



4106231546

ProQuest Number: 10290121

All rights reserved

INFORMATION TO ALL USERS

The quality of this reproduction is dependent upon the quality of the copy submitted.

In the unlikely event that the author did not send a complete manuscript and there are missing pages, these will be noted. Also, if material had to be removed, a note will indicate the deletion.



ProQuest 10290121

Published by ProQuest LLC (2017). Copyright of the Dissertation is held by the Author.

All rights reserved.

This work is protected against unauthorized copying under Title 17, United States Code
Microform Edition © ProQuest LLC.

ProQuest LLC.
789 East Eisenhower Parkway
P.O. Box 1346
Ann Arbor, MI 48106 – 1346

***CHARACTERISATION OF MPTP-
INDUCED NEUROTOXICITY IN A
NEUROBLASTOMA CELL MODEL
SYSTEM.***

Luigi A. De Girolamo

*A thesis submitted in partial fulfilment of the requirements of The
Nottingham Trent University for the Degree of Doctor of Philosophy*

This research programme was funded by Immutec, Nottingham, UK.

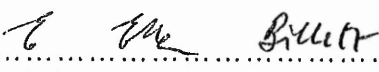
July 2000

DECLARATION

This work has not been accepted for any other degree and is not concurrently being submitted for any other degree.

This is to certify that the candidate carried out the work submitted. Due acknowledgement has been made of any assistance received.

Signed 
(Candidate)

Signed 
(Director of Studies)

Per Mamma, Pappa e Lisa

*Ma il mio mistero e chiuso in me,
il nome mio nessun sapra!
No, no sulla tua boca lo diro quando la luce splendera!
Ed il mio bacio scioglierà il silenzio
che ti fa mia*

*Il nome suo nessun sapra...
e noi dovrem, ahime, morir!*

Giacomo Puccini (1858-1924)

ACKNOWLEDGEMENTS

Without a doubt, this project would not have been possible if it were not for Dr. Ellen Billett and Dr. Alan Hargreaves. I will be forever grateful to them for investing their time, knowledge and guidance to give constant support and encouragement throughout. Thank you.

Many thanks go to friends and colleagues from all of Biochemistry Research, past and present. Alan, Cheryl, Debbie, Ghazi, James, Kevin, Lucy, Maxine, Nadine, Nathalie, Nico, Shiva and all others (whose absence from this acknowledgement is no reflection on their importance) for providing ideas, time, equipment, chemicals, and most of all friendship.

Thanks also go to technical staff from Biochemistry, Microbiology, Physiology and Radiochemistry departments. To Tracey Simmons for help with FACScan analysis, to Maggie Martin for providing photography and printing, to Dr. M Goedert for the synuclein antibody and Prof. R. Mayer for the ubiquitin antibody.

I would also like to express my sincere gratitude to my family, Mum, Dad, brother (Giovanni), sister (Rochina), Nigel and George for constant help, support and encouragement at every level, no matter what. I owe you everything. To Tina and Pat, for their friendship and help throughout.

Finally, to Lisa whose encouragement, strength, understanding and devotion have accompanied me down the long, windy and sometimes dark road. Thank you with all my heart.

ABSTRACT

Cell lines, as *in vitro* models, are useful tools in unravelling the detailed action and effects of many neurotoxic compounds. In this thesis, two specific CNS cell lines, mouse N2a neuroblastoma cells and rat C6 glioma cells, have been used to characterise the cytotoxic and neurotoxic effects of the Parkinsonian-inducing neurotoxin 1-methyl-4-phenyl-1,2,3,6-tetrahydropyridine (MPTP). The terms cytotoxic and neurotoxic are used separately here to define (i) cytotoxic; toxic insult which has caused apoptotic/necrotic cell death; or (ii) neurotoxic; sub-cytotoxic insult which may compromise molecular events, prior to any measurable cell death. The project will ultimately allow: (a) characterisation of the relative susceptibility of the two cell lines to the neurotoxin; (b) characterisation of N2a and C6 monoamine oxidase status (MAO); (c) provide a better understanding of the molecular events which occur during MPTP-induced neuronal degeneration; (d) identify possible early markers of neuronal toxicity; (e) provide a model which can be used to study potential neuroprotective agents.

Cytotoxicity assessments revealed that N2a cells exhibited an increased sensitivity to MPTP compared to C6 cells. In addition, cytotoxicity was increased when N2a cells were induced to differentiate by serum withdrawal and the addition of di-butyryl cyclic AMP. This increase in MPTP-induced cytotoxicity was shown to occur alongside a concomitant increase in total MAO activity. RT-PCR studies with MAO-specific primers revealed a predominance of MAO-A mRNA which increased accordingly in the differentiated state.

The use of sub-cytotoxic concentrations of MPTP on N2a cells have directed studies towards an understanding of the subtle molecular changes that occur following insult which may have particular relevance to neurodegeneration in Parkinson's Disease. Treatment of differentiating and differentiated neuroblastoma cells with sub-cytotoxic levels of MPTP led to an inhibition of axon outgrowth and retraction of axons, respectively. Biochemical characterisation by Western blotting revealed that MPTP had no significant effects on the levels of actin, α -tubulin or total neurofilament-H (NF-H). However, the use of phosphorylation state specific antibodies Rmd09 and Ta51 showed NF-H phosphorylation to increase following MPTP treatment. In addition, indirect immunofluorescence analysis revealed an accumulation of phosphorylated NF-H in the cell perikaryon, suggesting that altered NF-H distribution was associated with the observed effects of MPTP on cell morphology. Since these modifications occurred in the absence of a change in energy balance or mitochondrial membrane potential, and since NFs are components of Lewy bodies, aberrant NF-H hyper-phosphorylation could be considered to be an early marker of neurotoxicity.

The ability of potential neuroprotective agents to alleviate both MPTP-induced cell death (cytotoxicity) and MPTP-induced NF-H phosphorylation / reduction in axon outgrowth (neurotoxicity) was also investigated. Both the cytotoxic and neurotoxic effects of MPTP were reduced by the MAO inhibitors deprenyl and, to a lesser extent, clorgyline. Alleviation of both neurotoxicity and cytotoxicity was also achieved by glial conditioned medium, derived from C6 cells. In contrast, whilst the p38 mitogen-activated protein kinase inhibitor, SB202190, protected cells against MPTP-induced neurotoxicity, it could not maintain cell viability at high MPTP exposures. In each case neuroprotection involved maintenance of the differentiating phenotype linked with attenuation of NF-H hyper-phosphorylation; the latter may represent a mechanism by which neuronal cells can moderate MPTP-induced neurotoxicity. The use of a simplified neuronal cell model, which expresses subtle biochemical/molecular changes following neurotoxic insult, could therefore provide a valuable tool for the identification of potential neuroprotective agents.

Abbreviations

ADP	adenosine diphosphate
ATP	adenosine triphosphate
BCIP	bromochloroindolyl phosphate
bp	base pair
BSA	bovine serum albumin
CNS	central nervous system
dbcAMP	dibutyryl cyclic adenosine monophosphate
DMEM	Dulbecco's Modified Eagles Medium
DNA	deoxyribonucleic acid
DPM	disintegrations per minute
EDTA	ethylenediamine tetracetic acid
ERK	extracellular-regulated-signalling kinase
FAD	flavin adenine dinucleotide
FCS	foetal calf serum
FITC	fluorescein isothiocyanate
GDNF	glial-derived neurotrophic factor
GSH	reduced glutathione
GSSG	oxidised glutathione
Ig	immunoglobulin
JC-1	5,5',6,6'-tetrachloro-1,1',3,3'-tetraethylbenzimidazolylcarbocyanine iodide
JNK	c-jun-N-terminal kinase
kDa	kilodalton
LDH	lactate dehydrogenase
MAO	monoamine oxidase
MAPK	mitogen activated protein kinase
MPDP ⁺	1-methyl-4-phenyl-1,2,3-dihydropyridinium
MPP ⁺	1-methyl-4-phenylpyridinium ion
MPTP	1 methyl-4-phenyl-1,2,3,6-tetrahydropyridine
mRNA	messenger ribonucleic acid
MTT	3-(4,5-dimethylthiazol-2-yl)-2,5-diphenyltetrazolium bromide
NBT	nitroblue tetrazolium
NF-H	neurofilament heavy chain
NMDA	<i>N</i> -methyl- <i>D</i> -aspartate
NO	nitric oxide
O ₂ ⁻	superoxide
ONOO ⁻	peroxynitrite
p38 MAPK	p38 mitogen activated protein kinase
PBS	phosphate buffered saline
PCR	polymerase chain reaction
PD	Parkinson's disease
RT-PCR	reverse transcription - polymerase chain reaction
SAPK	stress-activated protein kinase
SD	standard deviation
SDS	sodium dodecyl sulphate
SDS-PAGE	sodium dodecyl sulphate – polyacrylamide gel electrophoresis
SEM	standard error of mean
SFM	serum free medium
TBS	tris buffered saline
TEMED	<i>N,N,N,N'</i> -tetramethylethylenediamine
Tween 20	polyoxyethylene sorbitan monolaurate

Figures

	Page
Chapter I	
Figure 1.1 Conversion of MPTP to MPP ⁺ by monoamine oxidase.	7
Figure 1.2 Proposed mechanism of MPTP-induced toxicity in vivo.	10
Figure 1.3 Simplified reaction catalysed by monoamine oxidase.	18
Figure 1.4 Chemical structure of MAO inhibitors clorgyline and deprenyl.	24
Figure 1.5 Diagrammatic representation of the sequence and basic structure of mammalian neurofilament subunits.	30
Figure 1.6 Two models for elaborating the axonal microtubule array.	34
Figure 1.7 Transport and dynamics of neurofilament transport in axons.	34
Chapter II	
Figure 2.1. Example of a protein standard curve (Lowry method).	56
Chapter III	
Figure 3.1 Determination of optimal incubation time for the MTT viability assay in glioma and neuroblastoma cell lines.	77
Figure 3.2 Validation of the MTT viability assay using mitotic C6 cells: Comparison with the Coomassie blue and LDH assay.	79
Figure 3.3 Validation of the MTT assay using differentiating N2a cells: Comparison with the LDH and Coomassie blue assays.	80
Figure 3.4 MPTP-induced cytotoxicity on mitotic N2a and C6 cells.	84
Figure 3.5 Cell viability assessment of mitotic C6 and N2a cell lines exposed to the neurotoxin MPTP for 48 hours.	85
Figure 3.6 Cell viability assessment of differentiating N2a neuroblastoma cells exposed to the neurotoxin MPTP for 24 and 48 hours.	86
Figure 3.7 Cell viability assessment of differentiating C6 glioma cells exposed to the neurotoxin MPTP for 72 hours.	87
Figure 3.8 Cell viability assessment of differentiating C6 and N2a cells exposed to the neurotoxic metabolite MPP ⁺ .	89
Figure 3.9 Cell viability assessment of differentiating N2a cells exposed to the neurotoxic metabolite MPP ⁺ in the presence of ATP.	90
Figure 3.10 Time course for the optimisation of MAO activity determination in C6 and N2a cell lines.	94
Figure 3.11 Inhibition of monoamine oxidase activity in mitotic C6 cells by clorgyline and deprenyl.	96
Figure 3.12 Identification of MAO-A and MAO-B mRNA present in the mitotic and differentiated state of C6 and N2a cells.	97
Chapter IV	
Figure 4.1 Time course of axon outgrowth in differentiating N2a cells.	120
Figure 4.2 The effect of sub-cytotoxic dose of MPTP on the morphology of differentiating N2a cells.	121
Figure 4.3 The effect of sub-cytotoxic dose of MPTP on axon outgrowth in differentiating N2a cells.	122
Figure 4.4 Time course of the expression of neurofilament-H protein during differentiation of neuroblastoma N2a cells.	123
Figure 4.5 Coomassie stained SDS PAGE gel of total cell extracts of differentiating N2a cells exposed to sub-cytotoxic concentrations of MPTP.	124
Figure 4.6 Western blotting analysis of cytoskeletal components from differentiating N2a cells exposed to sub-cytotoxic concentrations of MPTP.	125
Figure 4.7 Indirect immunofluorescence analysis of the effect of 10 μ M MPTP on neurofilament-H protein in differentiating N2a cells.	127

	Page
Figure 4.8 Analysis of JNK kinase activation in differentiating N2a cells.	132
Figure 4.9 The effect of sub-cytotoxic concentrations of MPTP on protein ubiquitination in differentiating N2a cells.	135
Figure 4.10 The effect of a sub-cytotoxic concentration of MPTP on synuclein levels in differentiating N2a cells	136
 Chapter V	
Figure 5.1 Cytotoxic protection afforded by clorgyline and deprenyl on differentiating N2a cells exposed to MPTP for 48 hours.	150
Figure 5.2 The effect of conditioned C6 medium and SB202190 on MPTP-induced cell death.	151
Figure 5.3 The effect of oestradiol and glutathione on MPTP-induced cell death induced.	152
Figure 5.4 The effect of potential neuroprotective agents on the morphology of differentiating N2a cells.	158
Figure 5.5 The effect of potential neuroprotective agents on of NF-H status from differentiating N2a cells exposed to sub-cytotoxic MPTP concentrations.	160
Figure 5.6 Determination of the presence of a GDNF-like protein in conditioned medium derived from rat C6 glioma cells.	162
Figure 5.7 Identification of Glial derived neurotrophic factor in conditioned medium harvested from the growth C6 cells.	163
 Chapter VI	
Figure 6.1 Time course of axon outgrowth in neuroblastoma N2a cells induced to differentiate in the presence and absence of conditioned C6 medium.	177
Figure 6.2 Characterisation of NF-H status in neuroblastoma N2a cells induced to differentiate in the presence or absence of conditioned C6 medium.	178
Figure 6.3 Cell viability assessment of pre-differentiated neuroblastoma N2a cells exposed to the neurotoxin MPTP for 8 and 24 hours.	180
Figure 6.4 Determination of axon maintenance in pre-differentiated N2a cells exposed to sub-lethal dose of MPTP.	182
Figure 6.5 Coomassie stained SDS PAGE gel of total cell extracts of pre-differentiated N2a cells exposed to sub -lethal dose of MPTP.	184
Figure 6.6 Western blotting analysis of cytoskeletal components from pre-differentiated N2a cells exposed to a sub-cytotoxic concentration of 10 μ M MPTP.	185

Tables

	Page
<i>Chapter I</i>	
Table 1.1 Substrates of MAO-A and MAO-B.	20
<i>Chapter II</i>	
Table 2.1. MAO sequence specific primers	59
Table 2.2 Formulation for SDS-PAGE minigels.	65
Table 2.3 Antibody profiles	68
<i>Chapter III</i>	
Table 3.1 Evaluation of the cytotoxicity of MPTP and MPP ⁺ towards two neural cell lines in culture.	88
Table 3.2 Total monoamine oxidase activity levels of C6 and N2a cells in the mitotic and differentiated state.	95
Table 3.3 Analysis of total glutathione levels (GSH + GSSG) in C6 and N2a cells (mitotic and differentiated state).	99
<i>Chapter IV</i>	
Table 4.1 Determination of sub-cytotoxic exposure of differentiating N2a cells exposed to MPTP	119
Table 4.2 Determination of ATP levels and mitochondrial membrane potential in differentiating N2a cells exposed to sub-cytotoxic MPTP concentration	131
<i>Chapter V</i>	
Table 5.1 Analysis of total glutathione levels in differentiating N2a cells following the addition of extracellular GSH.	153
Table 5.2 The effect of potential neuroprotective agents on axon outgrowth in differentiating N2a cells exposed to sub-cytotoxic MPTP concentrations.	157
<i>Chapter VI</i>	
Table 6.1 Determination of sub-cytotoxic exposure of pre-differentiated N2a cells exposed to MPTP.	181

CONTENTS

	<i>Page</i>
Chapter I: General Introduction	1
1.1 1-Methyl-4-Phenyl-1,2,3,6-Tetrahydropyridine (MPTP).	2
<i>1.1.1 The emergence of MPTP as a neurotoxin</i>	2
<i>1.1.2 Animal models of MPTP-induced Parkinsonism</i>	2
<i>1.1.3 MPTP-induced Parkinsonism as a valid model</i>	3
<i>1.1.4 Bioactivation of MPTP</i>	5
<i>1.1.5 Reaction mechanism of MPTP bioactivation</i>	6
<i>1.1.6 Selective toxicity of MPTP towards dopaminergic neurones</i>	7
<i>1.1.7 Metabolism and release of MPTP/MPP⁺ by glial cells</i>	9
<i>1.1.8 MAO-B expression and MPTP toxicity</i>	10
<i>1.1.9 Mechanisms of MPP⁺ induced cell death</i>	11
<i>1.1.9.1 Complex I inhibition</i>	11
<i>1.1.9.2 Production of reactive oxygen species</i>	13
<i>1.1.9.2.1 MPTP and antioxidant protection</i>	14
<i>1.1.9.2.2 Nitric oxide and MPTP-induced neurotoxicity</i>	15
<i>1.1.10 Glutamate excitotoxicity and MPTP-induced neurotoxicity</i>	16
1.2 Monoamine oxidase (MAO)	17
<i>1.2.1 General properties</i>	17
<i>1.2.2 MAO structure</i>	18
<i>1.2.3 Isozyme classification</i>	19
<i>1.2.4 Genetic studies</i>	20
<i>1.2.5 MAO location and distribution</i>	21
<i>1.2.5.1 Tissue distribution</i>	21
<i>1.2.5.2 Cellular distribution of MAO within the substantia nigra</i>	22
<i>1.2.5.3 Sub-cellular location of MAO</i>	23
<i>1.2.6 MPTP as a substrate for MAO</i>	23
<i>1.2.7 MAO inhibitors</i>	24
<i>1.2.7.1 Clorgyline</i>	25
<i>1.2.7.2 Deprenyl</i>	25
1.3 The neuronal cytoskeleton	26
<i>1.3.1 Components of the neuronal cytoskeleton</i>	26
<i>1.3.1.1 Microtubules</i>	27
<i>1.3.1.2 Microfilaments</i>	28
<i>1.3.1.3 Neurofilaments (NFs)</i>	28
<i>1.3.1.4 Neurofilament phosphorylation</i>	31
<i>1.3.2 The cytoskeleton and axonal growth</i>	32

	<i>Page</i>
1.4 Components of Lewy bodies	35
1.4.1 Ubiquitin	35
1.4.2 Synuclein	36
1.5 Neurotrophic Factors	37
1.5.1 Glial Derived Neurotrophic Factor (GDNF)	38
1.6 The use of MPTP in cellular systems for studying the pathogenesis of Parkinson's Disease.	39
1.6.1 Neuroblastoma (N2a) cell line	41
1.6.2 C6 Glioma cells	42
1.7 Aims of study	44
Chapter II: Materials and Methods	46
2.1 Materials	47
2.1.1 Specialised Equipment	47
2.1.2 Specialised Reagents	47
2.1.2.1 Chemical reagents	47
2.1.2.2 Antibodies	48
2.1.3 Tissue Culture Plastic-ware	48
2.1.4 Reagents	48
2.2 Methods	48
2.2.1 Cell lines	48
2.2.1.1 Mouse N2a neuroblastoma cells	48
2.2.1.2 Rat C6 glioma cells	49
2.2.1.3 Maintenance of cell lines	49
2.2.1.4 Freezing cells in liquid nitrogen	49
2.2.1.5 Thawing cells from liquid nitrogen	50
2.2.1.6 Passage of cells	50
2.2.2 Seeding of cells for experimentation	50
2.2.3 Differentiation of cells	51
2.2.3.1 Mouse N2a Neuroblastoma cells	51
2.2.3.2 Rat C6 Glioma cells	51
2.2.3.3 Glial C6 Conditioned Medium (Rat glial C6 cells)	52
2.2.4 Exposure of cells to MPTP/MPP⁺	52
2.2.5 Exposure of cells to neuroprotective agents	52
2.2.6 Viability Assays	53
2.2.6.1 MTT (Tetrazolium salt) viability assay	53

	<i>Page</i>
2.2.6.2 <i>Lactate dehydrogenase (LDH) viability assay</i>	53
2.2.6.3 <i>Trypan Blue exclusion assay</i>	54
2.2.7 <i>Protein Determination</i>	55
2.2.8 <i>Total Glutathione (GSH+GSSG) Determination</i>	56
2.2.9 <i>Monoamine oxidase analysis</i>	57
2.2.9.1 <i>Estimation of MAO activity</i>	57
2.2.9.2 <i>Selection of MAO-specific primers</i>	58
2.2.9.3 <i>Preparation of total RNA.</i>	59
2.2.9.4 <i>RNA quantitation</i>	60
2.2.9.5 <i>Reverse transcription-Polymerase chain reaction</i>	60
2.2.9.6 <i>Agarose gel electrophoresis</i>	61
2.2.10 <i>Preparation and analysis of protein cell extracts</i>	62
2.2.10.1 <i>Preparation of N2a cell extracts</i>	62
2.2.10.2 <i>Soluble and Insoluble Cell fractionation</i>	62
2.2.10.3 <i>Protein determination of cell extracts</i>	63
2.2.10.4 <i>Sample preparation</i>	63
2.2.11 <i>SDS-Polyacrylamide Gel Electrophoresis (SDS-PAGE)</i>	63
2.2.11.1 <i>Preparation of gels</i>	64
2.2.11.2 <i>Staining and destaining gels</i>	65
2.2.12 <i>Electrophoretic transfer of proteins</i>	66
2.2.12.1 <i>Western Blotting (electroblotting)</i>	66
2.2.12.2 <i>Staining of nitrocellulose blots for total protein pattern</i>	66
2.2.12.3 <i>Immunoprobng of blots for protein components</i>	67
2.2.12.4 <i>Antibodies</i>	68
2.2.12.5 <i>Quantification of blots</i>	68
2.2.13 <i>Quantification of axon outgrowth</i>	69
2.2.14 <i>Slide coating (Subbing)</i>	69
2.2.15 <i>Indirect Immunoflourescence analysis</i>	69
2.2.16 <i>Determination of ATP levels</i>	70
2.2.17 <i>Analysis of mitochondrial membrane potential</i>	71
2.2.18 <i>Statistical analysis</i>	71
Chapter III: Characterisation of MPTP-induced cytotoxicity in a cell model system.	72
3.1 <i>Introduction</i>	73
3.1.1 <i>Cell models: Characterisation</i>	73
3.2 <i>Results</i>	76
3.2.1 <i>Validation and optimisation of the MTT viability assay</i>	76

	<i>Page</i>
3.2.2 <i>Characterisation of the cytotoxicity of MPTP towards neuroblastoma and glioma cells</i>	81
3.2.3 <i>Characterisation of the cytotoxicity of MPP⁺ on neuroblastoma and glioma cells</i>	82
3.2.4 <i>Characterisation of monoamine oxidase activity in neuroblastoma and glioma cells</i>	91
3.2.4.1 <i>Determination of MAO isoform expression in C6 and N2a cell lines</i>	91
3.2.4.2 <i>Monoamine oxidase mRNA profiles in C6 and N2a cells</i>	92
3.2.5 <i>Analysis of total glutathione levels in N2a and C6 cells</i>	93
3.3 Discussion	100
3.3.1 <i>Cytotoxicity assay validation</i>	100
3.3.2 <i>Cytotoxicity of MPTP towards neuroblastoma and glioma cells</i>	101
3.3.3 <i>Cytotoxicity of MPP⁺ towards neuroblastoma and glioma cells</i>	104
3.3.4 <i>MAO activity and MAO-specific mRNA expression in neuroblastoma and glioma cell lines</i>	106
3.3.5 <i>Total glutathione (GSH + GSSG) status in C6 and N2a cells</i>	108
 Chapter IV: The neurotoxic effects of sub-cytotoxic MPTP insult on differentiating N2a neuroblastoma cells.	 109
4.1 Introduction	110
4.1.1 <i>Characterisation of MPTP-induced neurotoxic effects</i>	110
4.1.2 <i>NF-H antibodies</i>	111
4.1.3 <i>Abnormal cellular inclusions</i>	112
4.1.4 <i>MPTP-induced abnormalities in cell signalling cascades</i>	113
 4.2 Results	 115
4.2.1 <i>Assessment of sub-cytotoxic MPTP concentrations on differentiating N2a cells</i>	115
4.2.2 <i>Analysis of axon outgrowth in differentiating N2a cells</i>	115
4.2.3 <i>Analysis of neurofilament protein levels in differentiating N2a cells</i>	116
4.2.4 <i>Western blotting analysis of cytoskeletal components in differentiating N2a cells exposed to sub-cytotoxic concentrations of MPTP</i>	116
4.2.5 <i>Subcellular distribution of NF-H in differentiating N2a cells exposed to sub-cytotoxic MPTP concentration</i>	117

	<i>Page</i>
4.2.6 <i>ATP levels and mitochondrial membrane potential in differentiating N2a cells exposed to 10 μM MPTP.</i>	129
4.2.7 <i>Analysis of JNK/SAPK activation in differentiating N2a cells exposed to sub-cytotoxic concentrations of MPTP</i>	129
4.2.8 <i>Analysis of protein ubiquitination in differentiating N2a cells exposed to sub-cytotoxic concentrations of MPTP</i>	134
4.2.9 <i>Analysis of synuclein levels in differentiating N2a cells exposed to sub-cytotoxic concentrations of MPTP</i>	134
4.3 Discussion	137
4.3.1 <i>N2a cell differentiation</i>	137
4.3.2 <i>Sub-cytotoxic effects of MPTP on differentiating N2a cells</i>	137
4.3.3 <i>N2a cell energy status and mitochondrial integrity</i>	140
4.3.4 <i>Activation of the stress-activated protein kinase (SAPK) cascade</i>	141
4.3.5 <i>Protein ubiquitination in differentiating N2a cells</i>	141
4.3.6 <i>Synuclein expression in differentiating N2a cells</i>	142
 Chapter V: MPTP-induced neurotoxicity: Inhibition by potential neuroprotective agents.	 143
5.1 Introduction	144
5.1.1 <i>Neuroprotection</i>	144
5.2 Results	147
5.2.1 <i>The effect of MAO inhibitors on MPTP-induced cytotoxicity</i>	147
5.2.2 <i>The effect of potential neuroprotective agents on MPTP-induced cytotoxicity</i>	148
5.2.3 <i>Intracellular glutathione levels</i>	149
5.2.4 <i>Analysis of neuroprotective agents on axon outgrowth</i>	154
5.2.5 <i>Western blot analysis of NF-H in differentiating N2a cells exposed to MPTP and neuroprotective agents</i>	155
5.2.6 <i>Identification of glial-derived neurotrophic factor in C6 conditioned medium</i>	156
5.3 Discussion	164
5.3.1 <i>The protective efficacy of MAO inhibitors</i>	164
5.3.2 <i>The protective efficacy of glial conditioned medium</i>	165
5.3.3 <i>The protective efficacy of p38 MAPK inhibition</i>	167
5.3.4 <i>The protective efficacy of oestrogen (estradiol)</i>	168

	<i>Page</i>
5.3.5 <i>The protective efficacy of glutathione</i>	168
Chapter VI: The neurotoxic effects of sub-cytotoxic MPTP insult on pre-differentiated N2a cells.	171
6.1 <i>Introduction</i>	172
6.1.1 <i>Development of a pre-differentiated N2a model</i>	172
6.2 <i>Results</i>	174
6.2.1 <i>Analysis of N2a cell differentiation by conditioned medium</i>	174
6.2.2 <i>Characterisation of the cytotoxicity of MPTP on pre-differentiated N2a cells</i>	175
6.2.3 <i>Analysis of axon maintenance in pre-differentiated N2a cells</i>	176
6.2.4 <i>Western blotting analysis of cytoskeletal components in pre-differentiated N2a cells exposed to sub-cytotoxic MPTP concentration.</i>	183
6.3 <i>Discussion</i>	187
6.3.1 <i>Characterisation of a post-differentiated N2a cell model</i>	187
6.3.2 <i>Effect of MPTP on pre-differentiated N2a cells</i>	188
Chapter VII: General Discussion & Future work	192
7.1 <i>MPTP-induced neurotoxicity and neurodegeneration</i>	193
7.2 <i>The role of MPTP-induced signalling cascades</i>	196
7.3 <i>Neuroprotection</i>	199
7.4 <i>Summary</i>	200
References	203

CHAPTER I

General Introduction

1. INTRODUCTION

1.1 1-Methyl-4-Phenyl-1,2,3,6-Tetrahydropyridine (MPTP).

1.1.1 The emergence of MPTP as a neurotoxin.

The first scientifically reported synthesis of MPTP goes back to 1946 (Lee *et al.*, 1946) when studies on the synthesis of compounds derived from the basic chemical structure of morphine were undertaken in an attempt to obtain compounds with analgesic properties. MPTP was categorised as having no analgesic activity. However, in the late 1970's MPTP gained notoriety when a graduate student in the USA unwittingly synthesised MPTP while trying to reproduce a designer drug, 1-methyl-4-propion-oxypiperidine (MPPP), an analogue of the narcotic pethidine (meperidine). MPTP (a cyclic tertiary allylamine) is a variable by-product of the synthesis of MPPP, occurring at elevated temperatures and at low pH. Following administration of the drug (termed "new heroin") the individual was hospitalised exhibiting Parkinson-like symptoms. Upon his death, an autopsy revealed destruction of the substantia nigra pathologically similar to that seen in idiopathic Parkinson's disease (Davis *et al.*, 1979).

A similar incident, on a larger scale, occurred in 1982. A number of relatively young individuals with narcotic problems exhibited neurological symptoms closely resembling those seen in elderly Parkinson's disease patients. These symptoms responded to conventional L-Dopa therapy. Upon further investigation it was revealed that all the affected individuals were self-administering a contaminated batch of "new heroin", which on analysis was found to contain virtually pure MPTP (Langston *et al.*, 1983).

1.1.2 Animal models of MPTP-induced Parkinsonism.

A direct link between MPTP and its neurotoxic effect became evident when the compound was systemically administered to primates (Burns *et al.*, 1983; Langston *et al.*, 1984a). The clinical symptoms observed were typical of those seen in human Parkinsonism with respect to three principal manifestations: akinesia, rigidity and

hypokinesia, all of which responded to L-Dopa therapy (Burns *et al.*, 1983; Jenner *et al.*, 1984; Langston *et al.*, 1984a). In conjunction, MPTP treatment was shown to decrease monoamine neurotransmitter levels, particularly striatal dopamine and its metabolites (Burns *et al.*, 1983). Indeed, it was also observed that repeated MPTP treatment in the squirrel monkey produced a non-homogenous loss of dopamine (Langston, 1985); depletion being greater in the putamen than in the caudate, mimicking the deficiency pattern seen in idiopathic Parkinson's disease (PD) (Hornykiewicz, 1988). Similar pathological changes to that seen in idiopathic PD involving characteristic changes in the midbrain (i.e. degeneration of neurones in the zona compacta of the substantia nigra) have also been observed in primates on autopsy (Langston *et al.*, 1984a; Hantraye *et al.*, 1993).

The use of non-primate models has also been proposed in attempts to establish other suitable animal models of PD including the rat, mouse, cat, dog, sheep and goldfish (see Mari and Bodis-Wollner, 1997, for review). In general, some degree of the characteristic symptoms of PD are observed in the post-MPTP state in these animals. However, it is evident that significant species differences in sensitivity to MPTP exist. Rodents, for example, have been shown to be more resistant to the pathological effect of systemic MPTP treatment exhibiting fewer symptoms (Boyce *et al.*, 1984; Chiueh *et al.*, 1984; Heikkila *et al.*, 1984a) than primates. This is thought to be related to several mechanisms such as differences in monoamine oxidase, differences in the retention of pyridinium metabolites of MPTP in the brain (Markey *et al.*, 1984; Johannessen *et al.*, 1985), or the presence of neuromelanin in susceptible neurones (Irwin and Langston, 1985). In conjunction, there is evidence that older animals exhibit a higher sensitivity to MPTP (Gupta *et al.*, 1986; Ricaurte *et al.*, 1987).

1.1.3 MPTP-induced Parkinsonism as a valid model.

The symptomatological, neurochemical and pathological resemblance of MPTP-induced Parkinsonism with idiopathic PD have led to many workers suggesting it to be an ideal model for PD. However, along with the many characteristic similarities, there are some important differences to note. For example, MPTP-induced

Parkinsonian symptoms are not identical in all details to idiopathic PD. The most prominent clinical symptom lacking in MPTP induced Parkinsonism is resting tremor where it presents itself less frequently than in the disease itself (Tetrud and Langston, 1992).

Another proposed deficit of the MPTP induced Parkinsonism model is its variability in mimicking the clinical course of the PD process. PD has been described as a slow but relentlessly progressing neurodegenerative disease. However, in human and sub-human primate models of MPTP-induced Parkinsonism, progression and stabilisation have been reported along with incidence of spontaneous recovery occurring in some primate models (Langston, 1985).

The general absence of specific neuronal eosinophilic cytoplasmic inclusions called Lewy bodies (see section 1.4) in MPTP-treated animals is also a fundamental contrasting characteristic. The presence of Lewy bodies in PD is associated with its pathological confirmation (Gibb and Lees, 1988), although their presence is not exclusive to this disease, as they are seen in various other disorders and in normal ageing brain. However, work carried out by Forno *et al* (1986) has described the presence of similar inclusion bodies with partially different features to Lewy bodies, in MPTP-treated monkeys using a protracted dosing regimen. Recently, confirmation of similar eosinophilic inclusions *in vivo*, described as abnormal aggregates have been observed in other laboratories (Kowall *et al.*, 2000), supporting the possible presence of Lewy-type inclusions in MPTP-induced Parkinsonism.

Due to the increased number of different species proposed as animal models of MPTP-induced Parkinsonism the importance of well-defined and appropriate experimental criteria need to be realised. Several factors have been identified that may influence the clinical and biochemical aspects of MPTP-induced parkinsonism including species, age, total dose, dosing regimen and route of administration of MPTP (Mari and Bodis-Wollner, 1997).

Although the primate model of MPTP-induced Parkinsonism remains the closest model to Parkinson's disease to date, the use of other animal models has contributed significantly to the understanding of parkinsonism and are still of value for use in studies of anti-parkinsonian drug therapy. However, the use of animal models to determine the molecular events involved in MPTP-induced neurotoxicity may prove

difficult to interpret, in addition to continually arousing ethical questions. Therefore the application of a more simplified model may be of value in these situations.

1.1.4 Bioactivation of MPTP.

Following the recognition of the biological effects of MPTP workers turned their thoughts to the mechanism of action of the neurotoxin. Consideration of the chemical structure of MPTP suggested that, as a neutral molecule, it might readily pass the blood brain barrier; but since no highly reactive group is present its neurotoxic activity was unexpected. This led researchers to suggest that MPTP may be metabolised by tissue enzymes, known to metabolise tertiary amines, to a potentially more cytotoxic product to cause its neurotoxic effect.

Administration of [^{14}C]-MPTP to both monkeys and mice identified the corresponding pyridinium analogue, 1-methyl-4-phenylpyridinium cation (MPP^+), to be the major metabolite within the brain (Langston *et al.*, 1984b; Markey *et al.*, 1984). MPTP was also shown to be metabolised *in vitro* by rat brain mitochondrial fractions whereupon the major metabolite was again identified as MPP^+ (Chiba *et al.*, 1984; Castagnoli *et al.*, 1985). Indeed, MPTP appeared to decline from the primate brain while MPP^+ accumulated and persisted over a period of time (Johannessen *et al.*, 1985). Its positively charged conformation denies the metabolite the ability to cross the blood brain barrier and thereby indicates its formation must be within the brain. The direct toxicity of MPP^+ was demonstrated in culture initially by Mytilineou *et al.* (1985) in mesencephalic dopaminergic neurones where MPP^+ was more effective than MPTP.

Autoradiographic studies using [^3H]-MPTP revealed the neurotoxin to bind with high affinity to brain membranes in both rat and human brain. A high receptor density was observed in regions of the human brain including the caudate, substantia nigra, and locus coeruleus corresponding to the observed neurotoxicity and neurochemical imbalance obtained with MPTP administration (Javitch *et al.*, 1984). In contrast to humans, rat substantia nigra and caudate displayed only moderate receptor concentrations. This species difference further highlights the difficulty in producing selective nigrostriatal degeneration in rats.

In conjunction with the autoradiographic studies, the localisation of binding sites for [³H]-MPTP have been reported to resemble that of [³H]-pargyline (a MAO inhibitor) (Parsons and Rainbow, 1984; Rainbow *et al.*, 1985). MAO-B distribution, determined using immunohistochemical methods (Levitt *et al.*, 1982), also suggested the possible role of MAO in the neurotoxic process. These reports were further supported by the fact that pargyline and deprenyl (a MAO-B inhibitor) blocked the loss of dopaminergic neurones exposed to MPTP in explants of embryonic rat substantia nigra (Mytilineou and Cohen, 1984). They also prevented the biotransformation of MPTP *in vitro*, while clorgyline (a MAO-A inhibitor) could not (Chiba *et al.*, 1984). In association, pre-treatment of primates and mice with pargyline and deprenyl was shown to protect significantly against dopaminergic neurotoxicity preserving the levels of dopamine and its metabolites (Cohen *et al.*, 1984; Heikkila *et al.*, 1984b), while clorgyline treatment was less effective (Heikkila *et al.*, 1984b). These findings therefore suggested that the oxidative metabolism of MPTP to MPP⁺ was a critical feature in the neurotoxic process mediated by the enzyme monoamine oxidase, specifically the MAO-B isoform.

1.1.5 Reaction mechanism of MPTP bioactivation.

Research showing that cyclic tertiary amines undergo cytochrome P-450 catalysed α -carbon oxidation to form reactive iminium species prompted Castagnoli and co-workers to suggest a similar mechanism for the metabolism of MPTP by MAO (Chiba *et al.*, 1984; Castagnoli *et al.*, 1985). ¹H-NMR analysis proposed that MPTP is initially oxidised to an intermediate product 1-methyl-4-phenyl-1,2,3-dihydropyridinium (MPDP⁺) when added as a substrate to rat brain mitochondrial fractions (Chiba *et al.*, 1984). This reaction step, MPTP to MPDP⁺, was completely inhibited by pargyline. MPDP⁺ itself was found to be unstable and rapidly undergoes disproportionation to MPTP and MPP⁺, although pargyline has no inhibitory effect on the conversion of MPDP⁺ to MPP⁺ (Castagnoli *et al.*, 1985). The two step bioactivation process involves four electron oxidation. The reaction is initiated by the enzyme MAO-B whereupon the product, MPDP⁺, undergoes spontaneous oxidation to form the toxic metabolite MPP⁺ (see Fig. 1.1). The use of purified forms of MAO has

allowed further detailed investigation of the reaction mechanism *in vitro*. Contrary to early belief, both forms of MAO (A and B) are able to metabolise MPTP at appreciable rates; MAO-B expressing a higher affinity than MAO-A (Salach *et al.*, 1984).

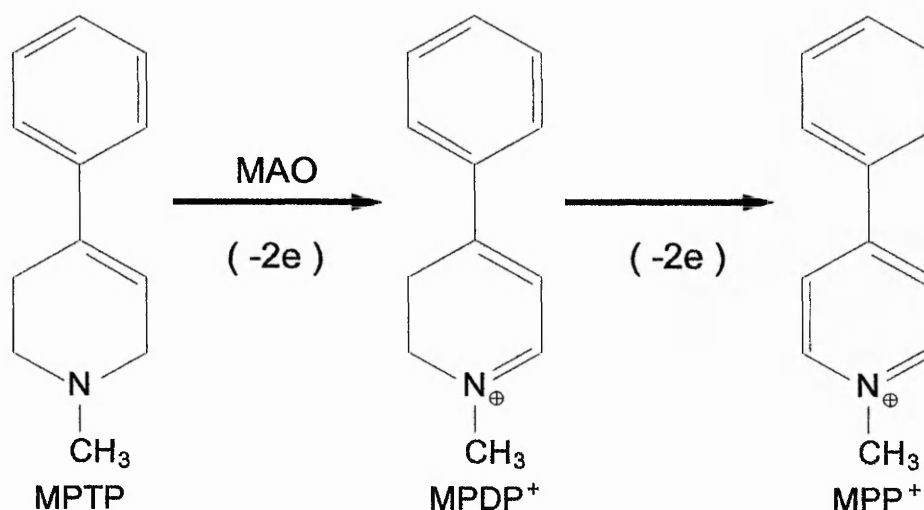


Figure 1.1 Conversion of MPTP to MPP⁺ by monoamine oxidase.

1.1.6 Selective toxicity of MPTP towards dopaminergic neurones.

While levels of MAO-B are high in the human substantia nigra and caudate, MAO-B also occurs in numerous other parts of the brain (Levitt *et al.*, 1982; Javitch *et al.*, 1984; Parsons and Rainbow, 1984) and thus MPP⁺ is formed from MPTP throughout the brain (Langston *et al.*, 1984a; Markey *et al.*, 1984). However, although the selective binding of MPTP and production of MPP⁺ by MAO-B is a necessary first step in eliciting toxicity, it cannot account for the selective effects on dopaminergic neurones. Indeed, the dopaminergic neurones of the nigrostriatal system have been reported to contain little MAO-B (Levitt *et al.*, 1982). In contrast, neighbouring glial cells and serotonergic neurones contain relatively high levels of the MAO-B isoform (Levitt *et al.*, 1982). Therefore the question arises of how reactive products from the oxidation of MPTP, formed in cells other than dopaminergic neurones, are selectively accumulated and able to exert their toxic effects on nigrostriatal dopamine containing neurones.

The ability of the neurotransmitter uptake systems within the brain to accumulate biogenic amines function in a relatively non-specific nature. This could therefore allow substances chemically related to biogenic amines, including neurotoxins, a possible entry pathway. The ability of catecholamine containing neurones in the corpus striatum and cerebral cortex to accumulate MPP⁺, but not MPTP, via the dopamine and norepinephrine re-uptake system was demonstrated by Javitch and co-workers (Javitch and Snyder, 1984; Javitch *et al.*, 1985). The K_m and V_{max} values for [³H]-MPP⁺ uptake were comparable to that of [³H]-dopamine uptake (Javitch *et al.*, 1985). Furthermore, blockade of dopamine uptake by dopamine uptake inhibitors, such as mazindol, are able to prevent MPTP neurotoxicity (Javitch *et al.*, 1984).

The cloning of both human and rat dopamine transporters (Giros *et al.*, 1992) and subsequent expression in cultured cells has demonstrated that MPP⁺ toxicity is directly correlated to the dopamine transport protein. Neuronal cell lines stably transfected with the dopamine transporter exhibited an increased susceptibility to the cytotoxic effects of low concentrations of MPP⁺ (Pifl *et al.*, 1993). However, there was no decisive difference between the rat and human dopamine transporter efficiencies that could explain the differences in susceptibility of these species to damage by MPTP.

Further *in vitro* studies, using the PC12 cell line and rat brain synaptosomes revealed an ATP-regulated dopamine transport pathway (low affinity/high capacity) that is a distinctly different transport process (Eshleman *et al.*, 1995) from that of basal dopamine transport (high affinity/low capacity). A subsequent report has shown that physiological levels of extracellular ATP can stimulate the transport of MPP⁺ into PC12 cells by 270% over basal levels (Dunigan and Shamoo, 1996) and suggests that the ATP-regulated dopamine transport pathway could be the major component of total MPP⁺ transport *in vivo*.

The vulnerability of dopaminergic neurones within the substantia nigra to MPTP toxicity has also been associated with the presence of neuromelanin. It is derived from the oxidation of dopamine and the polymerisation of other oxidation products of catecholamines. Neuromelanin is contained in the cell bodies of certain brain regions with particular reference to the locus coeruleus and substantia nigra,

whose dark pigmentation is characteristically due to the neuromelanin and seemingly increases with age (Mann *et al.*, 1977). MPP^+ has been shown to bind with high affinity to neuromelanin; it has therefore been postulated that it may act as a repository where MPP^+ can be stored and released gradually (D'Amato *et al.*, 1987). Interestingly, the presence of neuromelanin has not been identified in rats where a characteristic feature of MPTP administration is a rapid disappearance of the metabolite from the brain, contrasting to its extended retention in the primate brain (Irwin and Langston, 1985; Johannssen *et al.*, 1985).

1.1.7 Metabolism and release of MPTP/ MPP^+ by glial cells.

Experimental evidence indicates that glial cells are primarily responsible for the metabolic activation of MPTP in the CNS (Brooks *et al.*, 1989). Since MPP^+ is a positively charged molecule it is, in theory, ultimately unable to cross the blood brain barrier and cell membranes easily. MPP^+ must reach the extracellular space, once generated within glial cells, to be available for active accumulation by dopaminergic neurones. *In vitro* studies have demonstrated that the addition of MPTP to primary cultures of astrocytes results in the accumulation of MPP^+ extracellularly in the medium (e.g. Ransom *et al.*, 1987). This suggests MPP^+ may either be released from astrocytes after cell death or cause disruption of astrocyte membranes, due to its cytotoxic properties (DiMonte *et al.*, 1992). Alternatively, it has been proposed that diffusion of $MPDP^+$, the intermediate dihydropyridium species, through astrocyte membranes can occur through a series of events. $MPDP^+$ can exist in equilibrium with its conjugate base, 1,2-MPDP, at physiological pH (DiMonte *et al.*, 1992). 1,2-MPDP is lipophilic and therefore can diffuse across the astrocyte membrane and deposit itself extracellularly before undergoing auto-oxidation to MPP^+ (Singer *et al.*, 1986). The absence of auto-oxidation of 1,2-MPDP to MPP^+ within glia could be due to the presence of a highly reductive environment. Subsequently, MPP^+ is actively accumulated via the dopamine re-uptake system of neighbouring dopaminergic neurones. Once inside the cells MPP^+ is further accumulated within mitochondria disrupting oxidative metabolism, eventually leading to cell death (Fig. 1.2).

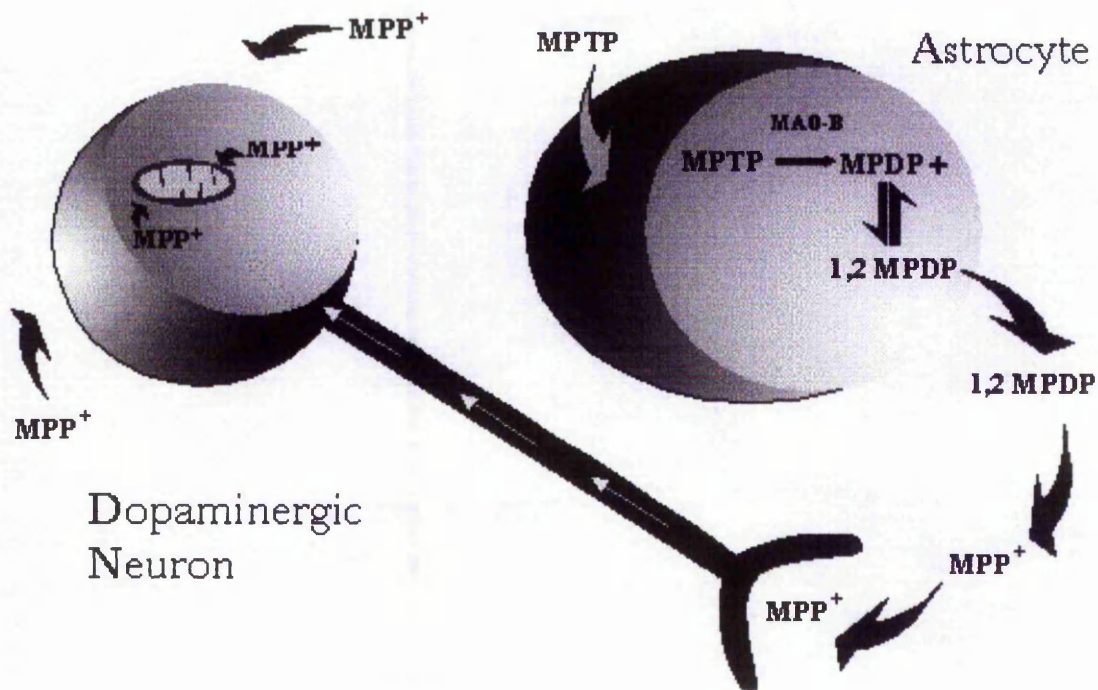


Figure 1.2 Proposed mechanism of MPTP-induced toxicity *in vivo*.

This mechanism is based on work carried out by DiMonte *et al* (1992) using primary cultures of mouse astrocytes under sub-lethal conditions whereupon MPP⁺ was shown to accumulate in the extracellular compartment during incubations with MPTP. Although still controversial, it has also been proposed that MPP⁺ could itself cross cell membranes, following a concentration-dependent gradient (Nernstian electrochemical gradient) (Scotcher *et al.*, 1991). What is clear is that *in vivo* glial cells play a paramount role in the MPTP neurotoxic process.

1.1.8 MAO-B expression and MPTP toxicity

Aberrant expression of high levels of MAO-B activity in neurones has been suggested to be a predisposing factor to the neurotoxic effects of MPTP. Indeed, *in vitro* studies using dopaminergic PC12 cells expressing elevated MAO-B levels showed a high level of free radicals and free radical damage, alongside an increased susceptibility of these cells to the toxin MPTP, compared to wild type cells (Wei *et al.*, 1996). However, in contrast, an *in vivo* study using transgenic mice expressing high

levels of MAO-B in neuronal cells was reported not to increase MPTP sensitivity. A comparable level of striatal dopamine, as well as similar tyrosine hydroxylase immunopositive cell numbers in the substantia nigra, after one week of MPTP administration, compared to age-matched non-transgenic litter mates was described. The study indicated that MAO-B levels and conversion of MPTP to MPP⁺ were not rate limiting steps in the toxicity of the compound (Andersen *et al.*, 1994). However, there are many factors that can influence the result in the more complicated *in vivo* situation. It has been suggested that variations in MPTP sensitivity in mice is a consequence of differences in levels of MAO-B activity in brain microvessels, which may act as a simple chemical blood brain barrier to obstruct MPTP entry into the brain. Alternatively, it is possible that endogenously high levels of MAO-B in other organs, particularly the liver, may restrict the amount of MPTP, introduced intraperitoneally, that reaches the brain (Andersen *et al.*, 1994).

1.1.9 Mechanisms of MPP⁺ induced cell death.

1.1.9.1 Complex I inhibition.

The intracellular localisation of MAO on the outer mitochondrial membrane is responsible for the conversion of MPTP to MPP⁺. This localisation of MAO also provides the proximity for MPP⁺ to be accumulated within mitochondria; a factor that is important when using *in vitro* cell cultures. MPP⁺ has been shown to be actively accumulated within the mitochondrial matrix by what is thought to be an energy dependent system capable of producing high intramitochondrial concentrations. The process is dependent on the electrochemical gradient of the mitochondrial membrane and is blocked by respiratory inhibitors and uncouplers (Ramsey *et al.*, 1986). The idea of a proposed carrier system within the mitochondria remains controversial. Direct measurement of mitochondrial uptake using an electrode selective for MPP⁺ has indicated that the initial rate of transport is non-saturable, therefore suggesting a less significant and important role played by a proposed carrier (Davey *et al.*, 1992).

Molecular orbital calculations have revealed that the positive charge of MPP⁺ is highly delocalised throughout the pyridinium ring and consequently it has been

postulated that MPP^+ may be able to diffuse down concentration or charge gradients therefore allowing entry into subcellular organelles e.g. mitochondria (Reinhard *et al.*, 1990). Several other studies utilising tetraphenylboron (TBP^-), a compound known to facilitate the entry of positively charged ions into mitochondria, have supported this argument by demonstrating that a passive Nerstian transport mechanism may be involved (see Tipton and Singer, 1993, for review).

Nicklas *et al* (1985) first reported that relatively high concentrations of MPP^+ interferes with mitochondrial respiration, acknowledging the necessity of mitochondrial MPP^+ accumulation. MPP^+ inhibited the ADP-stimulated and uncoupled oxidation of NADH-linked substrates with particular reference to pyruvate and glutamate oxidation, without affecting succinate oxidation. These observations were further supported by Vyas *et al* (1986) using mouse brain striatal slices that demonstrated changes consistent with the inhibition of mitochondrial oxidation. The changes included an increase in lactate formation and accumulation of the amino acids glutamate and asparagine and concomitant decrease in glutamine and aspartate. It was therefore proposed that MPP^+ is able to inhibit NAD-linked oxidation by interacting at the level of complex I of the electron transport system.

NADH:ubiquinone oxidoreductase (NADH dehydrogenase or complex I) is the proximal enzyme of the mitochondrial respiratory chain and is comprised of some thirty different subunits. One flavin mononucleotide (FMN) and as many as seven iron-sulphur clusters (Fe-S clusters), containing a total of 20-26 iron atoms, and probably one form of bound ubiquinone, participate in the electron pathway through the enzyme (see Weiss *et al.*, 1991, for review).

Electron paramagnetic resonance studies have shown no effect of MPP^+ on the reduction of the FMN moiety or Fe-S clusters of complex I suggesting that the inhibition site with which MPP^+ may interact is between the highest potential Fe-S cluster and ubiquinone (Q_{10}) (Ramsey *et al.*, 1987). This has also been proposed to be the general region where the classical electron transport chain inhibitors rotenone and piericidin A block NADH oxidation. Further evidence supporting the idea that MPP^+ inhibits complex I by binding at or near the same site as rotenone and piericidin was provided by radioligand binding and enzyme inhibitor studies (Ramsey *et al.*, 1991).

As a consequence of extensive complex I inhibition, reducing equivalents from complex I do not reach ubiquinone and thus oxidative phosphorylation is halted, resulting in rapid depletion of ATP and cell death. Many studies have implicated the involvement of energy depletion in MPP⁺ toxicity and has been demonstrated *in vitro* using rat hepatocytes (DiMonte *et al.*, 1986), rat brain mitochondria and *in vivo* within the mouse brain (Mari and Bodis-Wollner, 1997). The involvement of ATP depletion in MPP⁺ toxicity is further highlighted by the fact that complex I inhibition, ATP depletion and cell death are all reversible, below a threshold, and prevented when the neurotoxin is removed (Ramsey *et al.*, 1987; DiMonte *et al.*, 1992).

1.1.9.2 Production of reactive oxygen species

Although inhibition of mitochondrial respiration followed by energy depletion appears to be adequate to explain the observed neurotoxic effects of MPP⁺ there are some observations that indicate a more involved and complex action. The oxidative stress hypothesis for the biochemical basis of the neurotoxicity of MPP⁺, initially hypothesised by Johannessen *et al.* (1985), has been proposed to occur through a number of different possible pathways. Initially MAO-B catalyses the conversion of MPTP to MPDP⁺ which, at higher concentrations, disproportionates to MPTP and MPP⁺. Subsequently this not only impairs mitochondrial respiration but also has the ability to generate oxidative stress (Singer *et al.*, 1987). Although controversial, it is proposed that MPDP⁺ and MPP⁺ can interact directly with biomolecules to form deleterious free radical species (Adams and Odunze, 1991). For example, the non-enzymatic oxidation of MPDP⁺ to MPP⁺ may produce reactive oxygen species and, in part, may involve one-electron oxidation/reduction, thereby providing a pathway by which superoxide may be generated. Alternatively, MPP⁺ itself could be an instigator of free radicals. MPP⁺ reduction could produce a MPP[•] radical which, *in vitro*, can reduce oxygen to produce superoxide radical ion (Mari and Bodis-Wollner, 1997).

The functioning respiratory chain is a potent source of free radicals. Under normal circumstances the superoxide radicals generated are tightly bound to the chain and metabolised by the mitochondrial antioxidant system. However, inhibition of complex I by MPP⁺ can result in an increase in superoxide generation (Hasegawa *et*

al., 1990). This would suggest a secondary role for oxidative stress in MPTP-induced neurotoxicity. An increase in free radicals following complex I inhibition could cause irreversible damage to the respiratory chain directly and impair function or could be involved in other deleterious chemical reactions. Indeed, irreversible inactivation of complex I has been reported on prolonged incubation of mitochondria with MPP⁺, which the authors attributed to radical formation (Cleeter *et al.*, 1992).

The role of oxidative stress as a primary event in MPTP neurotoxicity is still unclear. Early work by Rossetti *et al* (1988) showed that when mitochondria isolated from mouse brain were incubated with MPTP, an electron resonance spin signal indicative of free radical formation could be detected. The addition of superoxide dismutase suppressed this signal consistent with MPP⁺ involving superoxide generation. Furthermore, pre-incubation of the mitochondria with deprenyl reduced the signal, suggesting MAO-B to be involved in its generation. More recently, Sriram *et al.* (1997) reported an increase in reactive oxygen species that preceded the inhibition of mitochondrial complex I in the mouse striatum, supporting the oxidative stress hypothesis.

1.1.9.2.1 MPTP and antioxidant protection.

The production of reactive oxygen species in MPTP neurotoxicity is further complicated by the fact that cytotoxicity is variably reduced in neuronal cell lines in the presence of antioxidants. The use of superoxide dismutase and catalase together partially alleviated MPTP-toxicity, although this protection was absent when the enzymes were used independently (Lai *et al.*, 1993). Similarly, embryonic rat ventral mesencephalic cells exposed to MPP⁺ along with various antioxidants (i.e. vitamin E, vitamin C, and coenzyme Q₁₀) partially alleviated the cytotoxic effects. However, the use of superoxide dismutase and allopurinol failed to exhibit any cytotoxic protection (Akaneya *et al.*, 1995). Transgenic mouse studies also support the role of reactive oxygen species in MPTP neurotoxicity since mice expressing increased Cu/Zn-superoxide dismutase activity showed increased resistance to MPTP-induced neurotoxicity (Przedborski *et al.*, 1992).

Glutathione acts as a major cellular antioxidant involved in the decomposition of H_2O_2 and whose levels have been observed to be reduced following MPTP administration (Adams and Odunze, 1991). This is of particular interest when comparing the MPTP model to Parkinson's disease as decreased glutathione levels have also been proposed in the substantia nigra of Parkinson patients brains (Riederer *et al.*, 1989). Furthermore, depletion of glutathione biosynthesis *in vivo*, achieved by administering L-buthionine sulphoximine (BSO) to preweanling mice and adult rats was shown to potentiate the toxic effects of MPTP and MPP^+ in nigral dopaminergic neurones (Wullner *et al.*, 1996). Reduced glutathione can also act as a protective agent (partial) when administered to mice prior to MPTP (Perry *et al.*, 1985).

In contrast to all of this, some workers have questioned the role of reactive oxygen species in MPTP neurotoxicity due to the absence of detectable oxy-radical damage, namely lipid peroxidation, both *in vitro* (DiMonte *et al.*, 1992; Lai *et al.*, 1993) and *in vivo* (Corongiu *et al.*, 1987) following MPTP administration. However, it has been postulated that lipid peroxidation is an end stage event which proceeds rapidly after lethal events have occurred (Lai *et al.*, 1993) and therefore factors such as assay sensitivity and MPTP concentration could be significant factors. Contrary to the MPTP model increases in the levels of lipid peroxidation, as measured by malondialdehyde levels and a decrease in polyunsaturated fatty acids, have been reported in the substantia nigra, but no other brain regions, in post-mortem Parkinson patients compared to age matched controls (Dexter *et al.*, 1989).

1.1.9.2.2 Nitric oxide and MPTP-induced neurotoxicity.

More recent reports have suggested a role for nitric oxide (NO) in conjunction with reactive oxygen species in directing MPTP-induced neurotoxicity. NO is a novel retrograde messenger in neurotransmission which has accumulated vast interest in recent years, and which has been linked to both normal and abnormal functions of the nervous system.

An increase in O_2^- formation due to MPP^+ can lead to O_2^- reacting with endogenous NO to form peroxynitrite ($ONOO^-$) (Packer *et al.*, 1996). Peroxynitrite is itself a potent oxidant that can directly oxidise thiol groups or decay rapidly to form

other reactive products. ONOO⁻ production has been shown to occur when MPP⁺ is incubated simultaneously with nitric oxide donors and mitochondrial membrane fractions. In conjunction, ONOO⁻ is implicated in producing mitochondrial depolarisation leading to calcium efflux in isolated mitochondria (Packer *et al.*, 1996). It has therefore ~~has~~ been proposed to be a contributory factor in MPTP-induced neurotoxicity. Indeed, inhibition of nitric oxide synthesis through the use of specific nitric oxide synthase inhibitors is able to reduce MPP⁺-induced hydroxyl radical formation (Smith *et al.*, 1994). Additionally, nitric oxide synthase inhibitors can prevent destruction of dopaminergic neurones alleviating parkinsonian symptoms in baboons treated with MPTP (Hantraye *et al.*, 1996). The role of NO in MPTP-induced neurotoxicity appears not to be a sole primary event but to exasperate the increase in oxidative stress produced by the neurotoxin. ? exacerbation?

1.1.10 Glutamate excitotoxicity and MPTP-induced neurotoxicity.

A new line of inquiry has suggested a role for *N*-methyl-*D*-aspartate (NMDA) receptors in MPTP-induced neurotoxicity *in vivo*, as part of an energy-linked excitotoxic hypothesis. Excitotoxicity is a receptor-mediated event involving glutamate. Excessive stimulation of glutamate receptors causes aberrant influx of extracellular calcium; the increase in cytoplasmic calcium can potentially activate a number of calcium dependent enzymes as well as increase nitric oxide formation and subsequently oxidative stress. This aberrant influx of calcium can therefore lead to cell death through a number of different pathways. Glutamate excitotoxicity linked to MPTP was first proposed when the use of NMDA antagonists provided significant protection against MPP⁺ neurotoxicity in animals (Turski *et al.*, 1991). However, the ability of NMDA antagonists to alleviate MPTP-induced neurotoxic effects is variable (Akaneya *et al.*, 1995; Camins *et al.*, 1997).

The role of the glutamatergic system in MPTP neurotoxicity is still not fully understood. MPP⁺ has been shown not to interact directly with NMDA receptors (Sundstrom and Mo, 1995), and therefore activation is thought to occur through energy deprivation suggesting an energy-excitotoxicity link (or indirect excitotoxicity). Indeed, Greenamyre (1998) has proposed a mechanism by which glutamate may

exasperate MPTP neurotoxicity. A reduction in ATP levels due to MPP^+ would result in a consequent reduction in Na^+/K^+ ATPase activity, leading to partial depolarisation of the neurone. This would relieve the voltage dependent magnesium block of the NMDA receptor causing the neurone to be overexcited by endogenous glutamate concentrations. This would allow aberrant calcium influx, disrupting cell homeostasis, whereupon cell death could proceed through a variety of mechanisms.

Most recently, glial cells have been implicated in providing a potential aberrant source of glutamate following neurotoxic exposure, *in vivo*. MPTP can evoke the release of glutathione from glia whose subsequent extracellular hydrolysis can provide a substantial pool of glutamate that could be detrimental to dopaminergic neurones via NMDA-receptor mediated excitotoxicity (Han *et al.*, 1999).

The primary neurotoxic mechanism and effect of MPTP is still debatable but it is becoming increasingly evident that the neurotoxin may exert its neurodegenerative effect via a combination of independent and linked events.

1.2 Monoamine oxidase (MAO)

1.2.1 General properties

Monoamine oxidase (amine:oxygen oxidoreductase deaminating flavin containing E.C.1.4.3.4.) was first extracted and characterised from rabbit tissue extracts by Hare in 1928, who initially termed the enzyme tyramine oxidase (Hare, 1928). The characterisation of similar enzymes by others prompted Blaschko and co-workers to demonstrate that all the proposed enzymes were in fact the same and introduced the term amine oxidase (Blaschko *et al.*, 1937). This was later modified to monoamine oxidase to reflect more accurately its substrate selectivity.

The substrate selectivity of MAO is relatively wide compared to other enzymes. In general all primary, secondary and tertiary monoamines in which the amine is attached to a free hydrocarbon chain and compounds containing an aromatic nucleus or an ethylamine side chain, can act as substrates. In addition, the dopaminergic neurotoxin MPTP (a tertiary cyclic allylamine) is an excellent substrate for MAO. The

net reaction catalysed by MAO can be described using a simplified equation (see Fig. 1.3).

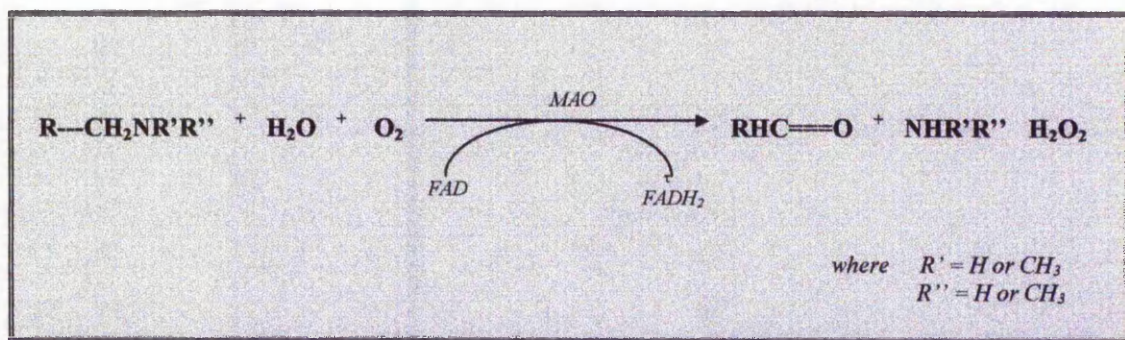


Figure 1.3 Simplified reaction catalysed by monoamine oxidase.

MAO is extensively distributed in the central nervous system and in peripheral tissues and plays an important role in the biological inactivation of a wide variety of biogenic amines. In the central nervous system MAO is the principle enzyme involved in the degradation, via deamination, of the catecholamine and indoleamine neurotransmitters to their corresponding aldehydes.

1.2.2 MAO structure

Two forms of the enzyme exist termed MAO-A and MAO-B, which were identified on the basis of the differences in molecular weight, substrate affinities, inhibitor sensitivities, and immunological properties (see section 1.2.3). The enzyme was initially shown to exhibit a total molecular weight of approximately 120 kDa containing two subunits with apparent molecular weight of 55-60 kDa, based on SDS-PAGE analysis (Minamiura and Yasunobu, 1978). In addition, it was originally estimated to contain one flavin adenine dinucleotide (FAD) as a prosthetic group. However, further studies using improved MAO purification methods, quantitative amino acid analysis and dithionite flavin titration showed a ratio of one FAD per 63 kDa and 57 kDa subunits for human MAO-A and MAO-B, respectively (Weyler, 1989). It was therefore concluded that MAO possessed one FAD per subunit or two per MAO protomer.

It appears that the FAD cofactor binds to a cysteine residue of the pentapeptide sequence; Ser-Gly-Gly-Cys-Tyr, with the attachment being via the $\delta\alpha$ CH₂ grouping of FAD (Kearney *et al.*, 1971). This sequence is identical in both isoforms as determined by peptide sequence studies with chymotrypsin and trypsin (Kearney *et al.*, 1971; Yu, 1981) and is required for normal enzyme activity.

1.2.3 Isozyme classification

Early studies initially suggested that MAO was a single enzyme with broad specificity. The possibility of more than one form of MAO was originally suggested in the early 1960s but was not conclusively demonstrated until 1968 (Johnston, 1968). Initially, MAO-A was shown to preferentially deaminate 5-hydroxytryptamine (serotonin), norepinephrine, and epinephrine (Table 1.1) and to be sensitive to inhibition by clorgyline (MAO-A inhibitor) (Johnston, 1968). MAO-B was later shown to preferentially deaminate β -phenylethylamine and benzylamine (Table 1.1) and to be sensitive to inhibition by deprenyl (MAO-B inhibitor) (Knoll and Magyar, 1972). However, no compound has yet been identified which shows absolute isozyme specificity. As such the aforementioned compounds (substrates and inhibitors) will interact with both forms of MAO under favourable conditions (i.e. concentration, affinity, turnover rate of substrate) (Berry *et al.*, 1994).

To establish protein uniformity and distribution the need to distinguish MAO-A and MAO-B proteins was achieved by immunological studies (Denny *et al.*, 1982; Levitt *et al.*, 1982). Differences in isotype structure were further supported by studies using partial proteolysis and peptide mapping. The two forms of MAO produced significantly different digestion maps indicating dissimilar proteolytic cleavage sites. (Cawthorn and Breakefield, 1979). Taken together, the above work provided supportive evidence for the presence and structural uniqueness of two forms of MAO.

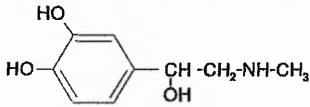
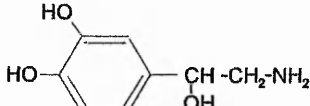
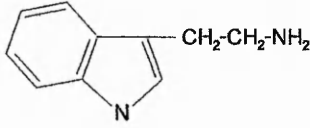
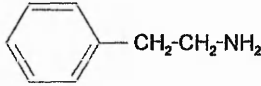
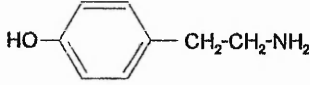
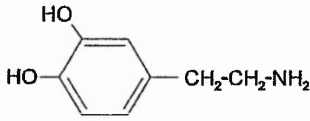
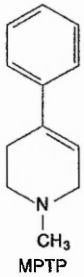
Substrates	Structure	A	B
Adrenaline (Epinephrine)		+	
Noradrenaline (Norepinephrine)		+	
Serotonin (5-hydroxytryptamine)		+	
Phenylethylamine			+
Tyramine		+	+
Dopamine		+	+
MPTP		+	+

Table 1.1 *Substrates of MAO-A and MAO-B.*

1.2.4 Genetic studies

In more recent years molecular biological techniques have confirmed that the two forms of MAO are indeed distinct proteins with differing primary amino acid

sequences, the products of separate genes. The genes for MAO-A and MAO-B were initially located on the X-chromosome (Kochersperger *et al.*, 1986) prior to specifically mapping them to the p11.23 region on the human X-chromosome (Lan *et al.*, 1989). In humans each gene has been shown to span at least 60 kb on the X-chromosome and contain 15 exons interrupted by 14 introns, with both isoforms exhibiting identical exon-intron organisation (Grimsby *et al.*, 1991). However, there are specific differences in the promoter region organisation for both MAO-A and MAO-B; a factor that may correspond to their different cell and tissue specific expression (Shih *et al.*, 1994).

Comparison of the deduced amino acid sequences of human liver MAO-A and MAO-B enzymes revealed that MAO-A consisted of 527 amino acids and MAO-B of 520 amino acids. Thus the subunit molecular weight was calculated to be 59,700 (MAO-A) and 58,800 (MAO-B) (Bach *et al.*, 1988), confirming the predictions of earlier work using SDS-PAGE analysis (Minamiura and Yasunobu, 1978). The amino acid sequence of MAO isoforms have now also been identified in several other species, e.g. rat and bovine (Ito *et al.*, 1988; Powell *et al.*, 1989), with a high degree of homology (approximately 70 %) existing between the amino acid sequences of A and B within a particular species (Bach *et al.*, 1988; Kwan and Abell, 1992). This may suggest that the two isoforms were originally derived from a common progenitor gene. A similar degree of amino acid homology has also been reported between the same isoforms of MAO in different species (Bach *et al.*, 1988; Powell *et al.*, 1989). However, more recently it has been suggested that MAO-A exhibits a greater sequence homology (approximately 85%) between species than does MAO-B (Kwan and Abell, 1992).

1.2.5 MAO location and distribution

1.2.5.1 Tissue distribution

In mammals, MAO has been found in all cell types with the exception of erythrocytes (see Berry *et al.*, 1994 for review). In the majority of tissues MAO-A and MAO-B appear to coexist with particularly rich sources occurring in the liver, skeletal

muscle, kidney, lung and brain. The brain is considered to exhibit a rich source of MAO, however, reports of relative abundance within the brain are variable. For example early reports suggested twice as much MAO-B as MAO-A (Fowler *et al.*, 1980). This relative abundance was questioned by other workers who reported a 4:1 distribution of MAO-B over MAO-A (Youdim and Finberg, 1991). However, the general consensus estimates a 2-4 fold greater abundance of MAO-B than MAO-A to be present within the brain (Berry *et al.*, 1994).

1.2.5.2 Cellular distribution of MAO within the substantia nigra.

The substantia nigra pars compacta, an area of the brain that is significantly affected in both Parkinson's disease and MPTP-induced parkinsonism, is generally populated by dopaminergic neurones and glial cells. Reports of distribution and quantification of MAO isoforms within these specific cell populations have produced variable results. Workers employing histochemical and immunochemical techniques, have demonstrated both the A and B forms of MAO to be present in glial cells (Konradi *et al.*, 1988; Westlund *et al.*, 1988), with histochemical analysis suggesting a predominance of MAO-B (Konradi *et al.*, 1989). In conjunction, dopaminergic neurones exhibited the absence of both forms of MAO (Konradi *et al.*, 1988; Konradi *et al.*, 1989). In contrast, work carried out using immunofluorescence cytochemistry and immunochemical methods, have reported the sole presence of very low levels of MAO-A (Moll *et al.*, 1988; Westlund *et al.*, 1988). In addition, the presence of MAO-B has been reported in a small sub-population of dopaminergic neurones from the dorsal portion of the substantia nigra (Damier *et al.*, 1996). The reported presence of MAO, especially MAO-B, within dopaminergic cells of the substantia nigra has been suggested has a possible contributory factor in their susceptibility to degeneration in PD. However, Damier *et al* (1996) has reported no significant difference in the number of MAO-B containing neurones in Parkinson disease midbrains compared to controls, suggesting that MAO-B in dopaminergic neurones does not directly contribute to vulnerability.

1.2.5.3 Sub-cellular location of MAO.

Both MAO-A and MAO-B are mitochondrial enzymes specifically associated with the outer mitochondrial membrane. However, the exact mechanism by which the protein is inserted into the outer mitochondrial membrane is not fully understood. It has been shown that MAO is synthesised by cytoplasmic polysomes prior to transportation to the mitochondrial membrane. However, since MAO is not synthesised as a pro-protein no cleavage residue that can act as a targeting sequence is present. It would therefore appear that a targeting sequence within the primary structure of the protein exists and would probably appear in a highly conserved region between MAO-A and B (Berry *et al.*, 1994).

1.2.6 MPTP as a substrate for MAO

Many other amines, in addition to biogenic amines, can serve as substrates for MAO. It was discovered that the dopaminergic neurotoxin MPTP (that causes parkinsonian symptoms in humans) is also an excellent substrate for MAO. The enzyme mediates the conversion of MPTP to a dihydropyridinium intermediate, which then spontaneously disproportionates to MPP^+ ion which is deleterious to dopaminergic neurones of the substantia nigra (see section 1.1.6).

The structure of MPTP, a tertiary allyamine, departs from the endogenous substrates for MAO in that the carbon-nitrogen bond oxidised is part of a six membered ring system that forms a relatively stable imine after oxidation. Contrary to initial thoughts, both MAO-A and MAO-B were shown to catalyse the oxidation of MPTP at substantial rates with MAO-B exhibiting a turnover number that is approximately 14 times greater than MAO-A (Salach *et al.*, 1984). Catalysis of MPTP by MAO-A was shown to express a K_m value of 0.14 mM and MAO-B a K_m value of 0.30 mM, both values comparable with K_m values of selective preferred substrates (e.g. kynuramine and benzylamine; MAO-A and B, respectively) (Salach *et al.*, 1984). In comparison, a V_{max}/K_m ratio of 143 and 523 for MAO-A and MAO-B, respectively, confirms the appreciable oxidation of MPTP by MAO-A (Yasuhara *et al.*, 1993).

Interestingly, it has been reported that the oxidation of MPTP by both forms of MAO is accompanied by progressive inhibition of both enzymes (Singer *et al.*, 1985). Thus it is therefore proposed that MPTP, MPDP⁺ and MPP⁺ can act as inhibitors of both MAO-A and MAO-B, with the B isoform expressing increased sensitivity to substrate inhibition, and the A isoform exhibiting sensitivity to product inhibition (Singer *et al.*, 1985).

1.2.7 MAO inhibitors

A number of MAO inhibitors were discovered in the 1960's which have helped to elucidate the mechanism and biochemical properties of MAO. However, their potential for use in clinical pharmacology was regarded as highly hazardous for several years due to their ability to potentiate the "tyramine pressor effect", which can sometimes cause fatal hypertensive reactions.

The emergence of two specific MAO inhibitors namely clorgyline (Johnston, 1968) and deprenyl (Knoll and Magyar, 1972), whose ability to specifically inhibit and thereby distinguish MAO-A and MAO-B, has provided the necessary chemical tools for the past few decades of research into MAO, MPTP toxicity and parkinsonism (see Fig. 1.4 for structures).

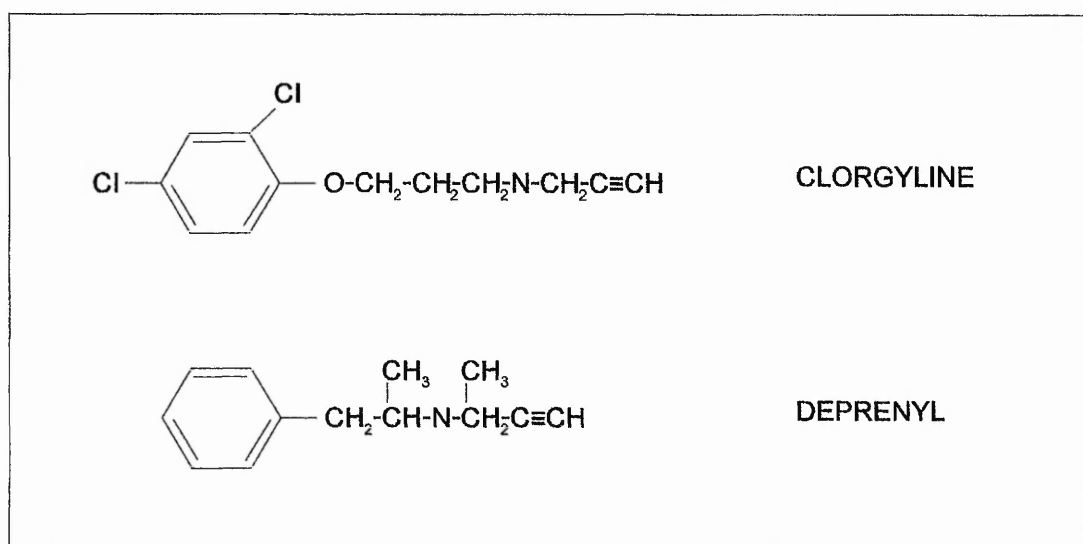


Figure 1.4 Chemical structure of MAO inhibitors clorgyline and deprenyl.

1.2.7.1 Clorgyline

Clorgyline was initially described by Johnston (1968) as a selective acetylenic inhibitor of MAO-A. This original classification has remained the basis for all studies carried out on MAO and was responsible for the identification of deprenyl as the selective inhibitor of the B isoform. Clorgyline belongs to the class of irreversible inhibitors also known as mechanism based or 'suicide inhibitors'. Clorgyline therefore binds to the active site of MAO to initiate inhibition. Due to its mode of inhibition *de novo* protein synthesis is required to alleviate the *in vivo* effects of clorgyline. Investigation of the behaviour of clorgyline has shown that its selectivity for MAO-A arises from the fact that it binds to this isoform with approximately 1000 times greater affinity than for the B-form (Fowler *et al.*, 1982). Therefore although termed a specific MAO-A inhibitor it can also inhibit MAO-B, albeit less efficiently. The use of clorgyline in clinical pharmacology is restricted to psychiatric therapy relating to its anti-depressant capacity. However, due to its irreversible inhibitor nature it can enhance a patients liability to tyramine related hypertension. Clorgyline has limited use in the treatment of PD. Indeed, it is unable to substantially inhibit MPTP-induced neurotoxicity *in vivo* (Heikkila *et al.*, 1984b), possibly relating to the MAO-B content of glial cells. In contrast, clorgyline is able to alleviate MPTP toxicity in *in vitro* studies through the use of homogenous cell populations (Buckman, 1991; Lai *et al.*, 1993).

1.2.7.2 Deprenyl

Deprenyl was originally synthesised as the D,L-racemic mixture by Knoll and co-workers (1965), who discovered that the L-isomer exhibited significantly more MAO inhibitory activity than the D-isomer and therefore became the compound of choice. Its ability to selectively inhibit MAO-B irreversibly (Knoll and Magyar, 1972) in the absence of the tyramine pressor effect heralded it as a pharmacological compound with a bright future.

Deprenyl is an enzyme-activated irreversible acetylenic inhibitor whose selectivity, like clorgyline, arises from a combination of greater affinity and greater

reactivity in combination with the B- isoform. In a first reversible step, deprenyl forms a non-covalent complex with the enzyme. Subsequent reaction of the inhibitor with MAO leads to a reduction of the enzyme bound FAD and simultaneous oxidation of deprenyl. This compound then forms a covalent bond with FAD at the N-5 position causing irreversible inhibition.

The inhibitor gained wide clinical acceptance following work carried out by Birkmayer who first suggested its usefulness in the treatment of PD. The subsequent long term clinical study (Birkmayer *et al.*, 1985) established deprenyl as the current mainstay of treatment of PD, in which it is used as a therapeutic adjunct to L-dopa therapy. In contrast to clorgyline, deprenyl is able to alleviate MPTP-induced neurotoxicity in both *in vivo* and *in vitro* models (Heikkila *et al.*, 1984b; Buckman, 1991; Lai *et al.*, 1993)

1.3 The neuronal cytoskeleton.

1.3.1 Components of the neuronal cytoskeleton.

The cytoskeleton plays a central role in the majority of cellular processes. Not only does it provide a dynamic 'skeleton' for cells, but also mediates organelle transport, mitosis, cytokinesis, secretion, cell polarity development, and the formation of cellular extensions. The neuronal cytoskeleton is therefore regarded as integral to the correct function of neurones. The neuronal cytoskeleton consists of a highly cross-linked network of microtubules, microfilaments, NFs and other specific associated proteins that govern the internal architecture and cellular processes of these cells. Interestingly, these components are capable of dramatic change in response to experimental injury and undergo significant modifications during the process of neuronal development and neuronal cell death. It is now recognised that modifications to cytoskeletal proteins are associated with a range of neurodegenerative conditions such as Alzheimer's disease and Parkinson's disease (Doering, 1993). Clearly, since the cytoskeleton is associated with numerous cellular processes it could represent a major target for neurotoxins associated with neurodegenerative disease. Of interest to

the work in this thesis are the potential changes to microtubules, microfilaments and NFs, the biochemical properties of which are described below.

1.3.1.1 Microtubules

Microtubules are hollow cylindrical organelles with an external diameter of approximately 25 nm. They are assembled primarily from heterodimers of α - and β -tubulin, in a process requiring GTP and a host of microtubule associated proteins or MAPs. Microtubules are comprised of 13 longitudinal protofilaments which express polarity, so that *in vitro* the two ends of a microtubule display different kinetics of subunit addition and loss. Thus, polymerisation proceeds by the net addition of tubulin subunits at the fast growing or plus ends of microtubules until a steady state is reached where the net tubulin association at the plus ends is equal to the net loss of subunits at the minus ends (Hargreaves, 1997). However, even in their steady state microtubules remain very dynamic whereby polymer mass remains constant but there can be drastic fluctuations in the length of individual microtubules; a phenomenon known as dynamic instability (Hargreaves, 1997).

Microtubules in association with microfilaments and neurofilaments have been implicated in many neuronal functions. These functions include cell division, transport of cytoplasmic components, maintenance of neuronal morphology, and growth of axons and dendrites. Microtubules in the axon are all orientated with the plus end toward the axon tip while microtubules in dendrites are thought to be of a mixed polarity orientation (Baas *et al.*, 1988). Immunofluorescence microscopy shows that during the time of axon outgrowth microtubules converge into growing processes forming dense bundles in the core of the axon (Marchisio *et al.*, 1978). This therefore provides a means for the selective bi-directional transport of components into axons or dendrites.

Tubulin, the major subunit component of microtubules, is a highly conserved acidic protein which is encoded by a multigene family. Tubulin isotypes fall into two main classes, α - and β -tubulin, each of which has an apparent molecular mass of approximately 55 kDa. The α/β heterodimer is the effective microtubule forming subunit which binds two molecules of GTP, one of which binds to α -tubulin the other

reversibly to β -tubulin and is hydrolysed during microtubule assembly. Tubulin can be post-translationally modified by phosphorylation, acetylation, tyrosination and glutamylation, alterations of which are involved in microtubule assembly and stability. The synthesis of tubulin is auto-regulated by the pool of unpolymerised tubulin; when microtubule assembly lowers this pool, tubulin synthesis is increased and vice versa.

1.3.1.2 Microfilaments

Microfilaments are composed of the protein actin, a highly conserved protein in all eukaryotic cells with a molecular mass of 42 kDa. Actin has a bi-lobal structure and is arranged helically during polymerisation with the resultant filament (F-actin) expressing an outer diameter of 5-7 nm (Hargreaves, 1997). Although actin is a major tissue protein, particularly abundant in muscle where it forms stable filaments that play a central role in muscle contraction, it also forms labile microfilaments in non-muscle cells. Here it is present in dynamic equilibrium in a range of other structures such as stress fibres, lamellipodia, filopodia and other networks and arrays, helping to regulate cellular morphology, anchorage and polarity.

F-actin formation itself occurs by a nucleated condensation mechanism in which polymerisation occurs (as in the case of tubulin assembly) by the net addition of monomeric actin subunits (G-actin) at the plus end of F-actin filaments. During the process of axon outgrowth actin is predominantly located at the cell periphery both in cell bodies and in cell processes. It appears to be present in areas of high surface motility and is especially abundant at the tip of the growth cone (Marchisio *et al.*, 1978). Indeed, actin based mechanisms probably underlie the marked motility and plasticity of the growth terminal.

1.3.1.3 Neurofilaments (NFs)

NFs belong to the intermediate family of polypeptides, all of which consist of filaments of about 10 nm in diameter as visualised by electron microscopy. In the mid-1970s, studies of axonal transport defined three proteins of apparent molecular weight of 200, 145 and 68 kDa, as determined by sodium dodecyl sulphate polyacrylamide gel

electrophoresis (SDS-PAGE). These were identified as subunits of NFs and were named the neurofilament triplet proteins (Hoffman and Lasek, 1975). They are now commonly referred to as NF-H, NF-M, and NF-L indicating high, middle and low apparent molecular weights, respectively. However, the apparent molecular weights for NF-H, NF-M and NF-L are considered gross overestimates versus the true chemical values of approximately 112 kDa, 102 kDa and 60 kDa, respectively (Lees *et al.*, 1988).

The NF subunits, like all intermediate filaments, have evolved from a common ancestral gene and therefore contain a highly conserved structure and sequence (Fig. 1.5). For example, all consist of a globular amino-terminal "head" domain, an α -helical rod domain, and a further globular carboxy-terminal "tail" domain (Geisler *et al.*, 1983). The central rod domain, consisting of 310 amino acid residues, remains constant between family members, so that the differences in molecular weight are mainly due to the variability in size of the head and tail domains (Shaw, 1991). In association, unique distinguishable sequences are located towards the C-terminal end of the protein containing the E segment and KSP regions (see Fig. 5). This central rod domain incorporates a heptad repeat of hydrophobic amino acids at positions 1, 4, and 7 repetitively along the sequence. The heptad pattern produces a helical strip of hydrophobic amino acids along the side of each α -helix, which can intercalate with hydrophobic amino acids on another similar α -helix to form a stable coiled-coil dimer. This is believed to be the first step in the formation of 10 nm filaments, which sees a dimer interacting with another dimer to produce an anti-parallel tetramer. This structure then interacts with other tetramers to build up a 10 nm filament (Geisler *et al.*, 1985).

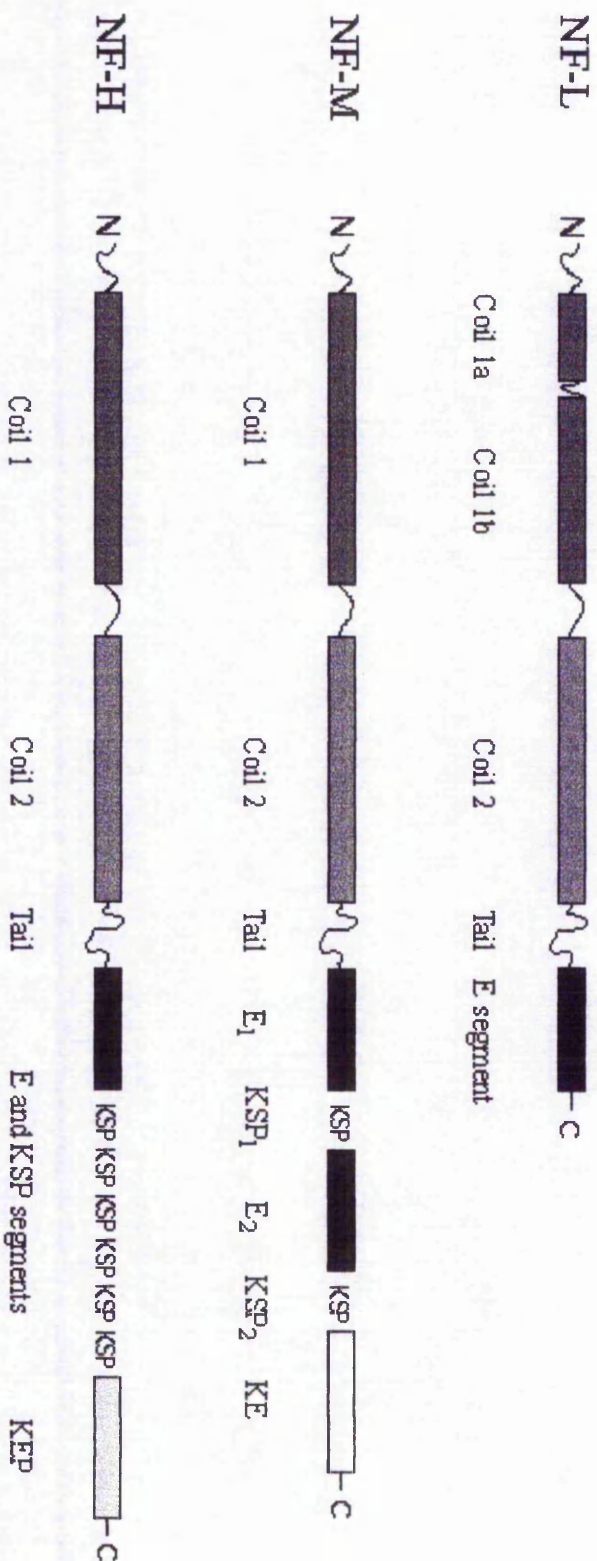


Figure 1.5 Diagrammatic representation of the sequence and basic structure of mammalian neurofilament subunits.

NF subunits are characterised by two large α -helical domains termed coil 1 and coil 2 (or coil 1a, 1b and 2 in the case of NF-L) containing heptad repeats of hydrophobic amino acids. These coils are separated by non-helical linkers. All three subunits contain a tail region which is followed by an E segment(s), containing sequences rich in glutamic acid. In NF-M and NF-H these are followed by KSP regions, sequences with variable numbers of lysine-serine-proline repeats which can be phosphorylated. There are two distinct sets of KSP regions in NF-M, separated by a further glutamic acid rich sequence, E₂. The carboxyterminus of NF-M is characterised by a KE domain due to the high content of lysine and glutamic acid. In NF-H the number of KSP containing sequences is vastly increased compared to NF-M, correlating to the ability of NF-H to be phosphorylated. The carboxyterminus of NF-H is rich in lysine, glutamic acid and proline and therefore termed the KEP segment, sequences involved in NF and non NF binding interactions.

1.3.1.4 Neurofilament phosphorylation

The carboxy-terminal tail domains of NFs are unique among intermediate filament proteins. Mammalian NF-M and particularly NF-H contain numerous serine residues that present themselves in a recurring lysine-serine-proline (KSP) motif which acts as a substrate for phosphorylation (Julien and Mushynski, 1983). More recent studies have shown NF-protein subunits can be phosphorylated at both the amino-terminal head domain and carboxy-terminal tails by different protein kinases (Nixon and Sihag, 1991). The fact that these subunits can be extensively phosphorylated has a marked effect on their mobility in SDS-PAGE resulting in their apparent increased molecular weight. Extensive phosphorylation of these NF subunits generates a host of micro-heterogenous isoforms (Carden *et al.*, 1987), whereupon it has been suggested that phosphorylation may mediate the interaction of NFs with each other and with other cytoskeletal constituents.

The site specific phosphorylation or dephosphorylation within the domains of each NF subunit is thought to regulate their assembly, axonal transport, and interactions with other cytoskeletal proteins (Nixon, 1993). The extensive phosphorylation of these domains, thought to project outward from the filament core, is considered as a mechanism by which neurofilaments cross-link with each other and with cytoplasmic organelles, thereby helping stabilise the axonal cytoskeleton (Carden *et al.*, 1985; Nixon, 1993; Shea and Beermann, 1994). Immunological studies have shown that NF-M and, particularly NF-H, become heavily phosphorylated in axons *in vivo*, but that the level of phosphorylation of these proteins is lower in cell bodies and short dendrites (Sternberger and Sternberger, 1983).

Studies of expression of neurofilament proteins have produced contradictions in the past, but the general consensus is that a hierarchical expression of neurofilament protein accompanies neuronal differentiation and neurite outgrowth, where neurofilaments undergo a series of progressive stabilising events. Initial expression of NFs in developing brain involves only NF-L and NF-M, whereas the appearance of NF-H is delayed (Carden *et al.*, 1987). Extensive phosphorylation of NF-H, which is associated with cytoskeletal stabilisation, is further delayed (Shea *et al.*, 1989).

Work carried out by Shea and co-workers using cultured neuronal cells, to study the dynamics of NF phosphorylation and assembly, has challenged the traditional view that assembly precedes NF phosphorylation. The differentiation of NB2a/d1 cells with dbcAMP causes the elaboration of axonal neurites and incorporation of NF subunits into the Triton-insoluble cytoskeleton (Shea *et al.*, 1990). In addition these cells contain substantial Triton-soluble pools of NF subunits, which incorporate modified isoforms of NF-H including extensively phosphorylated isoforms of NF-M and NF-H, prior to the extension of axonal neurites (Shea *et al.*, 1989, 1990; Shea, 1995). It is therefore proposed that NF phosphorylation and assembly represent separable processes (Shea *et al.*, 1990). Furthermore, it has been shown that the necessary kinases to effect extensive NF subunit phosphorylation are also present in the cell body. Thus leading to the suggestion that it is the residence time of a given subunit within the perikarya that determines whether or not it will undergo extensive phosphorylation, prior to axonal transport and assembly (Shea, 1995). These lines of reasoning are further supported by the transient observation of high levels of extensively phosphorylated NF-H in neuronal perikarya during early postnatal development in mice (Shea, 1995). The transient presence of large quantities of unassembled NF-H during development may, by incorporating into existing NFs, facilitate the timely stabilisation of the axonal cytoskeleton. Its continued presence at lower levels in more mature cells may support continued exchange of NF-H subunits with existing NFs (Shea and Beermann, 1994).

1.3.2 The cytoskeleton and axonal growth.

The formation of the axonal cytoskeleton at distances from the site of protein synthesis in the neuronal cell body/perikayon depends on the delivery of cytoskeletal components by slow axonal transport. The issue of whether microtubule proteins are transported as subunits or polymers remains controversial. In general, it is considered that microtubules form within growing axons largely by local subunit assembly (Nixon, 1998). Less clear is the source of the tubulin subunits used in this local assembly which originate either from free subunits transported along the axon or from

the disassembly of microtubule polymers transported into the axon (Fig 1.6) (Baas, 1997).

Radiolabel studies using ^{35}S -methionine suggests actin is generally transported in unassembled monomeric form and incorporates into the pre-existing stationary microfilament network along the axon (Nixon, 1998). The favoured hypotheses for neurofilament transport is that neurofilaments are transported as oligomers/polymers along axons where they are incorporated into existing neurofilament structures to maintain neurofilament integrity or help extend filament length. However, polymer transport is not the whole story and the early notion of neurofilaments as irreversible polymers is now being reconsidered. The key to this process is the phosphorylation events; cycles of phosphorylation and dephosphorylation involved in modulating transport, incorporation and stabilisation (Fig 1.7).

It is increasingly evident that axonal cytoskeleton is an orderly but dynamic structure that is regulated by a complex interactiveness involving regulation of subunits or polymers into the network, turnover of the network or transported elements and cross-bridging of polymers. These processes are modulated by a number of post-translational events of which phosphorylation is a major player.

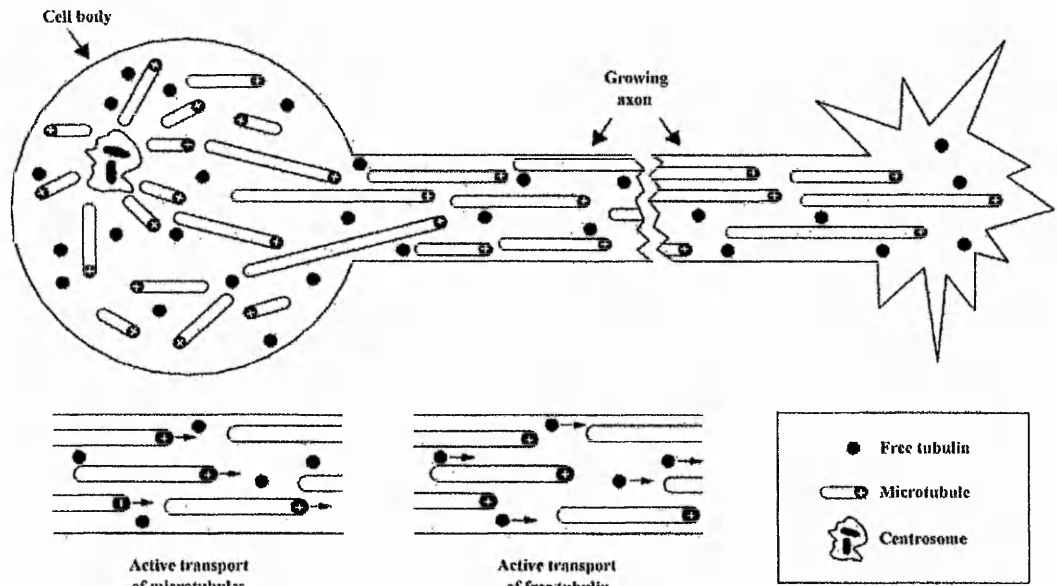


Figure 1.6 Two models for elaborating the axonal microtubule array.

Top: general schematic diagram of the microtubule array within the neuronal cell body and growing axon. Microtubules splay in many directions within the cell body, but are orientated with their plus ends distal to the cell body within the axon. The centrosome is capable of nucleating and releasing microtubules. A pool of free tubulin is present throughout the cell body and axon, and exchanges subunits with the microtubules. *Bottom:* two different models propose the possible form tubulin is actively transported down the axon. One model suggests that microtubules themselves are actively transported (plus ends leading), whereas the other model contends that free tubulin subunits (or small oligomers) are actively transported.

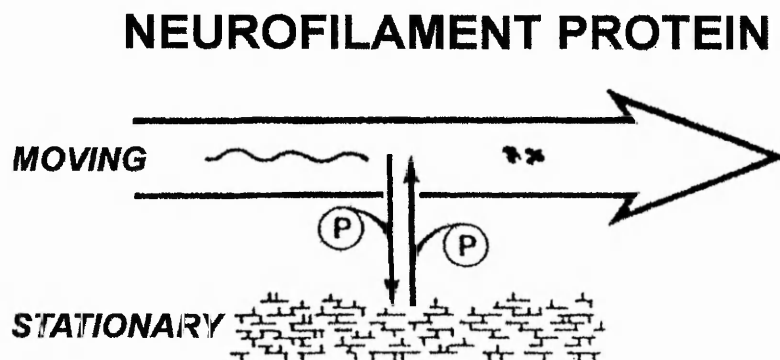


Figure 1.7 Transport and dynamics of neurofilament transport in axons.

Soon after synthesis NF protein attains an insoluble polymeric or oligomeric form and moves down the axon in equilibrium with a much slower moving or stationary pool of polymer. The transition between the moving and stationary pool may be governed by the phosphorylation state of NF protein; phosphate turnover on NF protein suggests that the process can be reversible. Work carried out by Shea *et al.*, 1990 also proposes the presence of assembly competent, soluble phosphorylated isoforms of NFs within the cell perikaryon.

1.4 Components of Lewy bodies.

Several degenerative diseases are characterised by the formation of abnormal structures within cells given the general term inclusion bodies. Within PD these inclusions are found in neuronal cells or neuronal cell processes of the substantia nigra and are termed Lewy bodies. Immunohistochemical techniques using antibodies raised to specific neurofilament polypeptides have demonstrated the inclusions to be based on aggregates of associated filaments (Forno *et al.*, 1983; Goldman *et al.*, 1983). Indeed, Lewy bodies exhibit immunohistochemical reactivity with a number of cytoskeletal proteins including tubulin, phosphorylated NFs and hyper-phosphorylated tau, to a lesser extent (Goldman *et al.*, 1983; Armstrong *et al.*, 1998). In addition, these abnormal inclusions show a high degree of ubiquitin and α -synuclein reactivity (Armstrong *et al.*, 1998). The presence of immunoreactive Lewy bodies within the substantia nigra are considered to be a pathological hallmark of idiopathic PD (Gibb and Lees, 1988). However, the absence of convincing Lewy body inclusions induced by MPTP remains a main criticism of MPTP-induced Parkinsonism model, although locus coeruleus lesions and eosinophilic inclusions have been reported in the MPTP-treated monkey (Forno *et al.*, 1986). This probably reflects the importance of concentration used, exposure time and dosing regimen. More recently, abnormal neuronal aggregates exhibiting characteristic epitopes have been reported in MPTP-treated baboons (Kowall *et al.*, 2000).

1.4.1 Ubiquitin

Ubiquitin is a 76-residue protein that exists in cells either free or covalently linked to other proteins. An initial insight into the role played by ubiquitin was demonstrated by Hershko and co-workers who identified ubiquitin as an essential component of the ATP-dependent proteolytic system (Hershko and Ciechanover, 1982). Indeed, ubiquitin initiates intracellular proteolysis through its ability to conjugate to abnormal or denatured proteins thereby "marking" them for degradation by the 26S proteasome - an ATP-dependent multisubunit protease. A highly sophisticated system sees a cascade of multi-ubiquitin chains conjugate to proteins

bearing degradation signals, thereby selectively destroying aberrant subunits. The degradation signal of a protein is related to the identity of a protein's N-terminal residue - a relation termed the N-end rule. Ubiquitin-dependent pathways have since been shown to play major roles in a host of biological processes, including cell differentiation, the cell cycle and stress responses (see review, Varshevsky, 1997).

Ubiquitin is also important in the development of the mammalian brain in the process of cell differentiation. Changes in ubiquitin immunoreactivity have been observed in the developing rat brain, where a decrease in the level of high molecular weight ubiquitin conjugates was observed in cell-soluble, mitochondrial and detergent-insoluble cytoskeletal fractions, likely due to tight protein regulation during development (Flann *et al.*, 1997). Changes in ubiquitin immunoreactivity following cell differentiation has also been confirmed in soluble and insoluble cytoplasmic extracts of PC12 cells following nerve growth factor-induced differentiation. Although no significant change in multi-ubiquitin chains was observed in urea-soluble cytoskeletal extracts, an increase in ubiquitination of nuclear proteins with a concomitant decrease in free ubiquitin was reported (OhtaniKaneko *et al.*, 1996), suggesting nuclear protein degradation following differentiation. Similarly, investigation of the levels and subcellular distribution of ubiquitin in neuroblastoma cell differentiation suggests that higher levels of cytoplasmic ubiquitin are needed during cAMP-induced differentiation (LaRosa *et al.* 1996), relating to the removal of proteins responsible for cell proliferation.

Since antibodies to ubiquitin react strongly with Lewy body inclusions (Lowe *et al.*, 1988) it suggests the cell has marked the accumulated abnormal or damaged proteins for degradation. However, the failure of the cell to effectively carry out the degradative process results in the observed accumulation and ubiquitin immunoreactivity characteristic of Lewy bodies.

1.4.2 Synuclein

Synuclein proteins are a class of highly conserved proteins predominantly expressed in the nervous system. Three different synuclein protein members have been identified all of which have a highly conserved amino-terminal repeat region, a

hydrophobic mid section, and a less conserved carboxyl terminal region. However, the exact function of synuclein in neuronal cells is unresolved. Although the proteins undergo post-translational modification, the exact modifications and their significance is not clear. Human α -synuclein and β -synuclein are 140 and 134 amino acid proteins, respectively, which have been found concentrated in presynaptic nerve terminals (Jakes *et al.*, 1994). Indeed, α -Synuclein was first identified in electric fish and named in recognition of its apparent localisation in presynaptic nerve terminals (Maroteaux *et al.*, 1988).

Recently, mutations in the α -synuclein gene have been reported in families susceptible to an inherited form of Parkinson's disease (Polymeropoulos *et al.*, 1996). In conjunction, α -synuclein has been shown to be a major component of Lewy bodies from idiopathic Parkinson's disease (Spillantini *et al.*, 1997). Thus it has been proposed that a mutation in the synuclein gene may promote the aggregation of α -synuclein into filaments (Spillantini *et al.*, 1997). This hypothesis is supported by work carried out by ElAgnaf *et al.* (1998) who have shown that human wild-type and mutant α -synuclein proteins can self-aggregate and form cytotoxic amyloid-like filaments inducing apoptosis in human neuroblastoma cells.

The use of chronic MPTP-mouse models *in vivo*, shows the expression of α -synuclein mRNA and protein to be increased following MPTP exposure (Jackson-Lewis *et al.*, 1998), suggesting the alterations induced by the toxin resembling the pathological process. It is therefore thought that targeting this protein for pharmacological intervention could modulate MPTP neurotoxicity and consequently PD.

1.5 Neurotrophic Factors.

It has long been known that glial cells can release factors into culture medium that are able to induce a significant degree of morphological differentiation when added to neuroblastoma cells in culture (Monard *et al.*, 1973; Shea and Husain, 1996). These factors are members of the neurotrophic factor family, a subclass of the large growth factor family. In general, these endogenous soluble proteins, with molecular weights between 13-24 kDa, are often active as homodimers. They are thought to

regulate the development, maintenance and survival of neurones, *in vivo*, in target derived, autocrine or paracrine fashion via cell surface receptors. The binding of these factors to receptors leads to a complicated cascade of reactions within the cell leading to intracellular molecular changes which then have a profound impact on cell development and survival. It is therefore thought that these factors may have beneficial effects in the treatment of neurodegenerative diseases.

1.5.1 Glial Derived Neurotrophic Factor (GDNF).

One such specific factor associated with astroglial cells is GDNF. GDNF is described as a distant member of the transforming growth factor β (TGF- β) superfamily isolated from the rat glial cell line, B49. It was initially characterised through its ability to promote, *in vitro*, the survival and differentiation of dopaminergic neurones from the embryonic midbrain (Lin *et al.*, 1993).

Sequence data suggests that GDNF is synthesised as a precursor that is processed and secreted as a mature disulphide-bonded homodimer of two 134 amino acid subunits (Lin *et al.*, 1993). The biological action of GDNF is thought to be mediated through a glycosylphosphatidylinositol-linked cell surface receptor (GDNFR- α). This receptor specifically binds GDNF; the complex formed then mediates activation of a signalling component, in this case a transmembrane protein termed c-Ret; a tyrosine kinase receptor (Treanor *et al.*, 1996).

Since GDNF was shown to be a neurotrophic factor involved in the survival of dopaminergic cells in culture, it was investigated whether GDNF could affect dopaminergic cell parameters following neurotoxic insult. Its ability to exert protective and regenerative effects *in vivo* was exhibited in the MPTP mouse model (Tomac *et al.*, 1995) where both dopamine levels and tyrosine hydroxylase-immunoreactive dopamine neurones were either maintained or restored, following administration of GDNF, before and after MPTP exposure. Similarly, primate recipients of GDNF exposed to MPTP exhibited significant improvements in behavioural performance in the majority of parameters including rigidity, bradykinesia and posture balance (see Lapchak *et al.*, 1996, review). An *in vitro* study by Hou *et al.* (1996) exposed mesencephalic dopaminergic cells to MPP⁺ and tested the effects of GDNF on cell

survival. They found that after removal of the neurotoxin, GDNF improved the survival of cells, prevented further cell death and stimulated the re-growth of dopaminergic fibres damaged by MPP⁺.

The possibility of a reduced GDNF expression within susceptible brain areas of diseased individuals could indicate the involvement of GDNF in the pathophysiology of PD. *In situ* hybridisation experiments on brain tissue sections of patients with PD along with age matched controls provided no detectable expression in either group of patients, suggesting GDNF expression to be very low in the adult brain and not upregulated under pathological conditions (Hunot *et al.*, 1996). At present, its involvement in the pathophysiology of the disease remains undetermined.

Overall, the results from diverse studies of the effects of GDNF on brain chemistry, behaviour and cell survival support the idea that GDNF may be therapeutically useful in the treatment of PD, slowing the degenerative process involved in the pathology of the disease (Lapchak *et al.*, 1996).

1.6 The use of MPTP in cellular systems for studying the pathogenesis of Parkinson's Disease.

Since the emergence of MPTP in the research field in 1983 the majority of investigators have carried out research to assess its mechanism of action, toxicity, and overall pathophysiology, focusing on the central nervous system of mammalian species *in vivo*. However, within the *in vivo* situation, MPTP exhibits selective differences including species specificity and cell selectivity (see section 1.1.2) for which the reasons are still not entirely understood. The elaborate pathways within the central nervous system and the complexity of cell types present further complicate these selective differences. Although still of paramount importance, animal models of MPTP neurotoxicity require well-characterised and defined parameters for valuable interpretation.

In more recent years the use of cloned cell lines as *in vitro* models have been shown to be very useful tools in deriving the detailed action and effects of many toxic substances. Cellular models present a number of apparent advantages over animal

models such as lower cost, speed, reproducibility, increased sensitivity, and it is often possible to establish a defined, effective concentration of a test compound.

The initial work carried out on isolated cells in culture employed primary cell lines and helped to elucidate and confirm the toxicity of MPTP (Mytilineou and Cohen, 1984) and its mechanism of action (Mytilineou *et al.*, 1985). Primary cultures have the advantage of maintaining excellent cell function closely resembling the cell's characteristics *in vivo*. However, primary cultures derived from the brain suffer from the fact that they are often obtained from embryonic tissue and require *in vitro* differentiation. In addition, these cultures are often a mixed cell population with a limited life span in commercial medium.

The use of continuous cell lines to investigate MPTP toxicity has in the past focused on the rat pheochromocytoma line, PC12 cells. These cells exhibit some properties associated with dopaminergic neurones and responds to nerve growth factor by extending neurites, acquiring the appearance of mature neurones. Some of the initial work using PC12 cells to assess MPTP toxicity was carried out by Denton and Howard (1984, 1987), who discovered that these cells exhibited increased resistance to MPTP by an alteration in energy metabolism. This was later proposed to be linked to the ability of PC12 cells to increase glycolytic metabolism to counteract the inhibition of mitochondrial respiration (Basma *et al.*, 1992).

However, PC12 cells have also been shown to exhibit changes in cellular morphology, prior to cell death, following exposure to the neurotoxin (Denton and Howard, 1984; Cappelletti *et al.*, 1995), suggesting a possible involvement of early disturbances in certain cellular components in expressing MPTP neurotoxicity. Indeed, other non-dopaminergic cell types, such as cultured fibroblasts, have exhibited cytotoxicity (Freyaldenhoven and Ali, 1996) and subtle changes in both cytoskeletal components (Cappelletti *et al.*, 1991; Urani *et al.*, 1994) and calcium levels (Urani *et al.*, 1994). These observations suggest that the characterisation of a neuronal cell culture model system that can express a mature morphology would be valuable for a more detailed investigation of the subtle degenerative effects of MPTP on cells.

The use of neural cell lines that are closely associated with MPTP neurotoxicity *in vivo* (i.e. neuronal and glial cells) has obvious advantages for this study. Established neuronal and glial cell lines have been employed in a variety of physiological,

biochemical and neuropharmacological studies. These include the neurotoxicity screening of a number of diverse compounds such as heavy metals (Kromidas *et al.*, 1990; Cookson *et al.*, 1995), organic compounds (Cookson *et al.*, 1995) and organophosphates (Henschler *et al.*, 1992; Flaskos *et al.*, 1998). The importance of these cellular model systems is that the cells represent a homogeneous population, thus permitting analyses of specific parameters on a large scale.

1.6.1 Neuroblastoma (N2a) cell line

The N2a neuroblastoma cell line is derived from the C1300 neuroblastoma (Klebe and Ruddle, 1969); a spontaneous tumour that has been maintained since 1940 at the Jackson Laboratories by serial transplantation in strain A/J mice (Haffke and Seeds, 1975). N2a cells typically express a round neuroblast morphology in suspension cultures and in the undifferentiated state. However, like many related clones of C1300 neuroblastoma, when given a surface on which to attach to, they undergo a striking change in morphology. The most prominent characteristic is the extrusion, from the cell body, of one to four elongated cytoplasmic processes referred to as neurites (axon like processes), which is accompanied by an increase in the size of the nucleus and perikaryon (Haffke and Seeds, 1975). Electron microscopy reveals neuroblastoma neurites to contain large numbers of neurofilaments which are characteristic of the axons and dendrites of mature neurones (Schubert *et al.*, 1969). This change in morphology can be augmented by the withdrawal of serum from the maintenance medium causing a reduction in cell division and promoting differentiation. This leads to a dramatic morphological increase in neurite outgrowth and a two fold biochemical increase in intracellular cyclic adenosine monophosphate (cAMP) levels (Prasad and Sinha, 1976). These changes are further enhanced by dibutyryl cyclic 3',5'-monophosphate (dbcAMP) which can mimic many of the actions of cAMP and promotes differentiation that is largely irreversible. The overall effect is a neuroblastoma cell population that can differentiate morphologically and biochemically to simulate a mature phenotype.

Accompanying the cellular morphological changes, neuroblastoma cells also have the ability to develop some electrophysiological and other biochemical related

characteristics of mature neurones. Intracellular recordings reveal that differentiated neuroblastoma cells are capable of spontaneous and repetitive depolarisation, in addition to generating action potentials in response to electrical stimulation (Haffke and Seeds, 1975).

Biochemically, the N2a clone is classed as an adrenergic neuroblastoma, containing high levels of tyrosine hydroxylase. This enzyme is the first, rate-limiting, enzyme in the biosynthetic pathway for the production of catecholamines and shows increased expression when neuroblastoma clones are treated with the differentiating agent dbcAMP (Waymire *et al.*, 1972). N2a cells have also been shown to contain small amounts of dopamine, norepinephrine and serotonin (Narotzky and Bondareff, 1974) and to express low levels of MAO (Nagutsu *et al.*, 1981). The low MAO activity phenomenon is also seen in dopaminergic neurones of the substantia nigra (the area of the brain affected in PD and MPTP-induced Parkinsonism) as reported by workers using immunofluorescence and immunological procedures (see section 1.2.5.2). These advantageous characteristics and the ability to differentiate to express a mature neuronal phenotype support the use of the N2a clone to investigate MPTP neurotoxicity in a cell model system study.

1.6.2 C6 Glioma cells

The glial cell strain, C6, was cloned from a Wistar rat glial tumour induced by N-nitrosomethylurea by Benda *et al* (1968) after a series of alternate culture and animal passages. The rat glial cell line has proven to be a valuable model of normal glia in a number of respects. For example, C6 cells possess antigens and enzymes characteristic of both astrocytes and oligodendrocytes found in glia *in vivo* and in primary cultures e.g. glycerol phosphate dehydrogenase, glutamine synthetase and lactate dehydrogenase (Kumar *et al.*, 1984); enzymes implicated in myelination and ammonia detoxification in the brain. The clone also produces S-100 protein, which is unique to brain glial tissue in vertebrates and has been found in numerous brain tumours in humans and other animals. Like neuroblastoma cell clones, C6 cells have also been employed to test various neurotoxicants, where they show similar neurotoxic

responses to primary astrocytes (Cookson *et al.*, 1995), supporting their use as a glial cell model.

C6 glioma cells are typically astroblastic in appearance when cultured *in vitro*, in that the cells are epithelioid in shape with spherical nuclei and irregular cell margins. Despite being a transformed cell line C6 cells can also be induced to differentiate using a variety of compounds. The short chain fatty acid sodium butyrate is commonly used and has been shown to produce reversible changes in morphology, growth rate and enzyme activities in several mammalian cell types (Kruh, 1982). The compound is known to induce hyperacetylation of chromatin proteins, which can be associated with gene expression and synthesis of specific proteins. Its addition to culture medium of transformed cells produces a progressive flattening associated with changes in the distribution of microtubules, microfilaments and intermediate filaments (Kruh, 1982). However, the precise mechanisms that mediate these general responses are still not fully defined.

Glioma C6 cells can develop short neurite-like processes which correlate to a change in tubulin distribution, when exposed to sodium butyrate (Hargreaves *et al.*, 1989). In conjunction, differentiating C6 cells increase expression of a spectrin-like protein related to fodrin which has been postulated to be involved in the organisation of the cytoskeleton in these cell processes (Hargreaves *et al.*, 1989).

In vivo, glial cells are crudely termed the mechanical and supporting cells of the nervous system, due to the fact that their precise roles are still not fully explained. The functional role of glia include mechanical support of neurones, removal of local tissue debris after cell death, provision of a filter system between blood and neurones, and control of the composition of extracellular fluid (Bradford, 1986). Glial cells are also considered to rapidly take up and inactivate chemical neurotransmitters released by neurones. Indeed, C6 glioma cells exhibit considerable MAO and acetylcholinesterase activities indicating a possible role in neurotransmitter inactivation (Skaper *et al.*, 1976).

Since MAO in glial cells is proposed to play an important role in the bioactivation of MPTP (see section 1.1.7), the use of these cells (which exhibit many similarities to primary astrocytes) will help to establish and characterise the toxic effects of MPTP in a controlled glial environment.

1.7 Aims of study.

It is becoming increasingly evident from the literature that the neurotoxin MPTP may exert its neurodegenerative effect via a combination of independent and linked events. However, despite the extensive work carried out the precise intraneuronal mechanisms by which this neurotoxin can evoke cellular changes that lead to neurodegeneration are still not fully understood. Studies employing animal models are complicated and prove difficult to interpret; involving the use of specifically defined ^{criteria} eriterion to eliminate experimental differences. This study will therefore utilise simplified *in vitro* cell model systems (employing C6 glioma and N2a neuroblastoma cells) representing glial and neuronal cells, to study MPTP-induced neurotoxicity. The two cell lines were chosen since they express appropriate receptors and mature characteristics suitable for studying the neurodegenerative effects of various neurotoxins (Cookson *et al.*, 1995; Flaskos *et al.*, 1998). The project will initially aim to characterise the two cell lines with respect to monoamine oxidase and glutathione status; relating these findings to glial and neuronal cell susceptibility to MPTP/MPP⁺.

In the past, investigators employing animal models have tended to use acute toxic doses of MPTP. Similarly, *in vitro* studies have focused on the toxic (i.e. lethal) effect of MPTP on cells. Recently, however it has been recognised that a low dose MPTP-induced animal model with extended survival times may be more valuable for studying neuronal damage and repair mechanisms (Bezard *et al.*, 1998). By the same token *in vitro* studies should therefore include the use of non-toxic doses of neurotoxin to allow investigation of the more subtle changes occurring during neuronal degeneration.

To achieve this MPTP-induced neurotoxicity will be investigated in neuroblastoma cells induced to express a maturing phenotype, to mimic the *in vivo* situation more closely. This approach will help to obtain a greater understanding of the molecular events that occur during MPTP-induced neurodegeneration with an aim to identifying possible early markers of toxicity. Characterisation and identification of these markers will ultimately lead to potential pharmacological targets for developing novel therapies. Indeed, the neuroblastoma model will be used to study the effects of

known and potential neuroprotective agents in their ability to alleviate MPTP-induced neurotoxicity. This will provide further support and accreditation for the use of neuronal cell model systems for preliminary pharmacological intervention studies.

CHAPTER II

Materials and Methods

2. Materials and Methods.

2.1 Materials

2.1.1 Specialised Equipment: -

Mettler AE 260 Delta balance (Metler, UK)
Gelaire BSB 4 Laminar Flow Hood, Class II (Flow Laboratories, UK)
MSE Centaur 2 centrifuge (MSE Scientific Instruments, UK)
Olympus CK2 Inverted light microscope (Olympus Optical Ltd, UK)
Neubauer Haemocytometer (Sigma-Aldrich, UK)
Phillips pH meter -PW9409 (Pye-Unicom, UK)
Fisons Whirlimixer (Fisons, UK)
Soniprep 150 (MSE Scientific Instruments, UK)
SM1 Magnetic stirrer (Stuart Scientific, UK)
Liquid Scintillation Counter -A 300 CD (Canberra Packard, USA)
Bio-Rad MiniProtean II electrophoresis kit (Bio-Rad, UK)
Bio-Rad PowerPac 300 (Biorad, UK)
Bio-Rad Trans-Blot electrophoretic transfer kit ((Bio-Rad, UK)
Quantiscan Image Analysis system, Version 1.5 (Biosoft, UK)
Desaspeed MH-2 microfuge
Schleicher and Schuell Bio-dot blot apparatus (Germany)
Ultrospec II spectrophotometer (Pharmacia LKB, UK)
Titertek Multiskan MCC/340 Mk2 ELISA reader (Titertek, UK)
PCR Thermal Cycler (Hybaid, USA)
Agarose gel electrophoresis kit (Bio-Rad, UK)
Leica CLSM Confocal Laser microscope (Leica, Germany)
Lucy I Microplate Luminometer (Anthos, UK)
FACScan Flow cytometer (Becton Dickinson, UK)

2.1.2 Specialised Reagents

2.1.2.1 Chemical reagents

Dulbecco's Modified Eagles Medium (DMEM), Foetal bovine serum (FBS), Glutamine/penicillin/streptomycin, Clorgyline, Deprenyl, 1-methyl-4-phenyl-1,2,3,6-tetrahydropyridine (MPTP), 1-methyl-4-phenyl-pyridinium (MPP+), ¹⁴C-tyramine hydrochloride, dibutyryl cyclic AMP (dbcAMP), 3-(4,5-dimethylthiazol-2-yl)-2,5-diphenyltetrazolium bromide (MTT), GSSG reductase, Oestradiol - All purchased from Sigma Aldrich Chemical Company Ltd (Poole, UK).

SB202190 - Calbiochem (Nottingham, UK).

ADP/ATP Vialight kit - Lumitech, (Nottingham, UK).

5,5',6,6'-tetrachloro-1,1',3,3'-tetraethylbezimidazolocarboxyanine iodide (JC-1) - Cambridge Bioscience (Cambridge, UK).

RNAasin[®], dNTP mix, M-MLV enzyme, Taq DNA polymerase - Promega (Southampton, UK).

RNA-STAT 60[™] - Biogenesis (Poole, UK)

Primers: MAO-A/B forward/reverse - Life Technologies (Gibco BRL).

2.1.2.2 Antibodies

Mouse anti-NF-H (N52; phosphorylation independent), mouse anti- α -tubulin (B512), rabbit (affinity isolated) anti-actin - Sigma Aldrich (Poole, UK).

Anti-NF-H monoclonal antibodies RMd09 (non-phosphorylation dependent) and Ta51 (phosphorylation dependent) were originally a kind gift from Dr. M. J. Carden (University of Kent, Canterbury).

Anti-mouse and anti-rabbit alkaline phosphatase-conjugates and fluorescein isothiocyanate (FITC) conjugates - Dako Ltd (Cambridge, UK).

Rabbit anti-a-synuclein antibody was a kind gift from Dr. M. Goedert (University of Cambridge, Cambridge)

Rabbit anti-ubiquitin-KLH antibody was a kind gift from Prof. R.J. Mayer (University of Nottingham, Nottingham).

Chicken anti-GDNF pAb, Rabbit anti-active@ JNK pAb, Goat anti-chicken IgY alkaline phosphatase secondary conjugate, Donkey anti-rabbit alkaline phosphatase secondary conjugate - Promega (Southampton, UK).

2.1.3 Tissue Culture Plastic-ware

All sterile tissue culture plastic-ware was of the highest quality and purchased from Scientific Laboratory Supplies (Nottingham, UK).

2.1.4 Reagents

All chemicals were of the highest grade and purchased from Sigma-Aldrich Chemical Company Ltd (Poole, UK) or BDH (Leicester, UK). Any chemicals or reagents purchased from alternative sources are specified in the text.

2.2 Methods

2.2.1 Cell lines

2.2.1.1 Mouse N2a neuroblastoma cells

The mouse neuroblastoma N2a cell line was originally deposited to the American Type Culture Collection (ATCC) by R.J. Klebe (1969). It is a subclone from the C1300 mouse neuroblastoma; a spontaneous tumour which has been maintained since 1940 at the Jackson Laboratories by serial transplantation in strain A/J mice (Haffke and Seeds, 1975). When maintained in the monolayer N2a cells typically express neuronal and amoeboid morphology. The cell line was obtained from Flow laboratories (Irvine, UK).

2.2.1.2 Rat C6 glioma cells

The rat C6 glioma cell line was originally deposited to the ATCC in the 30th serial passage by Benda *et al* (1968) and was cloned from a glial tumour induced by N-nitrosomethylurea in a Wistar rat. C6 glioma cells typically express a fibroblast-like morphology when cultured in monolayer. The cell line was obtained from Flow laboratories (Irvine, UK).

2.2.1.3 Maintenance of cell lines

Mouse N2a neuroblastoma and rat C6 glioma cells were both routinely maintained in monolayer in T25 flasks using Dulbecco's Modified Eagles Medium (DMEM) supplemented with 10% Foetal bovine serum, 2 mM L-glutamine, 100 units/ml penicillin, 10 mg/ml streptomycin, (*Growth medium*). Flasks were incubated in a humidified atmosphere of 95% air, 5% CO₂ at 37°C (Jouan IG150 incubator). Cells were typically kept and used for 30 passages following thawing from liquid nitrogen, whereupon they were discarded and a fresh batch thawed.

2.2.1.4 Freezing cells in liquid nitrogen

Cell lines were maintained in long term storage in liquid nitrogen. Cells were grown in monolayer, using growth medium, until they reached 70-90% confluency. Cells were then mechanically detached from the flask surface using growth medium and a Pasteur pipette. The cell suspension was transferred to a sterilin tube and harvested by centrifugation at 150 g for 7 minutes. The resultant supernatant was decanted and the pellet resuspended in 1 ml of *Freezing medium* (DMEM supplemented with 25% (v/v) foetal bovine serum, 5% (v/v) dimethyl sulphoxide, 2 mM L-glutamine, 100 units/ml penicillin, 10 mg/ml streptomycin) by carefully passing the cell suspension through a Pasteur pipette approximately 5 times. The cell suspension was then transferred to a freezing vial and placed in a freezing container (Nalgene) at -70°C overnight. Vials was finally transferred to liquid nitrogen and stored until required.

2.2.1.5 Thawing cells from liquid nitrogen

In order to maximise cell population recovery the thawing of cell lines was carried out rapidly. Vials were removed from liquid nitrogen and quickly placed into a 37°C waterbath to thaw. The cell suspension was transferred to a sterilin tube containing 10 ml growth medium (pre-warmed to 37°C) and the cells harvested by centrifugation at 150 g for 5 minutes. The resultant pellet was resuspended in 1 ml growth medium by passing the cell suspension approximately 5 times through a Pasteur pipette. The entire cell suspension was then transferred to a fresh T25 flask containing 10 ml growth medium and incubated overnight in a humidified atmosphere of 95% air, 5% CO₂ at 37°C. Growth medium was then carefully decanted from the flask and replaced with fresh growth medium and the cells re-incubated until they reached 70-90% confluency, whereupon they were sub-cultured.

2.2.1.6 Passage of cells

Cells were maintained in monolayer in T25 flasks and sub-cultured to a fresh culture vessel when growth reached 70-90% confluency (i.e. every 3-5 days). Cells were mechanically detached from the flask surface using a Pasteur pipette and growth medium. The cell suspension was transferred to sterilin tube and harvested by centrifugation at 150 g for 7 minutes. The resultant pellet was resuspended in 1 ml of growth medium (pre-warmed to 37°C) by carefully passing the cell suspension through a Pasteur pipette approximately 20 times. An aliquot of the cell suspension (typically 100-300 µl) was then transferred to a new T25 flask containing 10 ml fresh growth medium and incubated at 37°C in a humidified atmosphere of 95% air, 5% CO₂.

2.2.2 Seeding of cells for experimentation.

Cells were seeded to appropriate tissue culture plastic-ware for experimental analysis when growth reached approximately 70-90% confluency within the maintenance flasks. Cells were mechanically detached from the flask surface using a Pasteur pipette and growth medium. The cell suspension was transferred to a sterile

polycarbonate 'sterilin' tube and harvested by centrifugation at 150 g for 7 minutes. The resultant pellet was resuspended in 1 ml of growth medium by carefully passing the cell suspension through a Pasteur pipette approximately 20 times. To further desegregate the cells, the suspension was passed through a 19/21 gauge syringe needle 5 times. A 20 μ l aliquot was then transferred to a 1 ml microfuge tube containing 180 μ l growth medium (1:10 dilution) and a haemocytometer count carried out. Cells were then plated out using growth medium at a typical cell density of 50,000 cells/ml (T25 flasks, 500 000 cells per flask; 24 well plates, 25 000 cells per well; 96 well plates, 5 000 cells per well). Cells were incubated at 37°C in a humidified atmosphere of 95% air, 5% CO₂ to allow recovery.

2.2.3 Differentiation of cells.

2.2.3.1 Mouse N2a Neuroblastoma cells.

N2a cells were initially plated out at the required cell density in growth medium as described previously (section 2.2.2) and incubated overnight to allow recovery. Growth medium was carefully removed from the culture-ware, as to not disturb the attached cells, and replaced with an equal volume of serum-free Dulbecco's modified eagles medium supplemented with 2 mM L-glutamine, 100 units/ml penicillin, 10 mg/ml streptomycin solution (*serum-free medium*) and 0.3 mM dibutyryl cyclic AMP (dbcAMP). Cells were re-incubated at 37°C in an atmosphere of 95% air, 5% CO₂ for the required length of time.

2.2.3.2 Rat C6 Glioma cells.

C6 cells were initially plated out at the required cell density in growth medium as described previously (section 2.2.2) and incubated overnight to allow recovery. The growth medium was carefully removed from the culture-ware, as to not disturb the attached cells, and replaced with an equal volume of serum-free Dulbecco's modified eagles medium supplemented with 2 mM L-glutamine, 100 units/ml penicillin, 10

mg/ml streptomycin and 2 mM sodium butyrate. Cells were re incubated at 37°C in an atmosphere of 95% air, 5% CO₂ for the required length of time.

2.2.3.3 Glial C6 Conditioned Medium (Rat glial C6 cells).

Rat glial C6 cells were plated out in growth medium at a cell density of 100,000 cells/ml in T75 flasks and incubated for 48 h to allow growth to approach confluency. Growth medium was carefully decanted from the flask and replaced with an equal volume of SFM + 1 % (v/v) foetal bovine serum. Cells were re-incubated for a further 48 hours in an atmosphere of 95% air, 5% CO₂ prior to harvesting the medium. The medium was clarified of cells by centrifugation for 5 min at 500g. This cell free supernatant, termed C6 glial conditioned medium, was pooled prior to aliquoting into working volumes and stored under sterile conditions at -20°C, for up to 2 weeks, until required.

2.2.4 Exposure of cells to MPTP/MPP⁺

MPTP and MPP⁺ were dissolved in PBS (137 mM NaCl, 2.7 mM KCl, 10 mM Na₂HPO₄, 1.8 mM KH₂PO₄, pH 7.4) at stock concentration of 0.1 M. Cells were plated out at 50,000 cells/ml and incubated overnight to allow recovery. Growth medium was removed from the culture-ware and replaced with an equal volume of either fresh growth medium containing neurotoxin or differentiating medium (see section 2.2.3) containing neurotoxin. Cells were re-incubated at 37°C in an atmosphere of 95% air, 5% CO₂ for the required length of time.

2.2.5 Exposure of cells to neuroprotective agents

Clorgyline, deprenyl and estradiol were all dissolved in PBS (137 mM NaCl, 2.7 mM KCl, 10 mM Na₂HPO₄, 1.8 mM KH₂PO₄, pH 7.4) at stock concentrations of 0.1 M. SB202190 was dissolved in DMSO at a stock concentration of 0.1 M. Cells were plated out at 50,000 cells/ml and incubated overnight to allow recovery. Growth medium was removed from the culture-ware and replaced with an equal volume of

serum-free medium containing 0.3 mM dbcAMP in the presence or absence of MPTP and neuroprotective agent. Cells were re-incubated at 37°C in an atmosphere of 95% air, 5% CO₂ for the required length of time.

2.2.6 Viability Assays.

2.2.6.1 MTT (Tetrazolium salt) viability assay

The MTT {3-(4,5-dimethylthiazol-2-yl)-2,5-diphenyltetrazolium bromide} viability assay is a colorimetric assay for anchorage dependent cells. Viable cells intracellularly accumulate MTT whereupon it is reduced, primarily by enzymes of the endoplasmic reticulum (Berridge *et al.*, 1996), to yield a purple formazan product. This product is largely impermeable to cell membranes, thus resulting in its accumulation within healthy cells. Direct solubilisation of the product using dimethyl sulphoxide (DMSO) results in the liberation of the product, which can then be detected readily using a spectrophotometer. The ability of the cells to reduce MTT is largely dependent on the net rate of glycolytic NAD(P)H production by cells which may be interpreted as a measure of cell viability.

Cells exposed to neurotoxin were incubated for required time period prior to cell viability assessment. Typically, 1 h prior to the end of the incubation MTT (5 mg/ml in PBS) was added to each well (final conc. 0.5 mg/ml) and plates re-incubated at 37°C for 1 h. Medium was carefully aspirated from the wells, whereupon 1 ml dimethyl sulphoxide (DMSO) was added as solvent. Plates were gently agitated to dissolve the formazan product and the absorbance read at 570 nm within 30 minutes. Blank values were subtracted from each reading and the absorbance then expressed as a percentage of the value for the corresponding control (Cookson *et al.*, 1995).

2.2.6.2 Lactate dehydrogenase (LDH) viability assay.

The LDH viability assay method was adapted from Moldeus *et al.*, (1978) and is based on the measurement of lactate dehydrogenase activity released from the

cytosol of damaged cells into the supernatant. The quantification of extracellular LDH is directly related to cell lysis and can therefore be interpreted as cell death.

Cells incubated in the presence and absence of neurotoxin for the required time period were assessed for viability using the LDH assay. Activity of LDH was monitored in aliquots of cell-free medium and compared to the total activity achieved after total cell lysis. Typically, a 500µl aliquot of medium was removed from each well and made up to 900µl using 2% (v/v) Triton X-100 in serum-free medium (SFM) and incubated at room temperature for 5 minutes. The total cell LDH activity was achieved by the addition of 400 µl SFM + 500 µl 2% (v/v) Triton X-100 in SFM to each well and incubated at room temp for 5 minutes. The solution from the supernatant and total lysis samples were transferred to respective eppendorf tubes and made up to a final volume of 1000 µl through the addition of pyruvate (1.36 mM final conc.) and NADH (0.2 mM final conc.). Samples were instantly transferred to a cuvette and the rate of change of absorbance at 340 nm (due to NADH oxidation) was recorded. Cell viability was calculated thus:-

$$\% \text{ Cell Death} = \frac{\text{LDH activity (supernatant)}}{\text{LDH activity (total)}} \times 100\%$$

$$\% \text{ Cell Viability} = 100\% - \% \text{ Cell Death}$$

Neurotoxin-treated values were corrected for cell lysis in controls (i.e. incubated in the absence of MPTP) as follows:

$$\text{Corrected \% Cell viability} = \frac{\% \text{ Cell viability (MPTP)}}{\% \text{ Cell viability (control)}} \times 100\%$$

2.2.6.3 Trypan Blue exclusion assay.

Trypan blue is used in dye exclusion procedures for viable cell counting. This method is based on the principle that live cells exclude Trypan blue, whereas dead cells accumulate the dye.

Cells incubated in the presence or absence of neurotoxin were assessed for cell viability using the Trypan blue exclusion assay. Cells were mechanically detached from the monolayer using a Pasteur pipette and the cell suspension transferred to a sterilin tube. To ensure total cell detachment flasks were washed in 2 x 1 ml SFM and the suspension transferred to the sterilin tube. The cell suspension was then harvested

at 150 g for 7 min. The supernatant was carefully discarded and pellet resuspended in 100µl PBS. A 20 µl cell suspension was transferred to an eppendorf containing 60µl PBS, 20µl 0.4% (w/v) Trypan Blue. The suspension was then allowed to stand at room temperature for 5 min prior to a haemocytometer count. A separate count of viable and non-viable cells was obtained from which % cell viability could be assessed.

$$\text{Cells / ml} = \text{Average count per square} \times \text{dilution factor} \times 10^4$$

$$\text{Total cells} = \text{cells / ml} \times \text{original volume of cell suspension from which sample was removed}$$

$$\text{Cell viability (\%)} = [\text{Total viable cells (unstained)} \div \text{total cells (stained + unstained)}] \times 100$$

2.2.7 Protein Determination

Protein content of cell samples was determined using the method of Lowry *et al.* (1951) with modifications. On each occasion a BSA standard protein curve (0-100 µg) was prepared in parallel to cell samples. Cell suspensions were sonicated on ice for 2 x 5 sec using a Soniprep 150. Aliquots of protein standards and cell suspensions were made up to 90 µl with distilled water prior to the addition of 10 µl 1 % SDS. Stock reagent solution A [2.0 % (w/v) Na₂CO₃, 0.4 % (w/v) NaOH], solution B [1.0 % (w/v) CuSO₄.5H₂O] and solution C [2.7 % (w/v) sodium potassium tartrate] were dispensed to create a working solution comprising 50 ml solution A, 1.0 ml solution B, 1.0 ml solution C. To each sample 1.0 ml working solution was added, whereupon samples were vortex mixed and incubated at room temperature for 10 minutes. Following incubation, 100 µl Folin-Ciocalteu reagent (diluted 1:1 with dH₂O) was added to each sample and vortex mixed, prior to a further incubation of 30 minutes at room temperature. Absorbance readings were measured at 750 nm and protein content of samples was determined from the protein calibration curve (see Fig. 2.1 for typical example).

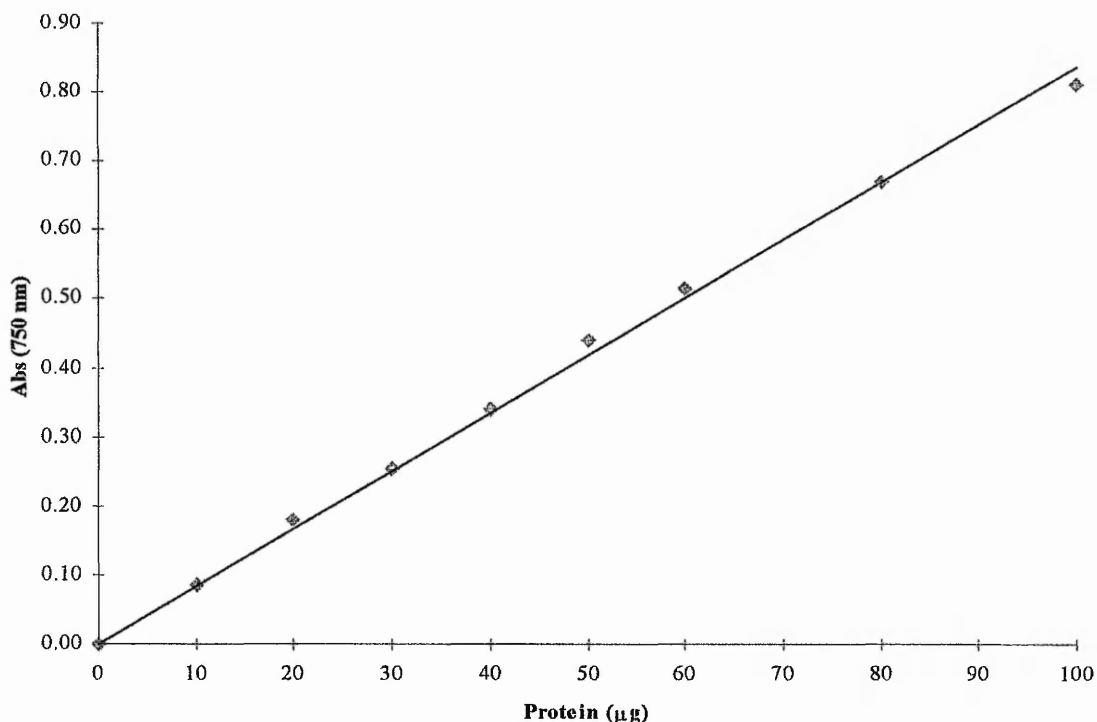
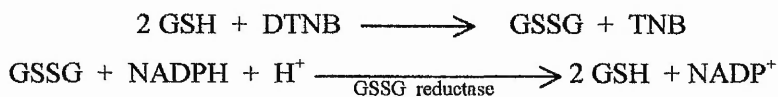


Figure 2.1. Example of Protein Standard Curve (based on method by Lowry, 1951).

2.2.8 Total Glutathione (GSH+GSSG) Determination

Total glutathione levels were determined using the DTNB-GSSG reductase recycling assay, based on the method described by Anderson, 1985, with minor modifications. The recycling assay for total glutathione (GSH + GSSG, in GSH equivalents) works on the basis of the following reactions:



N2a and C6 cells were plated out at constant cell density and incubated overnight in a humidified atmosphere of 95% air, 5% CO₂ at 37°C, to allow recovery. Cells were grown under mitotic conditions in growth medium for a further 24 h, or induced to differentiate in serum free medium supplemented with either 0.3 mM dbcAMP (N2a) or 2 mM sodium butyrate (C6) for 24 h. Following incubation medium was aspirated and the cells rinsed twice with 1.5 ml cold sterile PBS (137 mM NaCl,

2.7 mM KCl, 10 mM Na₂HPO₄, 1.8 mM KH₂PO₄, pH 7.4). The cells were then dislodged, centrifuged at 100 g for 7 min, and sonicated for 10 s in 250 µl 5-sulphosalicylic acid [final concentration 5 % (w/v)]. Samples were again centrifuged at 13,000 g for 10 min; total glutathione assays were performed on the supernatant, whereas protein was quantified in the pellet as described in section 2.2.7.

Reagents :- 5 sulphosalicylic acid (10 % w/v)
Stock buffer (143 mM sodium phosphate, 6.3 mM Na₄-EDTA)
NADPH buffer (0.25 mg/ml NADPH in stock buffer)
DTNB (6 mM DTNB in stock buffer)
GSSG reductase (200 U/ml)
GSH standards (0-10 nmol diluted in 5-sulphosalicylic acid
[final concentration 5 % (w/v)])

NADPH buffer (700 µl), DTNB solution (100 µl), sample (25 µl), 5-sulphosalicylic acid (25 µl) were added to microfuge tubes and made up to 990 µl with stock buffer. The tubes are pre-warmed in a 30°C water bath for 10 min prior to the addition of GSSG reductase (10 ml) with mixing, whereupon the formation of TNB is followed continuously for 5 min at 412 nm. Total glutathione levels are determined from a standard curve in which the GSH equivalents present are plotted against the rate of change of absorbance at 412 nm. A sample blank lacking GSH is used to determine the background rate. Values are finally expressed as glutathione nmol /mg protein.

2.2.9 Monoamine oxidase analysis.

2.2.9.1 Estimation of MAO activity.

Total MAO activity was determined using a radiochemical method as described by Russell and Mayer (1983) with modifications. The assay is based on the ability of MAO to convert the water soluble substrate [¹⁴C]-tyramine to its corresponding [¹⁴C]-aldehyde product which is soluble in the organic phase.

MAO activity was determined in both dividing and differentiated cells. In the case of dividing cells, cells were plated out in growth medium and left to grow for 48 hours prior to harvesting. In the case of differentiated cells, cells were plated out in growth medium and left to recover for 48 hours prior to inducing the cells to

differentiate as described previously. The cells were re-incubated for a further 24 hr before analysis. Cells were harvested by dislodging them from the substratum using medium and a Pasteur pipette and then collected by centrifugation at 100 g for 5 min. The pellet was resuspended in 1 ml DMEM and counted using a haemocytometer.

Equal cell aliquots of 250, 000 cells were made up to a final volume of 200 μ l using 0.02 M potassium phosphate buffer (pH 7.4) in plastic-scintillation-vial inserts and vortex mixed prior to incubation for 5 min at 37°C. In association with sample vials, blank vials were run in parallel and prepared by the addition of 0.5 M HCl prior to incubation. To each sample 20 μ l 1 mM [¹⁴C]-tyramine hydrochloride (1 mCi/mmol) was added whereupon samples were again vortex mixed and incubated for a further 60 min at 37°C. The reaction was terminated by the addition of 200 μ l 0.5 M HCl to each tube. Finally 3.0 ml of scintillant, 1% (w/v) 2,5-diphenyloxazole (PPO) in toluene:ethyl acetate (mixed 1:1) was added to each sample prior to vigorous vortexing and counting in a liquid scintillation counter. Extraction efficiency of the products into the upper organic phase was > 98 % and was not corrected for. Blank values were subtracted from sample values and activity expressed as pmol / min / mg protein.

2.2.9.2 Selection of MAO-specific primers

Sequence specific primers were selected from full cDNA sequences of rat MAO-A and MAO-B obtained from the GenBank Database (NCBI; National Library of Medicine, National Institute of Health, Bethesda, MD; www.ncbi.nlm.nih.gov). Sequence comparison of rat MAO-A and MAO-B cDNA with mouse counterparts using BLAST (Basic Local Alignment Search Tool) exhibits, in general, 95 % amino acid sequence identity. Sequence specific primers were selected using a primer design software program (Primer 3; www.genome.wi.mit.edu/cgi-bin/primer/primer3). To optimise primer design certain restrictions were applied to search protocol. For example probes were only identified towards the 5' end of the cDNA sequences and must cross an exon-intron boundary. Primer position between MAO-A and MAO-B were chosen to be within similar regions and produce similar (but distinctly different) product sizes to minimise potential discrepancies during normal transcription and allow individual identification (Table 2.1).

Primers for MAO-A are as follows (5' MAO-A-forward, 3' MAO-A-reverse), selected from rat cDNA exons 7 and 8, respectively. Primers for MAO-B are as follows (5' MAO-B-forward, 3' MAO-B-reverse), selected from rat cDNA exons 7 and 8, respectively.

Table 2.1 *MAO sequence specific primers*

<i>Oligonucleotide</i>	<i>Orientation</i>	<i>Location</i>	<i>Length</i>	<i>Sequence (5'-3')</i>	<i>Product size</i>
MAO-A forward	Sense	667-686	20 bp	GGT GGA TCT GGC CAA GTA AG	211 bp
MAO-A reverse	Anti-sense	877-858	20 bp	TCT CAG GTG GAA GCT CTG GT	
MAO-B forward	Sense	740-759	20 bp	GGG ACA GAG TGA AGC TGG AG	199 bp
MAO-B reverse	Anti-sense	938-919	20 bp	CCC AAA GGC ACA CGA GTA AT	

Confirmation of the specificity of the primers was achieved by carrying out a BLAST search of primer sequence to produce 100% identity hits exclusively for either MAO-A or MAO-B. Primers were purchased from Life Technologies, Gibco BRL.

2.2.9.3 Preparation of total RNA.

Total RNA was extracted from cultured cells based on a single step method of RNA isolation (Chomczynski and Sacchi, 1987). Cells were plated out at 100,000 cells/ml in growth medium prior to overnight recovery. Medium was removed from the cell monolayer and replaced with either fresh growth medium or differentiating medium. Following a 24 hour incubation medium was again aspirated from the monolayer and the cells lysed by the addition of 1 ml RNA-STAT 60™. To aid homogenisation the cell lysate was passed several times through a pipette and transferred to an eppendorf tube where it was incubated for 5 minutes at room temperature to permit the complete dissociation of nucleoprotein complexes. To each sample, 0.2 ml chloroform per 1 ml of RNA-STAT 60™ was added and shaken vigorously for 15 seconds prior to centrifugation at 12,000 g for 15 minutes at 4°C. The lysate separates into two phases: a lower red phenol chloroform phase, containing

DNA and proteins, and a colourless upper phase which contains RNA. The aqueous upper phase was then transferred a fresh eppendorf tube and mixed with 0.5 ml isopropanol per 1 ml of original RNA-STAT 60™. Samples were mixed by gentle inversion and incubated for 10 minutes at -20°C prior to centrifugation at 12,000 g for 10 minutes at 4°C . The supernatant was discarded and the RNA pellet washed with 1 ml 75 % (v/v) ethanol. The pellet was briefly vacuum dried for 5 minutes and then resuspended in 50 μl diethylpyrocarbonate (DEPC) treated water. Samples were either used immediately or stored at -70°C .

2.2.9.4 RNA quantitation

Quantification of RNA was achieved by spectrophotometric analysis. An aliquot of isolated RNA was diluted to 1 ml in DEPC treated water and absorbance read at wavelengths of 260 nm and 280 nm. The reading at 260 nm allows calculation of the concentration of nucleic acid in the sample with an A_{260} of 1.0 corresponding to approximately 40 μg /ml of RNA. The A_{260}/A_{280} ratio provides an estimate of the purity of the sample with a ratio reading of 2.0 suggesting a relatively pure nucleic acid sample.

2.2.9.5 Reverse transcription-Polymerase chain reaction.

A concentration of 5 μg total RNA was reverse transcribed in a total reaction volume of 50 μl as defined below. Reagents used below were purchase from Promega (Southampton, UK).

	<i>Volume</i>	<i>Final conc.</i>
5 x M-MLV reaction buffer	10 μl	1 x
dNTP mix (10 mM of each dNTP)	1 μl	0.2 mM each
MAO-A/B forward primer	2 μM	100 pmol
Template (RNA)	x μl	5 μg
RNAsin (40u/ μl)	1 μl	0.8 u/ μl
M-MLV enzyme (200 u/ μl)	1 μl	4 u/ μl
Nuclease free water	x μl	(to a final vol. of 50 μl)

Prior to addition of M-MLV enzyme samples were heated to 65°C for 5 min to denature any secondary structure. Samples were then immediately transferred to ice. Reverse transcription was achieved by the addition of the aforementioned M-MLV enzyme and incubation at 37°C for 60 min. A subsequent incubation at 95°C for 5 min was carried out to denature any remaining enzyme activity.

The resultant cDNA was then used for PCR as described below

	<i>Volume</i>	<i>Final conc.</i>
10 x Reaction buffer	5 µl	1 x
dNTP mix (10 mM of each dNTP)	1 µl	0.2 mM each
MgCl ₂ (25 mM)	3 µl	1.5 mM
MAO-A/B forward primer	2 µM	100 pmol
MAO-A/B reverse primer	2 µM	100 pmol
Template (RT sample)	12.5 µl	
*Taq DNA polymerase (5u/µl)	0.5 µl	0.05 u/µl
ddH ₂ O	x µl	(to a final vol. of 50 µl)

*The resultant reaction mix was overlaid with 25 µl mineral oil and heat denatured for 7 min prior to the addition of Taq DNA polymerase to initiate the reaction. The cycling protocol was as follows:

denaturation 95°C , 45 seconds	40 cycles
annealing 55°C, 1 minute	
elongation 72°C, 2 minutes	

This was followed by a final elongation at 72°C for 7 minutes.

2.2.9.6 Agarose gel electrophoresis

PCR products were analysed by agarose gel electrophoresis. A 1.8 % agarose gel was prepared with Tris-borate-EDTA buffer (TBE: 89 mM Tris-borate, pH 8; 2 mM EDTA) and carefully heated until dissolved. The solution was cooled for 3 min prior to the addition of ethidium bromide (final concentration 0.5 mg/ml). The agarose gel was then poured into a minigel cassette, with the comb in place and allowed to set at room temperature. PCR samples were prepared for analysis as follows:

	<i>Volume</i>	<i>Final conc.</i>
PCR sample	10 μ l	
Loading Buffer (10 x)	2 μ l	1 x
Ethidium bromide (5 μ g/ml)	2 μ l	0.5 μ g/ml
ddH ₂ O	x μ l	final vol. 20 μ l

The minigel was immersed in TBE (x1) within the electrophoresis apparatus and samples loaded into individual wells. A voltage of ~5 volts/cm was applied to the gel for approximately 30-60 min. Following completion of electrophoresis gels were viewed with a UV light source and photographed.

2.2.10 Preparation and analysis of protein cell extracts

2.2.10.1 Preparation of N2a cell extracts

Cells differentiated in the presence or absence of neurotoxin / neuroprotective agents were assessed, following the required exposure period. Medium was carefully removed from the tissue culture-ware and the cell monolayer extracted into 1 ml extraction buffer [1 % (w/v) SDS, 125 mM Tris-HCl, pH 6.8]. Samples were boiled for 2 min prior to the removal of aliquots for protein estimation.

2.2.10.2 Soluble and Insoluble Cell fractionation

N2a cells induced to differentiate in the presence and absence of sub-cytotoxic MPTP concentrations were fractionated into Triton-insoluble and -soluble fractions according to procedure described by Shea and Beermann, 1994. Cells were rinsed in TBS, pH 6.8 and then harvested into cold 1 % (v/v) Triton X-100 in 50 mM Tris-HCl (pH 6.8), 5 mM EDTA, 2 mM phenylmethylsulphonyl fluoride (PMSF) and 50 μ g/ml leupeptin. The samples were sonicated for 10 s and centrifuged at 13,000 g for 10 min at 4°C. Sedimented material, defined as the insoluble fraction, was resuspended in 1 % (w/v) SDS in the above buffer. The supernatant was defined as the soluble fraction. Protein estimations were carried out on both soluble and insoluble fractions using the method described in section x.x.x. The appropriate soluble and insoluble buffers were added to each bovine serum albumin standard to optimise accurate protein estimation.

2.2.10.3 Protein determination of cell extracts.

The protein content of cell extract samples was determined using the method of Lowry *et al.* (1951) as described previously (see section 2.2.7) with minor modifications. On each occasion a BSA standard protein curve (0-100 μg) was prepared in parallel to cell samples. Briefly, 10 μl aliquots of samples originally extracted into extract buffer [1.0 % (w/v) SDS, 125 mM Tris-HCl, pH 6.8] were made up to a final volume of 100 μl . BSA standards were made up to 90 μl with distilled water, prior to the addition of 10 μl 1.0 % (w/v) SDS, 125 mM Tris-HCl, pH 6.8 solution. A working solution comprising 50 ml solution A, 1.0 ml solution B, 1.0 ml solution C was prepared (see section 2.2.7). To each sample 1.0 ml working solution was added, whereupon samples were vortex mixed and incubated at room temperature for 10 minutes. Following incubation, 100 μl Folin-Ciocalteu reagent (diluted 1:1 with dH_2O) was added to each sample and vortex mixed, prior to a further incubation of 30 minutes at room temperature. Absorbance readings were measured at 750 nm and protein content of samples was determined from the protein calibration curve.

2.2.10.4 Sample preparation

Equal protein cell extract samples (20-40 μg) were dissolved in reducing electrophoresis sample buffer [x2] (250 mM Tris-HCl, pH 6.8; 2 % (w/v) SDS; 10 % (v/v) glycerol; 5 % (v/v) 2-mercaptoethanol; 0.01 % (w/v) bromophenol blue) to give a 1x final concentration. Prior to electrophoresis samples were immersed in boiling water for 5 min to ensure dissolution / denaturation. Samples were then carefully loaded into wells using gel loading tips and electrophoresed.

2.2.11 SDS-Polyacrylamide Gel Electrophoresis (SDS-PAGE).

SDS-PAGE was carried using the method of Laemmli (1970), modified for use in a vertical slab gel electrophoresis system.

2.2.11.1 Preparation of gels

The gel mould apparatus (Bio-Rad mini-protean 11 system) was assembled according to the manufacturers instructions. Firstly, glass plates were cleaned with detergent, followed by dH₂O and ethanol. Gel spacers were used to produce 0.75 mm or 1.5 mm thick gels and placed in between the glass plates prior to clamping the mould together. Solutions and volumes required for the preparation of resolving gels can be seen in table 2.2. Here, an example of the preparation of 20 ml of a 7.5 % denaturing gel, enough for two 1.5 mm thick minigels, is described. The resolving gel (7.5 %, w/v, acrylamide) was prepared by mixing 3.75 ml acrylamide stock solution [40% (w/v)], 5 ml 1.5 M Tris buffer, pH 8.8; 200 µl SDS stock solution [10 % (w/v)]; and 11.05 ml dH₂O in a small buckner flask. The solution was then degassed for 10 min at room temperature. Immediately, before the gels were to be poured 100 µl ammonium persulphate [10 % (w/v)] and 10 µl N,N,N',N'-tetramethylethylenediamine (TEMED) was added to the solution (to catalyse the polymerisation of the acrylamide) and carefully mixed as to not introduce air bubbles. The solution was poured into the gel mould, taking care to exclude air bubbles, to a height of approximately 6 cm (minigel). The gel solution was overlaid with water-saturated butan-2-ol and the gel left to polymerise for up to 1 hr at room temperature. Prior to the application of the stacking gel, the butan-2-ol was removed and the surface of the gel washed with 1.5 M Tris buffer, pH 8.8, and any excess buffer absorbed with filter paper.

The stacking gel solution [4 % (w/v) acrylamide] was prepared by mixing 1 ml acrylamide stock solution [40% (w/v)], 2.5 ml Tris buffer (0.5 M, pH 6.8), 100 µl SDS stock solution [10 % (w/v)], 6.4 ml dH₂O and degassed as before. To the solution 50 µl ammonium persulphate [10 % (w/v)] and 20 µl TEMED was added and mixed whereupon it was poured on top of the resolving gel to fill the remaining space. A comb was immediately introduced for the formation of sample wells and placed as to leave approximately 1 cm between the bottom of the sample wells and the top of the resolving gel. Polymerisation was allowed to proceed for up to 1 hr at room temperature before sample application.

The comb was carefully removed and the wells washed and overlaid with electrode buffer. Samples were applied to the base of the wells using a gel loading tips.

The remaining electrophoresis apparatus was assembled and the chambers filled with electrode buffer (25 mM Tris base; 192 mM glycine; 0.1 % (w/v) SDS, pH 8.3). Electrophoresis was performed at a constant current 20 mA per gel for approximately 2-3 hours.

Molecular weight protein standards were also electrophoresed adjacent to samples to allow estimation of sample protein molecular weights.

Table 2.2 *Formulation for SDS-PAGE minigels.*

Formulation for resolving gel (to make 20 ml)				
<i>Components</i>	<i>Volumes for acrylamide gel concentration (ml)</i>			
	<i>7.5 %</i>	<i>10 %</i>	<i>12 %</i>	<i>15 %</i>
40 % (w/v) Acrylamide stock solution	3.75	5.0	6.0	7.5
1.5 M Tris buffer, pH 8.8	5.0	5.0	5.0	5.0
10 % (w/v) SDS	0.2	0.2	0.2	0.2
dH ₂ O	11.05	9.8	8.8	7.3
TEMED	10 µl	10 µl	10 µl	10 µl
10 % (w/v) Ammonium persulphate	100 µl	100 µl	100 µl	100 µl
Formulation for stacking gel (to make 10 ml)				
<i>Components</i>	<i>Volume (ml)</i>			
40 % (w/v) Acrylamide stock solution	1.0			
1.5 M Tris buffer, pH 8.8	2.5			
10 % (w/v) SDS	0.1			
dH ₂ O	6.4			
TEMED	20 µl			
10 % (w/v) Ammonium persulphate	50 µl			

2.2.11.2 Staining and destaining gels.

Following electrophoresis, gels were carefully removed from the glass mould and stained in a large glass tray using Coomassie blue staining solution (50 % (v/v) methanol; 10 % (v/v) acetic acid, 0.25 % (w/v) Coomassie blue R-250) for up to 3 hours at room temperature with agitation. Gels were then destained in destain solution (10 % (v/v) methanol; 5 % (v/v) acetic acid) at room temperature with agitation, until the background was clear.

2.2.12 Electrophoretic transfer of proteins

2.2.12.1 Western Blotting (electroblotting).

Electrotransfer of proteins from cell extracts that had been subjected to SDS-PAGE was performed as described by Towbin *et al.* (1979) with modifications, using the 'tank' buffer system. Following electrophoresis the gel was immersed in electroblotting buffer (39 mM glycine; 48 mM Tris base; 0.0375 % w/v SDS; 20 % v/v methanol) to allow partial removal of excess SDS. Four filter papers (3MM Whatman chromatography paper) and a sheet of nitrocellulose (pore size 0.45 mm) per gel, cut slightly larger than the size of the gel were soaked in electroblotting buffer by slow immersion to allow saturation by capillary action. Each blotting cassette was assembled taking care not to introduce air bubbles between individual surface layers. The position and orientation of the gel on the nitrocellulose was marked. The cassette was placed into the Bio-Rad wet electroblotting unit, which was filled with electroblotting buffer, ensuring the nitrocellulose faced the anode and the adjacent SDS-PAGE gel faced the cathode. A current of 100 mA was applied across the electrodes at room temperature overnight or 250 mA for 1 hour at room temperature, using the ice pack cooling system incorporated in the unit. A voltage gradient of 6 V/cm for 1 hour or 20 V overnight was applied.

2.2.12.2 Staining of nitrocellulose blots for total protein pattern.

Staining of the blot for the total protein pattern is of interest to confirm the efficiency of transfer, or when the signal is to be located with respect to other proteins on the gel such as the molecular weight standards.

Electroblots were immersed in 0.05 % (w/v) copper phthalocyanine-3,4-tetrasulphuric acid tetrasodium salt in 12 mM HCl for 2-3 min then transferred to distilled water to assess transfer. At this stage blots could be sectioned into strips for probing with different primary antibodies etc. or trimmed to appropriate size. To remove copper stain electroblots were transferred to 12 mM NaOH solution and

agitated until destaining was complete. Blots were then briefly washed in distilled water, placing them in a position to be immunoprobed.

2.2.12.3 Immunoprobing of blots for protein components.

Nitrocellulose electroblots were initially washed in Tris-buffered saline (TBS) (50 mM Tris-HCl; 150 mM NaCl, pH 7.4) for 5 min to equilibrate the blot. Nitrocellulose blots were then blocked in 3% (w/v) Bovine serum albumin (BSA) in TBS for 1 hour at room temperature with agitation. Antibodies raised to cytoskeletal proteins were diluted to the appropriate concentration (see section 2.2.12.3: Antibody library) in 3% (w/v) BSA/TBS and incubated with the blot at 4°C overnight. Following primary antibody incubation the blot was washed 3 x 15 min in TBS/Tween (50 mM Tris-HCl; 150 mM NaCl; 0.1 % v/v Tween 20, pH 7.4) and then incubated with an alkaline phosphatase conjugated anti-primary IgG diluted in 3% (w/v) BSA/TBS to the appropriate concentration (see section 2.2.12.3: Antibody library) for 2 hours at room temperature. Nitrocellulose blots were again washed for 3 x 15 min in TBS/Tween followed by a single wash in dH₂O and then equilibrated in substrate buffer (0.75 M Tris base, pH 9.5) for 10 min. Blots were finally incubated in substrate buffer containing 44 µl nitro-blue tetrazolium (NBT) [50 mg/ml in 70 %, v/v, dimethylformamide] and 33 µl bromochloroindolyl phosphate (BCIP) [75 mg/ml in 100, % v/v, dimethylformamide]. To ensure optimal conditions nitrocellulose blots were developed in the dark until bands appeared. Development was stopped by extensive washing with dH₂O and dried by blotting between sheets of filter paper.

2.2.12.4 Antibodies.

Table 2.3 *Antibody library – working concentrations.*

Primary Antibodies	Isotype	Working Dilutions	
		Western Blotting	Immunofluorescence
Antibody (monoclonal)			
Anti-Neurofilament 200 (N52) (phosphorylated + non-phosphorylated)	Mouse IgG	1:500	1:100
Anti-Neurofilament-H (Ta51) (phosphorylation dependent epitope)	Mouse IgG	1:200	1:100
Anti-Neurofilament-H (RMd09) (non-phosphorylation dependent epitope)	Mouse IgG	1:200	1:100
Anti-actin	Rabbit IgG	1:100	1:50
Anti α -tubulin	Mouse IgG	1:2000	1:250
Antibody (polyclonal)			
Anti-recombinant human glial-derived neurotrophic factor	Chicken IgY	1:1000	-
Anti-ACTIVE™ JNK (pTPpY)	Rabbit IgG	1:5000	-
Anti-ubiquitin pAb: (<i>Ub-KLH</i> , 968215)	Rabbit IgG	1:1000	-
Anti-synuclein pAb (<i>PER 4</i>)	Rabbit IgG	1:500	-

2.2.12.5 Quantification of blots

Densitometric scanning of nitrocellulose blots was performed by using the image analysis system Quantiscan (Version 1.5, Biosoft) interfaced to a high resolution CCD video camera. Blots were digitised and the cytoskeletal protein levels were quantified by directly relating antibody reactivity to specific protein level. Using the features of the Quantiscan software program individual lanes were superimposed

over the region of interest from which a peak profile could be constructed. An arbitrary value of the peak area was then calculated and corrected for by subtracting the background profile; calculated as the subtraction of the mean of the lowest values within the lane.

2.2.13 Quantification of axon outgrowth.

Cultures differentiated in the presence or absence of sub-cytotoxic concentrations of MPTP in 24-well plates were washed in Tris-buffered saline (TBS) (50 mM Tris-HCl; 150 mM NaCl, pH 7.4) prior to fixation with ice-cold 90 % (v/v) methanol in TBS at -20°C for 20 minutes. Cells were stained using Coomassie brilliant blue for 2 min at room temperature. Cells were viewed using an inverted light microscope at 200 x magnification. The total number of cells and axon-like processes (whereby an axon was defined as a cellular extension greater than two cell body diameters in length) were recorded (Keilbaugh *et al.*, 1991). Five random fields were examined from each well, giving a total cell count of at least 200 cells per well.

2.2.14 Slide coating (Subbing)

Glass slides (25 x 75 mm) were placed in a suitable slide rack and immersed in 2 % (v/v) Decon detergent solution for 15 minutes. Slides were then washed thoroughly in running water to remove all traces of detergent. Excess water was drained and the slides then immersed in acetone for 2 minutes and then transferred to fresh acetone containing 2 % (v/v) 3-aminopropyltriethoxysilane for 5 minutes. Slides were removed and excess solution drained prior to washing the slides briefly in dH₂O. Slides were then allowed to dry at room temperature overnight prior to use.

2.2.15 Indirect Immunofluorescence analysis

N2a cells were initially plated out at 50,000 cells/ml in petri dishes containing 3-aminotriethoxysilane coated glass slides. Following overnight recovery cells were induced to differentiate in the presence or absence of 10 µM MPTP for 24 hours. Slides containing the attached cells were initially fixed in 90 % (v/v) methanol in TBS

at -20°C for 20 minutes. Cells were permeabilised for 10 min using 1 % (v/v) Triton in TBS at room temperature. Slides were then washed in TBS and incubated in blocking solution containing 3% (w/v) bovine serum albumin (BSA) in TBS for 1 hour at room temperature. Cells were incubated with specific monoclonal cytoskeletal antibodies diluted appropriately (see table 2.3) in 3 % (w/v) BSA in TBS, overnight in a humidified chamber. Following extensive washing in 4 x TBS/0.1 % (v/v) Tween-20 for a total of 1 hour, cells were incubated with fluorescein isothiocyanate (FITC)-conjugated goat anti-mouse or goat anti-rabbit immunoglobulins (1:40 in 3% (w/v) BSA in TBS) for 2 hours at room temperature. Slides were again washed in TBS/Tween for 1 hour prior to mounting with anti-fade mountant (Vectashield). Cells were viewed under a Leica CLSM confocal laser microscope equipped with epifluorescent optics.

2.2.16 Determination of ATP levels

ATP levels of N2a cells differentiated in the presence or absence of sub-cytotoxic concentrations of MPTP were assessed in 24-well plates. Following exposure, 400 µl medium from a total of 500 µl were aspirated from wells and replaced with 100 µl nucleotide releasing reagent. Plates were incubated for 5 minutes at room temperature with gentle agitation prior to transfer of the lysate to a white-walled 96-well luminometer plate. Plates were placed in an Anthos Lucy I luminometer where 20 µl ATP monitoring reagent were automatically dispensed into each well. Bioluminescence exhibited by each sample corresponded directly to cellular ATP levels and was recorded as relative light units. Samples were allowed to stand for 10 minutes prior to determination of ADP levels, to allow the ATP bioluminescent signal to decay. To determine ADP/ATP ratios 20 µl of ADP converting reagent (500 u/ml pyruvate kinase, 100 mM phosphoenol pyruvate, 2 mM potassium acetate) was dispensed into each well and an ADP₀ measurement taken (corresponding to ADP levels at time zero). Following 5 min incubation 20 µl of ATP monitoring reagent was again dispensed into each well and a further measurement taken (ADP₅, corresponding to ADP converted to ATP). ADP/ATP ratio was then determined by the equation:

$$\frac{ADP_5 - ADP_0}{ATP} = \text{ratio}$$

2.2.17 Analysis of mitochondrial membrane potential

Differentiating N2a cells were incubated in the presence and absence of 10 μ M MPTP for 24 hours. Medium was aspirated from the wells and replaced with phosphate buffered saline (PBS) containing a dual emission potential sensitive probe, JC-1 (10 μ g/ml final concentration). JC-1 solution was prepared by diluting a stock concentration of 5mg/ml in PBS and filtering the solution through a 0.45 μ M disc filter (Nalgene, UK). Cells were re-incubated for 60 min at 37°C in an atmosphere of 95 % air/5% CO₂. Cells were finally harvested in to 1 ml of fresh PBS and analysed using FACscan flow cytometer where between 2000-5000 events were analysed at an excitation wavelength of 485 nm. Results are expressed as the percentage of intact mitochondrial membrane potentials of the total population, i.e. j-aggregates (red) – healthy mitochondria and green monomers – unhealthy mitochondria.

2.2.18 Statistical analysis

Values are expressed as means \pm SEM. The Mann Whitney *U*-test was used to assess statistical differences between the control and neurotoxin treated samples using a 95 % confidence interval, when sample number < 12. The students *t* test was used when sample number > 12. In all cases, p values < 0.05 are considered to be statistically significant.

CHAPTER III

**Characterisation of MPTP-induced cytotoxicity in a
cell model system.**

3.1 Introduction

3.1.1 Cell models: Characterisation.

Administration of MPTP to mammalian species produces an experimental syndrome similar to Parkinson's disease (Burns *et al.*, 1983; Langston *et al.*, 1984a; Heikkila *et al.*, 1984a). This is primarily characterised by a degeneration of dopaminergic neurones in the pars compacta of the substantia nigra. However, resistance to MPTP toxicity exists and not all brain areas, cell types or dopaminergic neurones are equally affected (Boyce *et al.*, 1984; Langston *et al.*, 1984a). This specificity and cell selectivity is not entirely understood and is compounded by the complexity of the pathways and numerous cell types present in the central nervous system. This makes investigation of specific parameters very difficult.

In order to assess accurately MPTP neurotoxicity *in vitro*, a variety of approaches will undoubtedly be required, from complex systems to more simple systems such as cell lines. The ability of MPTP to exert toxicity on dopaminergic cells (e.g. pheochromocytoma cells, Denton and Howard, 1987) and non-dopaminergic cells (e.g. hepatoma cells, DiMonte *et al.*, 1986, and fibroblasts Cappelletti *et al.*, 1991) in culture, suggests that a common mechanism of action exists. Therefore the use of an appropriate, simplified *in vitro* system could provide a valuable tool giving insight to MPTP neurotoxicity.

With the intention of establishing a cell model system to investigate MPTP neurotoxicity, the cytotoxic effects of MPTP and its metabolite, MPP⁺, are to be examined on the rat C6 glioma and mouse N2a neuroblastoma cell line. The former is considered to be a valuable model of normal glia in brain, expressing both astrocytic and oligodendrocytic characteristics (see section 1.6.2). The latter is an established neuronal cell line that has been shown to be a useful tool for studies of neuronal development, differentiation and toxicity assessments, expressing appropriate receptors and neurotransmitters. Indeed, they are also able to differentiate both morphologically and biochemically displaying a typical neuronal phenotype. Their close association with catecholaminergic neurones makes them an appropriate candidate for this study (see section 1.6.1).

In vivo, glial cells are proposed to play an important role in the action of the neurotoxicant MPTP, since they are a primary locus of the MAO mediated conversion of MPTP (Chiba *et al.*, 1984). Because of this role in the bioactivation process, glial cells would be expected to be targets of the cytotoxic properties of MPP⁺. However, degeneration of glial cells, *in vivo*, does not appear to be an obvious neuropathological feature of MPTP exposure. Reactive proliferation of glial cells has instead been described in the striatum of animals injected with MPTP (Hess *et al.*, 1990). This gliosis may mask the damaging effects of MPTP towards glial cells, thereby explaining, at least in part, the failure to observe obvious cytotoxicity *in vivo*. Therefore a simplified *in vitro* cell system, which expresses similar characteristics to astrocytes within the brain, can be used to assess the genuine cytotoxicity of MPTP and its metabolite MPP⁺ towards glial cells. In addition, this will also provide a comparison with the neuronal model.

Initially the validity of the MTT viability assay will be assessed by comparison with two other viability assays, in order to establish a reliable cytotoxicity assay. The three assays measure different properties that can be related to cell death. The Coomassie blue assay measures total cell protein; whilst the lactate dehydrogenase leakage assay reflects cell membrane integrity and the MTT assay measures formazan production relating to cellular metabolism.

The loss of cell viability using the MTT reduction assay has often been used as a measure of mitochondrial function (e.g. Johnston *et al.*, 1993). The mechanism of MTT conversion has been questioned by Berridge *et al* (1996), who indicated that the cellular conversion of MTT to its formazan product could occur outside the mitochondria. Indeed, MTT is reduced by the majority of dehydrogenase enzymes and by pyridine cofactors NADH and NADPH to its formazan product. This however, does not invalidate the assay system from a cytotoxicity viewpoint, reflecting cellular metabolism, and has the added advantages of being relatively simple to perform, inexpensive and widely applicable.

The cytotoxic effects of MPTP and MPP⁺ will be assessed in both neuroblastoma and glioma cell lines in the mitotic and differentiating state. Differentiation will be achieved by incubating N2a and C6 cells in serum free medium supplemented with dbcAMP and sodium butyrate, respectively. These treatments have

the effect of reversing the transformed characteristics of the clone and for the cells to adopt a mature phenotype, thereby representing the *in vivo* situation more closely.

The toxic effects of MPTP towards cultured cells are thought to be related to the activity of MAO present, since both A and B isoforms of the enzyme catalyses the conversion of MPTP to its toxic metabolite at appreciable rates (Salach *et al.*, 1984). Therefore to further characterise the cell model systems the MAO status of proliferating and differentiating N2a/C6 cells will be assessed. Identification of the predominant isoform will be achieved using both MAO specific inhibitors (i.e. clorgyline and deprenyl) of activity and also RT-PCR to gene transcripts using MAO sequence-specific primers.

To determine total monoamine oxidase activity within the two cell lines a radiometric assay will be used. This will incorporate the use of ^{14}C -tyramine as substrate since it is oxidised to a similar extent by both MAO-A and MAO-B. Clorgyline will be used to inhibit MAO-A, deprenyl to inhibit MAO-B, in order to estimate the relative activities of MAO-A and MAO-B in the cells. Detection of MAO-A and/or MAO-B – mRNA in total cellular RNA extracts by RT-PCR will utilise sequence specific primers selected from full cDNA mouse sequences of MAO-A and MAO-B (see section 2.2.9.2).

MPTP-induced cell death may be related to the production of reactive oxygen species and therefore the antioxidant status of the cell lines used in this study will be addressed. Total glutathione levels will be investigated in both N2a and C6 cell lines, again under different growth conditions.

In accordance with the findings from this chapter, the sensitivity of the cells to MPTP and MPP^+ will be discussed in relation to the activity and expression of MAO, antioxidant status and the phase of cell growth (i.e. mitotic or differentiating state).

3.2 Results

3.2.1 Validation and optimisation of the MTT viability assay.

In order to use the MTT assay successfully, it was initially necessary to compare and optimise the incubation period of MTT within the two cell lines in culture. An optimal cell density of 50,000 cells/ml was used which produced a homogenous distribution of cells within the culture vessels producing absorbance readings within the range 0.0-1.5 absorbance units when analysed. Formazan production was observed to increase linearly when MTT was incubated over a period of 60 minutes within both the C6 and N2a and cell lines (Fig. 3.1). The conversion of MTT was reduced in the presence of 1 mM MPTP (48 hr exposure) over the 60 minute time period. This corresponded to the presence of shrunken cell morphology and the absence of formazan production in both C6 and N2a cells exhibiting signs of cell death (compare Fig 3.4 a, c with 3.4 b, d). Since the reaction proceeded in a linear manner over the time course of 60 minutes, a time point of 60 minutes was chosen as a suitable incubation period to assess cell viability in both N2a and C6 cell lines, as also chosen by Cookson *et al.* (1985) for toxicity assessments.

Validation of the MTT viability assay was achieved by comparing the viability data with data from other cell viability assays. The MTT assay was compared against the Coomassie blue total protein and LDH assay in mitotic C6 cells (Fig. 3.3) and differentiating N2a cells (Fig 3.4). Although the mean % cell viability reported using the Coomassie blue assay was slightly lower in both cell lines than the values reported by the MTT assay, a similar profile of cell viability was seen. The LDH assay also provided comparable cell viability profiles for both N2a and C6 cells exposed to MPTP over a 24 and 48 hour period, respectively.

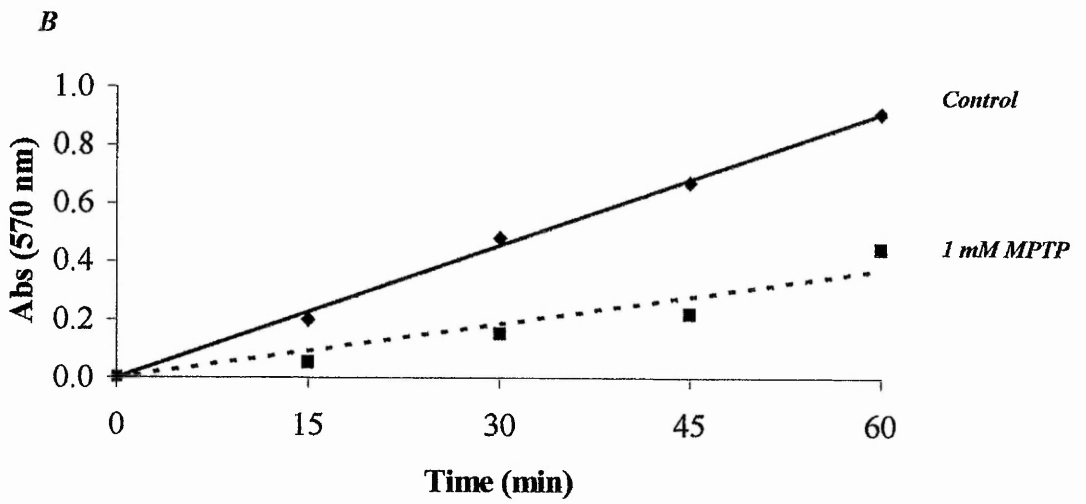
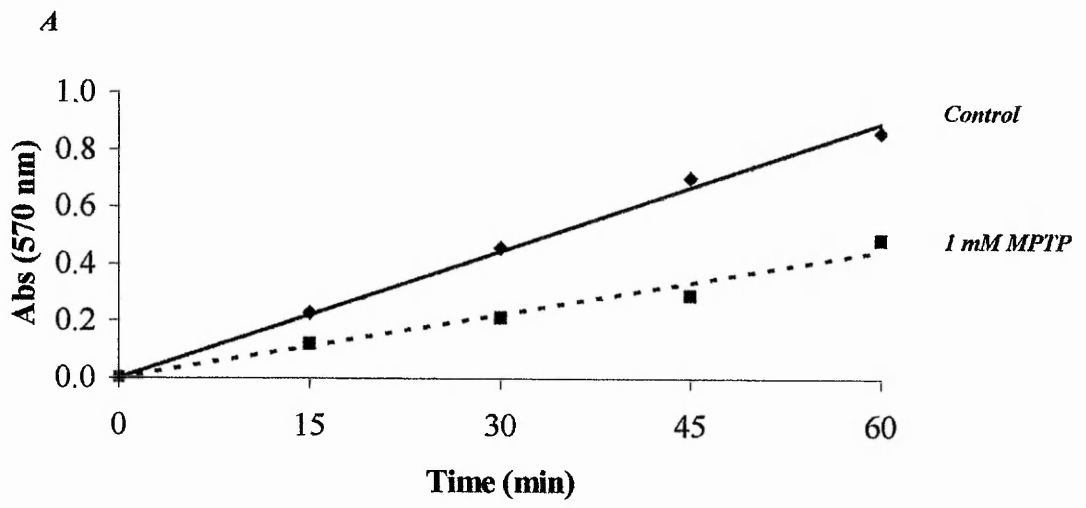


Figure 3.1 *Determination of optimal incubation time for the MTT viability assay in glioma and neuroblastoma cell lines.*

Cells were plated out in growth medium at a density 50,000 cells/ml and incubated overnight at 37°C in an atmosphere of 95% air/5% CO₂, to allow recovery. Growth medium was carefully aspirated from the wells and replaced with fresh growth medium alone (*control*) or growth medium + 1 mM MPTP (*1 mM MPTP*). Cells were re-incubated for a further 48 hours prior to assessment. MTT was added to each well (final conc. 0.5 mg/ml) at the appropriate time point prior to the end of the experiment. Medium was aspirated from the wells and the formazan product dissolved in DMSO prior to reading the absorbance (570 nm). (*A*) C6 glioma, (*B*) N2a neuroblastoma. Results are expressed as the mean of two and three separate experiments, respectively.

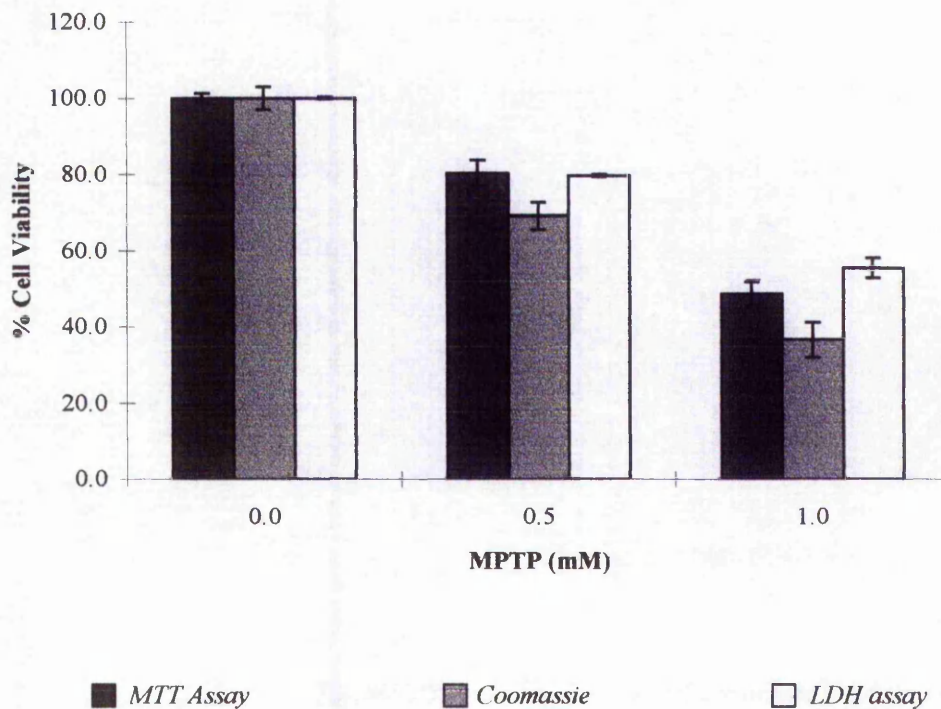


Figure 3.2 Validation of the MTT viability assay using mitotic C6 cells: Comparison with the Coomassie blue and LDH assay.

C6 cells were plated out in growth medium at a density 50,000 cells/ml prior to overnight incubation at 37°C in an atmosphere of 95% air/5% CO₂, to allow recovery. Growth medium was carefully aspirated from the wells and replaced with fresh growth medium alone or growth medium + MPTP. Cells were re-incubated for a further 48 hours prior to assessment. Cell viability was assessed via the MTT, Coomassie blue or LDH assay as described in Materials and Methods (section 2.2.6.2). Results are expressed as mean % cell viability ± SEM, where MTT, n=18; Coomassie, n=12; LDH, n=4.

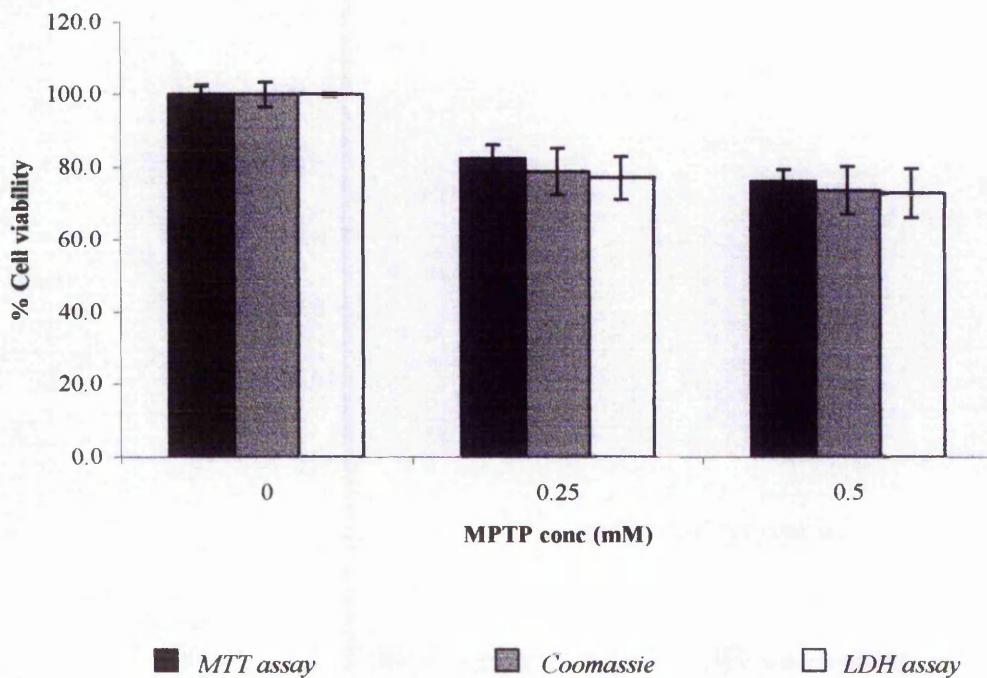


Figure 3.3 Validation of the MTT assay using differentiating N2a cells: Comparison with the LDH and Coomassie blue assays.

N2a cells were plated out in growth medium at a density 50,000 cells/ml prior to overnight incubation at 37°C in an atmosphere of 95% air/5% CO₂, to allow recovery. Growth medium was carefully aspirated from the wells and replaced with SFM containing 0.3 mM dbcAMP alone or SFM + 0.3 mM dbcAMP + MPTP. Cells were re-incubated for a further 24 hours prior to assessment. Cell viability was assessed via the MTT, lactate dehydrogenase or Coomassie blue assays as described in Materials and Methods (section 2.2.6.2). Results are expressed as mean % cell viability ± SEM, where MTT, n=12; LDH, n=11; Coomassie, n=8.

3.2.2 Characterisation of the cytotoxicity of MPTP towards neuroblastoma and glioma cells.

To initially establish the cytotoxicity of MPTP towards the two cell lines cultured cells were treated with increasing concentrations of MPTP under proliferative conditions for up to 48 hours. Cell death was assessed by the MTT reduction assay. The cytotoxic effect of MPTP on mitotic N2a and C6 cells was not evident after 24 hours treatment. However, when exposure time was increased to 48 hours a noticeable change in cellular morphology was evident, as demonstrated in Figure 3.4. MPTP induced a combination of cell shrinkage, cell lysis and detachment of cells from the monolayer which directly correlated to a decrease in viable cell MTT reduction. This phenomenon was more obvious in the N2a neuroblastoma cell line than the C6 glioma cell line with N2a cells exposed to 1 mM MPTP exhibiting ~70% cell death while C6 cells exhibiting ~50% cell death (Fig 3.5). In contrast, both mitotic C6 and N2a cells exposed to 125 μ M MPTP for 48 hours exhibited no significant cell death. Further calculation of MPTP-induced cell death by MTT reduction revealed N2a cells to express an $EC_{50} = 749 \mu$ M while C6 $EC_{50} = 998 \mu$ M (Table 3.1).

Following treatment with dbcAMP N2a cells exhibited a typical maturing neuronal morphology characterised by long unipolar or bipolar neurites. Exposure of N2a cells to relatively low doses of MPTP (i.e. 100 μ M) during the differentiation process produced a dramatic drop in cell viability after 48 hours exposure (Fig. 3.6B). However, at this point an increase in MPTP concentration did not produce dramatic increases in cell death. The sensitivity of N2a cells to MPTP had significantly increased when compared to N2a cells in the proliferative state ($EC_{50} = 32 \mu$ M, Table 3.1). Indeed, cytotoxicity was also evident in differentiating N2a cells after only 24 hours exposure to MPTP (Fig 3.6A) which had previously been absent in mitotic N2a cells exposed for same time period. However, cell death was much lower in differentiating N2a cells following 24 hr exposure than 48 hr; i.e. $EC_{50} > 1.0$ mM and $EC_{50} = 32 \mu$ M, respectively (Table 3.1). Viewing differentiating N2a cells exposed to MPTP for 24 hours, using phase contrast microscopy, revealed morphological alterations to the cell population, characterised by a loss of neurites.

C6 glioma cells induced to differentiate by serum withdrawal and addition of sodium butyrate exhibited a more flattened, fibroblast-like morphology and the presence of short processes. Differentiating C6 cells exposed to MPTP for 48 hours displayed no significant cell death (data not shown, $EC_{50} > 1.0$ mM) in contrast to mitotic C6 cells, which did display cytotoxicity following 48 hour exposure (see Fig 3.6). Cytotoxicity was evident in differentiating C6 cells when exposed to MPTP for 72 hours (Fig 3.7) although $EC_{50} = 1127$ μ M (Table 3.1). Phase contrast microscopy revealed that cells within this population that did not reduce MTT exhibited a round/shrunken morphology (results not shown) with many of the cells detached from the substratum.

3.2.3 Characterisation of the cytotoxicity of MPP^+ on neuroblastoma and glioma cells.

The cytotoxic capacity of MPP^+ (toxic metabolite of MPTP) was investigated under mitotic and differentiating conditions in the two cell lines. Both mitotic N2a and C6 cells exposed to MPP^+ (up to 1mM) over a 24 and 48 hour period exhibited no significant decrease in cell viability (Table 1; $EC_{50} > 1000$ μ M). A similar cytotoxic resistance to MPP^+ was seen when N2a and C6 cells were exposed under differentiating conditions for 24 hours (data not shown; table 3.1, $EC_{50} > 1000$ μ M). However, N2a cells induced to differentiate in the presence of 1 mM MPP^+ for 48 hours did show a proportion of cell death (24.8 %, $p < 0.01$) (Fig. 3.8B), but again the EC_{50} value could not be estimated (i.e. $EC_{50} > 1000$). Likewise, C6 cells induced to differentiate in the presence of increasing concentrations of MPP^+ demonstrated resistance, in terms of cell death, to MPP^+ than its parent compound MPTP. Cell viability assessment using the MTT assay revealed only a 15.1 % drop ($p < 0.01$) in viability (Fig. 3.8A) in these differentiating cells exposed to 1 mM MPP^+ .

The ability of ATP to increase MPP^+ -induced cell death was assessed in differentiating N2a cells. Firstly, the effect of ATP was evaluated by comparing the extent of cell death in the presence and absence of ATP alone. ATP itself was found to be cytotoxic to differentiating N2a cells, with increasing ATP concentrations causing a decrease in cell viability (Fig. 3.9). The addition of 2 mM ATP caused a 28.5 %

decrease in cell viability compared to control cells. However, the simultaneous addition of MPP⁺ and ATP (0.5-2.0 mM) produced a consistent increase in cell death when compared to the corresponding ATP control (assigned 100 % values to allow comparison with increasing MPP⁺ concentrations).

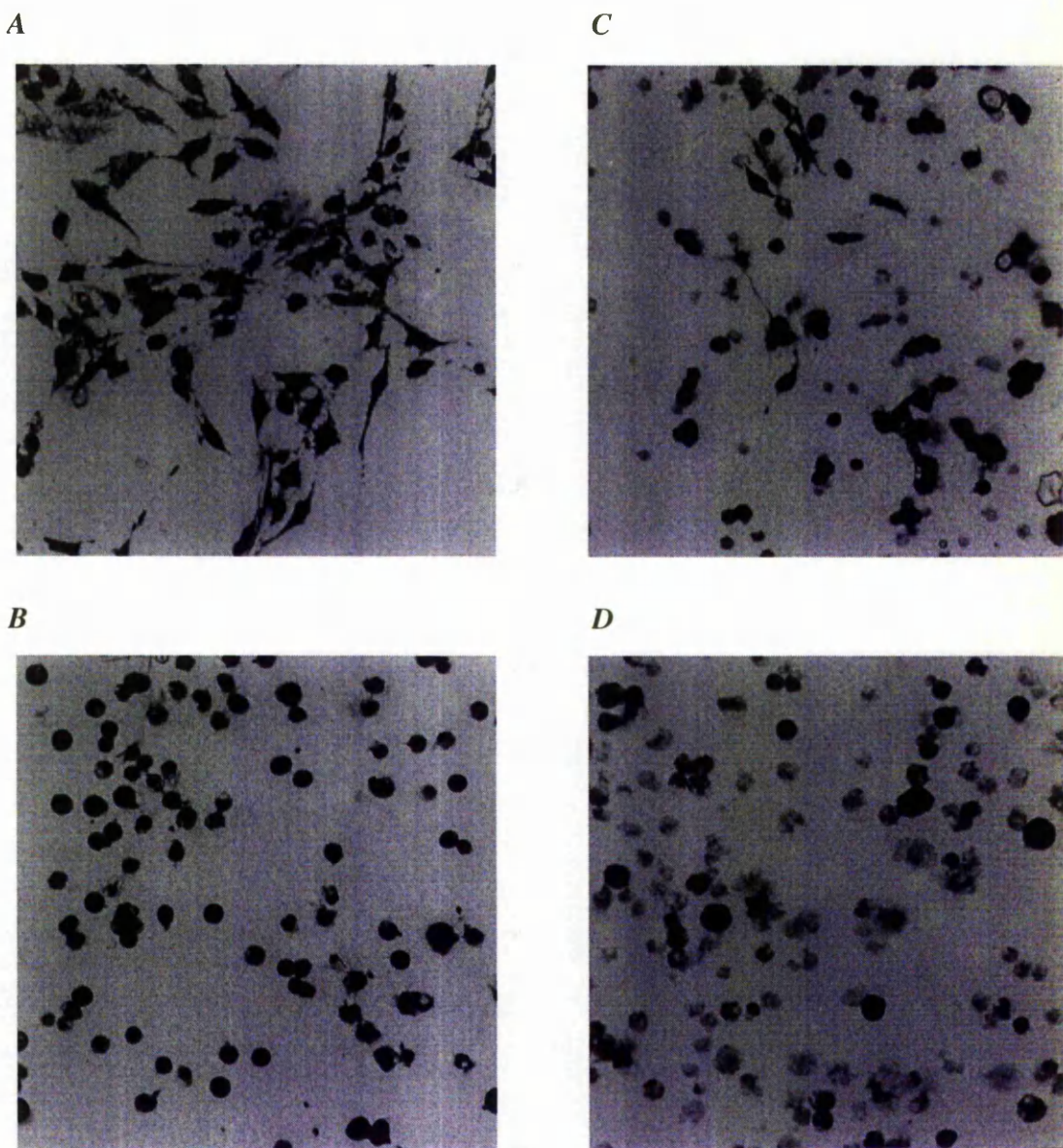


Figure 3.4 *MPTP-induced cytotoxicity on mitotic N2a and C6 cells.*

Cells were plated out at a density 50,000 cells/ml (C6: A, C; N2a: B, D) and incubated overnight at 37°C in an atmosphere of 95% air/5% CO₂, to allow recovery. Growth medium was carefully aspirated from the wells and replaced with fresh growth medium alone (A, B) or growth medium + 1 mM MPTP (C, D). Cells were re-incubated for a further 48 hours prior to the addition of MTT (final conc. 0.5 mg/ml) for 60 min. Cells were visualised using phase contrast microscopy at x 100 magnification.

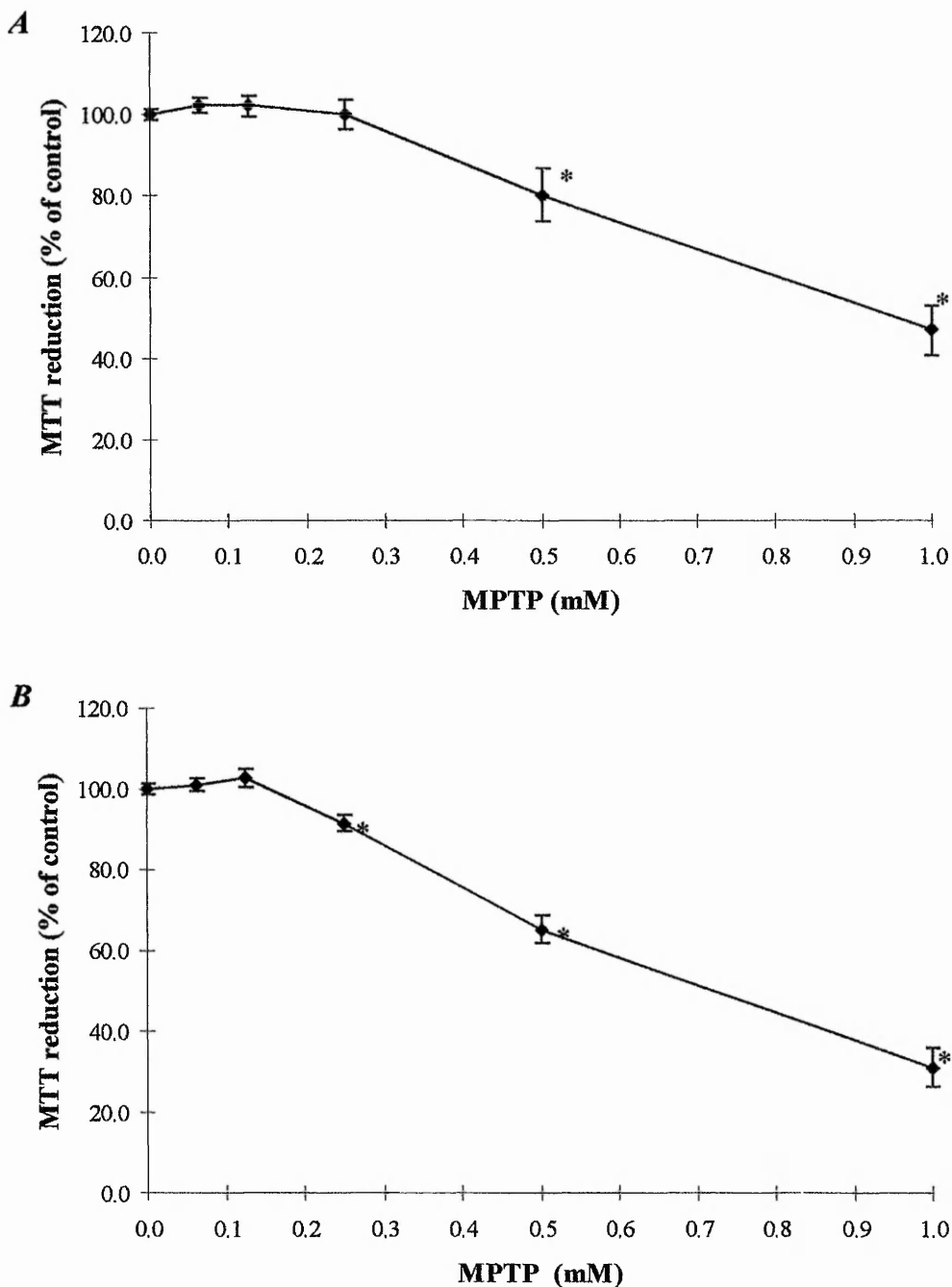


Figure 3.5 Cell viability assessment of mitotic C6 and N2a cell lines exposed to the neurotoxin MPTP for 48 hours.

C6 glioma (A) and neuroblastoma N2a (B) cells were plated out in growth medium at a density 50,000 cells/ml in 24-well plates prior to overnight incubation at 37°C in an atmosphere of 95% air/5% CO₂, to allow recovery. Growth medium was aspirated from the wells and replaced with fresh growth medium alone or growth medium + MPTP. Cells were re-incubated for a further 48 hours prior to assessment. Cell viability was assessed via the MTT reduction assay as described in (section 2.2.6.1). Results are expressed as mean % MTT reduction ± SEM. Statistical analysis was carried out using the student's t-test, where n=18 or n=20 for C6 and N2a, respectively. * p < 0.05 vs control.

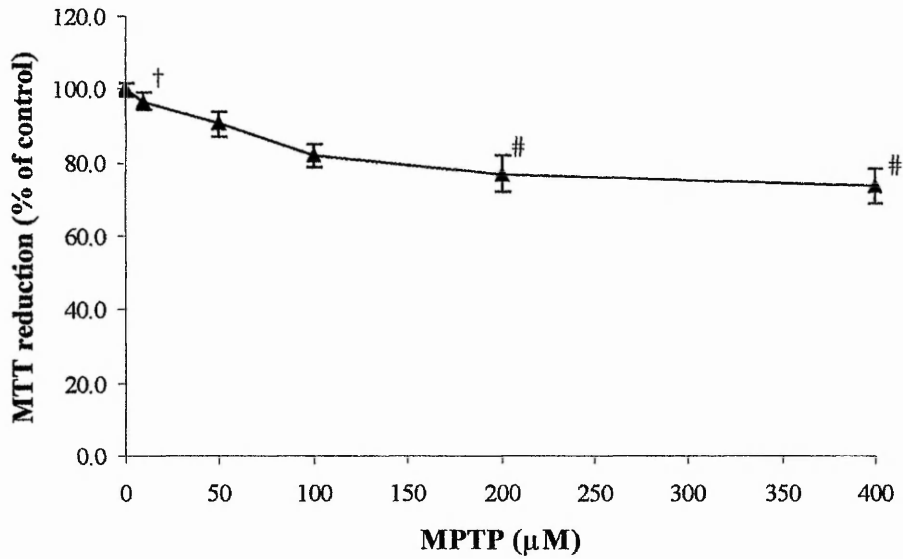
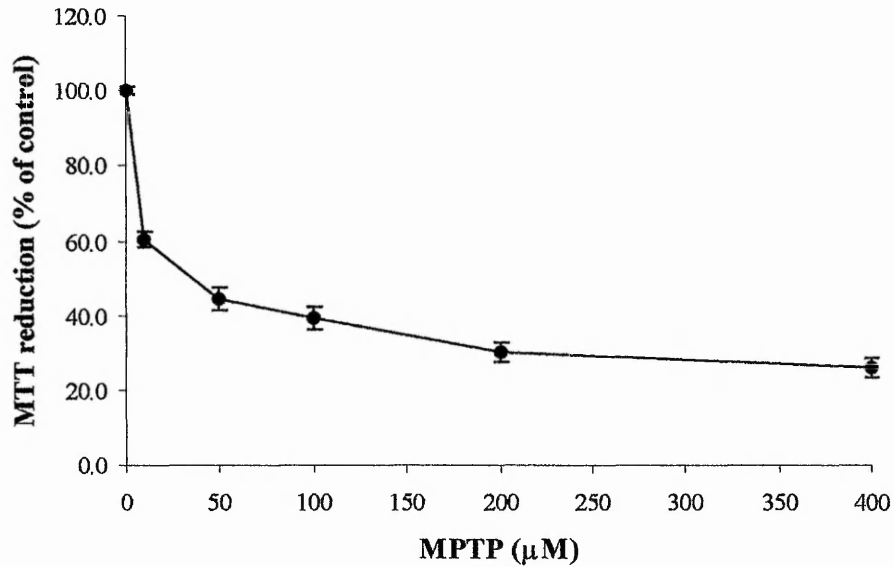
A**B**

Figure 3.6 Cell viability assessment of differentiating N2a neuroblastoma cells exposed to the neurotoxin MPTP for 24 and 48 hours.

N2a cells were plated out in growth medium at a density 50,000 cells/ml in 24-well plates prior to overnight incubation at 37°C in an atmosphere of 95% air/5% CO₂, to allow recovery. Growth medium was carefully aspirated from the wells and replaced with SFM containing 0.3 mM dbcAMP alone or SFM + 0.3 mM dbcAMP + MPTP. Cells were re-incubated for a further 24 hours (A) or 48 hours (B) prior to assessment. Cell viability was assessed via the MTT viability assay. Results are expressed as mean % MTT reduction \pm SEM. Statistical analysis was carried out using the student's t-test, where n=16 for both 24 and 48 hour exposure except #, where n=12. All values p < 0.05 vs control except †.

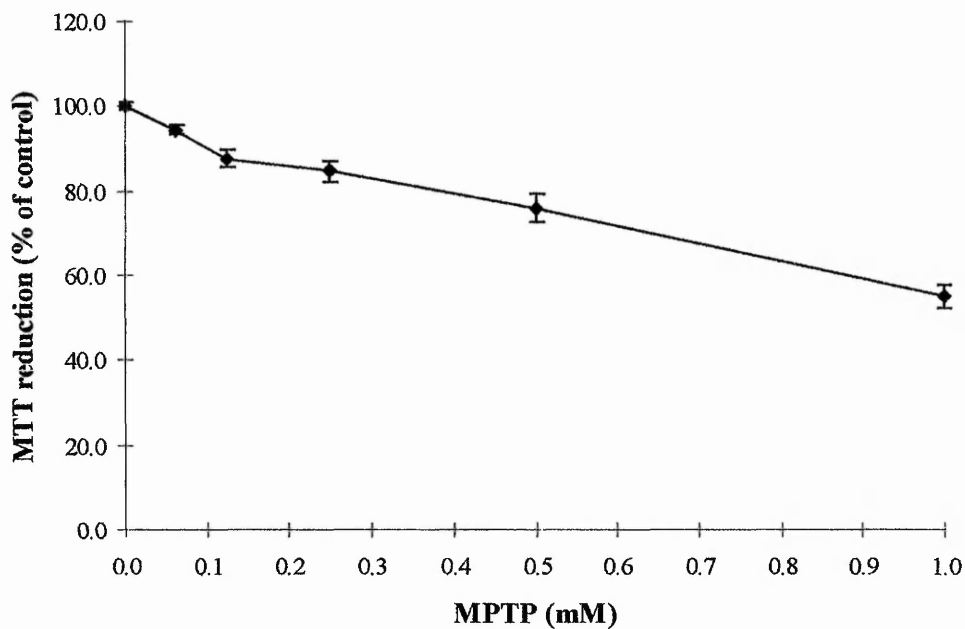


Figure 3.7 Cell viability assessment of differentiating C6 glioma cells exposed to the neurotoxin MPTP for 72 hours.

C6 cells were plated out in growth medium at a density 50,000 cells/ml in 24-well plates prior to overnight incubation at 37°C in an atmosphere of 95% air/5% CO₂, to allow recovery. Growth medium was aspirated from the wells and replaced with SFM containing 2 mM sodium butyrate alone or SFM + 2 mM sodium butyrate + MPTP. Cells were re-incubated for a further 72 hours prior to assessment. Cell viability was assessed via the MTT reduction assay as described in Materials and Methods (section 2.2.6.1). Results are expressed as mean % MTT reduction ± SEM. Statistical analysis was carried out using the student's t-test, where n=16. All values p < 0.05 vs control.

<i>Neurotoxin</i>	<i>Exposure time (hr)</i>	<i>EC₅₀ value (μM)</i>			
		<i>Mitotic N2a</i>	<i>Differentiating N2a</i>	<i>Mitotic C6</i>	<i>Differentiating C6</i>
MPTP	24	> 1000	> 1000	> 1000	> 1000
MPTP	48	749	32	998	> 1000
MPTP	72	-	-	-	> 1127
MPP ⁺	24	> 1000	> 1000	> 1000	> 1000
MPP ⁺	48	> 1000	> 1000	> 1000	> 1000
MPP ⁺	72	-	-	-	> 1000

Table 3.1 *Evaluation of the cytotoxicity of MPTP and MPP⁺ towards two neural cell lines in culture.*

Neuroblastoma N2a and glial C6 cells were exposed to MPTP and MPP⁺ over an increasing time period under mitotic and differentiating conditions. Cells were plated out in growth medium at a density 50,000 cells/ml in 24-well plates prior to overnight incubation at 37°C in an atmosphere of 95% air/5% CO₂, to allow recovery. Cells were exposed to the neurotoxin in either the mitotic or differentiating state for the stated time period, prior to assessment. Cell viability was assessed via the MTT reduction assay. The EC₅₀ values for cell death are expressed as approximate values that were estimated directly from the graphs using a line of best fit in the Microsoft Excel 7.0 package.

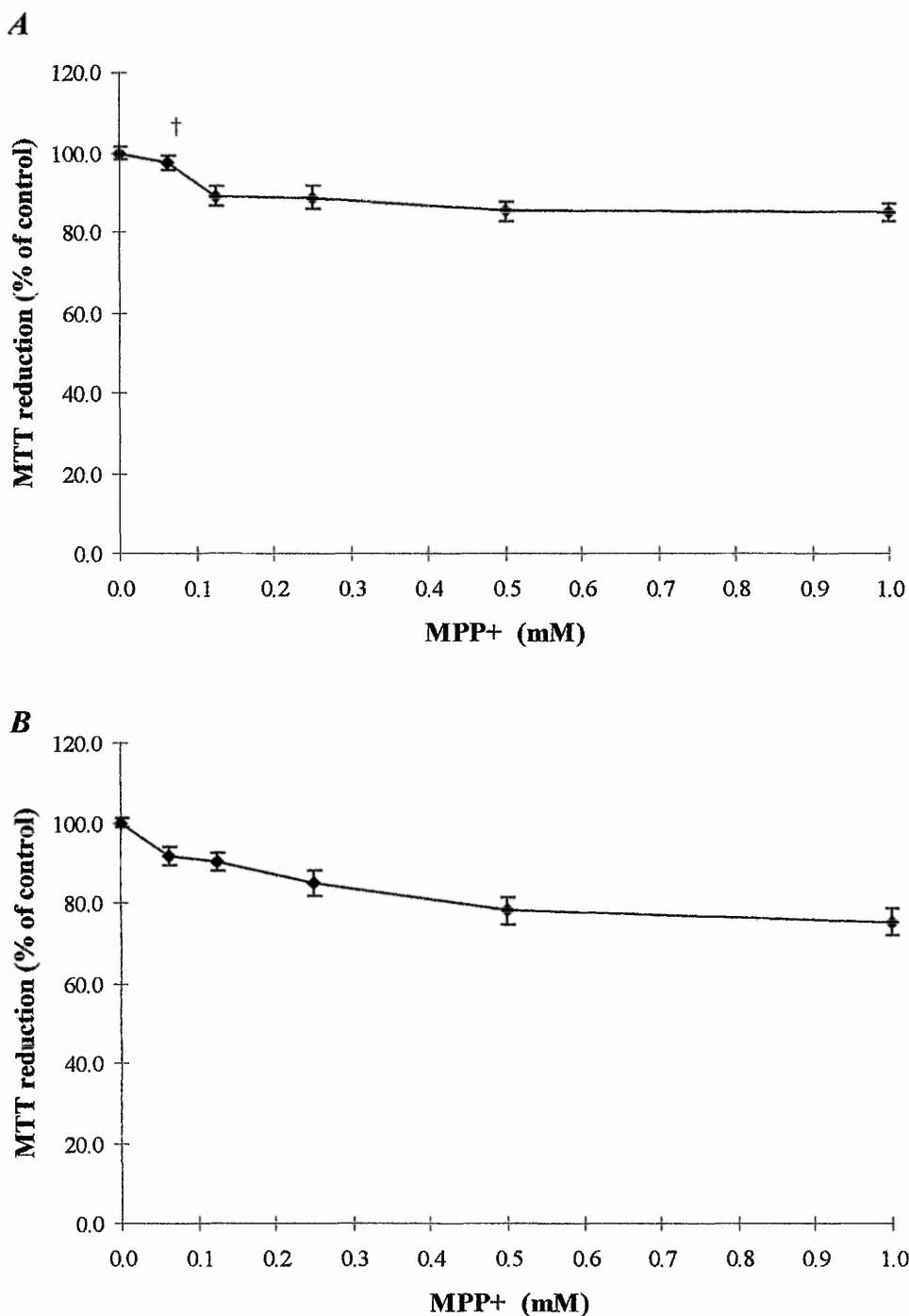


Figure 3.8 Cell viability assessment of differentiating C6 and N2a cells exposed to the neurotoxic metabolite MPP^+ .

C6 (A) and N2a (B) cells were plated out in growth medium at a density 50,000 cells/ml in 24-well plates prior to overnight incubation at $37^{\circ}C$ in an atmosphere of 95% air/5% CO_2 , to allow recovery. Growth medium was aspirated from the wells and replaced with SFM containing 2 mM sodium butyrate alone / SFM + 2 mM sodium butyrate + MPP^+ (C6) or SFM containing 0.3 mM dbcAMP alone / SFM + 0.3 mM dbcAMP + MPP^+ (N2a). Cells were re-incubated for a further 48 hours (N2a) or 72 hours (C6) prior to assessment. Cell viability was assessed via the MTT reduction assay. Results are expressed as mean % MTT reduction \pm SEM. Statistical analysis was carried out using the student's t-test, where $n=12$. All values $p < 0.05$ vs control except †.

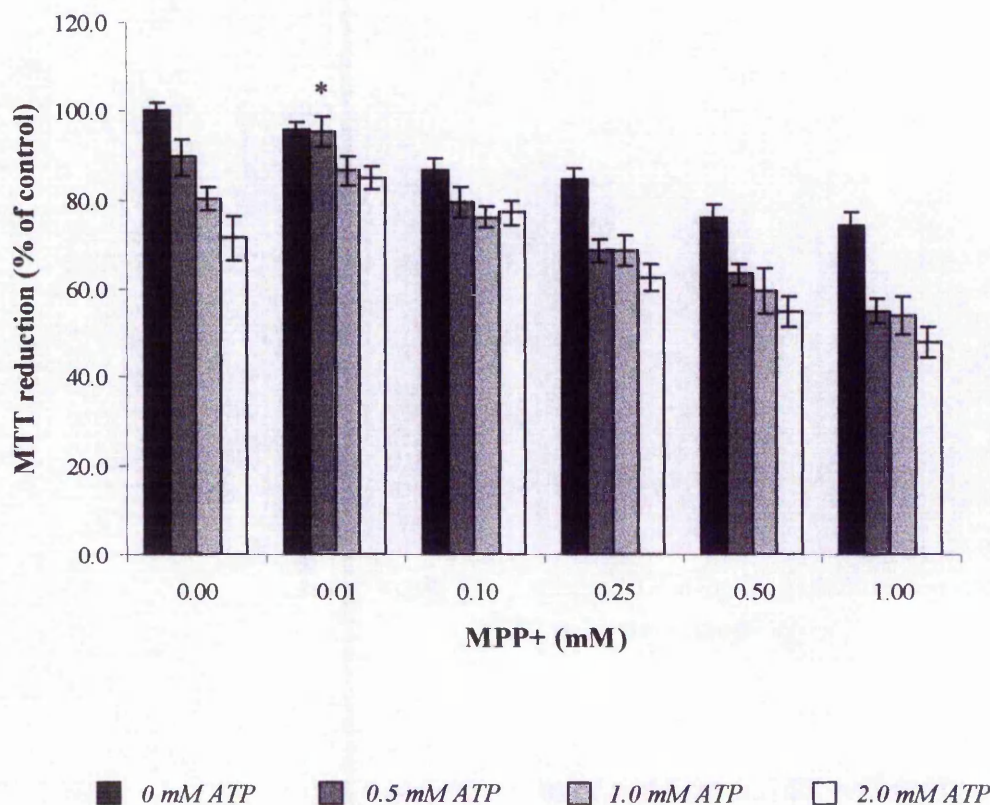


Figure 3.9 Cell viability assessment of differentiating N2a cells exposed to the neurotoxic metabolite MPP⁺ in the presence of ATP.

N2a cells were plated out at a density 50,000 cells/ml prior to overnight incubation at 37°C in an atmosphere of 95% air/5% CO₂, to allow recovery. Growth medium was carefully aspirated from the wells and replaced with SFM containing 0.3 mM dbcAMP in the presence or absence of MPP⁺ and ATP. Cells were re-incubated for a further 48 hours prior to assessment. Cell viability was assessed via the MTT reduction assay. The effect of ATP on cell viability was assessed by reference to '0 mM ATP' treatment. The effect of MPTP on cell viability was assessed by reference to the corresponding control. Results are expressed as mean % MTT reduction ± SEM, compared to the corresponding ATP control (assigned 100 % value). Statistical analysis was carried out using the Mann Whitney *U*-test, where n=7. Results obtained in the presence of ATP were compared against the results obtained in its absence. All values p < 0.05 vs control except *.

3.2.4 Characterisation of monoamine oxidase activity in neuroblastoma and glioma cells.

Total MAO activity, using tyramine as a substrate was assessed over a time course using C6 and N2a cells at a constant cell density. The ability of MAO, derived from C6 cells, to oxidise tyramine appeared to increase linearly over a time period of approximately 75 minutes (Fig. 3.10a). Similarly, MAO activity in N2a cells was linear for 60 min, although activity was significantly lower in this cell line (Fig. 3.10b). Under these conditions (cell density and substrate concentration) a time point of 60 minutes was chosen as representative of the initial rate of total MAO activity.

Total MAO activity measurements in both mitotic and differentiating C6 and N2a cells can be seen in Table 3.2. Mitotic C6 cells expressed a total MAO activity of 266.99 pmol/min/mg protein, while mitotic N2a cells expressed a significantly lower (greater than 10-fold) total MAO activity of 12.76 pmol/min/mg protein.

In order to assess any changes in the total MAO activity, the two cell lines were induced to differentiate in serum-free medium supplemented with dbcAMP (N2a) and sodium butyrate (C6). Any change in MAO activity was calculated compared to cells cultured under proliferating/mitotic conditions (assigned as controls). Differentiated N2a cells again expressed a relatively low total MAO activity of 14.73 pmol/min/mg protein. Although small, this represents a significant increase (17.94%) in total MAO activity, compared to mitotic cells (Table 2). This increase in total MAO activity in the N2a cell line following differentiation was reflected in the C6 cell line but to a greater extent. C6 cells induced to differentiate expressed a total MAO activity of 339.23 pmol/min/mg protein; a mean % increase of 30.68%, compared to mitotic C6 cells. Although independent, the increases in MAO activity occurred alongside changes in cell morphology in both cell lines, as described previously.

3.2.4.1 Determination of MAO isoform expression in C6 and N2a cell lines.

Examination of the effects of the specific MAO inhibitors clorgyline and deprenyl (MAO-A and MAO-B inhibitors, respectively) on MAO activity was carried out to assess which isoforms were present (Fig. 3.11). MAO activity in C6 cells was more sensitive to clorgyline than to deprenyl. Clorgyline inhibited MAO activity at a

concentration approximately three orders of magnitude lower than deprenyl (i.e. 5×10^{-9} M clorgyline; 5×10^{-6} M deprenyl) based on IC_{50} values. This would suggest a predominance of MAO-A activity within the C6 cell line. However, the inhibitor profiles obtained with clorgyline and deprenyl indicate approximately 95 % MAO-A and approximately 5% MAO-B activity (ratio 19:1). The fact that both inhibitors are not entirely specific and can inhibit both MAO isoforms in a concentration dependent manner makes this estimation more difficult.

Due to the low MAO activity levels in N2a cells, it was not possible to use inhibitors to confidently determine the isoform profile. However, total MAO activity was inhibited in the N2a cell line using concentrations as low as 10^{-9} M clorgyline, while a 10^{-6} M deprenyl had a similar total inhibitory effect (data not shown). Although the data for this is limited the results do suggest a predominance of MAO-A, as seen in the C6 cell line.

3.2.4.2 Monoamine oxidase mRNA profiles in C6 and N2a cells.

MAO radioactivity assays performed on C6 and N2a cells (see above) revealed the presence of different MAO total activities in both cell types. In addition, inhibitor studies provided indications of the predominant MAO isoform. The technique of RT-PCR was used to enhance and consolidate the MAO isotype profile in both cell lines. RT-PCR results using MAO-A and MAO-B specific primers confirmed the presence of mRNA coding for both isotypes in the C6 and N2a cell lines. As predicted from primer design definitive products were generated for each isoform; a 211 bp product and a 199 bp product for MAO-A and MAO-B, respectively. It is recognised that quantitative conclusions are difficult to make using RT-PCR, however, in an attempt to qualify the predominant isoform within each cell type a constant amount of total RNA (5 μ g) was used as template. Assuming efficiency of amplification is equal for both isotypes, both the C6 and N2a cells exhibited a predominance of MAO-A mRNA with C6 cells expressing a greater signal compared to N2a cells (Fig 3.12a). However, both cell lines also expressed definite MAO-B mRNA, albeit to a much lesser extent than MAO-A mRNA. RT-PCR was also carried out on total RNA isolated from C6 and N2a cells following differentiation. The use of equal RNA concentrations (i.e. 5 μ g) was again

used in an attempt to qualify the MAO profiles present in the two cell lines. Differentiation of C6 and N2a cells increased the individual signals obtained for both MAO-A and MAO-B mRNA (Fig 3.12b). The increase in MAO expression was again characterised by a predominance of MAO-A mRNA in both differentiating C6 and N2a cells.

3.2.5 Analysis of total glutathione levels in N2a and C6 cells.

In order to obtain an indication of antioxidant status within C6 and N2a cells total glutathione levels (GSH + GSSG) were determined using the DTNB-GSSG reductase recycling assay. Comparison of mitotic C6 glioma and N2a neuroblastoma cells revealed the two cell types to express comparable levels of total glutathione of 14.10 nmol/ μ g protein and 13.80 nmol/ μ g protein, respectively (Table 3.3). Treatment of C6 cells with serum free medium supplemented with 2 mM sodium butyrate to induce differentiation produced a concomitant rise in glutathione levels to 24.90 nmol/ μ g protein; an increase of 70.2%. Likewise, N2a cells induced to differentiate for 24 hours produced a 45.5 % increase in glutathione levels compared to mitotic N2a cells.

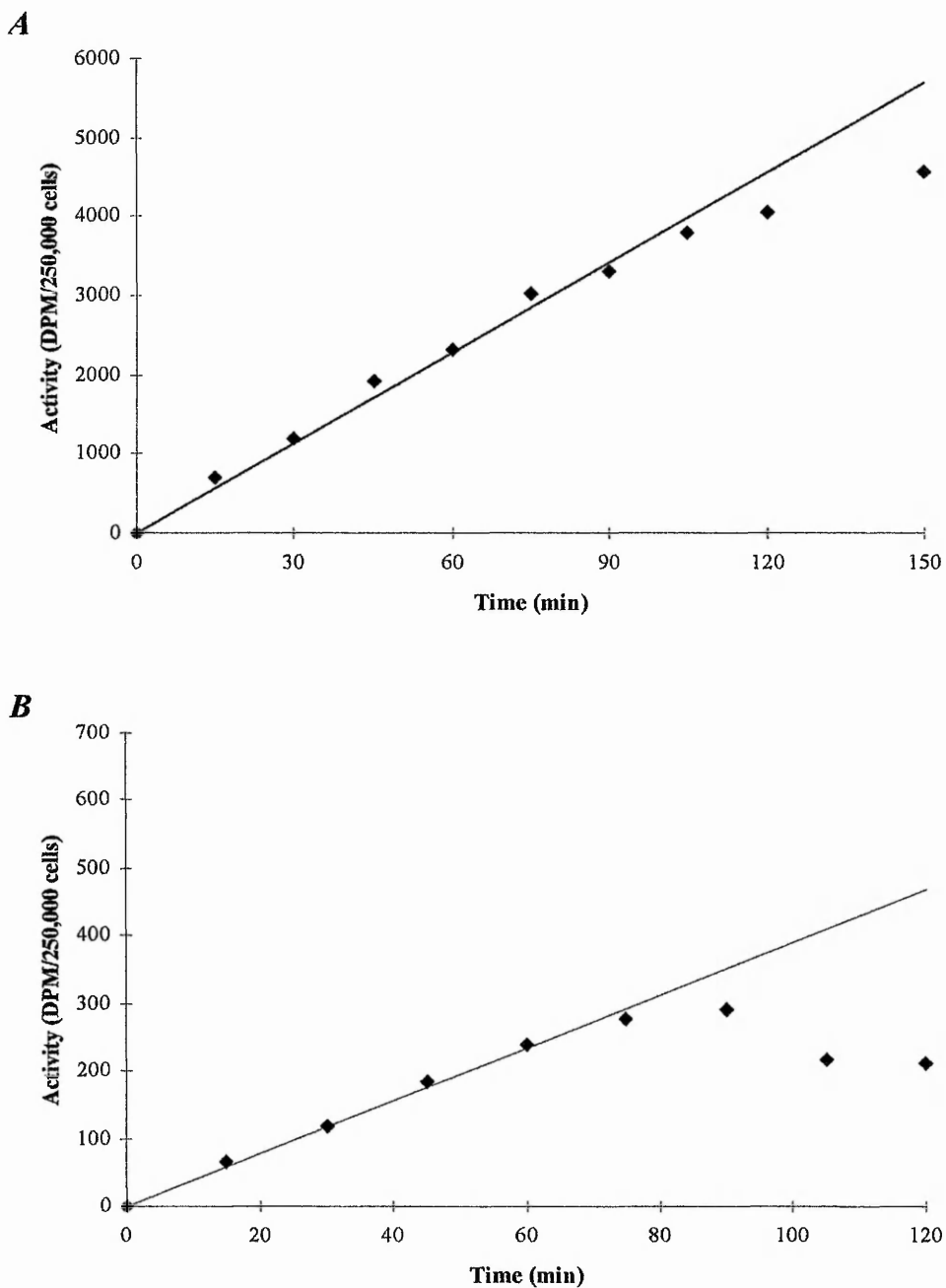


Figure 3.10 Time course for the optimisation of MAO activity determination in C6 and N2a cell lines.

C6 (A) and N2a (B) cells were seeded into T25 flasks and grown to approximately 80-100% confluency in an atmosphere of 95% air/5% CO₂. Cells were then mechanically detached from the monolayer and harvested by centrifugation at 1000 rpm for 5 minutes prior to a cell count using a haemocytometer. Equal cell aliquots were used per sample tube for the assessment of total MAO activity using the radiometric method (section 2.2.9.1). Samples were incubated at 37°C for the appropriate time in the presence of 1 mM ¹⁴C-tyramine (1 mCi/mmol) as substrate. Radioactive products were counted in a toluene based scintillation mixture at an efficiency > 90%. Blank values were subtracted from sample values. Results are the mean of two experiments each carried out in duplicate.

Cell type	Cell status (Activity = pmol / min / mg protein)		% Increase (Total MAO Activity)	p value
	Mitotic	Differentiated		
Neuroblastoma (N2a)	12.76 ± 3.43	14.73 ± 3.48	17.94 ± 6.90	0.0347
Glioma (C6)	266.99 ± 33.61	339.23 ± 71.89	30.68 ± 8.45	0.0377

Table 3.2 Total monoamine oxidase activity levels of C6 and N2a cells in the mitotic and differentiated state.

Cells were plated at a cell density of 100,000 cells/ml and incubated for 24 hr at 37°C in an atmosphere of 95% air/5% CO₂, to allow recovery. Cells for MAO activity assessment in the mitotic state were incubated in fresh growth medium for a further 24 hr. Cells for MAO activity assessment in the differentiated state were treated as follows:

C6 cells were induced to differentiate with SFM containing 2 mM sodium butyrate. Cells were re-incubated for a further 24 hours prior to assessment.

N2a cells were induced to differentiate with SFM containing 0.3 mM dbcAMP. Cells were re-incubated for a further 24 hours prior to assessment.

Cells were counted and aliquots removed for protein determination. Equal cell aliquots of 250,000 cells were used per sample tube for the assessment of total MAO activity. Samples were incubated for 60 min at 37°C in the presence of 1 mM ¹⁴C-tyramine (1 mCi/mmol) as substrate. Blank values were subtracted from sample values. Results are expressed as mean Activity (pmol / min / mg protein ± SEM), where n=6 (N2a) and n=5 (C6) (comprised of at least five replicates). Statistical analysis was carried out using the Mann-Whitney U-test to compare MAO activity in the mitotic and differentiated state. Both p values < 0.05 compared to MAO activity in the mitotic state (control).

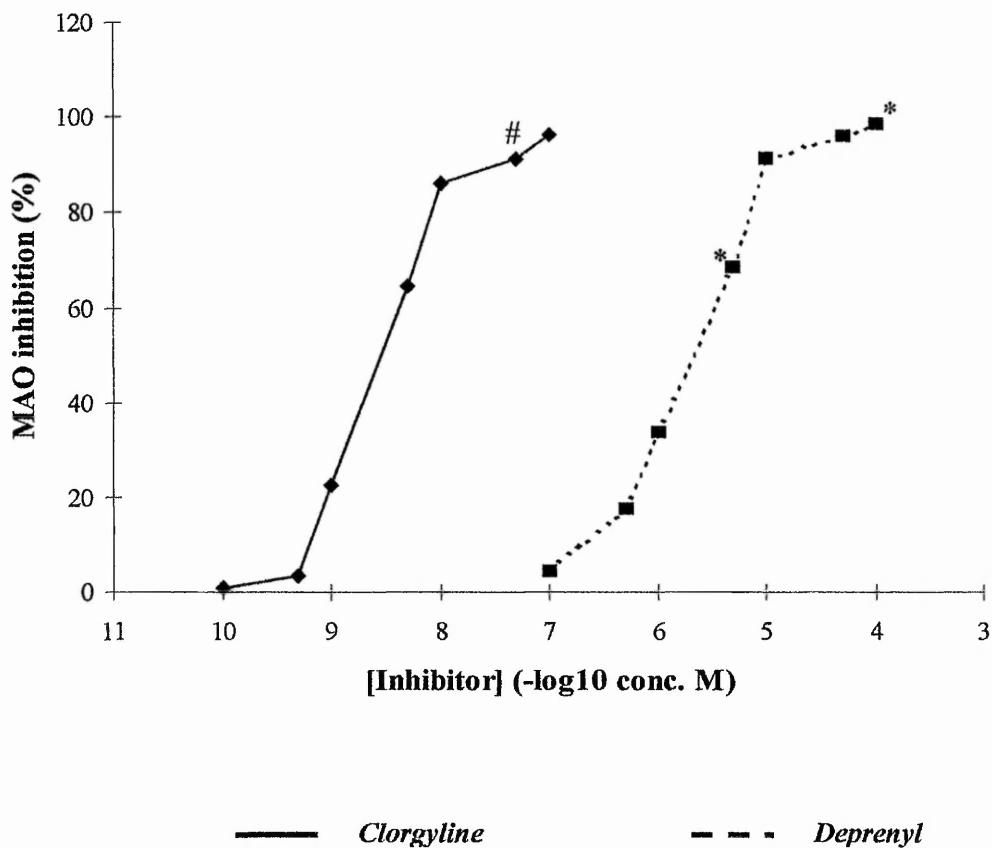
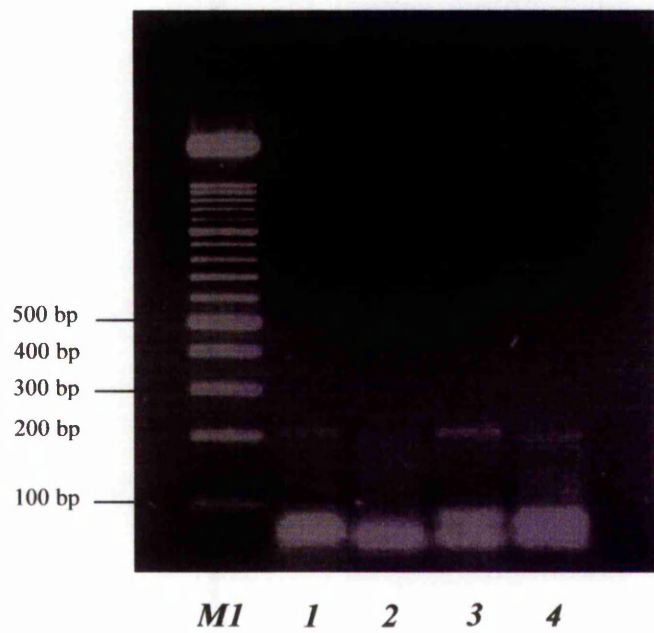


Figure 3.11 Inhibition of monoamine oxidase activity in mitotic C6 cells by clorgyline and deprenyl.

C6 cells were seeded into T25 flasks and grown to approximately 80-100% confluency in an atmosphere of 95% air/5% CO₂. Cells were harvested prior to a cell count. Equal cell aliquots of 250,000 cells were used per sample tube for the assessment of total MAO activity using the radiometric method (section 2.2.9.1). Samples were incubated for 60 min at 37°C in the presence of 1 mM ¹⁴C-tyramine (1 mCi/mmol) and increasing concentrations of MAO inhibitor (clorgyline or deprenyl). Blank values were subtracted from sample values and the results expressed as mean % inhibition of MAO activity compared to corresponding controls, where n=5, except* (where n=3) and # (where n=2).

A



B

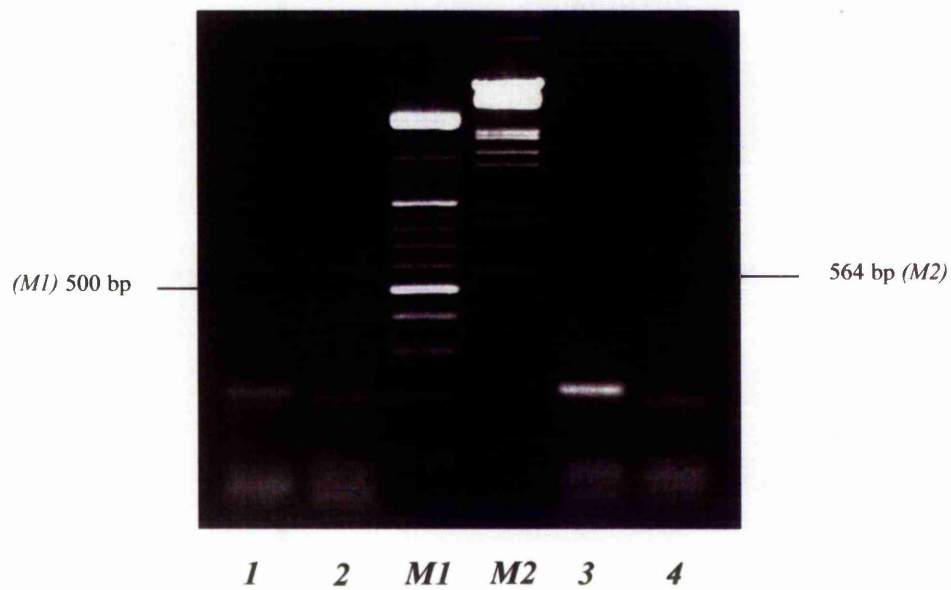


Figure 3.12 *Identification of MAO-A and MAO-B mRNA present in the mitotic and differentiated C6 and N2a cells.*

Cells were plated at a cell density of 100,000 cells/ml in growth medium. The cells were incubated for 24 hr at 37°C in an atmosphere of 95% air/5% CO₂, to allow recovery. C6 and N2a cells for MAO mRNA assessment in the mitotic state were continually incubated in fresh growth medium for a further 24 hr. C6 and N2a cells for MAO mRNA assessment in the differentiated state were treated as follows:

C6 cells were induced to differentiate by replacing the growth medium with SFM containing 2 mM sodium butyrate. Cells were re-incubated for a further 24 hours prior to assessment.

N2a cells were induced to differentiate by replacing growth medium with SFM containing 0.3 mM dbcAMP. Cells were re-incubated for a further 24 hours prior to assessment.

Sequence specific MAO-A or MAO-B primers were used to for reverse transcription of C6 and N2a total RNA (5 µg). Reverse transcription products were then amplified by PCR and revealed using electrophoresis on ethidium bromide stained agarose gels (1.8 %).

A. mitotic

- | | | | |
|---------------|---------------|----------------|----------------|
| 1. C6 – MAO-A | 2. C6 – MAO-B | 3. N2a – MAO-A | 4. N2a – MAO-B |
|---------------|---------------|----------------|----------------|

B. differentiated

- | | | | |
|---------------|---------------|----------------|----------------|
| 1. C6 – MAO-A | 2. C6 – MAO-B | 3. N2a – MAO-A | 4. N2a – MAO-B |
|---------------|---------------|----------------|----------------|

M1 = 100 base pair ladder

M2 = Lamda DNA *Hind* III marker

Cell type	Total Glutathione (GSH + GSSG) (nmol / mg protein)		% Increase (Total Gluathione)	p value
	Mitotic	Differentiated		
Neuroblastoma (N2a)	13.80 ± 5.53	20.08 ± 5.19	45.5%	0.0214
Glioma (C6)	14.10 ± 5.03	24.00 ± 8.12	70.2%	0.0116

Table 3.3 Analysis of total glutathione levels (GSH + GSSG) in C6 and N2a cells (mitotic and differentiated state).

Cells were plated at a cell density of 100,000 cells/ml and incubated for 24 hr at 37°C in an atmosphere of 95% air/5% CO₂, to allow recovery. Mitotic cells were incubated in fresh growth medium for a further 24 hr prior to analysis. Cells for glutathione assessment in the differentiated state were treated as follows:

C6 cells were induced to differentiate by replacing the growth medium with SFM containing 2 mM sodium butyrate. Cells were re-incubated for a further 24 hours prior to assessment.

N2a cells were induced to differentiate by replacing growth medium with SFM containing 0.3 mM dbcAMP. Cells were re-incubated for a further 24 hours prior to assessment.

Following extraction samples were analysed for protein content and total glutathione levels. Total glutathione is expressed as nmol/mg protein, where n = 7. Statistical analysis was carried out using the Mann-Whitney *U* test to compare mitotic against differentiated cells. Both p values < 0.05 compared to glutathione levels in the mitotic state (control).

3.3 Discussion

3.3.1 Cytotoxicity assay validation.

The data presented at the beginning of this chapter (Fig 3.1, 3.2 and Fig 3.3.) validates the use of the MTT reduction assay for monitoring cell viability. Initially, cell death was measured by monitoring three independent parameters (i.e. total cell protein, cell membrane integrity, and cellular metabolism) in both the C6 and N2a cell line. Several methods have been developed to assay cytotoxicity, however all have associated problems. Although it has been suggested that the MTT assay may be prone to insensitivity at high cell densities, comparison of this assay with the additional Coomassie and LDH cytotoxicity assays shows there was a strong correlation between the results obtained with these assays and the preferred MTT assay.

The apparent increase in cell death reported by the Coomassie blue assay could in fact be due to the assay method which involves prior fixation of the cell monolayer by the addition of methanol which must then be removed prior to staining and washing. These manipulations on a previously stressed population may cause greater cell detachment and thereby represent an overestimate of cell death. This may be countered by the fact that because the assay measures total protein it will only distinguish dead cells if they have become completely detached from the monolayer. Although the preliminary results obtained using the Coomassie blue assay were comparable to the other assays the limitations described suggest it would not be the ideal candidate for further cytotoxicity assessments.

The major disadvantage of the LDH assay was time consumption due to the fact that the rate of NADH oxidation must be measured within the supernatant and total cell lysate for each well. This would involve continual environmental changes during processing. In comparison, the MTT assay requires only one measurement and produced a comparable viability profile. The comparison of the MTT assay with the Coomassie blue and LDH assays in both proliferating and differentiating cells demonstrates the usefulness and validity of the MTT assay for use within the proposed cellular models. Indeed, the assay has been used successfully in other studies to measure toxicity (e.g. Cookson *et al.*, 1995).

3.3.2 Cytotoxicity of MPTP towards neuroblastoma and glioma cells.

Following 48 hours exposure, mitotic N2a cells exhibited greater sensitivity to MPTP than mitotic C6 cells with EC_{50} values of 749 μ M and 998 μ M, respectively. A similar study carried out by Notter *et al.*, (1988) using C6 glioma cells and a subclone of the N2a cell line, termed N₂AB-1 found these cell lines to be relatively resistant to 33.7 μ M MPTP over a similar time course. Likewise, a toxicological screen carried out by Cookson *et al.*, (1995) employing C6 cells only and MPTP, among other toxicants, found no significant cell death when mitotic C6 cells were exposed to a relatively high MPTP concentration of 4.7 mM, over a 24 hour period. Although at first the present data appears conflicting, Notter *et al.* (1988) used MPTP up to a concentration of 33.7 μ M only, while Cookson *et al.* (1995) exposed confluent C6 cultures for only 24 hours. In addition, Cookson cultured C6 cells in a high glucose medium supplemented with an increased serum concentration of 17.5 %; factors that alone or in combination, could influence cell sensitivity to toxicants (Bohets *et al.*, 1994). In the present study there was no significant cell death in either the N2a or C6 cells exposed to MPTP concentrations up to 125 μ M and 250 μ M, respectively, over a 48 hour period. However, concentrations above this did inflict a cytotoxic response. Thus it would seem that MPTP is certainly toxic to these cells, but only above a threshold concentration, the latter dependent on exposure time. The fact that increasing MPTP concentration over a short time period (i.e. 24 hours) does not increase cytotoxicity suggests that diffusion and metabolism of the neurotoxin could be the rate limiting factors. Therefore the cytotoxic effects of MPTP to mitotic neuroblastoma and glioma cells observed after 48 hour exposure are proposed to be the consequence of increased MPTP oxidation by MAO to its toxic metabolite, MPP⁺.

MPTP was markedly more cytotoxic to differentiating than mitotic N2a cells following a 48 hour exposure with EC_{50} values being 32 μ M and 749 μ M, respectively. Although cell death was also evident in differentiating N2a cells after 24 hours an EC_{50} value could not be calculated. However, phase contrast microscopy revealed MPTP to exert some early signs of toxicity. Differentiating N2a cells exhibited an inability to extend neurites and cell detachment from the substratum, while some cells exhibited cell surface blebs and a reduction in cell volume

(observations only). It is likely that MAO plays an important factor in this differential sensitivity. MAO activity studies presented in this chapter suggest mitotic N2a cells to express a low, predominantly MAO-A activity. Thus the conversion of MPTP to MPP⁺ would be expected to be low. On differentiation N2a cells exhibit elevated mRNA levels coding for both MAO-A and MAO-B accompanied by an increase in total MAO activity (17.94%), factors that lead to an observed increase in cell death. Indeed, elevation of MAO activity levels in PC12 cells results in a similar phenomenon, i.e. increased sensitivity to MPTP (Wei *et al.*, 1996).

The increased resistance to MPTP exhibited by glial C6 cells, when compared to neuroblastoma N2a cells, is a phenomenon analogous to the *in vivo* situation. Glial cells are thought to play an essential role in the bioactivation of MPTP *in vivo*. However, they also appear to be able to withstand insult while the susceptible dopaminergic neurones are readily destroyed by the neurotoxin. The differential sensitivities of N2a and C6 cells to MPTP evident in this *in vitro* study could be due to a number of factors. For example it could relate to MPTP-induced inhibition of mitochondrial respiration (Nicklas *et al.*, 1985). This inhibition leads to depletion of ATP stores and therefore the energy requirements of a particular cell type could be a factor in determining cell sensitivity. Indeed, work carried out using a PC12 cell line variant resistant to MPTP suggests increased resistance could occur through alterations in energy metabolism (Denton and Howard, 1987). C6 and N2a cells may be able to maintain ATP stores differently by switching metabolism to favour ATP production via glycolysis. An indication that this has occurred in the MPTP treated cells following a 48 hr exposure (but not 24 hrs exposure) was acidification of the growth medium (i.e. slight discoloration of growth medium due to the pH indicator phenol red). Initial inhibition of complex I by the neurotoxin would impair the normal mitochondrial utilisation of pyruvate generated by glycolysis, thereby increasing the concentration of cellular NADH. High levels of pyruvate and NADH would drive the reaction catalysed by lactate dehydrogenase to the production of lactate causing medium acidification.

Another factor that could be of importance in this *in vitro* cell model is based on an earlier observation by Notter *et al* (1988). Using electron microscopy Notter indicated that C6 cells contain a large number of mitochondria. Although this could reflect high energy requirements by the cells it could also suggest the need for a

greater concentration of neurotoxin to cause inhibition of complex I sufficient enough to cause cell death. This difference in cell line susceptibility to MPTP-cytotoxicity could also extend to mechanisms that trap the toxic metabolite, MPP^+ , within cells. *In vivo* MPP^+ is known to bind to neuromelanin present in susceptible dopaminergic neurones (D'Amato *et al.*, 1987). *In vitro*, Umemura *et al.* (1990) has suggested that MPTP cytotoxicity could be dependent on cellular melanin content. One could speculate that, if present, neuroblastoma and glioma cells could differ in neuromelanin content relating to neurotoxin susceptibility.

In vivo, it is generally accepted that glial cells help maintain neuronal glutathione levels which contain less glutathione than glial cells (Makar *et al.*, 1994). Thus neuronal cells are unable to mount sufficient protection against the potential oxidative stress produced by toxic insult, i.e. MPTP. However, determination of total glutathione levels in C6 and N2a cells reveals the two cell lines to express similar levels; 14.10 nmol/ μ g protein and 13.80 nmol/ μ g protein, respectively; the comparable levels not corresponding to the differential cell sensitivities. Cell differentiation also leads to an increase in total glutathione in both C6 and N2a cells. However, increased glutathione levels in the latter are unable to promote cell survival in the presence of MPTP, suggesting possibly that oxidative stress is not a primary cytotoxic-inducing event and that cell energy requirements may have more influence on cell susceptibility in these models.

The cytotoxic effects of MPTP on differentiating C6 cells compared to mitotic C6 cells are in contrast to that seen with the neuroblastoma population. Differentiating C6 cells exposed to MPTP exhibited increased resistance with only a small reduction in cell viability evident after 72 hours exposure. This was unexpected since total MAO activity assessment indicates that differentiation of C6 cells causes a significant increase in MAO activity. This in turn would seemingly cause an increase in MPTP metabolism, therefore potentially increasing cytotoxicity, as proposed to be a contributing factor in the neuroblastoma cell model. However, 90% cell viability was maintained in the differentiating C6 cell line following 72 hours exposure to 1 mM MPTP. Work carried out by Cookson *et al.* (1995) also reported no increase in cytotoxicity in C6 cells that had been pre-differentiated for 48 hours prior to exposure to 4.7 mM MPTP for 24 hours, when compared to the mitotic population. It would

therefore seem that C6 cells express relative insensitivity to MPTP than N2a cells, over the concentration and time periods investigated.

3.3.3 Cytotoxicity of MPP^+ towards neuroblastoma and glioma cells.

The neurotoxic metabolite, MPP^+ , derived from MPTP (Markey *et al.*, 1984) is thought to be the mediator of toxicity. Therefore to directly assess the cytotoxic potential of MPP^+ within the cell systems, the neurotoxic metabolite was added directly to mitotic and differentiating N2a and C6 cell lines and cell viability monitored using the MTT reduction assay.

The effect of MPP^+ on both cell lines was unexpected. MPP^+ concentrations of up to 1 mM exerted little effect on viability of both mitotic neuroblastoma and glial cells over a 48 hour exposure period. A lack of cytotoxicity was also the case when neuroblastoma and glioma cells were induced to differentiate in the presence of MPP^+ , over a 48 hr and 72 hr (Table 3.1) exposure period, respectively. Differentiating C6 cells expressed greater resistance than differentiating N2a cells to MPP^+ , the former requiring a longer incubation period to achieve similar cytotoxic levels. The use of phase contrast microscopy revealed no dramatic morphological effects on either cell types, although differentiating N2a cells did exhibit some cell detachment and rounding of cells.

This lack of increased susceptibility to MPP^+ (compared to MPTP) is not unique and has also been reported in the rat neuronal B65 cell line of dopaminergic origin (Lai *et al.*, 1993). It has also been demonstrated that MPP^+ can exert a mitogenic effect on differentiated N₂A-B1 cells at low concentrations (Notter *et al.*, 1988). Cells treated with MPP^+ (33.7 μ M) for 48 hours exhibited growth stimulation as determined by cell counts. This phenomenon was not assessed in the present cell models. However, some cells did express a round morphology that could be associated with either neurotoxin-induced changes in cell morphology or mitogenic-induced changes.

Since MPP^+ is a charged molecule it is unable to readily traverse cell membranes. Therefore a key event in the expression of MPP^+ neurotoxicity is the active cellular uptake of the metabolite and accumulation within the mitochondria of

susceptible cells. Intercellular accumulation of MPP^+ has been proposed to occur via the catecholamine uptake system (Chiba *et al.*, 1984; Javitch *et al.*, 1985), where ATP has been suggested to be involved in the bulk transfer of MPP^+ (Dunigan and Shamoo, 1996). Differences in the intrinsic properties of the uptake systems in different cell lines exists which can affect the level of cytotoxicity expressed. For example, rat dopaminergic neurones were reported to be killed by 10 μM MPP^+ (Michel *et al.*, 1990) where measurements of MPP^+ uptake in related synaptosomes was recorded as 2750 ± 213 fmol/min/mg protein. In comparison, PC12 cells were reported to be killed by 100-fold higher concentrations of 1-3 mM MPP^+ ; these cells exhibited a 10-fold lower uptake rate of MPP^+ of 198 ± 17 fmol/min/mg protein (Itano *et al.*, 1994).

Since the maintenance medium used in these studies lacks ATP, its inclusion could influence the rate of MPP^+ uptake into cells (Dunigan and Shamoo, 1996). This was addressed by the addition of 0.5-2.0 mM ATP (physiological ATP levels ~ 1.0 mM) to N2a cells in the presence of MPP^+ prior to assessing cell viability. Indeed, ATP did increase MPP^+ -induced cytotoxicity in differentiating N2a cells in a dose dependent manner (Fig 3.9). However, it was evident from observing control values in the absence of MPP^+ that increasing ATP concentration also increased N2a cytotoxicity. Although it would seem that ATP did increase active MPP^+ uptake, control data suggests this could be related, in part, to a non-specific increase in membrane permeability mediated by ATP. It is therefore likely that a relatively inefficient catecholamine uptake system exists within the N2a cell line.

Comparison of mitotic and differentiating N2a cells shows differentiating cells to be more susceptible to MPP^+ -induced cytotoxicity. This increased sensitivity accompanying differentiation has also been observed in PC12 cells. An increase in MPP^+ uptake has also been associated with the morphological differentiation of PC12 cells treated with nerve growth factor (Itano *et al.*, 1994). Therefore the possibility exists that the small increase in cytotoxicity in differentiating N2a cells could be associated, in part, with an increase or low level activation of MPP^+ uptake.

Work carried out by DiMonte *et al.* (1992) has suggested that MPP^+ can itself cross the plasma membrane towards the extracellular space, in mouse astrocytes, once generated within the cell. Whether this phenomenon is a consequence of membrane permeability or a capability of particular cells remains to be determined. However, it

does suggest that the cytotoxicity of MPTP and MPP⁺ could be influenced by the relative rate of MPP⁺ accumulation by mitochondria compared to the rate of release into the medium by the cells. Differences in this balance could explain, in part, the relative resistance to the neurotoxin exhibited by different cell lines (i.e. C6 versus N2a).

3.3.4 MAO activity and MAO-specific mRNA expression in neuroblastoma and glioma cell lines.

Neural cells were grown in parallel under conditions conducive to proliferation and differentiation, prior to total MAO assessment. Total MAO activity was greatest in glial C6 cells compared to neuroblastoma N2a cells; a phenomenon similar to the distribution of activity seen *in vivo*, in neuronal and glial cells of the substantia nigra (Oreland *et al.*, 1983). The low MAO activity exhibited by N2a cells is similar to the dopaminergic neurones in the *in vivo* situation, where substrates not utilised are accumulated. Indeed, these neuroblastoma cells have been shown to contain varying amounts of the neurotransmitters dopamine, norepinephrine and serotonin (Narotzky and Bondareff, 1974), all physiological substrates with differing affinities for MAO. The use of MAO-specific primers surprisingly revealed the presence of both MAO-A and MAO-B mRNA in the N2a cells, the former predominating. However, the identification of specific messenger levels within cells does not necessarily correlate to the translation of mature protein expressing enzyme activity. *In vivo*, the presence of MAO-B in dopaminergic neurones is conflicting (see Westlund *et al.*, 1988 and Damier *et al.*, 1996) although it is generally accepted that dopaminergic neurones contain very low MAO activity (Westlund *et al.*, 1988).

On dbcAMP-induced differentiation N2a cells exhibited an increase in total MAO activity of 17.94 %. This correlates with an increase in MAO messenger levels for both MAO-A and MAO-B as determined by RT-PCR. Increased MAO activity following dbcAMP differentiation has also been demonstrated in another mouse C1300 clone, N4 neuroblastoma. These cells expressed a mean MAO activity of 8.9 nmol/h/mg protein under differentiating conditions compared to 7.4 nmol/h/mg protein under mitotic conditions (Skaper *et al.*, 1976) an increase of ~20%, although the increase was deemed not to be statistically significant, in this case. It must be noted,

however, that these cells were differentiated in serum containing medium supplemented with dbcAMP where the extent of cellular differentiation was not defined. Therefore it is possible, in this case, that a significant increase in MAO activity could be masked by the attenuating effect of serum.

Other neuroblastoma cells cloned from the original C1300 clone have been shown to exhibit marked increases in tyrosine hydroxylase activity, in conjunction with morphological differentiation, when cells were grown in the presence of dbcAMP (Waymire *et al.*, 1972). This would perhaps lead to an increase in the concentration of L-dopa and subsequently dopamine (a MAO substrate). The authors considered the elevation in tyrosine hydroxylase to be mediated through both dbcAMP and butyric acid, which can be formed from the hydrolysis of dbcAMP. In conjunction, the addition of sodium butyrate (whose biological structure closely resembles neurobiologically active compounds i.e. γ -aminobutyric acid) to cell lines has been associated with an ability to induce hyperacetylation linked to gene expression and leading to general protein synthesis (Kruh, 1982). Early studies (Waymire *et al.*, 1972; Prasad and Sinha, 1976) using neuroblastoma cells showed butyrate to increase the specific activity of several enzymes including choline acetyltransferase, acetylcholine esterase and tyrosine hydroxylase. Indeed, it would seem that differentiation can activate many enzymes involved in the control of neurotransmitters.

In the C6 cell line sodium butyrate-induced differentiation resulted in a larger (30.68 %) increase in total MAO activity. This occurred alongside an increase in MAO expression of both MAO-A and MAO-B mRNA levels, compared to mitotic cells. Culture conditions have been implicated in influencing MAO activity in primary rat astrocytes, with particular reference to serum content (Carlo *et al.*, 1996). Primary rat astrocytes cultured in serum supplemented defined medium showed significantly lower MAO activity than cells cultured in chemically defined medium devoid of serum. The authors suggested that the increase in MAO activity in the absence of serum is linked to morphological differentiation of the rat astrocytes. Indeed, serum free medium has been shown to elicit both morphological differentiation (Haffke and Seeds, 1975) and changes in other enzyme activities of cultured cells (Borg *et al.*, 1985). Therefore it would seem that the constituents of serum in addition to the presence of a differentiating agent could influence changes in MAO activity.

3.3.5 Total glutathione (GSH + GSSG) status in C6 and N2a cells.

Contrary to the *in vivo* situation where it is generally considered that glial cells contain more glutathione than neuronal cells (Makar *et al.*, 1994), both the C6 and N2a cells lines, in the mitotic state, expressed comparable glutathione concentrations of 14.1 and 13.8 nmol/ μ g protein, respectively. However, differentiation resulted in increased glutathione concentrations in the both cell lines. This increase was greater in C6 cells compared to the N2a cells; 20.08 and 24.00 nmol/ μ g protein, mimicking the *in vivo* situation more closely.

Reduced glutathione (GSH) is by far the predominant form within cells exhibiting greater than 99.5 % of total glutathione levels. Glutathione plays a fundamental role in protecting cells from damage by oxidative stress. Indeed, depletion of glutathione, *in vivo*, can increase MPTP-induced neurotoxicity in mice (Wullner *et al.*, 1996). However, in this *in vitro* model cell susceptibility to MPTP does not correlate with total glutathione levels; N2a cells exhibit a greater susceptibility to MPTP while expressing comparable glutathione levels as C6 cells. In addition, increases in glutathione levels on differentiation do not correlate with a decrease in cell susceptibility to MPTP. This could suggest that MPTP-induced cell death in these cell lines does not occur primarily through oxidative stress and may follow an initial cytotoxic-inducing event (i.e. energy deprivation). There is also a suggestion that the neurotoxin can evoke the release of intracellular glutathione (Han *et al.*, 1999) causing a depletion in levels thereby attenuating cellular antioxidative capacity. Indeed, preliminary evidence from this study using differentiating N2a cells exposed to 1 mM MPTP for 24 hours resulted in a decrease in total glutathione levels compared to control. However, this decrease in total glutathione levels could be due, in part, to cell lysis resulting from cell death rather than specific glutathione release.

CHAPTER IV

**The neurotoxic effects of sub-cytotoxic MPTP insult
on differentiating N2a neuroblastoma cells.**

4.1 Introduction.

4.1.1 Characterisation of MPTP-induced neurotoxic effects

Although viability is a common endpoint to determine if toxicants are affecting cells in culture it is a relatively insensitive marker which can mask subtle changes to a cell population resulting from neurotoxic insult. A significant observation made in the previous chapter (Chapter III) was the dramatic change in cell morphology of differentiating N2a cells exposed to the neurotoxin, MPTP. Light microscopy revealed that MPTP-treated differentiating N2a cells exhibited a range of detrimental effects including vacuole formation, detachment of cells from the substratum and cell lysis; characteristics commonly associated with the onset of cell death. However, more interestingly, the inability of a large population of viable cells to extend neurites was also evident even at lower MPTP concentrations (i.e. $< 100 \mu\text{M}$).

Changes in cell morphology as a consequence of exposure to various toxins has been reported by a number of workers (e.g. Cookson *et al.*, 1995; Hartley *et al.*, 1997; Flaskos *et al.*, 1998). More specifically, studies using clonal cells that express a neuronal phenotype have indicated that MPTP is able to significantly alter neuronal morphology following exposure. For example, Denton and Howard (1984) noted that pheochromocytoma cells were unable to extend neurites in the presence of high doses of MPTP (i.e. 1 mM MPTP). Likewise, Notter *et al.* (1988) made a similar observation using neuroblastoma cells exposed to MPP⁺ (f 0.33 μM). However, detailed analyses have not been carried out.

The neuroblastoma N2a cell line used in this study is ideal, with respect to monitoring initial morphological changes, due to its ability to extend neurites rapidly in response to serum withdrawal and addition of dbcAMP. The survival and normal function of neuronal cells requires membrane integrity and a sustainable energy supply. In order to investigate the morphological and biochemical effects of the neurotoxin, MPTP, on differentiating N2a cells it is first necessary to establish a sub-lethal dose to ensure that any changes that do occur are not consequent to a secondary or lethal cytotoxic effect. In Chapter III evidence suggests that exposure of differentiating N2a cells to 10 μM MPTP for 24 hours was not cytotoxic; this was

therefore confirmed by trypan blue exclusion and the determination of cell energy status (ATP levels).

Changes in cell morphology are usually analogous with alterations to the cytoskeleton. Indeed, the cytoskeleton is important in maintaining cellular architecture and internal organisation with clear involvement in defining cell shape, in cell division, and a range of other cellular processes (Doering, 1983). For example, neuronal differentiation, *in vitro*, is accompanied by profound morphological alterations, characterised by the elaboration of neurites. The development of this polarity is also accompanied by specific distribution of cytoskeletal components including NF subunits, which are associated with aspects of axon outgrowth and axon calibre (Carden *et al.*, 1987; Hoffman *et al.* 1987). In general, as axon outgrowth proceeds NF levels may increase and undergo post-translational events, namely phosphorylation. Interestingly, disruption of the normal NF phosphorylation patterns have been associated with a variety of neuropathologies *in vivo* (Nixon, 1993).

NF-H, the largest of the NF subunits, contains numerous serine residues that present themselves in a recurring lysine-serine-proline (KSP) motif which acts as a substrate for post-translational phosphorylation (Julien and Mushynski, 1983). This has led to the development of monoclonal antibodies that can distinguish between phosphorylated and unphosphorylated KSP domains of NF-H (Sternberger and Sternberger, 1983; Lee *et al.*, 1987).

In order to characterise further any morphological changes to neuroblastoma cells in this chapter, it is necessary to monitor related biochemical parameters associated with the cytoskeleton. Therefore representatives of the microtubule and microfilament components, namely α -tubulin and actin, respectively will be assessed in differentiating N2a cells exposed to MPTP. Similarly, NF-H levels, NF-H phosphorylation state and NF-H distribution will also be assessed.

4.1.2 NF-H antibodies.

Three distinct monoclonal antibodies directed to NF-H will be used to characterise NF-H levels and post-translational status. The commercially available mouse monoclonal N52 raised to dephosphorylated pig NF-H recognises both the phosphorylated and non-phosphorylated forms in a wide variety of species, and will be

used to monitor total NF-H levels. NF-H antibodies, Ta51 and RMd09, were obtained from Dr. M. J. Carden and were prepared from purified native rat NF-H proteins, i.e. phosphorylated rat NF-H and enzymatically dephosphorylated rat NF-H, respectively. The antibodies were part of a large panel of monoclonals raised to NFs (Lee *et al.*, 1987).

The antibodies recognise epitopes in the COOH terminus of the NF-H subunit and therefore can discriminate the different isoforms of NF-H to a large extent, depending on the phosphorylation state of each variant. The antibodies were assigned to one of four categories based on their performance in immunoblots of progressively de-phosphorylated rat NF samples and by immunohistochemistry of adult rat nervous tissue (Lee *et al.*, 1987). P[-] antibodies preferentially stained neuronal perikarya and dendrites recognising only extensively de-phosphorylated (alkaline phosphatase treated) and non-phosphorylated NF-H. P[+] antibodies stained axons more strongly ^{than} that perikarya, and primarily recognised phosphorylated forms of NF-H subjected to limited enzymatic de-phosphorylation, but not non-phosphorylated forms of NF-H on immunoblots. RMd09 and Ta51 are typical candidates from each of these two categories, i.e. P[-] and P[+] respectively.

4.1.3 Abnormal cellular inclusions.

PD is characterised by Lewy body inclusions typically found within neuronal cell bodies or neuronal cell processes of the substantia nigra. These inclusions have been shown to react with a number of antibodies directed to neuronal proteins including the cytoskeletal proteins tubulin, NFs, tau and others such as ubiquitin and α -synuclein (Armstrong *et al.*, 1998). Recently, abnormal neuronal aggregates have been reported in MPTP-treated baboons (Kowall *et al.*, 2000). Initial observations using the differentiating N2a cell model suggest exposure of cells to MPTP induce noticeable changes in both cell morphology and cell survival (Chapter III). Therefore it is conceivable that these changes are linked to neurotoxic-induced stress.

Cellular arrest and differentiation of cells involves alterations in ubiquitin-dependent pathways. In conjunction, some stress responses can include activation of these pathways (Varshevsky, 1997), however, the exact alterations are not yet clearly defined. Differentiation of neuroblastoma cells has been associated with alterations in

the level of free ubiquitin (LaRosa *et al.*, 1996) suggesting the ability of a cell to anticipate the future degradation of redundant proteins. MPTP may influence intracellular ubiquitin levels during neuronal differentiation. This could potentially lead to MPTP-induced ubiquitination of abnormal proteins marking them for intracellular degradation. Therefore a polyclonal anti-ubiquitin antibody, which recognises ubiquitin-conjugated proteins, will be used to analyse changes in ubiquitination following exposure of cells to the neurotoxin.

Recent findings using the MPTP mouse and baboon models have reported the increased expression of the pre-synaptic protein α -synuclein within the substantia nigra (Jackson-Lewis *et al.*, 1998; Kowall *et al.*, 2000). In PD α -synuclein is also expressed in Lewy bodies, where it is considered to be a major component (Spillantini *et al.*, 1997). The presence of modified basal levels of this protein within MPTP exposed neuroblastoma cells could insinuate its role in regulating neurotoxic cell deterioration. Therefore a polyclonal anti-synuclein antibody, which recognises α - and β -synuclein, will be used to assess the levels of cellular synuclein following differentiation of N2a cells exposed to sub-lethal doses of MPTP.

4.1.4 MPTP-induced abnormalities in cell signalling cascades.

Changes in protein phosphorylation are commonly involved in cellular regulation. The state of phosphorylation of intracellular proteins is determined by the interplay between protein kinases and protein phosphatases with some enzymes requiring phosphorylation for activity, others de-phosphorylation. A variety of stimuli can initiate signalling reaction cascades; by transducing signals through a cascade of kinases, several control points are introduced for amplifying and/or modifying the output signal.

The mitogen activated protein kinase cascades (MAPK) encompasses three parallel pathways termed the extracellular regulated protein kinase pathway (ERK), the stress activated protein kinase pathway (SAPK) and the p38 pathway (Tibbles and Woodgett, 1999). These pathways are involved in neuronal growth, differentiation and survival. However, in neuronal cells little is known about these pathways and their downstream effectors and substrates in response to stress.

The SAPK cascade can be activated by a variety of extracellular cellular stresses mediated through membrane bound receptors. However, it is becoming increasingly clear that various intracellular stressors such as large increases in reactive oxygen species or aberrant calcium fluxes can activate the SAPK pathways (i.e. JNK/p38 kinase (Tibbles and Woodgett, 1999)). Therefore this suggests that perturbation of intracellular homeostasis by a stressing agent, such as a neurotoxin, could potentially activate the stress signalling cascade. Indeed, a rise in reactive oxygen species and intracellular calcium levels has been documented following MPTP exposure (Kass *et al.*, 1988). Therefore the activation of the SAPK pathway following exposure of differentiating N2a cells to MPTP will be investigated using a polyclonal antibody that recognises the dually phosphorylated (active) form of JNK.

4.2 Results

4.2.1 Assessment of sub-cytotoxic MPTP concentrations on differentiating N2a cells.

Initial cytotoxicity assessments using the 3-(4,5-dimethylthiazol-2-yl)-2,5-diphenyltetrazolium bromide (MTT) reduction assay on differentiating N2a cells revealed that significant cell death occurred with MPTP concentrations of 50 μ M and above, following a 24 hour exposure (Chapter III, Figure 3.6A). Lower concentrations of MPTP (i.e. 10 μ M) revealed no cell death, as determined by the MTT reduction assay (Chapter III, Figure 3.6A). The trypan blue exclusion assay was used to monitor and confirm viable/dead cell numbers following 24 hours exposure to concentrations of 5 μ M and 10 μ M MPTP. No significant cell death was observed (Table 4.1), although changes in cell morphology were evident.

4.2.2 Analysis of axon outgrowth in differentiating N2a cells.

Characterisation of axon outgrowth in N2a cells induced to differentiate by serum withdrawal and the addition of 0.3 mM dbcAMP, was carried out over a 48 hour time period. Measurement of axon numbers was achieved by viewing Coomassie blue stained cells by light microscopy at a magnification of x 200. Axons were defined as extensions greater than two cell body diameters in length. Cells cultured in growth medium alone (Fig 4.1, time zero) exhibited a very low level of axon numbers (i.e. 4.8 axons / 100 cells). However, when cultured under differentiating conditions N2a cells exhibited a steady increase in axon outgrowth, with axon numbers reaching a plateau at approximately 32 hours (i.e. 33.8 axons / 100 cells). Axon counts carried out on N2a cells induced to differentiate for 48 hours showed a slight decrease in actual axon numbers. Although following 48 hours differentiation a proportion of the cells exhibited longer axon-like processes; it was evident that some cells were becoming detached from the substratum.

Observing Coomassie stained cells induced to differentiate in the presence of a sub-cytotoxic dose of MPTP revealed a reduction in the number of axon-like processes following 24 hours incubation, compared to control cells (Fig 4.2, compare b vs a). Indeed, cells exposed to sub-cytotoxic MPTP concentrations showed an inhibition in

axon numbers with cells exposed 10 μ M MPTP exhibiting approximately 40 % inhibition of axon outgrowth, compared to control values (Fig. 4.3).

4.2.3 Analysis of neurofilament protein levels in differentiating N2a cells.

Biochemical characterisation of cellular NF-H protein levels and phosphorylation state was carried out to complement the morphological changes observed during neuronal differentiation. NF-H status was monitored over a 48 hour differentiation time period by western blot analysis of cell extracts probed using three distinct antibodies. RMd09 preferentially recognises non-phosphorylation dependent epitope of NF-H, Ta51 recognises a phosphorylation dependent epitope of NF-H, and N52 recognises NF-H independent of phosphorylation state. In general, NF-H levels were low in cells cultured in growth medium alone (i.e. 0 hr) but increased concomitantly when differentiation was induced. This was characterised by an increase in axon outgrowth over the 48 hour time period (see Fig. 4.3).

The observed increase in total NF-H levels, as determined by N52 reactivity (Fig. 4.4A), resembled the pattern seen with the RMd09 antibody (Fig 4.4B), complementing a time dependent differentiation of N2a cells. In contrast, levels of phosphorylated NF-H, as determined by Ta51 reactivity (Fig 4.4C) were expressed at a much later time point during the differentiation process. Levels of phosphorylated NF-H remained low until approximately 16 hours where upon Ta51 reactivity dramatically increased. Therefore during the initial process of differentiation N2a cells are dominated by hypo-phosphorylated NF-H subunits which over time undergo post-translational modification contributing to axon stability/maturity.

4.2.4 Western blotting analysis of cytoskeletal components in differentiating N2a cells exposed to sub-cytotoxic concentrations of MPTP.

Biochemical characterisation of specific cytoskeletal component levels was carried out to investigate the molecular basis of the morphological changes observed during neuronal differentiation. Equal protein aliquots of cell extracts were separated on a 7.5 % SDS PAGE gel (e.g. Fig 4.5) prior to protein transfer to nitrocellulose. In addition to the NF-H subunit status, actin and α -tubulin protein levels were

specifically monitored by immunoprobings Western blots of total cell extracts of differentiating N2a cells, exposed to MPTP for 24 hours. To monitor NF-H status, three distinct antibodies were used, which preferentially recognised a non-phosphorylation dependent epitope of NF-H, a phosphorylation dependent epitope of NF-H (RMd09 and Ta51, respectively; Lee *et al.*, 1987), and an epitope of NF-H independent of phosphorylation state (N52).

Figure 4.6 shows the result of Western blot analysis (left panel) from a typical experiment where extracts were probed with five anti-cytoskeletal antibodies. In addition, densitometric analysis was performed on blots obtained from three different experiments (right panel). Visual and densitometric analysis of the probed blots indicates that differentiating N2a cells exposed to MPTP for 24 hours (lanes 2, 3) exhibited no apparent change in the levels of α -tubulin or actin (representatives of microtubule and microfilament components, respectively), compared to controls. However, NF-H status appeared modified by treatment with MPTP. MPTP treated cells probed with the phosphorylation independent antibody (N52) exhibited no significant change in NF-H levels, compared to the control. Conversely, a decrease in the level of RMd09 reactivity with a concomitant net increase in the level of Ta51 reactivity (compared to controls) was observed (Fig. 3d, 3e, right panel). Indeed densitometric analysis of cells exposed to 5 μ M and 10 μ M MPTP showed that RMd09 reactivity was reduced to 73.7 ± 9.6 and 46.4 ± 17.7 % respectively, compared to controls. This was in contrast to an increase in Ta51 reactivity to 132.5 ± 15.8 % and 191.2 ± 51.0 % for 5 μ M and 10 μ M MPTP, respectively.

4.2.5 Subcellular distribution of NF-H in differentiating N2a cells exposed to sub-cytotoxic MPTP concentration.

The possible involvement of cytoskeletal disruption as an effect of sub-cytotoxic dose of MPTP on differentiating N2a cells was examined by indirect immunofluorescence using antibodies RMd09, Ta51 or anti-actin. Cells were grown on coated glass slides and induced to differentiate in the presence and absence of 10 μ M MPTP, prior to fixation and antibody probing. In control differentiating N2a cells the NF-H isoform recognised by RMd09 staining was evident in the perikarya and in axon-like processes (Fig. 4.6a). However, MPTP-treated cells exhibited a reduction in

axon outgrowth where RMD09 staining intensity was considerably reduced. In this case cell perikarya expressed lower levels of RMD09 staining intensity (Fig 4.6b). The NF-H isoform recognised by Ta51 was characteristically detected in axon-like processes in control cells, in which axons exhibited a greater staining intensity than the cell body, where staining seemed more diffuse (Fig 4.6c). Conversely, MPTP-treated cultures produced many cells lacking axon processes that exhibited a significant increase in Ta51 staining intensity. This increase in phosphorylated NF-H reactivity was confined invariably to the cell perikaryon (Fig 4.6d). By contrast, MPTP did not affect the distribution of actin filaments, with the possible exception of small actin positive outgrowths in MPTP-treated cells, as revealed by probing MPTP exposed and non-exposed differentiating cells with an anti-actin antibody (compare Fig. 4.6e and 4.6f).

	MPTP (μM)		
	<i>Control</i>	<i>5</i>	<i>10</i>
Cell death (%)	8.90 ± 1.98	11.24 ± 3.08	9.12 ± 2.76

Table 4.1 *Determination of sub-cytotoxic exposure of differentiating N2a cells exposed to MPTP.* N2a cells were induced to differentiate in the presence or absence of MPTP for 24 hours at 37°C in an atmosphere of 95% air / 5% CO₂. Cell death was assessed via the trypan blue exclusion assay as described in Materials and Methods, section 2.2.6.3. Results are expressed as mean % cell death \pm SEM. Statistical analysis was carried out using the Mann-Whitney *U* test, where n=5. All values $p < 0.05$ versus control.

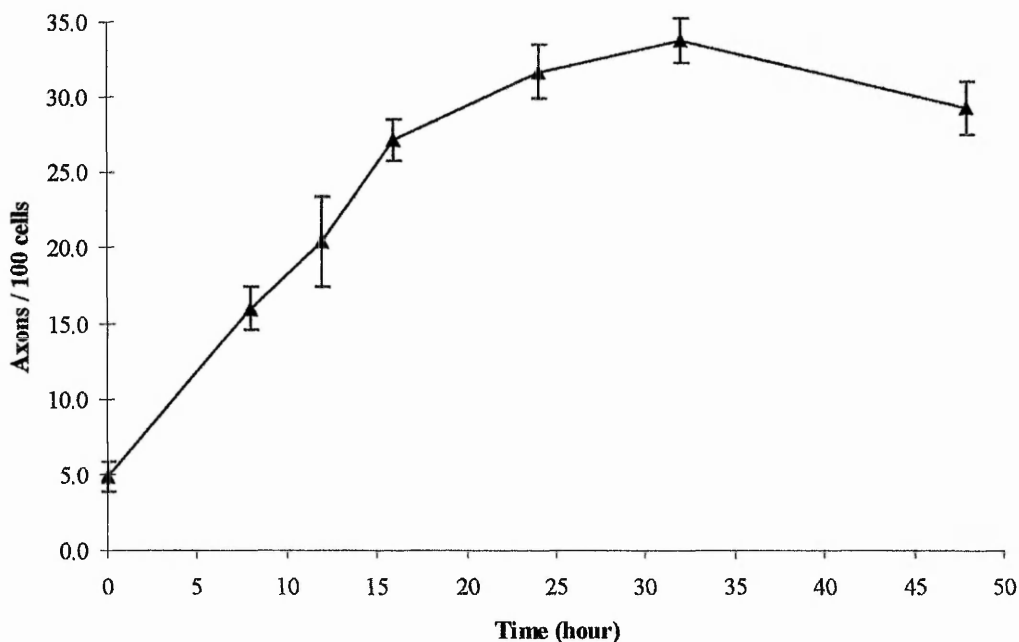
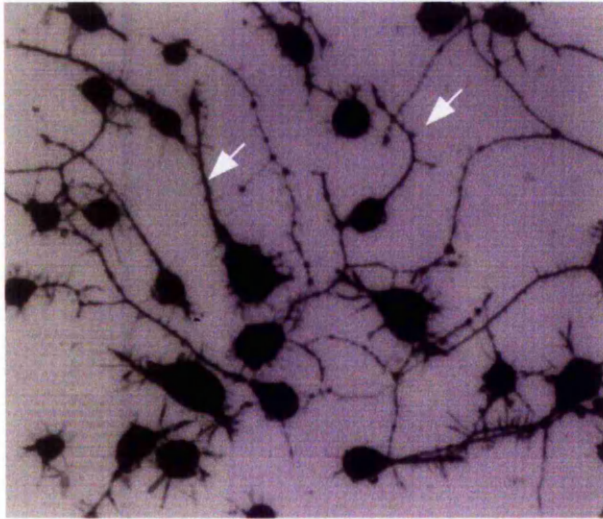


Figure 4.1 *Time course of axon outgrowth in differentiating N2a cells.*

N2a cells were induced to differentiate in SFM containing 0.3 mM dbcAMP. Cells were incubated at 37°C for increasing time periods, in an atmosphere of 95% air/5% CO₂, prior to morphological assessment. Cells were fixed in ice-cold methanol and stained with Coomassie blue as described in Materials and Methods (section 2.2.13). Quantification of axon outgrowth was achieved using an inverted light microscope (Magnification: × 200). The number of axon-like processes (defined as extensions greater than two cell body diameters in length) were counted in five random fields per well. Results are expressed as mean Axons/100 cells ± SEM, where n=4.

(a). Control



(b). 10 μ M MPTP

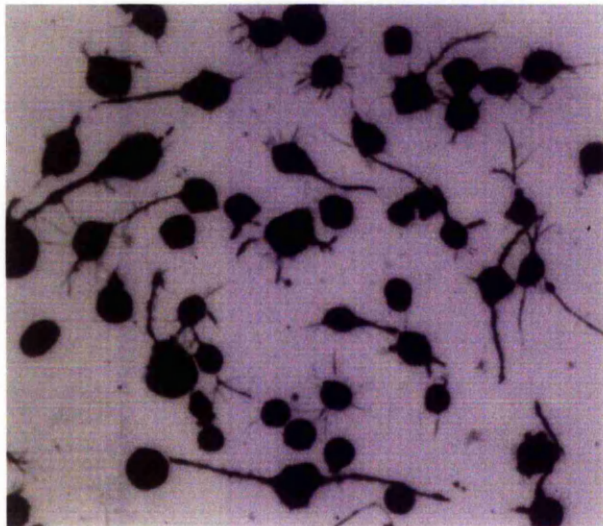


Figure 4.2 *The effect of sub-cytotoxic dose of MPTP on the morphology of differentiating N2a cells.*

N2a cells were induced to differentiate for 24 hours alone (a) or in the presence of 10 μ M MPTP (b). Cells were fixed in ice-cold methanol and stained with Coomassie blue as described in Materials and Methods (section 2.2.13). Cells were viewed on an inverted light microscope at x 200 magnification. Arrows indicate typical axon-like processes. Note the reduction in axon-like processes following treatment with MPTP.

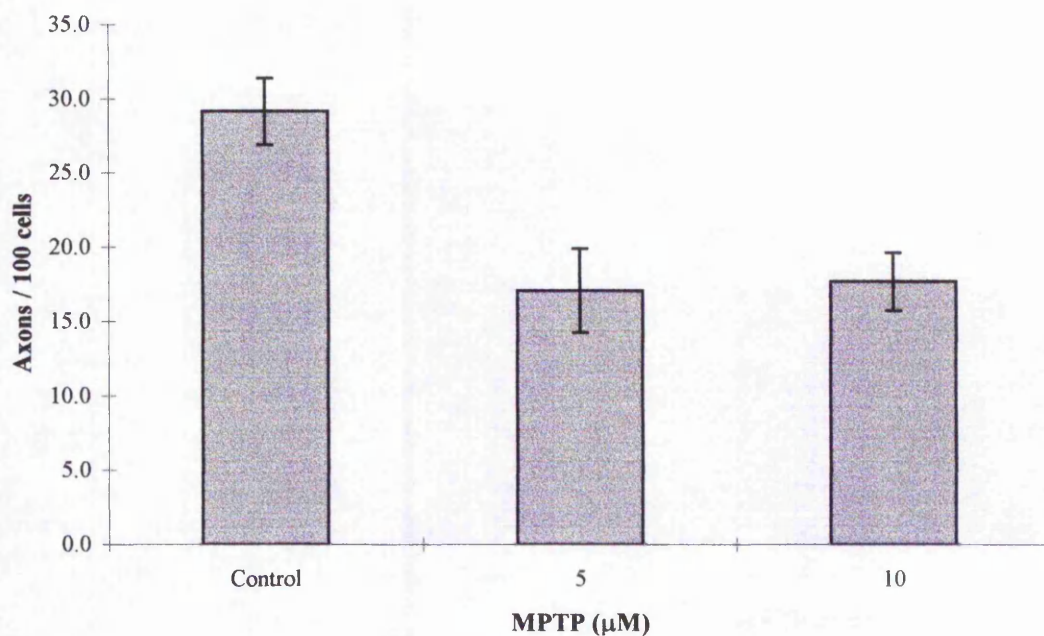


Figure 4.3 *The effect of sub-cytotoxic dose of MPTP on axon outgrowth in differentiating N2a cells.*

N2a cells were induced to differentiate in the presence or absence of MPTP for 24 hours prior to morphological assessment. Cells were fixed stained as described in Materials and Methods (section 2.2.13). Quantification of axon outgrowth was achieved using an inverted light microscope (Magnification: x 200). The number of axon-like processes (defined as extensions greater than two cell body diameters in length) were counted in five random fields per well. Results are expressed as mean number of axons / 100 cells \pm SEM. Statistical analysis of control vs. neurotoxin treated cells was carried out using the Mann-Whitney *U* test, where n=12 wells. All p values < 0.05 compared to control.

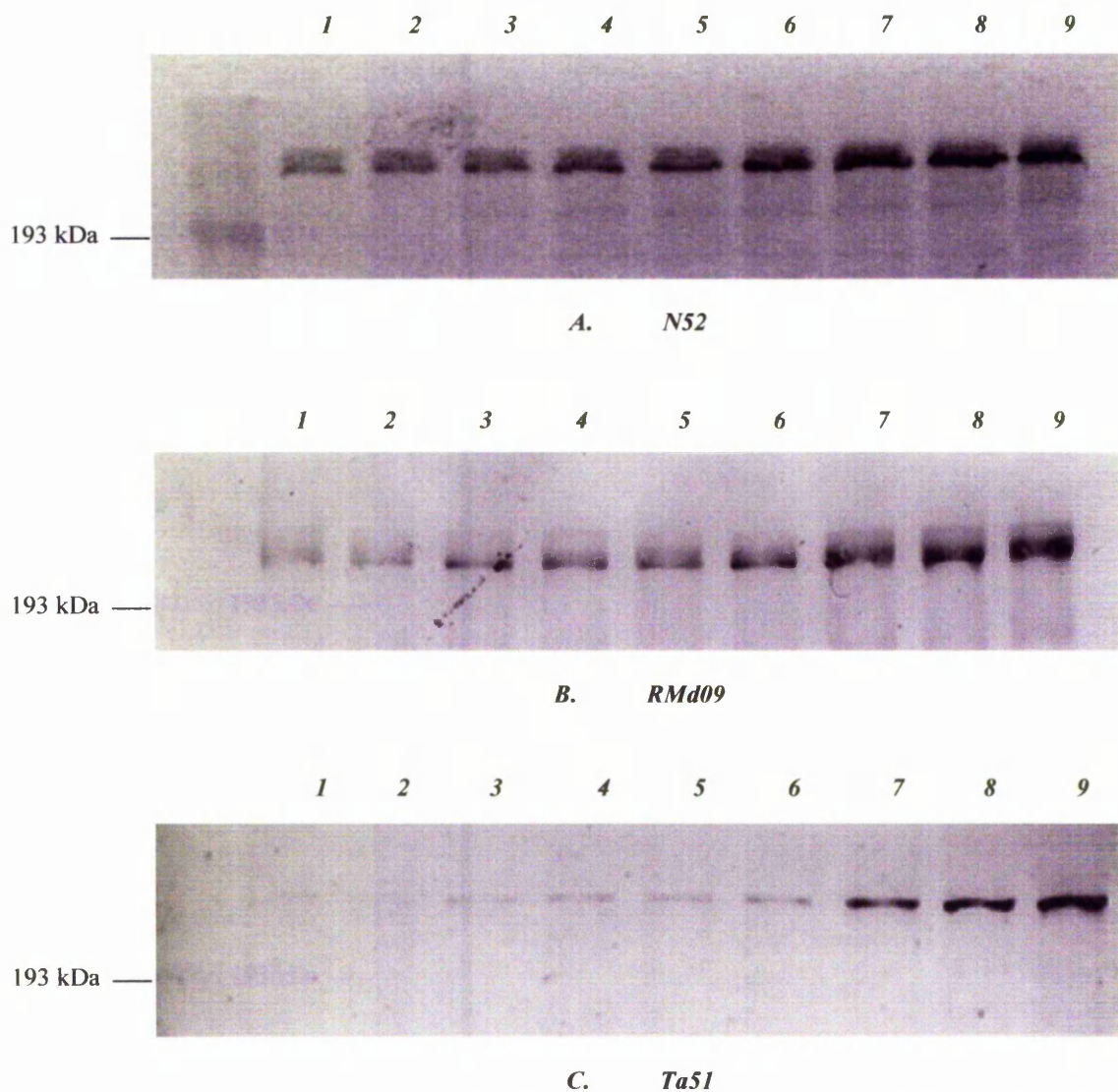


Figure 4.4 Time course of the expression of neurofilament-H protein during differentiation of neuroblastoma N2a cells.

N2a cells were induced to differentiate in SFM containing 0.3 mM dbcAMP. Cells were incubated at 37°C for increasing time periods, in an atmosphere of 95% air/5% CO₂, prior to extraction of the cell monolayer. Equal protein aliquots (20 µg) of cell extracts were loaded onto a 7.5% SDS-PAGE gel and electrophoresed. Samples were then transferred onto nitrocellulose membrane and probed with mouse antibodies N52, RMd09 and Ta51. The signal was developed using a rabbit anti-mouse alkaline phosphatase secondary conjugate.

- A. N52
 (1) 0 hr (2) 4 hr (3) 8 hr (4) 12 hr (5) 16 hr (6) 20 hr (7) 24 hr (8) 32 hr (9) 48 hr.
- B. RMd09
 (1) 0 hr (2) 4 hr (3) 8 hr (4) 12 hr (5) 16 hr (6) 20 hr (7) 24 hr (8) 32 hr (9) 48 hr.
- C. Ta51
 (1) 0 hr (2) 4 hr (3) 8 hr (4) 12 hr (5) 16 hr (6) 20 hr (7) 24 hr (8) 32 hr (9) 48 hr.

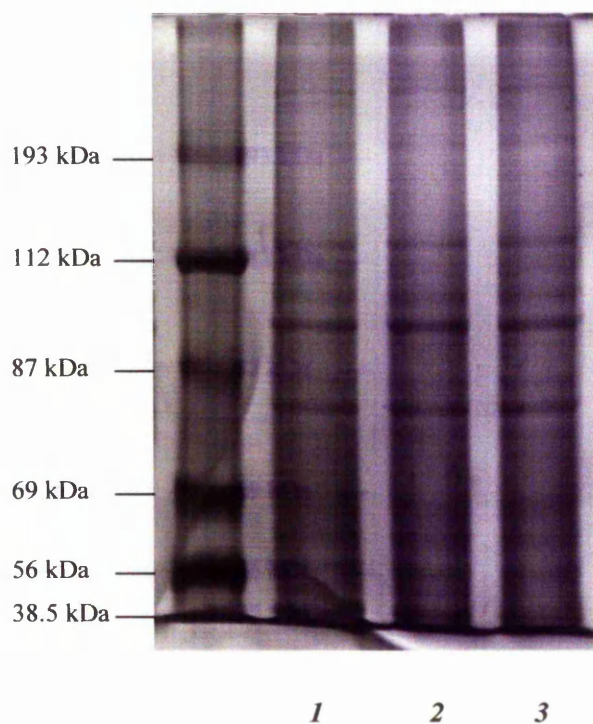
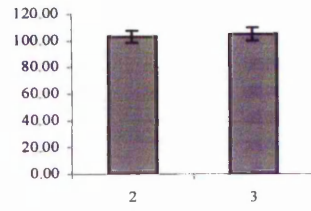
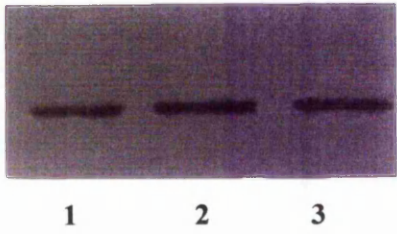


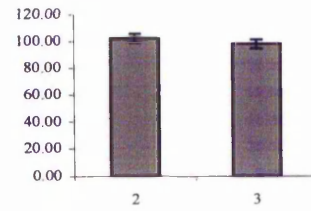
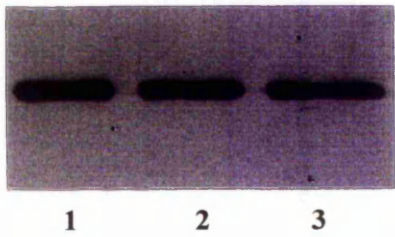
Figure 4.5 *Coomassie stained SDS PAGE gel of total cell extracts of differentiating N2a cells exposed to sub-cytotoxic concentrations of MPTP.*

Equal protein aliquots (20 μg) of cell extracts of MPTP exposed differentiating cells were loaded onto a 7.5% SDS-PAGE gel and electrophoresed. Lane 1, control; lane 2, 5 μM MPTP; Lane 3, 10 μM MPTP. Gel was stained with Coomassie blue to reveal protein pattern band formation and confirm the equality of sample loadings.

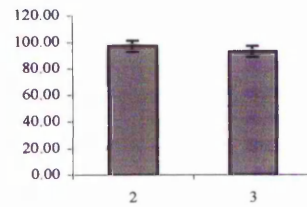
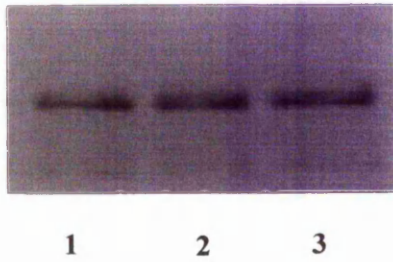
(a). Actin



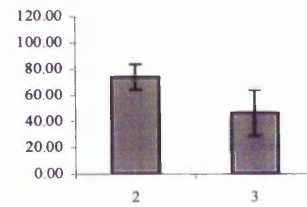
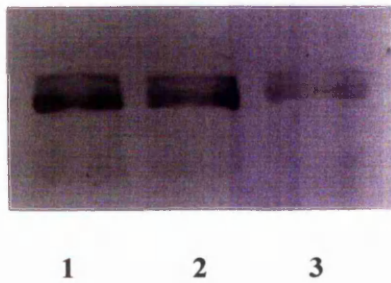
(b). α -tubulin



(c). N52



(d). RMd09



(e). Ta51

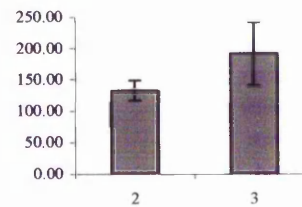
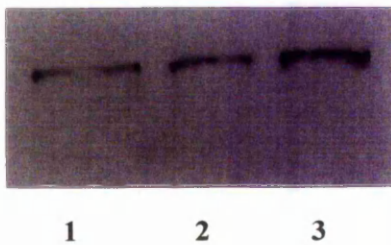


Figure 4.6 *Western blotting analysis of cytoskeletal components from differentiating N2a cells exposed to sub-cytotoxic concentrations of MPTP.*

Left panel: N2a cells were induced to differentiate in the presence or absence MPTP for 24 h, prior to extraction of the cell monolayer. Equal protein aliquots (20 μ g) of cell extracts were electrophoresed on a 7.5% SDS-PAGE gel and transferred onto nitrocellulose membrane filters. Blots were then probed with antibodies that recognise anti-actin (a); α -tubulin (b); or neurofilament epitopes (c-e). The signal was developed using either mouse or rabbit alkaline phosphatase secondary conjugates. Shown are control cells (lanes 1), cells exposed to 5 μ M MPTP (lanes 2) and 10 μ M MPTP (lanes 3) for 24 h during differentiation.

Right panel: Blots were digitised and changes in antibody reactivity were densitometrically analysed using the Quantiscan Analysis software package. Net area values (arbitrary units) representing the area beneath the peak, automatically corrected for background interference, were obtained. Presented are the mean % peak area values (y-axes) of three separate experiments \pm SEM, in which the change in densitometry of cells exposed to 5 μ M MPTP (2) and 10 μ M MPTP (3) is expressed relative to its corresponding control (assigned 100% value).

a.



b.



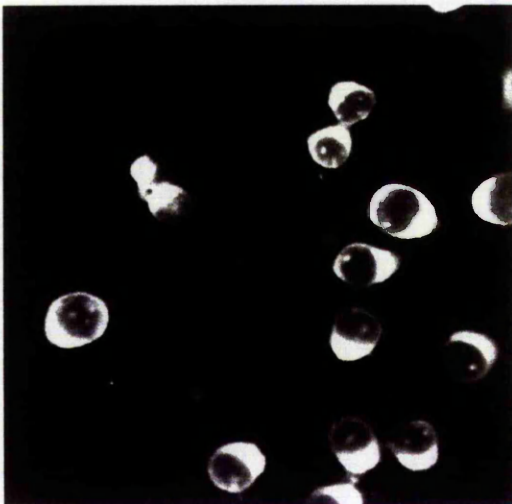
c.



d.



e.



f.



Figure 4.7 *Indirect immunofluorescence analysis of the effect of 10 μ M MPTP on neurofilament-H protein in differentiating N2a cells.*

N2a cells were induced to differentiate in the presence and absence of 10 μ M MPTP for 24 hours, prior to fixation. Cells were fixed in methanol and then probed with antibodies RMd09, Ta51 and anti-actin, as described in Materials and Methods. The signal was revealed using a mouse or rabbit FITC-conjugated secondary antibody and visualised on a confocal microscope. Shown are control cells (a, c, e) and MPTP-treated cells (b, d, f) stained with RMd09 (a, b); Ta51 (c, d) and anti-actin (e, f) respectively. Scale bar: 20 μ M.

4.2.6 ATP levels and mitochondrial membrane potential in differentiating N2a cells exposed to 10 μ M MPTP.

ATP levels and ADP/ATP ratios can provide an alternative indication of cell viability by monitoring cell energy status and therefore were used to investigate the effect of 10 μ M MPTP on cell status. Differentiating N2a cells exposed to 10 μ M MPTP for 24 hours exhibited no significant decrease in ATP levels, compared to control cells. In contrast, exposure of differentiating N2a cells to 0.05% H₂O₂ produced a dramatic drop in cellular ATP levels. This reduction in ATP levels was reflected in the ADP/ATP ratio of hydrogen peroxide exposed cells. However, exposing differentiating N2a cells to 10 μ M MPTP did not show a significant change in ADP/ATP ratios, when compared to control cultures (Table 4.2).

The use of the potentiometric dye JC-1 allowed monitoring of mitochondrial status in both control and 24 hr-neurotoxin treated cells. Healthy mitochondria accumulate JC-1 to form aggregates (termed j-aggregates) that fluoresce in the red spectrum. However, comparison of control and neurotoxin exposed cells loaded with JC-1 exhibited no obvious differences in the number of mitochondria exhibiting a normal mitochondrial potential profile when quantified using FACScan analysis (values of 43.7 % and 42.6 %, respectively, Table 4.2).

4.2.7 Analysis of JNK/SAPK activation in differentiating N2a cells exposed to sub-cytotoxic concentrations of MPTP.

For this study, treated N2a cell extracts cells were electrophoresed on a 12 % SDS-PAGE gel prior to probing with a polyclonal antibody (JNK pAb). This antibody recognises the active, dually phosphorylated form of the enzyme, binding specifically to the phosphorylated amino acid residues threonine and tyrosine of the Thr-X-Tyr consensus sequence (representing the catalytic core of the active JNK enzyme).

Positive activation of JNK kinase (JNK 1,2) was achieved by the treatment of differentiating N2a cells with 0.5 M sorbitol. Figure 4.8A reveals the transient activation of JNK kinase by sorbitol over a 6 hour period, resulting in maximal activation following 30 min exposure to 0.5 M sorbitol. Active JNK kinase was characterised by a 46 and 54 kDa banding pattern representing JNK 1 and JNK2,

respectively. Observation of the cells during this exposure typically revealed a shrunken spherical morphology, associated with osmotic shock, with cells detaching from the substratum at the later time points.

Total cell extracts derived from N2a cells induced to differentiate by serum withdrawal and the addition of dbcAMP for up to 40 hours resulted in no activation of JNK kinase (results not shown). Total cell extracts, derived from differentiating N2a cells exposed to sub-cytotoxic MPTP (10 μ M) for up to 40 hours, revealed very low level but sustained activation of JNK from approximately 20 hours exposure onwards (results not shown). However, the characteristic banding pattern was very faint and included additional band reactivity.

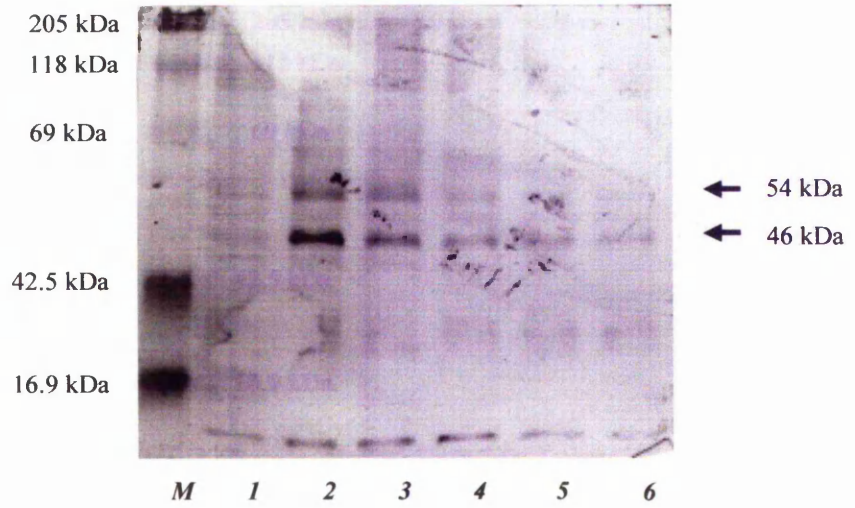
To enhance blot development Triton soluble and insoluble extracts were prepared (see materials and methods, section 2.2.10.2) from N2a cells induced to differentiate in the presence and absence of MPTP for 24 hours. Activation of JNK kinase by 0.5 M sorbitol for 30 minutes resulted in JNK 1 and 2 reactivity within the Triton-soluble fraction (Fig 4.8B, lane 3a) and a concomitant increase in NF-H phosphorylation (as indicated by an increase in Ta51 reactivity) in the insoluble fraction (Fig 4.8B, lane 3b). In conjunction, differentiating N2a cells exposed to MPTP for 24 hours exhibited a faint banding pattern, characteristic of JNK activation, within the Triton soluble cell extract (Fig 4.8B, lane 2a). A concomitant increase in Ta51 reactivity was also present in the Triton-insoluble extract, compared to control untreated sample (compare Fig 4.8B, lanes 1b and 2b).

	<i>ATP</i> (relative light units)	<i>ADP/ATP</i>	<i>% J aggregates</i>
<i>Control</i>	181.55 ± 9.49	0.877 ± 0.016	43.7
<i>10 μM MPTP</i>	166.69 ± 7.25*	0.930 ± 0.024*	42.6*
<i>0.05 % H₂O₂</i>	1.15 ± 0.19	0.4918 ± 0.104	-

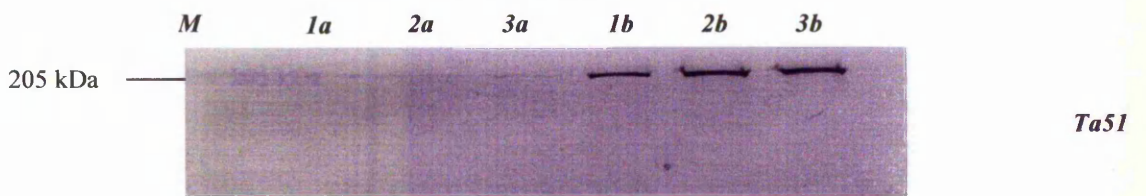
Table 4.2 *Determination of ATP levels and mitochondrial membrane potential in differentiating N2a cells exposed to sub-cytotoxic MPTP concentration.*

Differentiating N2a cells incubated in the presence and absence of MPTP and H₂O₂ were assessed for total ATP levels, ADP/ATP ratios and mitochondrial membrane potential as described in material and methods. ATP results are expressed as mean relative light units ± SEM and ADP/ATP results expressed as means ± SEM, where n=12 in both cases. Mitochondrial membrane potential of MPTP exposed and non-exposed cells are expressed as a percentage of j-aggregate formation (representing active mitochondria). Statistical analysis was carried out using Mann-Whitney *U* test to compare control and neurotoxin treated samples. All p values < 0.05 except *.

A. 0.5 M sorbitol



B. 10 μ M MPTP



C. anti-JNK kinase

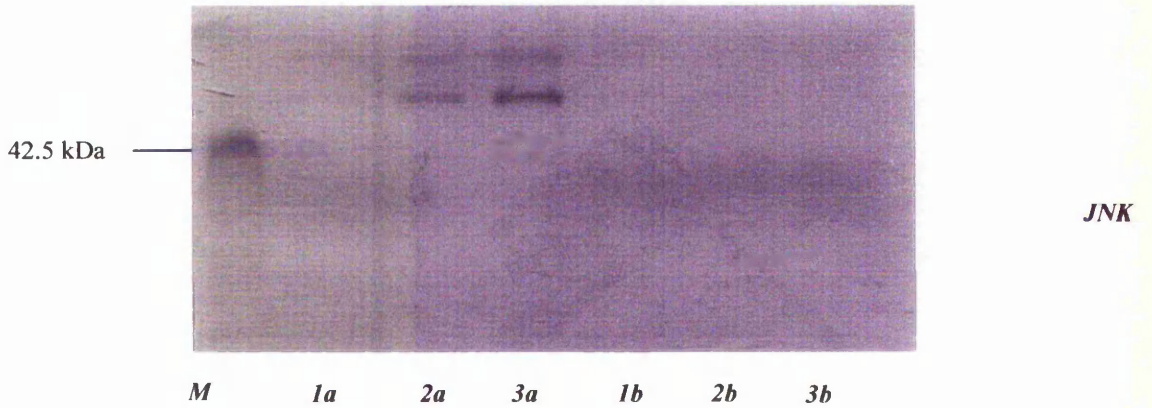


Figure 4.8 *Analysis of JNK kinase activation in differentiating N2a cells.*

N2a cells were plated out in growth medium and incubated at 37°C for 24 hours, in an atmosphere of 95% air/5% CO₂, to allow recovery. Growth medium was carefully aspirated and replaced with an equal volume of SFM containing 0.3 mM dbcAMP + 0.5 M sorbitol (A) or SFM + 0.3 mM dbcAMP + 10 μM MPTP (B). Cells were re-incubated for the required time period prior to extraction of the cell monolayer as described in Materials and Methods (section 2.2.10.2). Equal protein aliquots (20 μg) of total (A) and soluble/insoluble cell extracts; B(a) and B(b), were electrophoresed on a 12 % SDS-PAGE gel and transferred onto nitrocellulose membrane filters. Blots were then probed with a rabbit anti-JNK polyclonal antibody; A and B(b) and Ta51; B(b). The signal was developed using a donkey anti-rabbit alkaline phosphatase secondary conjugate or a goat anti-mouse alkaline phosphatase secondary conjugate, respectively. Activated JNK 1 and JNK 2 produces 54 and 46 kDa bands, respectively. (ρ) represents position of activated forms, *M* represent molecular weight marker.

A. Cells induced to differentiate for 24 hours + sorbitol treatment.

(1) 0 hr (2) 30 min (3) 1 hr (4) 2 hr (5) 4 hr (6) 6 hr

B. Cells induced to differentiate for 24 hours in the presence or absence of MPTP.

(1a) No MPTP (soluble) (2a) 10 μM MPTP (soluble) (3a) 0.5 M sorbitol [30 min] (soluble)
(1b) No MPTP (insoluble) (2b) 10 μM MPTP (insoluble) (3b) 0.5 M sorbitol [30 min] (insoluble)

4.2.8 Analysis of protein ubiquitination in differentiating N2a cells exposed to sub-cytotoxic concentrations of MPTP.

Analysis of abnormal ubiquitinated protein patterns was carried out by probing total cell extracts derived from differentiating N2a cells exposed to sub-cytotoxic doses of MPTP. Western blots probed with a polyclonal anti-ubiquitin antibody (a kind gift from Prof. R.J. Mayer) produced a characteristic smearing pattern corresponding to ubiquitin-conjugated proteins. A distinct increase in reactivity was observed from extracts of differentiating N2a cells (Fig. 4.9, 24 hr differentiation, lane 2), compared with extracts obtained from mitotic N2a cells (Fig 4.9, 0 hr differentiation, lane 1). Although less distinct, an increase in antibody reactivity, corresponding to an increase in ubiquitin-conjugated proteins, was also evident in MPTP treated samples. However, the characteristic smearing of bands on the blots, unfortunately would not allow the identification of any specific ubiquitin-conjugated proteins.

4.2.9 Analysis of synuclein levels in differentiating N2a cells exposed to sub-cytotoxic concentrations of MPTP.

Western blots analysis of total N2a cell extracts and rat / mouse brain soluble cell extracts, were probed with a polyclonal anti-synuclein (PER 4) antibody (a kind gift from Dr. M. Goedert). Soluble protein cell extracts from rat and mouse brains produced positive reactivity, with a band present at approximately 19 kDa (Fig 4.10, lane 3, 4). Synuclein reactivity was not detected in total cell extracts derived from N2a cells induced to differentiate in the presence (Fig 4.10, lane 2) and absence (Fig 4.10, lane 1) of MPTP. However, N2a cells extracts and to a lesser extent, soluble rodent brain cell extracts exhibited an unidentified faint reactive band with an apparent molecular weight of approximately 80 kDa (lanes 1-4).

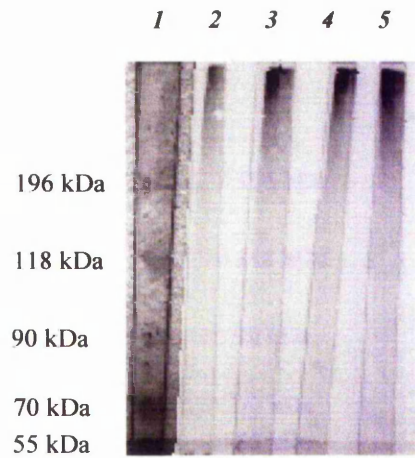


Figure 4.9 *The effect of sub-cytotoxic concentrations of MPTP on protein ubiquitination in differentiating N2a cells.*

N2a cells were induced to differentiate in the presence or absence MPTP for 24 h, prior to extraction of the cell monolayer. Equal protein aliquots (20 μ g) of cell extracts were loaded onto a 7.5% SDS-PAGE gel and electrophoresed. Samples were then transferred onto nitrocellulose membrane whereupon the membrane was autoclaved for 20 min prior to probing with a rabbit anti-ubiquitin polyclonal antibody (*Ub-KLH, 968215 pAb*). The signal was developed using a goat anti-rabbit alkaline phosphatase secondary conjugate. Shown are SDS-PAGE pre-stained molecular weight markers (lane 1), non-differentiated N2a cells (lane 2), cells induced to differentiate for 24 hours (lane 3), cells induced to differentiate in the presence of 5 μ M MPTP (lane 4) and 10 μ M MPTP (lane 5).

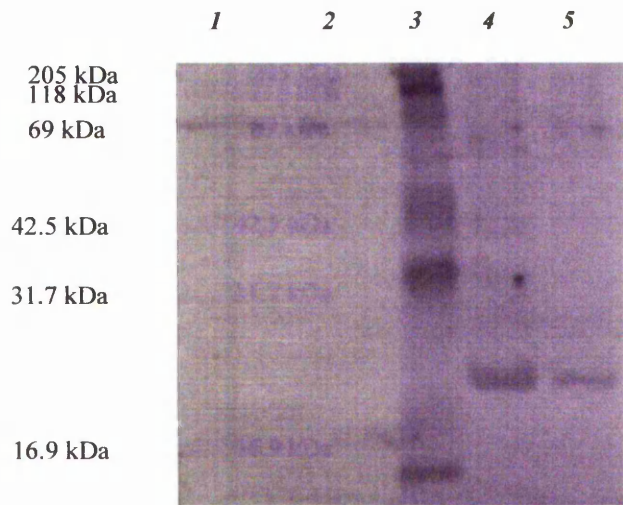


Figure 4.10 *The effect of a sub-cytotoxic concentration of MPTP on synuclein levels in differentiating N2a cells.*

N2a cells were induced to differentiate in the presence or absence MPTP for 24 h, prior to extraction of the cell monolayer. Soluble brain extracts from a Wistar rat and Balb-c mouse were prepared whereupon protein aliquots (20/40* μg) of extracts were loaded onto a 7.5% SDS-PAGE gel and electrophoresed. Samples were then transferred onto nitrocellulose membrane filters prior to probing with a rabbit anti-synuclein antibody. The signal was developed using a goat anti-rabbit alkaline phosphatase secondary conjugate. Shown are N2a cells induced to differentiate for 24 hours (lane 1), cells induced to differentiate in the presence of 10 μM MPTP (lane 2), pre-stained molecular weight marker (lane 3), rat brain soluble cell extract (lane 4*), and mouse brain soluble cell extract (lane 5).

4.3 Discussion

4.3.1 N2a cell differentiation.

Differentiation of N2a neuroblastoma cells, by serum withdrawal and the addition of dbcAMP, substantially reduced cell division accompanied by a dramatic change in cell morphology. This was typically characterised by the outgrowth of axon-like processes from the cell perikaryon. Indeed, characterisation of axon outgrowth in differentiating N2a cells revealed a steady increase in axon numbers over a 32 hour differentiation period. This was accompanied by a steady increase in total NF-H levels as determined by N52 reactivity. Similarly, levels of hypo-phosphorylated NF-H, as defined by RMd09 reactivity and phosphorylated NF-H as defined by Ta51 reactivity, also increased over this time period. It was evident from observing the levels of phosphorylated NF-H that this post-translational modification was expressed at a later stage, when compared to the levels of hypo-phosphorylated NF-H. For example, N2a cells induced to differentiate for up to 8 hours revealed the absence of significant Ta51 reactivity. This delay in NF-H phosphorylation has been seen by others (Carden *et al.*, 1987, Shea *et al.*, 1990) and is related to the process of NF assembly and axon stabilisation (Carden *et al.*, 1985; Nixon, 1993). Differentiation of N2a cells for 48 hours revealed a slight decline in the number of axons formed suggesting maximal cell differentiation had been achieved under the conditions used. In contrast, total NF-H levels continued to show a slight increase along with the levels of phosphorylated NF-H. This may be associated with axon calibre and length, factors that correspond with maturation and stabilisation of axons (Carden *et al.*, 1985; Nixon, 1993).

4.3.2 Sub-cytotoxic effects of MPTP on differentiating N2a cells.

Results presented in Chapter III suggest that differentiating N2a cells exhibit a greater sensitivity to MPTP than their mitotic, non-differentiating counterparts. In addition, differentiating N2a cells exposed to MPTP exhibited changes in cell morphology, even at concentrations that produced no measurable cell death. This was further investigated and confirmed in this chapter indicating that sub-cytotoxic doses of MPTP can inhibit the outgrowth of axon-like processes of differentiating N2a cells.

Indeed the number of axon-like processes in cells exposed to 10 μ M MPTP for 24 hours was 40 % less than in control differentiating cells. This effect is in agreement with earlier observations (Denton and Howard, 1984; Notter *et al.*, 1988), where a change in neuronal cell morphology was noted but has been quantified for the first time in the present study.

Since the cytoskeleton provides the framework that defines, supports and maintains the shape of neurones, a change in cell morphology could be attributed to alterations within the cytoskeleton. Western blots probed with anti-actin and anti- α -tubulin antibodies exhibited no obvious change in protein levels. In addition, observation of the actin network using confocal microscopy exhibited no visible spatial alterations. These observations contrast with work on Swiss 3T3 fibroblasts, which indicated that high levels of MPTP (1.5 mM) does modify the spatial organisation of the microfilament and microtubule networks following 6 hours exposure (Cappelletti *et al.*, 1991; Urani *et al.*, 1994). Indeed, it has also been reported that the direct exposure of pre-differentiated PC12 cells to the active metabolite MPP⁺ (15 μ M for 24 hours) can alter the regulatory balance of α - and β -tubulin (Cappelletti *et al.*, 1995). These reported changes possibly reflect an acute effect to high levels of MPTP or prolonged exposure to the active metabolite, respectively.

NFs are characteristically major components of the axonal cytoskeleton, with the expression and post-translational modification of NF-H associated with axon maturation, calibre and stability (Carden *et al.*, 1987). Exposure of differentiating N2a cells to MPTP produced an altered NF-H reactivity with RNd09 and Ta51 but not N52. A decrease in RNd09 reactivity in the presence of a concomitant increase in Ta51 reactivity suggests that differentiating N2a cells exposed to sub-cytotoxic levels of MPTP exhibit a net increase in NF-H phosphorylation which may be associated with the observed inhibition of axon outgrowth.

Increased NF-H phosphorylation has been observed *in vivo* in neuropathologies induced by treatment with acrylamide (Gold *et al.*, 1988), aluminium (Johnson and Jope, 1988) and in streptozotocin-induced diabetic neuropathy (Pekiner and McLean, 1991). The observed change in cell morphology and NF-H phosphorylation state within the differentiating N2a cell model may therefore indicate a subtle alteration consequential to cellular stress. These phenomena have also been observed in other

neuroblastoma cell models using different proposed neurotoxicants. For example, Shea *et al.*, (1995) reported an increase in NF-H phosphorylation following aluminium exposure using a subclone N2a model, NB2a/d1. In addition, Flaskos *et al.*, (1998) reported a reduction in axon outgrowth in differentiating N2a cells, although in this case NF-H levels were reduced. The effect of MPTP on differentiating N2a cells in this study could be attributed to its mode of action, possibly reflecting some specific effects on NF-H. However, it is evident that other neurotoxins may cause similar changes in the NF network of differentiating cells, possibly through other pathways, lending further support to the use of NF-H phosphorylation as an early neurotoxicity marker.

The consequence of changes in NF-H phosphorylation following MPTP treatment on the spatial arrangement of the NF-H network was studied by indirect immunofluorescence using RMd09 and Ta51. RMd09 preferentially stains neuronal perikarya and short processes in adult rat nervous tissue (Lee *et al.*, 1987) and the proximal regions of axon-like processes in differentiated N2a and PC12 cells (Flaskos *et al.*, 1998). This was reflected in the pattern of staining in control differentiating N2a cells. However, cultures that had been exposed to MPTP for 24 hours expressed a reduction in perikaryal RMd09 staining countered by an increase in Ta51 reactivity, particularly in cells lacking significant axon growth.

The appearance and accumulation of phosphorylated NF-H isoforms within the perikayon of NB2a/d1 cells has been reported in both undifferentiated and differentiated cells, following exposure to aluminium (Shea *et al.*, 1995). It has also been shown that aluminium can disrupt NF translocation into axon-like neurites (Shea *et al.*, 1997) contributing to an accumulation of NF-H within the perikaryon. In addition, the neurotoxins acrylamide and 2,5 hexanedione have been shown to induce accumulation of NFs in the perikarya of differentiated human SH-SY5Y neuroblastoma cells (Hartley *et al.*, 1997). There is also evidence of altered phosphorylation of NFs after exposure to these two neurotoxins (Watson *et al.*, 1991; Reagan *et al.*, 1994) suggesting the disruption of NF phosphorylation could lead to NF disorganisation and accumulation.

Cultured neuronal cells contain substantial Triton-soluble pools of NF subunits, including partially phosphorylated NF-H and extensively phosphorylated isoforms of

NF-H, prior to the elaboration of neurites (Shea *et al.*, 1989, 1990). In addition, the necessary kinases to effect NF subunit phosphorylation have been shown to be present in the cell perikaryon (Polotrak and Freed, 1988). Pulse chase analysis has suggested that a proportion of soluble NF-H may represent precursors for NF assembly and that their phosphorylation before assembly and axonal transport is a function of their extended residence time within perikarya (Shea *et al.*, 1990). The possibility therefore arises that premature NF-H phosphorylation could contribute to its aberrant accumulation within the cell perikaryon (Shea *et al.*, 1994). The inhibition of axon outgrowth produced following MPTP exposure seen in the present study could therefore be consequential to disruption of phosphorylation state affecting normal cytoskeletal distribution.

4.3.3 N2a cell energy status and mitochondrial integrity

Although no measurable cell death was seen with 10 μ M MPTP over 24 hr, changes in N2a cell morphology and the cytoskeleton were evident (see above). Morphological and ultrastructural changes, particularly to mitochondria, have also been reported in human neuroblastoma cells at concentrations and exposure times much lower than that needed to induce cell death (Song *et al.*, 1997). Uncoupling of mitochondrial respiration can produce a number of secondary events including loss of ATP, elevations in intracellular calcium and increased oxidative stress (Chan *et al.*, 1991). However, exposure of differentiating N2a cells to 10 μ M MPTP produced only a small reduction in ATP levels, characterised by an increase in the ADP/ATP ratio, changes that were not significant. This was confirmed by the determination of the mitochondrial membrane potential in control and MPTP exposed cultures, resulting in no significant change in j-aggregate formation. This suggests that the morphological (i.e. axon outgrowth inhibition) and biochemical changes (i.e. increase in NF-H phosphorylation) observed in differentiating N2a cells exposed to sub-cytotoxic MPTP concentrations occurs prior to changes to mitochondrial integrity or significant inhibition of mitochondrial respiration.

4.3.4 Activation of the stress-activated protein kinase (SAPK) cascade.

Activation of the SAPK cascade is associated with events leading to cell death and has been shown to be triggered by oxidative stress (Turner *et al.*, 1998) and calcium fluxes (Tibbles and Woodgett, 1999); factors also associated with MPTP neurotoxicity. Indeed, inhibition of the SAPK pathway by an analogue of K252a (protein kinase inhibitor) has been shown to protect against the loss of dopaminergic cells in a low-dose MPTP mouse model. (Saporito *et al.*, 1999). Sorbitol-induced activation of JNK by osmotic shock imparted dramatic changes on differentiating N2a cellular morphology, namely the rounding up of cells. This resulted in a transient activation of JNK over a 6 hour exposure period in addition to an increase in NF-H phosphorylation following 30 minutes sorbitol exposure.

Differential extraction of N2a cells exposed to 10 μ M MPTP revealed a low, but clear activation of JNK, following 24 hours exposure. In addition, insoluble extracts revealed a concomitant increase in NF-H phosphorylation (as defined by Ta51 reactivity) compared to control differentiating cells. Interestingly, Giasson and Mushynski (1996) have reported that activation of the SAPK pathway can lead to hyper-phosphorylation of perikaryal NF-H. Although MPTP caused only low level JNK activation (compared to sorbitol) in N2a cells, exposure lasted 24 hours. This continual prolonged exposure during differentiation could conceivably elicit the cumulative alteration in NF-H phosphorylation state as a consequence of triggering the stress activated pathway. Although, these results provide a preliminary indication that MPTP may activate a stress-induced signalling cascade it does not, of course, exclude the possibility that non-JNK related pathways may be involved in aberrant NF-H phosphorylation following exposure to MPTP.

4.3.5 Protein ubiquitination in differentiating N2a cells.

N2a cells induced to differentiate for 24 hours typically expressed an increase in protein ubiquitination compared to corresponding cells maintained in the mitotic state. This increase in ubiquitination is reminiscent of the levels of free ubiquitin seen in differentiating neuroblastoma cells, compared to proliferating cells (LaRosa *et al.*, 1996). Immunostaining for ubiquitin increased markedly within the cell cytoplasm

when neuroblastoma cells were induced to differentiate. It has been suggested that this increase may be due to the need for the increased removal of proteins responsible for cell proliferation (LaRosa *et al.*, 1996). Although small, changes (i.e. increased antibody reactivity) were observed between control differentiating N2a cells and cells induced to differentiate in the presence of MPTP over a 24 hour period. Reactivity was localised to proteins with molecular weights in excess of approximately 180 kDa. However, due to the extent of basal protein ubiquitination in differentiating cells and the possibility of multi-ubiquitination of proteins any changes to specific proteins were masked, making interpretation difficult. Nevertheless, the failure of a cell to eliminate ubiquitinated proteins can disrupt cellular homeostasis leading to cell degeneration and cell death (AlvesRodriguez *et al.*, 1998). Indeed, differentiating N2a cells exposed to MPTP for 48 hours does lead to a reduction in cell viability (see Chapter III).

4.3.6 Synuclein expression in differentiating N2a cells.

Although recent reports have suggested that MPTP can provoke an increase in α -synuclein expression within the nigrostriatal pathway mice *in vivo* (Jackson-Lewis *et al.*, 1998; Vila *et al.*, 2000), N2a cells induced to differentiate in the presence of MPTP did not exhibit synuclein reactivity. Indeed, the expression of α/β -synuclein (19 kDa) in N2a cells was undetectable both in the mitotic (results not shown) and control differentiating states, suggesting its role in these cells to be of limited importance under normal basal conditions. Interestingly, synuclein mRNA and protein has been reported in normal mouse brain with particular emphasis on the midbrain including the substantia nigra (Vila *et al.*, 2000). The absence of basal reactivity in N2a cells could therefore prejudice its potential involvement in MPTP neurotoxicity in this cell line. PER 4 (anti-synuclein antibody) did react with an 80 kDa band in N2a cells extracts, a band that was less distinct in control rat and control mouse brain cell extracts. Although one could speculate that this could be the consequence of synuclein aggregates induced by α -synuclein mutation as seen by ElAgnaf *et al.* 1998, in human neuroblastoma cells, it is more likely that this is due to antibody cross reactivity. The involvement of α/β -synuclein in MPTP induced neurotoxicity in the differentiating N2a cell model remains undetermined.

CHAPTER V

MPTP-induced neurotoxicity: Inhibition by potential neuroprotective agents.

5.1 Introduction.

5.1.1 Neuroprotection

The cytotoxic capacity of MPTP on differentiating N2a cells was initially established in Chapter III. *In vivo*, MPTP is thought to be oxidised to an active toxic metabolite 1-methyl-4-phenylpyridinium (MPP⁺) by the catecholaminergic enzyme monoamine oxidase (MAO) found in neighbouring glial cells (Markey *et al.*, 1984). The mechanisms of action of MPTP/MPP⁺ have been studied by several authors who have suggested the possible involvement of many factors. These include the inhibition of mitochondrial oxidative processes in particular complex I (Nicklas *et al.*, 1985; Ramsey *et al.*, 1986), generation of toxic reactive oxygen species (Lai *et al.*, 1993; Sriram *et al.*, 1997), changes in intracellular calcium levels (Kass *et al.*, 1988; Packer *et al.*, 1996) and induction of glutamate-mediated excitotoxicity (Turski *et al.*, 1991), to name but a few. However, the precise intraneuronal mechanisms by which MPTP can evoke cellular changes that lead to neurodegeneration are still not fully understood. Nevertheless, these discoveries have greatly influenced Parkinson's disease research in identifying possible targets for pharmacological intervention and potential therapeutic agents. The use of differentiating N2a cells will provide a model with which to investigate potential neuroprotective agents to alleviate MPTP-induced neurotoxicity.

Since MPTP can exert its neurotoxic effect through biological activation by MAO (Markey *et al.*, 1984), inhibition of this enzyme could therefore potentially afford neuroprotection. *In vivo*, inhibition of MPTP-induced dopaminergic neurotoxicity has been achieved using the MAO-B specific inhibitor deprenyl, while the MAO-A specific inhibitor clorgyline exhibited little protective effect (Heikkila *et al.*, 1984a; Langston *et al.* 1984a). Indeed, deprenyl has gained wide clinical acceptance as a useful form of adjunct therapy in the treatment of Parkinson's disease. In contrast, *in vitro* studies using neuronal cell model systems have reported that clorgyline, in addition to deprenyl, can confer protection from MPTP-induced cell death (Buckman *et al.*, 1991; Lai *et al.*, 1993) suggesting clorgyline may still play a role in alleviating toxin induced degeneration.

A primary role for oxidative stress in MPTP-induced neurotoxicity still remains disputable. Generation of cytotoxic free radicals following MPTP treatment has been reported in MPTP-treated mouse brain (Sriram *et al.*, 1997) and in cultured human neuroblastoma cells (Kitamura *et al.*, 1999), prior to complex I inhibition. In contrast, treatment of dopaminergic neurones with MPP⁺ produced a small increase in reactive oxygen species that could not be directly related to cell death (Lotharius *et al.*, 1999). The absence of significant levels of lipid peroxidation products in MPTP-treated neuronal cell lines also confuses the situation (Lai *et al.*, 1993). The protective capacity of various antioxidants in alleviating cell death has also produced conflicting results. Pre-treatment of mouse brain slices with the general cellular reductant glutathione can partially attenuate MPTP toxicity in mouse brain slices (Sriram *et al.*, 1997). In addition, depletion of glutathione can potentiate nigrostriatal cell death in MPTP-treated mice (Wullner *et al.*, 1996). In contrast, other antioxidants such as allopurinol or superoxide dismutase were unable to rescue MPP⁺-induced cell death in cultured dopaminergic neurones, while other antioxidants tested could only provide partial protection (Akaneya *et al.*, 1995). The ability of glutathione (a non-protein reductant) to protect differentiating N2a cells from MPTP-induced toxicity will be investigated, also allowing an indication of the extent of involvement of reactive oxygen species.

Glial cells play a variety of supporting roles to brain neurones. *In vivo*, these cells secrete a variety of factors (termed neurotrophic factors) that specifically influence neuronal migration, survival and neurite outgrowth (Shea and Hussain, 1996). The fact that these neurotrophic factors are implicated in the normal functional activity of neuronal cells and play a role in plasticity suggests they may exhibit neuroprotective properties. Indeed, glial-derived neurotrophic factor (GDNF), found as a trophic factor for midbrain dopaminergic neurones (Lin *et al.*, 1993), has received much attention as a potential therapeutic agent for the treatment of neurodegenerative diseases (reviewed by Airaksinen *et al.*, 1999). The fact that glial cells release factors is a phenomenon that can be mimicked in culture by utilising conditioned medium derived from glial cultures. The ability of conditioned medium to confer protection against MPTP-induced neurotoxicity will therefore be investigated.

A cell's response to stress is often complex, involving multiple signalling pathways that can act alone or in concert to influence cell fate. Of growing interest is the role of the mitogen activated protein kinase signalling cascades in mediating neurotoxicity, since *in vivo* studies have recently suggested that MPTP-induced cell death can be attenuated by inhibition of the stress-activated signalling cascade (SAPK) (Saporito *et al.*, 1999). Interestingly, inhibition of the p38 kinase pathway has been proposed to promote cell survival in neuronal cells (Horstmann *et al.*, 1998). However, the role of the p38 mitogen-activated protein kinase cascade in MPTP neurotoxicity has yet to be determined. The use of a specific p38 inhibitor will attempt to address the potential involvement of the p38 mitogen-activated protein kinase cascade in MPTP neurotoxicity.

Increasing evidence also suggests the role of oestrogen as a neuroprotective compound that can act dependently or independently of oestrogen receptor activation. Indeed, oestrogen has been shown to prevent MPTP-induced dopamine depletion in mice (Behl and Holsboer, 1999) and recently oestrogen replacement therapy has been suggested as a potential pharmacological approach for the prevention and treatment of Alzheimer's and Parkinson's disease (Inestrosa *et al.*, 1998; Marder *et al.*, 1998). The ability of oestrogen to protect N2a cells from MPTP-induced cell death will therefore be investigated.

This chapter will therefore investigate the ability of various potential neuroprotective agents to attenuate MPTP-induced cell death in differentiating N2a cells. The neuroprotectants will include the use of MAO inhibitors clorgyline and deprenyl, glutathione, glial conditioned medium, oestrogen and a specific p38 inhibitor (SB202190). Although viability is a common endpoint to determine if toxicants are affecting cells in culture it can be a relatively insensitive marker which can mask subtle changes to a cell population resulting from neurotoxic insult. Indeed, the previous chapter demonstrated that MPTP could interfere with cellular biochemical processes and cell morphology, characterised by an inhibition of axon outgrowth and an increase in neurofilament-H phosphorylation, prior to measurable cell death. Therefore in addition to cytoprotection, the ability of potential neuroprotective agents to maintain neuronal cell morphology and attenuate the MPTP-induced changes to differentiating N2a cells will be assessed.

5.2 Results

5.2.1 The effect of MAO inhibitors on MPTP-induced cytotoxicity.

The ability of the MAO inhibitors clorgyline and deprenyl to inhibit MPTP-induced cytotoxicity was investigated using the MTT reduction assay (Fig 5.1 A, B). Previous experimental work showed that total MAO activity was inhibited in intact N2a cells by 0.5 μM clorgyline or 50 μM deprenyl (Chapter III, section 3.2.4.1). Concentrations of 0.5 μM and 50 μM clorgyline had no significant effect on cell viability; however, at higher concentrations (100 μM and 250 μM) clorgyline significantly reduced cell viability compared to controls (i.e. 250 μM clorgyline reduced viability by 22 % compared to control values). Nevertheless, when values were normalised against their corresponding clorgyline control, clorgyline (50-250 μM) was able to partially protect differentiating N2a cells from MPTP-induced cell death (Fig 5.1 A). In general, a reduction in MPTP-induced cell death was seen with an increase in clorgyline concentration at low MPTP concentrations. This protective effect was greater in cultures exposed to 0.1 mM MPTP than cultures exposed to 1.0 mM MPTP, viability increasing by approximately 20 % and 10 %, respectively, with 250 μM clorgyline. However, since clorgyline at concentrations of 50 μM and above is toxic, overall cell viability in the presence of MPTP is not improved by these higher concentrations of clorgyline treatment.

In comparison, deprenyl alone (50-250 μM) exhibited no significant toxic effect to differentiating N2a cells; cell viability in the presence of deprenyl alone producing comparable values to control cell viability. Additionally, deprenyl reduced cell death to a greater extent than clorgyline, at concentrations between 50-250 μM , with cytoprotection again being dependent on MPTP concentration (Fig 5.1 B). Indeed, deprenyl (250 μM) increased cell viability by approximately 36 % and 16 % when cells were exposed to 0.01 and 0.1 mM MPTP, respectively, compared to controls in its absence.

5.2.2 The effect of potential neuroprotective agents on MPTP-induced cytotoxicity.

Glial conditioned medium, derived from C6 glioma cells, was able to reduce neurotoxin-induced cytotoxicity of differentiating N2a cells exposed to MPTP for 48 hours, producing up to ~20% increase in cell viability at the MPTP concentrations investigated (Fig. 5.2 A). Indeed, by increasing the concentration of glial conditioned medium (from 1:8 to 1:2 dilution), MPTP-induced cytotoxicity was consistently reduced. Differentiating N2a cells exposed to conditioned medium alone exhibited no significant increases in MTT reduction (i.e. viability), although observing the cells using light microscopy revealed definite changes to cell morphology (see section 5.2.4).

Inhibition of the p38 MAPK pathway using SB202190 did not dramatically effect viability of N2a cells with viability increasing by up to 19 %, compared to cells induced to differentiate in its absence. However, SB202190 was unable to confer significant protective capacity to cells exposed to MPTP concentrations in excess of 10 μ M for 48 hours. Nevertheless, cells exposed to 10 μ M MPTP in the presence of SB202190 did exhibit increased survival, with viability increasing by up to ~20 %, in conjunction with a rise in inhibitor concentration (1-20 μ M) (Fig. 5.2 B).

The ability of oestradiol to alleviate MPTP-induced cell death was also investigated using the MTT reduction assay. Cells differentiated in the presence of oestradiol alone exhibited an increase in MTT reduction (i.e. viability) with cells exposed to 1 mM oestradiol displaying a dramatic 63 % increase, compared to control cells (Fig 5.3 A). However, oestradiol was only able to confer cytoprotection to MPTP exposed cells when used at concentrations of 100 μ M or above. The use of 0.01 mM estradiol could not alleviate MPTP-induced cell death. In addition, protection was only afforded to differentiating N2a cells exposed to MPTP concentrations up to 400 μ M for 48 hours; cells exposed to higher concentrations of 800 μ M and 1000 μ M MPTP were not protected.

The potential capacity of glutathione to alleviate MPTP-induced cell death was addressed using glutathione in its reduced form (GSH). The addition of reduced glutathione (0.1-2.0 mM) alone to differentiating N2a cells produced a dramatic increase in MTT reduction. For example the addition of 2 mM glutathione produced a 118 % increase in cell viability as suggested by MTT reduction (Fig 5.3 B). In

contrast, the presence of 0.1–1 mM glutathione was unable to alleviate MPTP-induced cell death to any significant extent, although the addition of 2 mM glutathione to MPTP exposed cells did produce minor increases in cell viability.

5.2.3 Intracellular glutathione levels

Table 5.1 shows changes in cellular glutathione levels after the addition of extracellular glutathione (GSH) to differentiating N2a cells. Cells were exposed to glutathione (1-2 mM) for 48 hours prior to assessment. The addition of 1 mM glutathione to N2a cells produced a 37 % increase in endogenous glutathione levels. Glutathione levels were maintained when 2 mM glutathione was added to differentiating cells with cells expressing a 34% increase compared to control. Differentiating N2a cells exposed to 1 mM MPTP for 48 hours exhibited a similar glutathione content (21.79 nmol/mg protein) as control cells (20.00 nmol/mg protein).

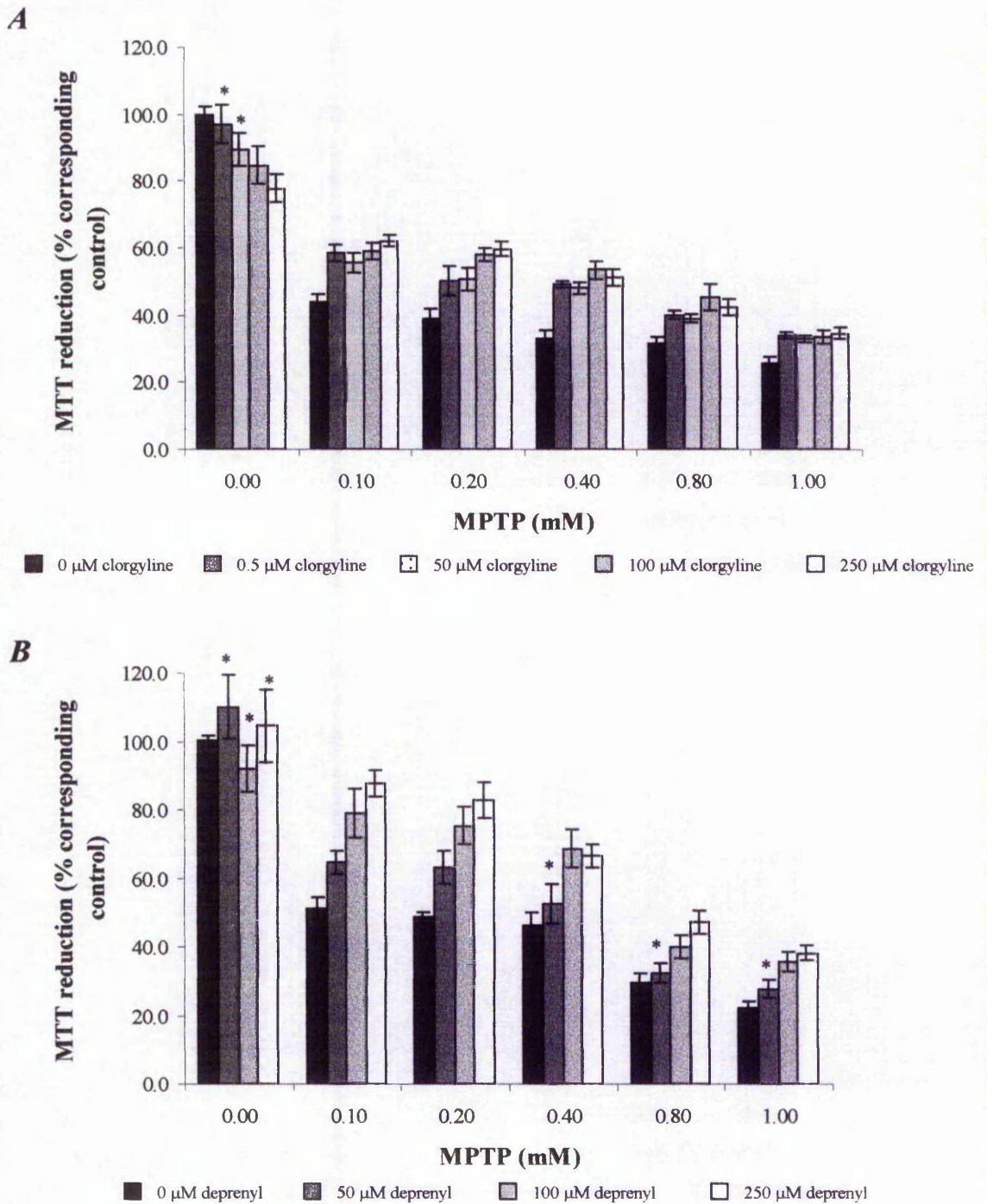
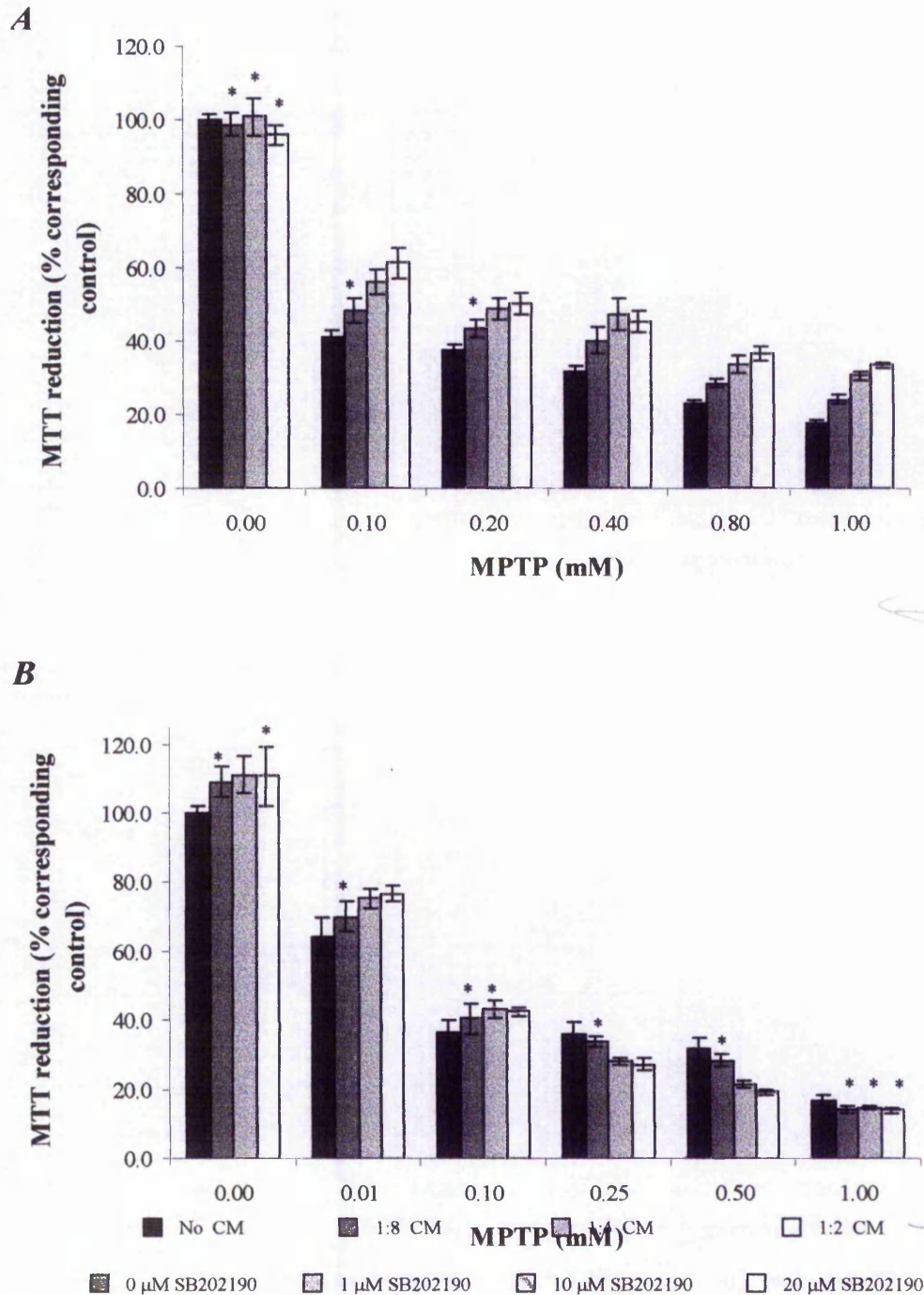


Figure 5.1 Cytotoxic protection afforded by clorgyline and deprenyl on differentiating N2a cells exposed to MPTP for 48 hours.

N2a cells were induced to differentiate in the presence of MPTP and clorgyline (A) or deprenyl (B). Cells were re-incubated for a further 48 hours prior to cell viability assessment via the MTT reduction assay. All results are expressed as mean % MTT reduction \pm SEM, compared to corresponding MAO inhibitor control. The effect of MAO inhibitor alone on cell viability was assessed by reference to (0 μ M "MAO inhibitor") control. Statistical analysis was carried out using the Mann-Whitney *U* test, where $n=8$. Results obtained in the presence of MAO inhibitor were compared against the results obtained in its absence. All values $p < 0.05$ except *.



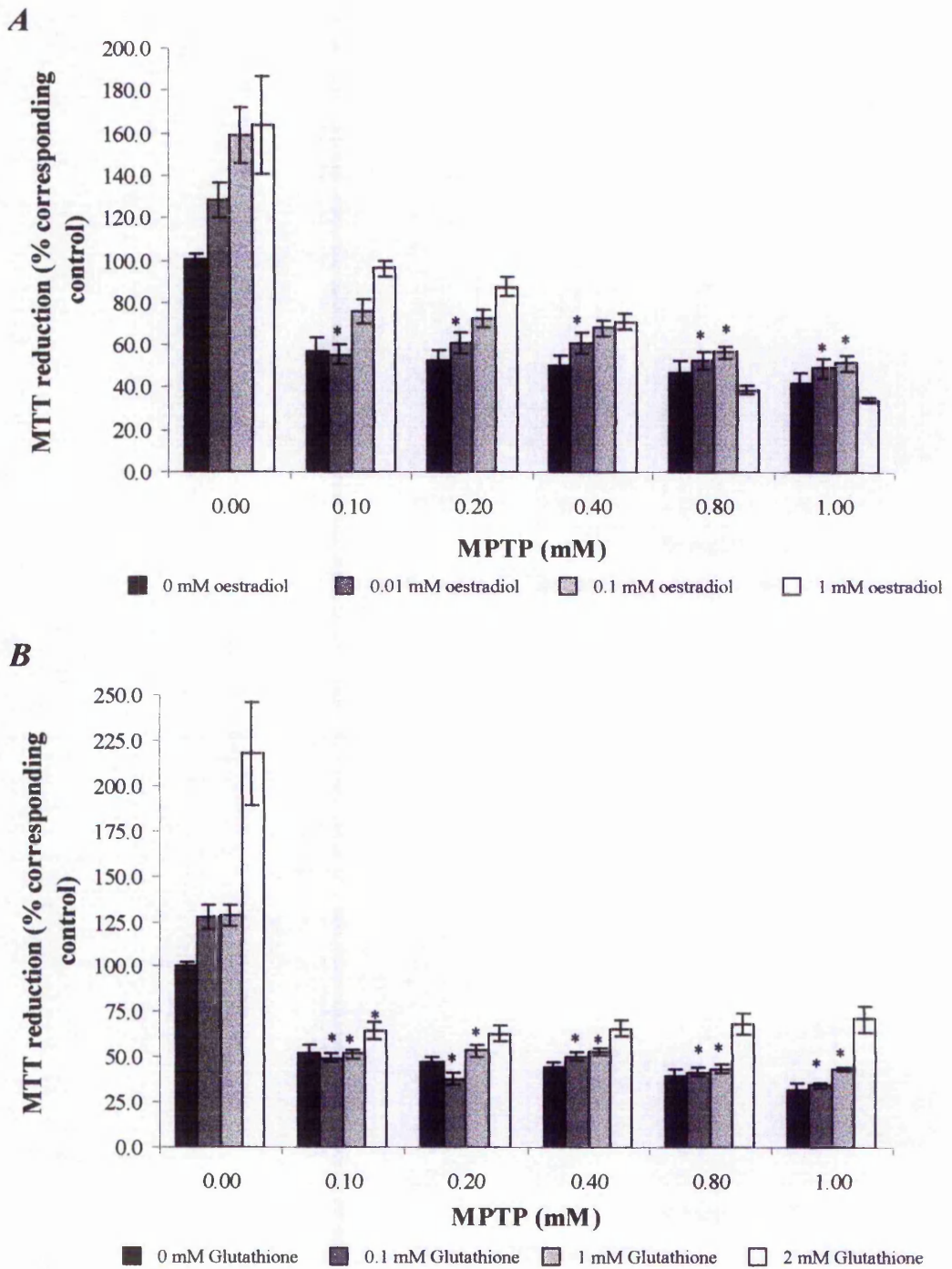


Figure 5.3 *The effect of oestradiol and glutathione on MPTP-induced cell death induced.* N2a cells were induced to differentiate in the presence of MPTP and either oestradiol (**A**) or glutathione (**B**). Cells were re-incubated for a further 48 hours prior to cell viability assessment via the MTT reduction assay. All results are expressed as mean % MTT reduction \pm SEM, compared to corresponding control. The effect of “neuroprotectant” alone on cell viability was assessed by reference to viability in its absence (0 mM MPTP; control). Statistical analysis was carried out using the Mann-Whitney *U* test, where $n=8$. Results obtained in the presence of “neuroprotectant” were compared against the results obtained in its absence. All values $p < 0.05$ except *.

	<i>Total Glutathione(nmol/mg protein)</i>	
	<i>Mean ± SEM</i>	<i>% change ca. control</i>
<i>Control[#]</i>	20.00 ± 1.66	-
<i>1 mM glutathione</i>	27.51 ± 1.74	+ 37.6 %
<i>2 mM glutathione</i>	26.86 ± 3.89	+ 34.3 %
<i>1 mM MPTP</i>	21.79 ± 2.96	+ 9.0 %*

Table 5.1 Analysis of total glutathione levels in differentiating N2a cells following the addition of extracellular GSH.

N2a cells were induced to differentiate in the presence or absence of reduced glutathione (1- 2 mM) for 48 hours, prior to assessment. Similarly, N2a cells were also induced to differentiate in the presence of 1 mM MPTP for 48 hours. Following extraction, samples were analysed for protein content and total glutathione levels (GSH + GSSG). Total glutathione is expressed as nmol/mg protein, where n=4, except #, where n=8. Statistical analysis was carried out using the Mann-Whitney *U*-test to compare control differentiating N2a cells against treated cells. All p values < 0.05 except *.

5.2.4 Analysis of neuroprotective agents on axon outgrowth.

Changes in morphological cell differentiation characterised by axon outgrowth were carried out. N2a cells were induced to differentiate in the presence of dbcAMP and a potential neuroprotective agent, over a 24 hour time period. The ability of N2a cells to extend axon-like processes in the presence and absence of sub-cytotoxic MPTP concentrations was initially investigated. In order to quantify any changes in cell morphology treated cells were fixed and stained with Coomassie blue and examined by light microscopy. A sub-cytotoxic concentration of MPTP (10 μ M) was able to inhibit the formation of axon-like processes by approximately 40 % (Table 5.2 and Chapter IV; section 4.2.2). The ability of various agents to alleviate this inhibition of axon outgrowth was similarly investigated. MPTP treated differentiating N2a cells were incubated in the presence and absence of the MAO inhibitors clorgyline (0.5 μ M) and deprenyl (50 μ M); concentrations that fully inhibit MAO, in intact N2a cells, but are not cytotoxic. Clorgyline partially protected the cells from the MPTP-induced inhibition of axon outgrowth, axon counts being reduced by approximately 16 % compared to axon counts in the presence of clorgyline alone. In contrast, the addition of 50 μ M deprenyl alleviated the action of MPTP on axon outgrowth returning axon counts to control values. In both instances, the addition of clorgyline or deprenyl alone to differentiating N2a cells did not dramatically affect N2a cell morphology (compare Fig 5.4a with Fig 5.4b and 5.4c, respectively). N.B. Figures of MPTP treated cells plus neuroprotectant have been omitted; cell morphology and axon counts resembling appropriate controls.

The addition of glial conditioned medium (1:4) produced a dramatic increase (43%) in the elaboration of axon-like processes in differentiating N2a cells (Table 5.2 and Fig 5.4d). This level of axon outgrowth remained unchanged in cultures exposed to 10 μ M MPTP. Additionally, the use of the p38 mitogen activated protein kinase inhibitor, SB202190 (10 μ M) also produced an increase (20%) in axon outgrowth (Table 5.2 and Fig 5.4e), compared to control cells, the increase being unaffected by treatment with 10 μ M MPTP (Table 5.2). In contrast to these agents, the addition of estradiol (100 μ M) to N2a cells dramatically reduced the extent of N2a cell differentiation with cells typically exhibiting a round mitotic morphology (compare

Fig 5.4a and 5.4f). Therefore the ability of oestrogen to alleviate the MPTP-induced inhibition of axon outgrowth could not be investigated.

5.2.5 Western blot analysis of NF-H in differentiating N2a cells exposed to MPTP and neuroprotective agents.

Biochemical characterisation of NF-H subunit status in the presence of MPTP (10 μ M) was carried out to further investigate the potential protective capacity of various neuroprotective agents. NF-H phosphorylation state were monitored by immunoprobng Western blots of total cell extracts of cells induced to differentiate in the presence of MPTP and neuroprotective agent. Three distinct antibodies were used, which preferentially recognised a non-phosphorylation dependent epitope of NF-H, a phosphorylation dependent epitope of NF-H (RMd09 and Ta51, respectively; Lee *et al.*, 1987), and an epitope of NF-H independent of phosphorylation state (N52).

Figure 5.5 shows the results of Western blot analysis using four different neuroprotective agents. Cell extracts obtained from cultures exposed to 10 μ M MPTP alone exhibited a modified NF-H status, compared to the NF-H profile of control cell extracts. This was characterised by a decrease in RMd09 reactivity with a concomitant increase in the level of Ta51 reactivity, while N52 reactivity remained unchanged (Fig. 5.5A, compare lanes 1 and 2). MPTP treated N2a cells incubated in the presence of 0.5 μ M clorgyline (Fig. 5.5B) or 50 μ M deprenyl (Fig. 5.5C) displayed an unaltered NF-H phosphorylation profile with N52, RMd09 and Ta51 reactivity remaining unchanged, compared to control extracts, i.e. the inhibitors had blocked the effect of MPTP on NF-H phosphorylation. Similarly, cultures exposed to sub-cytotoxic concentrations of MPTP and the neuroprotective agent, conditioned C6 medium (1:4) or SB202190 (10 μ M), exhibited an unaltered NF-H phosphorylation profile compared to extracts of cultures exposed to conditioned C6 medium or SB202190 alone (Fig. 5.5D and Fig. 5.5E, respectively). In these cases, NF-H levels and NF-H phosphorylation state of MPTP exposed cells remained comparable to control levels.

5.2.6 Identification of glial-derived neurotrophic factor in C6 conditioned medium.

C6 glioma cells were cultured in growth medium for 48 hours prior to replacing the medium with SFM containing 0 %, 1% and 10 % foetal bovine serum. Cells were re-incubated for a further 48 hours prior to harvesting of the “conditioned medium” and protein analysis. An initial screen to monitor the presence of a GDNF-like protein was carried out. Dot blot analysis of cell-free conditioned medium using a polyclonal antibody raised to recombinant human GDNF initially characterised the presence of a GDNF-like protein in all medium derived from the growth of rat glioma C6 cells (Fig 5.6). Reactivity was greatest in conditioned medium that had been supplemented with 10 % foetal calf serum (Fig 5.6D, lanes 1-3). However, serum free conditioned medium also expressed GDNF-like protein reactivity (Fig 5.6B, lanes 1-3). GDNF reactivity was absent from serum free medium that had not been in contact with C6 cells (Fig 5.6B, lane 4), but some cross reactivity was seen in serum supplemented medium devoid of contact with C6 cells (Fig. 5.6C and 5.6D, lane 4). This suggests the antibody may show some cross reactivity with serum or particular components of serum.

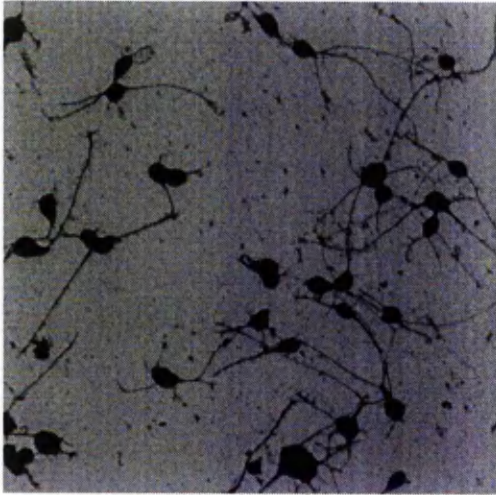
To further characterise and identify the presence of GDNF, equal aliquots of conditioned medium were concentrated by acetone precipitation, prior to protein estimation and solubilisation of the extract in electrophoresis sample buffer. In conjunction, a cell extract of C6 cells and recombinant human GDNF were also prepared. Total extracts (50 µg) were separated on a 12 % SDS-PAGE gel and the proteins transferred to nitrocellulose. Immunoprobings of the blot revealed recombinant human GDNF to express a molecular weight of approximately 30 kDa (Fig 5.7, lane 1). Similarly, serum free conditioned medium exhibited the presence of a 30 kDa anti-GDNF reactive band (Fig 5.7, lane 2). Unfortunately, no 30 kDa band reactivity was observed in conditioned medium extracts that had been supplemented with 1 % and 10 % foetal calf serum (lanes 3 and 4; respectively). C6 total cell extracts (lane 5) expressed a number of reactive bands ranging in size, possibly representing the cross reactivity displayed by the antibody or protein precursors of GDNF present in C6 cells, prior to processing. However, the C6 cell extract did include a 30 kDa reactive protein band akin to recombinant human GDNF.

<i>Axons / 100 cells</i>					
	<i>Control</i>	<i>Clorgyline (0.5 μM)</i>	<i>Deprenyl (50 μM)</i>	<i>C6 medium (1:4)</i>	<i>SB202190 (10 μM)</i>
<i>0 μM MPTP</i>	30.07 ± 0.65	27.73 ± 0.96	31.57 ± 1.61	42.92 ± 1.97	36.15 ± 1.38
<i>10 μM MPTP</i>	17.32 ± 0.56	23.43 ± 1.34	29.55 ± 1.02	42.73 ± 2.02	35.03 ± 0.49

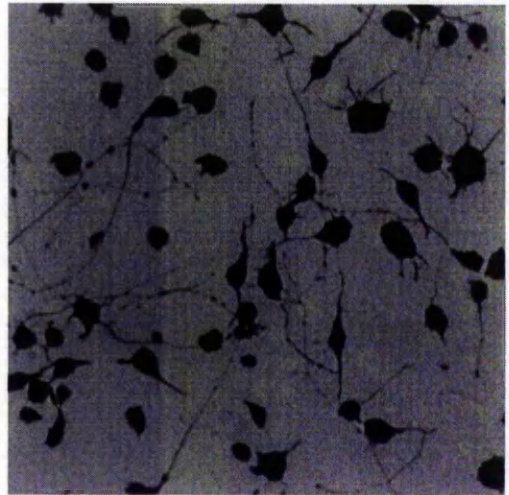
Table 5.2 *The effect of potential neuroprotective agents on axon outgrowth in differentiating N2a cells exposed to sub-cytotoxic MPTP concentrations.*

N2a cells were induced to differentiate in the presence or absence of various “neuroprotectants” and MPTP for 24 hours prior to morphological assessment. Cells were fixed in methanol and stained with Coomassie blue. Quantification of axon outgrowth was achieved as described previously. Results are expressed as mean number of axons/100 cells ± SEM. Statistical analysis was carried out to compare axon counts in the presence and absence of “neuroprotectants” using the Mann-Whitney U test, where $n = 4$. All p values < 0.05 compared to corresponding “0 μM MPTP” control.

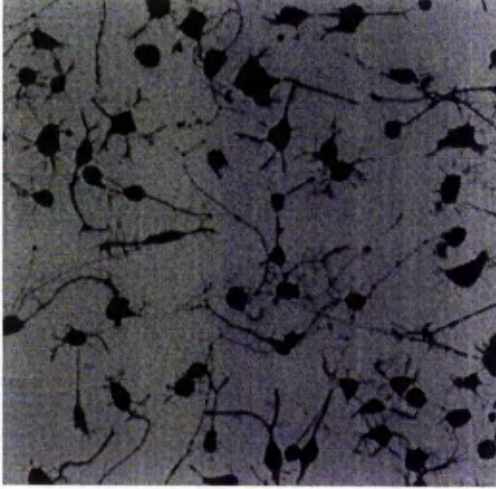
a



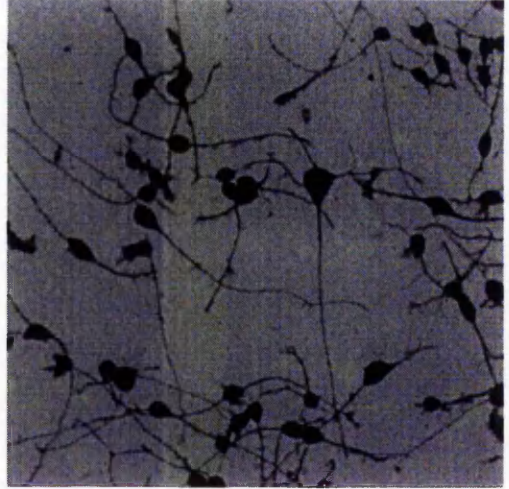
b



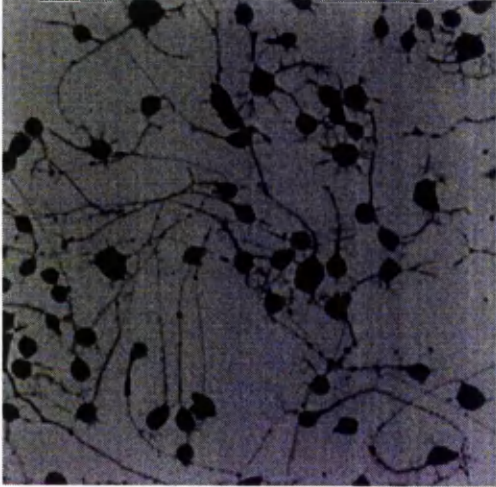
c



d



e



f

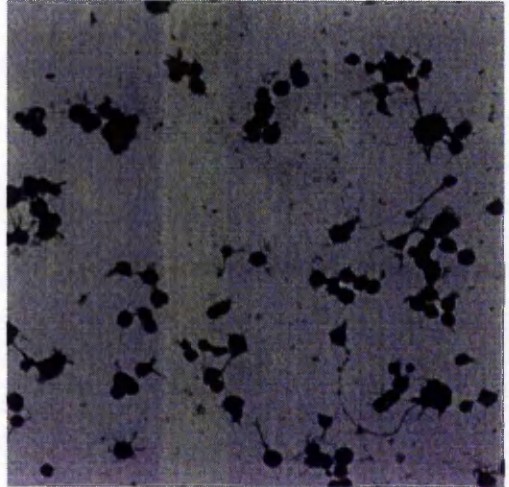


Figure 5.4 *The effect of potential neuroprotective agents on the morphology of differentiating N2a cells.*

N2a cells were induced to differentiate for 24 h alone (a) or in the presence of clorgyline [0.5 mM] (b), deprenyl [50 mM] (c), conditioned C6 medium [1:4] (d), SB202190 [10 μ M] (e) or estradiol [100 μ M] (f). Cells were fixed in ice-cold methanol and stained with Coomassie blue prior to air drying. Cells were then viewed on a light microscope at x 100 magnification.

N52

RMd09

Ta51

1

2

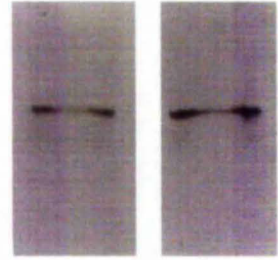
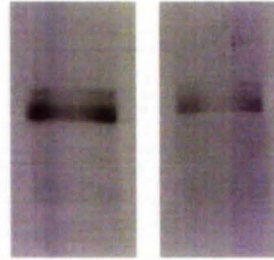
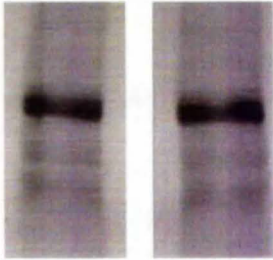
1

2

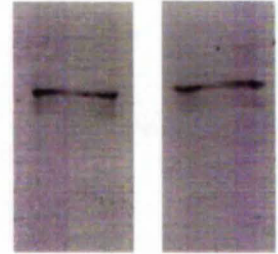
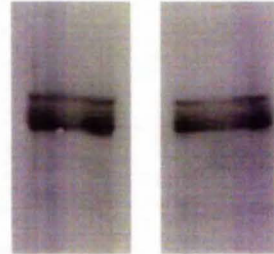
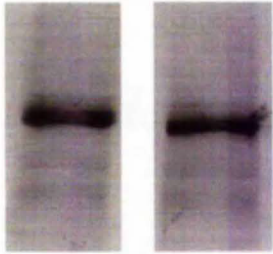
1

2

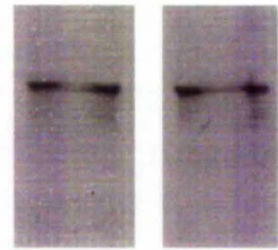
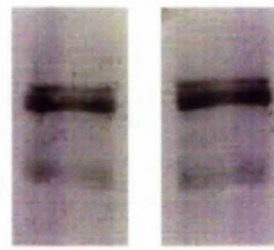
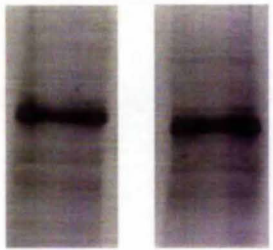
A



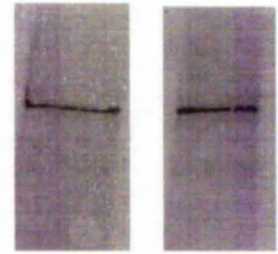
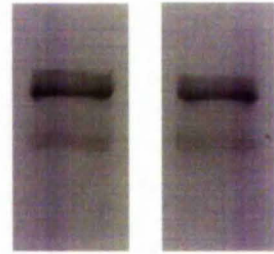
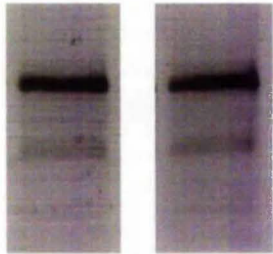
B



C



D



E

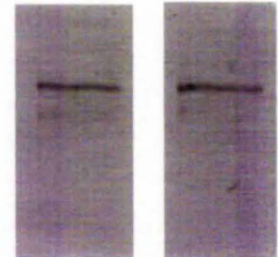
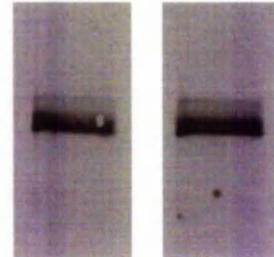
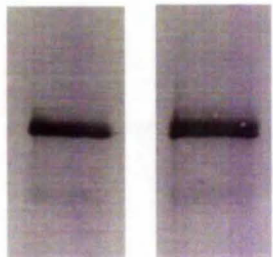


Figure 5.5 *The effect of potential neuroprotective agents on of NF-H status from differentiating N2a cells exposed to sub-cytotoxic MPTP concentrations.*

N2a cells were induced to differentiate in either the absence or presence of MPTP and a neuroprotective agent: control (A); clorgyline (B); deprenyl (C); conditioned medium (D); SB202190 (E) for 24 h, prior to extraction of the cell monolayer. Equal protein aliquots (20 μ g) of cell extracts were electrophoresed on a 7.5% SDS-PAGE gel and transferred onto nitrocellulose membrane filters. Blots were then probed with NF-H antibodies N52; RMd09; or Ta51. The signal was developed using either mouse or rabbit alkaline phosphatase secondary conjugates. Shown are cells induced to differentiate for 24 h in the absence of MPTP (lanes 1) or the presence of 10 μ M MPTP (lanes 2).

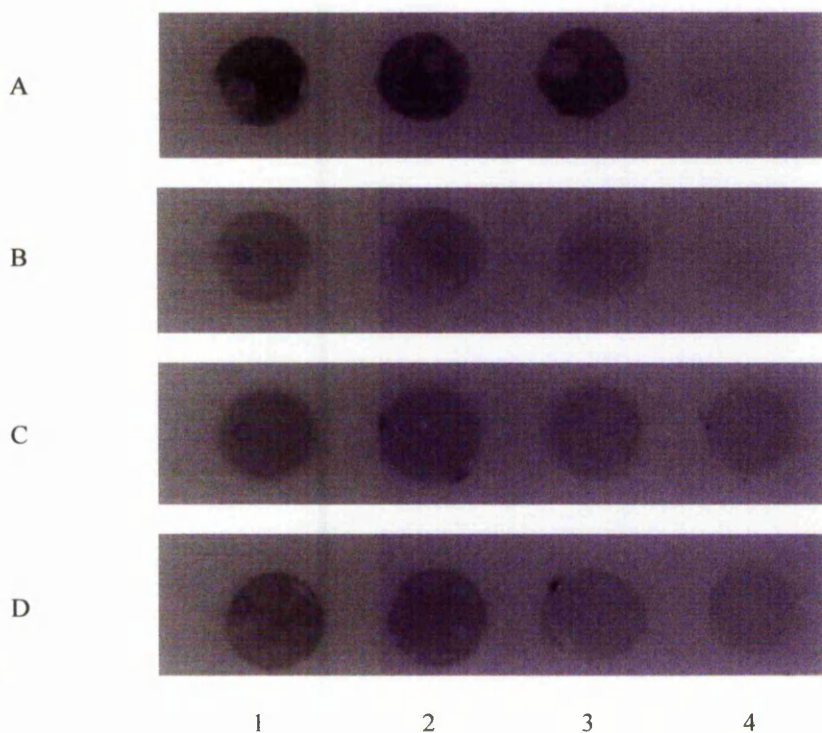


Figure 5.6 Determination of the presence of a GDNF-like protein in conditioned medium derived from rat C6 glioma cells.

C6 cells were plated out in growth medium at a cell density of 100,000 cells/ml in T75 flasks and incubated for 48 hours to allow cell growth. Growth medium was removed from the flasks and replaced with:

Flask 1: Serum free medium.

Flask 2: Growth medium (1 % Foetal bovine serum).

Flask 3: Growth medium (10 % Foetal bovine serum)

Cells were re-incubated for 48 hours whereupon the medium was decanted and clarified of cells by centrifugation. A bio-dot blot was performed on the conditioned medium obtained from the three culture conditions. Dilution of each medium was made up to a final volume of 250 μ l and passed through a nitrocellulose membrane under vacuum. The membrane was blocked prior to probing with a polyclonal Ig Y antibody raised to recombinant human GDNF. The signal was developed using an anti-chicken Ig Y alkaline phosphatase conjugate.

Aliquots of 250 μ l of each sample was loaded:

A. Recombinant Human GDNF

(1) 62.5 ng (2) 31.25 ng (3) 15.625 ng (4) TBS (Control)

B. Conditioned medium [Serum free medium]

(1) 250 μ l (2) 125 μ l (3) 62.5 μ l (4) Medium control

C. Conditioned medium [Growth medium; 1% Foetal bovine serum].

(1) 250 μ l (2) 125 μ l (3) 62.5 μ l (4) Medium control

D. Conditioned medium [Growth medium; 10 % Foetal bovine serum]

(1) 250 μ l (2) 125 μ l (3) 62.5 μ l (4) Medium control

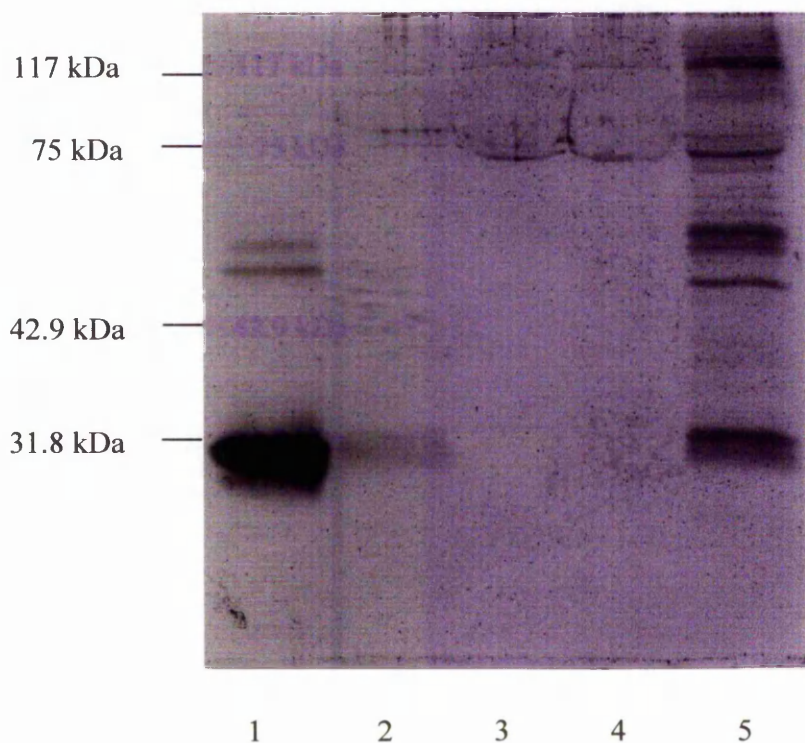


Figure 5.7 Identification of Glial derived neurotrophic factor in conditioned medium harvested from the growth C6 cells.

C6 cells were plated out in growth medium at a cell density of 100,000 cells/ml in T75 flasks and incubated for 48 hours to cell growth. Growth medium was removed from the flasks and replaced with an equal volume of:

Flask 1: Serum free medium.

Flask 2: Growth medium (1 % Foetal bovine serum).

Flask 3: Growth medium (10 % Foetal bovine serum)

Flask 4: Growth medium (10 % Foetal bovine serum)

Cells were re-incubated for a further 48 hours whereupon the medium was decanted and clarified of cells by centrifugation. Equal aliquots (200 μ l) of each medium was acetone precipitated prior to protein estimation. Protein aliquots (50 μ g) were solubilised in 2x electrophoresis reducing sample buffer. C6 cell extract (50 μ g) was also prepared from cells grown in growth medium. Extracts of samples were run on 12 % SDS-PAGE gel and proteins transferred to nitrocellulose prior to being probed with anti-human GDNF pAb (1 μ g/ml). Blot revealed using an anti chicken IgY alkaline phosphatase conjugate (1:1000).

1. Recombinant Human GDNF (1 μ g).

2. Conditioned medium [Serum free medium]

3. Conditioned medium [Growth medium; 1% Foetal bovine serum].

4. Conditioned medium [Growth medium; 10 % Foetal bovine serum].

5. C6 glioma cell extract [Growth medium; 10 % Foetal bovine serum].

5.3 Discussion.

5.3.1 The protective efficacy of MAO inhibitors.

The initial step in MPTP toxicity has long been recognised to involve the metabolism of the neurotoxin to its toxic metabolite, MPP⁺ (Chiba *et al.*, 1984; Markey *et al.*, 1984). This reaction is mediated by MAO and therefore inhibition of this enzyme, in theory, could alleviate the cytotoxic action. Chapter III initially demonstrated that differentiating N2a cells exposed to increasing concentrations of MPTP only exhibited a dramatic reduction in viability following 48 hours exposure. It appears therefore that MPTP-induced cell death in N2a cells is a time dependent event, likely relating to the production of the toxic metabolite MPP⁺, mediated by MAO (Markey *et al.*, 1984). Therefore inhibition of MPP⁺ production could confer cytoprotection.

Although N2a cells are considered to express low, predominantly MAO-A activity (Nagatsu *et al.*, 1981; Chapter III, section 3.3.4), work suggests differentiation of these cells causes an increase in total MAO activity which can be totally inhibited by 0.5 μ M or 50 μ M clorgyline or deprenyl (Chapter III, section 3.3.4). Concentrations of the lipophilic MAO inhibitors, clorgyline and deprenyl used here are therefore in excess of that needed to inhibit total MAO activity. The addition of clorgyline (0.5 μ M - 250 μ M) to differentiating N2a cells exposed to MPTP was able to partially alleviate MPTP-induced cell death over a 48 hour exposure. In general, an increase in clorgyline concentration resulted in the reduction of MPTP-induced cell death (0.1-1.0 mM MPTP). Preliminary early work using clorgyline *in vivo* reported that clorgyline was unable to confer neuroprotection to MPTP-treated animals (Chiba *et al.*, 1984; Heikkila *et al.*, 1984b). However, this phenomenon seems to be reversed *in vitro*. Pre-treatment of rodent cell lines in culture with clorgyline has previously been shown to protect cells from MPTP-induced death (Buckman, 1991; Lai *et al.*, 1993). These findings are in agreement with the results obtained in this chapter, using the differentiating N2a cell model. Interestingly, clorgyline was able to maintain N2a cell morphology and in doing so was also able to partially alleviate the sub-cytotoxic effect of MPTP. In this instance 0.5 μ M

clorgyline alleviated the inhibition of axon outgrowth and maintained NF-H levels and NF-H phosphorylation state, following MPTP exposure. These protective properties of clorgyline are possibly due to its MAO inhibitory properties. The difference in clorgyline protection between *in vivo* and *in vitro* models is possibly due to the high MAO-B activity found in the neurotoxin activating glial cells of the substantia nigra (Berry *et al.*, 1994), which contributes considerably to MPTP metabolism.

In comparison to clorgyline, deprenyl at concentrations between 50-250 μM , was able to alleviate cell death to a greater extent. Indeed, increasing deprenyl concentrations consistently increased cell viability. It has been suggested that in addition to its MAO inhibitory properties, deprenyl can exhibit neuroprotective properties (Tatton and Chalmers-Redman, 1996). This notion initially stems from the findings reported by Mytilineou and Cohen (1985) who showed that deprenyl maintained dopamine levels and dopamine uptake in mesencephalic explants following treatment with the active metabolite MPP^+ . Therefore deprenyl could reduce dopaminergic neuronal damage by a mechanism other than blocking the conversion of MPTP to MPP^+ . In this current study, incubation of MPTP treated cells with deprenyl also alleviated the inhibition of axon outgrowth and reversed the increase in NF-H phosphorylation associated with sub-cytotoxic MPTP neurotoxicity (see Chapter IV). Interestingly, deprenyl was able to maintain N2a cell morphology and alleviate MPTP-induced toxicity to a greater extent than clorgyline. It has been suggested that deprenyl could in fact possess additional neuroprotective properties. Indeed, deprenyl has previously been shown to modulate gene expression (such as free-radical scavenger enzymes) and protein synthesis in neuronal cells independent of MAO inhibition (Tatton *et al.*, 1994; Tatton and Chalmers-Redman, 1996).

5.3.2 The protective efficacy of glial conditioned medium.

The use of conditioned medium derived from rat glioma C6 cells protected differentiating N2a cells from exposure to increasing concentrations of MPTP. Protection was evident at low as well as high MPTP concentrations. Furthermore, the addition of conditioned medium to differentiating N2a cells caused a dramatic increase in axon outgrowth of 43 %, compared to N2a cells induced to differentiate

by dbcAMP alone. Of greater significance was that axon outgrowth was maintained in the presence of the inhibitory action of sub-cytotoxic MPTP concentrations. This protective influence was also extended to alleviate the aberrant change in NF-H phosphorylation state resulting from exposure to MPTP.

In vivo, astroglial cells secrete a variety of factors that are involved in the support of neurite outgrowth and neuronal survival (Shea and Husain, 1996), suggesting that conditioned medium harvested from glioma C6 cells in this study to be able to mimic these phenomena (Shea, 1994). It has been shown that axon outgrowth in neuroblastoma cells is influenced by alterations in signal transduction protein kinases, including induction by protein kinase C inhibition and by protein kinase A activation (Shea *et al.*, 1992). Glial conditioned medium is proposed to mediate axon outgrowth via the protein kinase C signal transduction pathway, independent of protein kinase A mediated pathways (Shea and Husain, 1996). Since in this study conventional N2a cell differentiation is mediated by dbcAMP (a protein kinase A activator), the additional presence of conditioned medium can function cooperatively producing a synergistic effect on axon outgrowth (Shea *et al.*, 1992).

It is difficult to determine exactly which or how many neurotrophic factors are important in this mechanism, since the identification of all the factors secreted by glial cells are unknown. However, C6 cells have previously been shown to express significant levels of GDNF mRNA (Suter-Crazzolara and Unisicker, 1996). Interestingly, GDNF is a potent neurotrophic factor that has been shown to alleviate MPTP-induced neurotoxicity *in vivo* (Tomac *et al.*, 1995). It is gaining increasing clinical support for use as a neuroprotective agent in the treatment of Parkinson's disease.

Preliminary dot blot analysis of glial conditioned medium using a polyclonal GDNF antibody revealed the presence of GDNF-like protein reactivity which was absent from cell free medium controls. The culture conditions of C6 cells also seemed to influence the extent of GDNF secretion. Dot blot analysis revealed medium harvested from C6 cells grown in the presence of 10 % (v/v) foetal calf serum produced greater GDNF reactivity than equivalent cells grown in 1 % (v/v) foetal calf serum or serum free conditions. However, SDS-PAGE analysis revealed only C6 cells grown in serum free conditions to express a 130 kDa GDNF protein

band, all be it at low levels. The absence of significant detectable immunoreactivity from serum containing conditioned medium is related to the relatively low concentration of the factor compared to serum. Therefore when loading equal protein aliquots on gels the percentage of GDNF protein compared to other proteins is considerably reduced.

Conditioned medium derived from C6 cells grown under serum free conditions was ideal for use experimentally. The use of foetal bovine serum containing conditioned medium was considered inappropriate as it could influence cell proliferation and therefore adversely affect cell differentiation. GDNF itself has been shown to exhibit a highly potent activity with an average half-maximal effective concentration in midbrain cultures of 1.2 pM (Lin *et al.*, 1993). Indeed, glial conditioned medium was effective on N2a cells when diluted 1:8 with serum free medium, although a concentration of 1:4 was found to be optimal.

The observed changes in N2a cell differentiation and N2a survival from MPTP induced neurotoxicity following the addition of conditioned C6 medium treated could suggest the possible involvement of GDNF. However, medium derived from the growth of glial cells contains a number of neurotrophic factors (Shea, 1994) whose presence and involvement in maintaining N2a cell morphology cannot be dismissed.

5.3.3 The protective efficacy of p38 MAPK inhibition.

Inhibitors of the p38 MAPK pathway are reported to promote neuronal survival *in vitro* (Horstmann *et al.*, 1998). This phenomenon is reflected when differentiating N2a cells are exposed to SB202190 producing an abundant increase in cell viability and differentiation. This survival promoting ability is also evident when cells are exposed to sub-cytotoxic concentrations of MPTP. Inhibition of p38 MAPK can repress the MPTP-induced effects on N2a cell morphology and NF-H phosphorylation state. However, recent work suggests that p38 kinases are not involved in the stress-induced hyperphosphorylation of perikaryal NF-H (Giasson and Mushynski, 1997). This suggests that SB202190 induced protection is possibly upstream of MPTP-induced effects or is via an alternative mechanism that can indirectly affect MPTP-induced NF-H phosphorylation. It is also clear that the

protection afforded by p38 inhibition is limited, since cells exposed to cytotoxic concentrations of MPTP still undergo cell death.

5.3.4 The protective efficacy of oestrogen (estradiol).

It has recently been postulated that estradiol may have neuroprotective functions at various cellular levels independent of the classical genomic action via its receptor (Toran-Allerand *et al.*, 1999). These include intrinsic antioxidative properties (Behl and Holsboer, 1999) and the ability to enhance growth and differentiation of axons in developing brain through activation of the extracellular-signal regulated kinase pathway (Toran-Allerand *et al.*, 1999). These diverse neuroprotective properties are concentration dependent (nanomolar to millimolar range) and sometimes in excess of variable physiological concentrations (~ 10 nM; Lee and Eghbali-Webb, 1998). However, effective treatment might need to reach high pharmacological concentrations in the brain rather than physiological plasma concentrations (Behl and Holsboer, 1999). In the present study, micromolar concentrations (10-1000 μ M) of estradiol were required to prevent MPTP-induced cell death. However, this was only achieved at concentrations which blocked cell differentiation in response to dbcAMP. This cytoprotective response could be a consequence of estradiol's antioxidative capacity or related to estradiol's ability to enhance a mitogenic/proliferative response within these cells, as seen in cardiac fibroblasts (Lee and Eghbali-Webb, 1998). Although lower physiological concentrations of estradiol were not cytoprotective, lower concentrations may have beneficial effects on MPTP-induced neurotoxicity. However, preliminary work using lower concentrations of estradiol (i.e. 100 nM) also affected N2a cell morphology. This unfortunate characteristic excludes the use of estradiol as a potential neuroprotective agent in this particular neuroblastoma model.

5.3.5 The protective efficacy of glutathione.

The depletion of intracellular glutathione, *in vivo*, has been shown to potentiate the cytotoxic effect of MPTP (Wullner *et al.*, 1996). Therefore since glutathione is important in the detoxification of free radicals it is not unreasonable to

assume that an increased glutathione presence could impart protection against MPTP-induced cell death, possibly quenching oxidative stress. However, treatment of differentiating N2a cells exposed to MPTP for 48 hours with up to 2 mM GSH did not convincingly inhibit cell death. Treated cells supplemented with GSH expressed a similar level of cell death as cells devoid of the tripeptide.

Although glutathione alone seemed to exhibit an effect on N2a cell viability it was found to interfere considerably with the MTT reduction assay. Cell counts proved that N2a cell numbers were not affected by glutathione (results not shown), as seemed to be the case with the MTT reduction assay. In spite of this, glutathione was still unable to protect differentiating N2a cells from MPTP-induced toxicity. In addition, exposure of differentiating N2a cells to 1 mM MPTP did not significantly affect total glutathione levels. However, due to the limitations of the assay changes in GSH/GSSG ratios were not measured which could give a clearer indication of the extent of oxidative stress.

Some reports have questioned the ability of glutathione to cross cell membranes (e.g. Meister *et al.*, 1984). However, determination of intracellular glutathione content revealed N2a cells to increase total glutathione levels by up to 38 % when supplemented with 1 mM GSH. The extent of intracellular glutathione levels remained fairly constant when cells were supplemented with 2 mM GSH. Indeed, Kromadis *et al.*, (1990) showed that the extracellular addition of 10 mM glutathione to neuroblastoma cells only resulted in a doubling of intracellular reduced glutathione (GSH) suggesting uptake efficiency to be the limiting factor. The mechanism of glutathione uptake described by Kromadis *et al.*, (1990) suggests GSH in the extracellular medium is auto-oxidised to GSSG, prior to being transported into the cell. Here it is reduced to GSH by the action of glutathione reductase. It could therefore be loosely suggested that MPTP could affect the activity of glutathione reductase thereby inhibiting the intracellular conversion and therefore elevation of reduced glutathione. This action would relieve the cell of its ability to compensate for the toxic action of neurotoxin. However, to date the ability of MPTP to affect this enzyme activity has not been thoroughly explored, although the activity of glutathione reductase is depleted by peroxynitrite (ONOO⁻). Increased production of

this oxidising species has been linked to the cytotoxic action of MPTP (Packer *et al.*, 1996), in a concentration dependent manner.

An alternative hypothesis for the inability of glutathione to prevent cytotoxicity could relate to the involvement of oxidative stress. The cytotoxic action of MPTP may not initially involve oxidative stress (Lotharius *et al.*, 1999) and occur as a consequential secondary event to mitochondrial respiratory inhibition. The ability of glutathione to then alleviate this cascade would therefore be limited.

CHAPTER VI

**The neurotoxic effects of sub-cytotoxic MPTP insult
on pre-differentiated N2a neuroblastoma cells.**

6.1 Introduction

6.1.1 Development of a pre-differentiated N2a model.

The process of differentiation within the N2a cell line, through serum withdrawal, causes a number of morphological and biochemical changes as described by a number of workers (e.g. Seeds *et al.*, 1970; Waymire *et al.*, 1972; Prasad, 1975). These typically include inhibition of cell division, initiation of axon outgrowth and regulation and synthesis of cellular enzymes. The neurotoxic capacity of MPTP on differentiating mouse N2a cells was initially established and characterised in Chapter IV. This was characterised by marked changes in the formation of the archetypal differentiating cell, namely inhibition of axon outgrowth. In addition, changes to the neurofilament component of the cytoskeleton, namely alterations in both basal neurofilament-H phosphorylation status and neurofilament-H spatial arrangement during the differentiation process were also evident.

In an attempt to obtain conditions more akin to neuronal cells *in vivo*, it was thought advantageous to pre-differentiate N2a cells to allow investigation of the neurotoxic effects of MPTP on a mature neuronal phenotype. Such a model would therefore focus more closely on axon maintenance rather than development and would lend further support to the use of N2a cells to investigate neurodegenerative events associated with PD. However, the process of differentiating N2a cells using serum free conditions can only be achieved over a 48 hour time period. Interruption during this differentiation process enhances cell detachment and results in poor axon maintenance and thus was deemed an unsuitable protocol for developing a pre-differentiated model.

Workers using a differentiating neuroblastoma subclone to investigate axon stability and maintenance for extended periods have suggested using serum-supplemented medium (Shea and Beermann, 1994). However, preliminary studies using this regimen with N2a cells in this project, indicated that cell division continued at an appreciable rate. In addition, the extent of cell differentiation (defined as axons/100 cells) was less convincing than traditional differentiation in chemically defined serum free medium; low axon numbers making screening for aberrant morphological changes more difficult. Therefore it was deemed necessary to firstly define an efficient protocol to maximise N2a cell differentiation so that the neurotoxic

effects of sub-cytotoxic MPTP concentrations on pre-differentiated cells could be investigated.

The use of conditioned medium derived from primary astroglial cells has been shown to promote the rapid elaboration of axon-like processes in undifferentiated neuroblastoma cells (Shea, 1994). Indeed, conditioned medium derived from rat C6 glioma cells produces a similar response (see Chapter V). Differentiation was therefore induced by culturing cells in serum free medium supplemented with conditioned C6 medium [4:1] and 0.3 mM dbcAMP. Following differentiation, medium was replaced with dbcAMP supplemented serum free medium whereupon cells were incubated in the presence or absence of MPTP.

The morphological and biochemical changes that may occur following challenge by sub-lethal doses of MPTP were monitored via a study of changes in axon maintenance and cytoskeletal components associated with cell morphology, as described in Chapter IV.

6.2 Results

6.2.1 Analysis of N2a cell differentiation by conditioned C6 medium.

The differentiation of N2a cells in the presence and absence of conditioned C6 medium, derived from rat C6 glioma cells, was quantified by monitoring axon outgrowth; axons were defined as perikaryal extensions greater than two cell body diameters in length, as previously noted. N2a cells were induced to differentiate by conventional serum withdrawal supplemented with dbcAMP, termed *conventional differentiation*, or by conditioned medium supplemented with dbcAMP, termed *conditioned differentiation*.

The conventional method of differentiation of N2a cells, by serum withdrawal and addition of dbcAMP, produced a steady increase in axon numbers over a 24 hour time period. Axon counts increased from 4.9 to 30.3 axons/100 cells between 4 hours and 24 hours, respectively (Fig. 6.1). In comparison, the incorporation of conditioned C6 medium produced a substantial increase in axon outgrowth with axon numbers increasing to 42.1 axons/100 cells, following 24 hours conditioned differentiation. It is evident, through observation of the cell populations, that withdrawal of serum from the maintenance medium promptly stimulated the early stages of neuritogenesis. Indeed, both conventional differentiation and conditioned differentiation produced a number of short neurites following 4 hours incubation, although the number of processes that qualified as axons was significantly greater in conditioned medium treated cells; increasing by approximately 101%. The rate of axon outgrowth is seemingly increased by conditioned differentiation, compared to conventional differentiation (Fig. 6.1). An incubation period of 16 hours with conditioned C6 medium produced axon numbers comparable to that of conventional differentiation of cells incubated for 24 hours; 30.3 and 32.2 axons/100 cells, respectively.

To further characterise the morphological increase in cell differentiation produced by conditioned C6 medium, total cell extracts of N2a cells differentially induced to stimulate axon outgrowth were analysed by Western blotting. Since conditioned differentiation for 16 hours produced a morphological profile similar to conventional differentiation for 24 hours, the comparative NF-H status was analysed. Cells induced to differentiate in the presence and absence of conditioned C6 medium

over a 16 and 24 hour time period were analysed by immunoblotting with specific antibodies directed to differentially phosphorylated NF-H isoforms. In general, total NF-H levels, as described by N52 reactivity (Fig 6.2A), increased from 16 to 24 hours with both conventional (lanes 1 and 2) and conditioned differentiation (lanes 3 and 4). In addition, conditioned differentiation for 16 hours displayed comparable total NF-H levels to that of conventional differentiation over the longer incubation period of 24 hours. This profile is mimicked by RMd09 reactivity (Fig 6.2B), with cells undergoing conditioned differentiation expressing comparable NF-H levels to cells induced for a 24 hours by conventional means.

In contrast, the appearance of phosphorylated NF-H isoforms, highlighted by Ta51 reactivity, in cells differentiated by conventional means for 16 hours is low (Fig 6.2C, lane 1). However, conditionally differentiated N2a cells express comparable Ta51 reactivity levels to that of conventionally differentiated N2a cells following 24 hours incubation (Fig 6.2C, lanes 2, 3). The appearance of phosphorylated NF-H isoforms is therefore rapidly increased, in conjunction with axon outgrowth, by treatment of N2a cells with conditioned C6 medium.

6.2.2 Characterisation of the cytotoxicity of MPTP on pre-differentiated N2a cells.

The cytotoxic effects of MPTP on pre-differentiated N2a cells were initially monitored using the MTT viability assay. N2a cells were differentiated with conditioned C6 medium and dbcAMP for 16 hours prior to exposure to the neurotoxin. Medium was removed and replaced with serum free medium supplemented with dbcAMP alone in the presence or absence of MPTP, whereupon cells were re-incubated for the required exposure time. In general, an increase in MPTP exposure from 8 hours to 24 hours caused a successive increase in N2a cell death. For example, exposure of pre-differentiated N2a cells to 500 μ M MPTP for 24 hours produced a 42 % decrease in cell viability, relative to control. Similarly, pre-differentiated N2a cells exposed to 500 μ M MPTP for 8 hours resulted in a 23 % decrease in cell viability (Fig. 6.3). However, exposure of cells to 10 μ M MPTP for 8 hours did not significantly increase cell death. Observation of these cells by light microscopy revealed obvious changes in cell morphology, in terms of axon maintenance (see below). However, it was apparent that the ability of pre-differentiated cells to remain attached was

diminished following this protocol, i.e. a small proportion of viable cells in both the control and drug treated wells became detached.

To obtain an independent assessment of cell death the trypan blue exclusion assay was employed. Exposure of cells to 10 μ M MPTP had no significant effect on cell death, relative to control (Table 6.1). However, although a dose of 20 μ M MPTP did increase cell death by 11 % the increase was not statistically significant.

6.2.3 Analysis of axon maintenance in pre-differentiated N2a cells.

The effect of sub-cytotoxic MPTP concentration (10 μ M) on axon maintenance was carried out on N2a cells initially pre-differentiated for 16 hours with conditioned C6 medium, prior to exposure to the neurotoxin in serum free medium supplemented with dbcAMP alone, for 8 hours. The maintenance of axonal processes was assessed by axon counts based on the criterion described in Materials and Methods (section 2.2.13). Control cultures (conditioned differentiation - 16 hours, conventional differentiation - 8 hours) resulted in axon counts of 28.4 axons / 100 cells (Fig. 6.4). However, exposure of pre-differentiated N2a cells to 10 μ M MPTP for 8 hours produced a decrease in axon number by approximately 38 %, compared to control values.

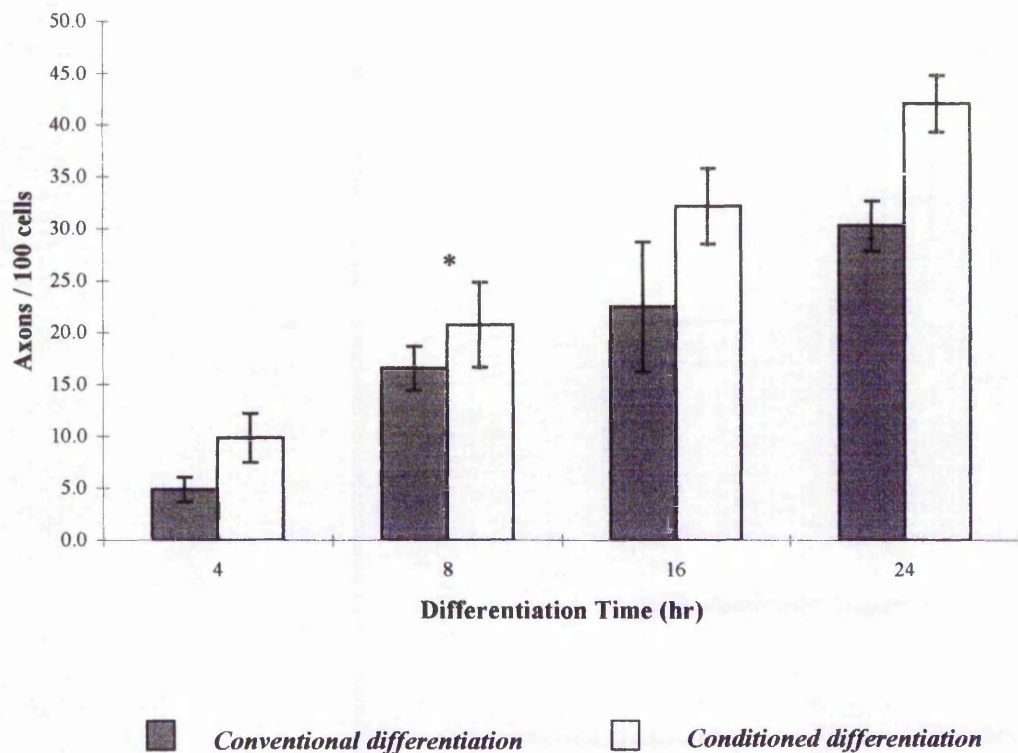
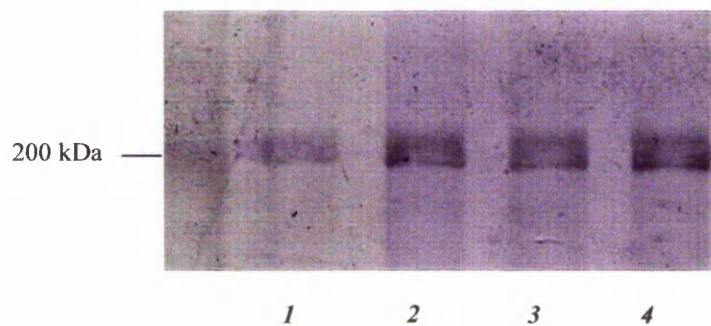


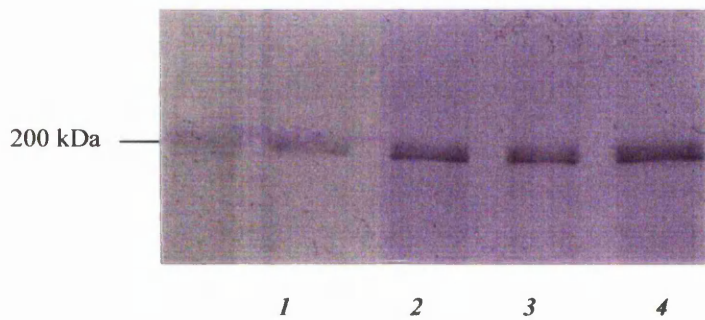
Figure 6.1 Time course of axon outgrowth in neuroblastoma N2a cells induced to differentiate in the presence and absence of conditioned C6 medium.

N2a cells were plated out in growth medium at a density of 50,000 cell/ml in 24 well plates, prior to overnight incubation at 37°C in an atmosphere of 95% air/5% CO₂, to allow recovery. Growth medium was carefully aspirated from the wells and replaced with an equal volume of either SFM + 0.3 mM dbcAMP (*conventional differentiation*) or with SFM:CM [4:1] containing 0.3 mM dbcAMP (*conditioned differentiation*). Cells were re-incubated for the required time course prior to morphological assessment. The number of axon-like processes (defined as extensions greater than two cell body diameters in length) were counted in five random fields per well. Results are expressed as mean Axons/100 cells ± Standard deviation. Statistical analysis was carried out using the Mann-Whitney *U* test, where n=4. Results obtained with conventional differentiation were compared against conditioned differentiation. All values p < 0.05 vs control except *.

A. N52



B. RMd09



C. Ta51

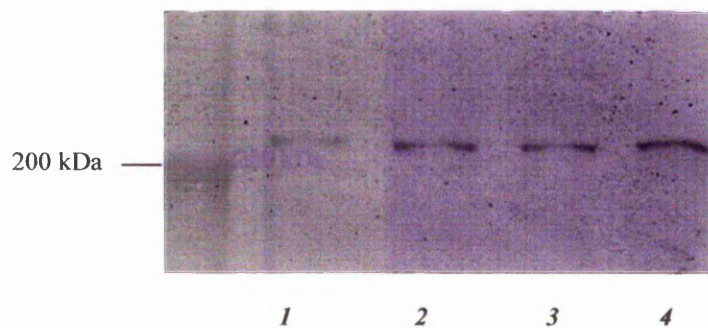


Figure 6.2 *Characterisation of NF-H status in neuroblastoma N2a cells induced to differentiate in the presence or absence of conditioned C6 medium.*

N2a cells were plated out in growth medium at a density of 50,000 cell/ml, prior to overnight incubation to allow recovery. Growth medium was aspirated from the flasks and replaced with an equal volume of SFM containing 0.3 mM dbcAMP alone (*conventional differentiation*) or SFM:CM [4:1] + 0.3 mM dbcAMP (*conditioned differentiation*). Cells were re-incubated for a further 16-24 hr, prior to extraction of the cell monolayer. Equal protein aliquots (20 µg) of cell extracts were electrophoresed on a 7.5% SDS-PAGE gel. Protein was then transferred to nitrocellulose and probed with specific mouse antibodies directed to non-phosphorylation dependent NF-H protein (RMd09), phosphorylation dependent NF-H protein (Ta51) and phosphorylation independent NF-H protein (N52). The signal was developed using a mouse alkaline phosphatase secondary conjugate.

A.	N52				
(1) 16 h (conventional)	(2) 16 h (conditioned)	(3) 24 h (conventional)	(4) 24 h (conditioned)		
B.	RMd09				
(1) 16 h (conventional)	(2) 16 h (conditioned)	(3) 24 h (conventional)	(4) 24 h (conditioned)		
C.	Ta51				
(1) 16 h (conventional)	(2) 16 h (conditioned)	(3) 24 h (conventional)	(4) 24 h (conditioned)		

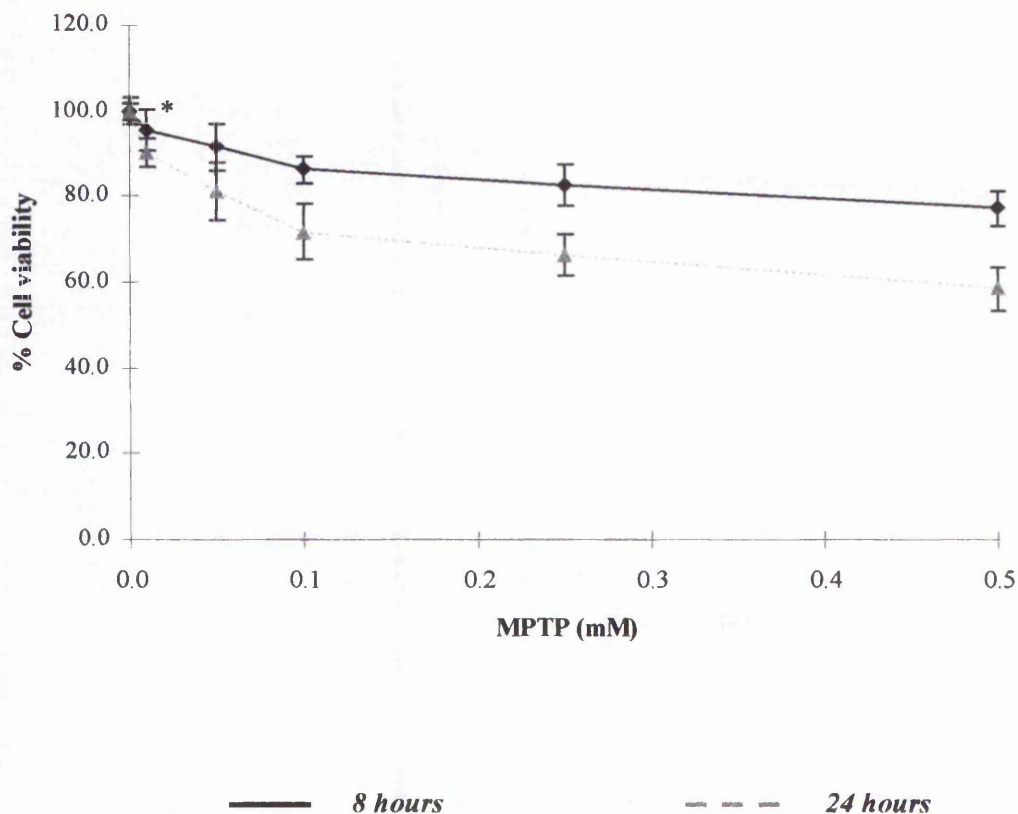


Figure 6.3 Cell viability assessment of pre-differentiated neuroblastoma N2a cells exposed to the neurotoxin MPTP for 8 and 24 hours.

N2a cells were plated out in growth medium at a density 50,000 cells/ml, prior to overnight incubation at 37°C in an atmosphere of 95% air/5% CO₂, to allow recovery. Growth medium was carefully aspirated from the wells and replaced with SFM:CM [4:1] containing 0.3 mM dbcAMP to induce differentiation, for a period of 16 hours. Following differentiation medium was again aspirated from the wells and replaced with SFM + 0.3 mM dbcAMP + MPTP. Cells were re-incubated for a further 8 hours or 24 hour, prior to viability assessment. Cell viability was assessed via the MTT viability assay. Results are expressed as mean % cell viability ± SEM. Statistical analysis was carried out using the Mann-Whitney *U* test, where n=8 for both 8 and 24 hour exposure. All values p < 0.05 vs control except *.

	MPTP (μ M)		
	<i>Control</i>	<i>10</i>	<i>20*</i>
% Cell Death	16.71 \pm 3.40	19.75 \pm 3.01	27.32 \pm 2.95

Table 6.1 Determination of sub-cytotoxic exposure of pre-differentiated N2a cells exposed to MPTP.

N2a cells were plated out in growth medium at a density 50,000 cells/ml prior to overnight incubation at 37°C in an atmosphere of 95% air/5% CO₂, to allow recovery. Growth medium was carefully aspirated from the wells and replaced with SFM:CM [4:1] containing 0.3 mM dbcAMP to induce differentiation, for a period of 16 hours. Following differentiation medium was again aspirated from the wells and replaced with SFM + 0.3 mM dbcAMP + MPTP. Cells were re-incubated for a further 8 hours prior to viability assessment. Cell death was assessed via the Trypan blue exclusion assay. Results are expressed as mean % cell death \pm SEM. Statistical analysis was carried out using the Mann-Whitney *U* test, where n=5, except * where n=4. All values $p \gg 0.05$ vs control.

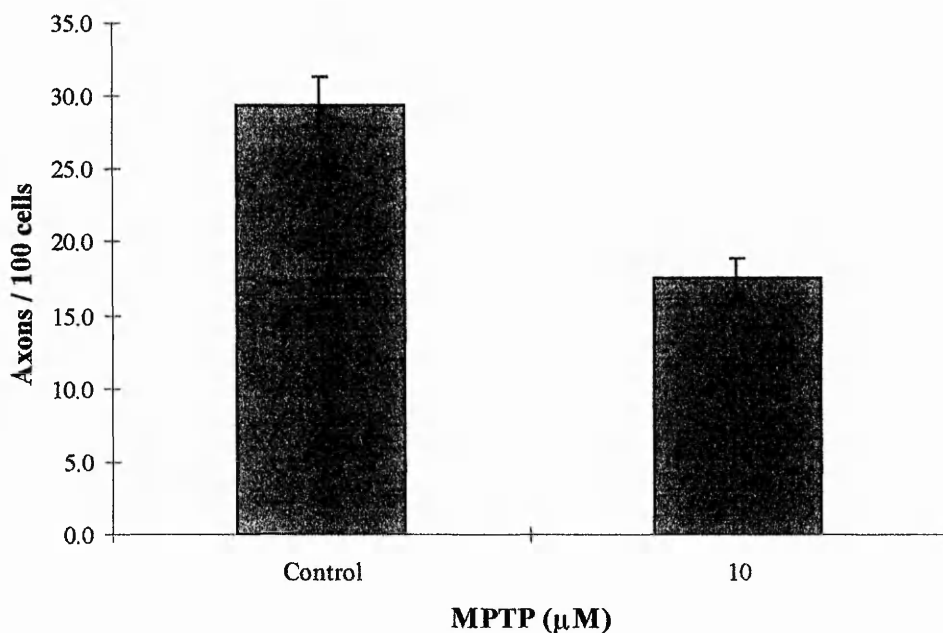


Figure 6.4 Determination of axon maintenance in pre-differentiated N2a cells exposed to sub-lethal dose of MPTP.

N2a cells were plated out in growth medium at a density 50,000 cells/ml in T25 flasks prior to overnight incubation. Growth medium was carefully aspirated from the wells and replaced with SFM:GCM [4:1] containing 0.3 mM dbcAMP to induce differentiation, for a period of 16 hours. Following differentiation medium was again aspirated from the wells and replaced with SFM + 0.3 mM dbcAMP + MPTP. Cells were re-incubated for a further 8 hours prior to morphological assessment. The number of axon-like processes (defined as extensions greater than two cell body diameters in length) were counted in five random fields per well, giving a total cell count of at least > 200 cells per well. Results are expressed as mean Axons/ 100 cells \pm SEM. Statistical analysis was carried out using the Mann Whitney *U*-test, where $n=8$ and p value < 0.05 compared to control.

6.2.4 Western blotting analysis of cytoskeletal components in pre-differentiated N2a cells exposed to sub-cytotoxic MPTP concentration.

Biochemical characterisation of specific cytoskeletal components was carried out to further investigate the morphological changes observed through the exposure of pre-differentiated N2a cells to MPTP. Pre-differentiated N2a cells were incubated in the presence or absence of 10 μ M MPTP for 8 hours prior to extraction of the monolayer to obtain a total protein cell extract. Equal protein extracts were then electrophoresed on a 7.5% SDS PAGE gel (e.g. Fig. 6.5) prior to transfer to nitrocellulose filters. Cytoskeletal proteins were then analysed by probing western blots with antibodies N52, RMD09, Ta51, anti-actin and anti- α -tubulin. Densitometric analysis was performed on blots obtained from three separate experiments, except α -tubulin where only two individual blots were analysed.

In general, the cell protein levels/profile of control and drug-treated samples remained comparable following 8 hours exposure (Fig. 6.6). Indeed, visual and densitometric analysis of the probed blots indicates that pre-differentiated N2a cells exposed to 10 μ M MPTP for 8 hours exhibited no dramatic change in the levels of actin or α -tubulin (Fig 6.6 a, b), the latter increasing the most by approximately 9 %. In contrast, NF-H status did appear modified by treatment with MPTP. Although blots probed with the N52, phosphorylation independent, antibody displayed comparable reactivity levels between control and drug treated samples (Fig. 6.6 c), blots probed with RMD09 exhibited a 28 % reduction in reactivity (Fig 6.6 d), following MPTP exposure. This decrease in reactivity was countered by an MPTP-induced increase in Ta51 reactivity of 19 %, compared to control values (Fig 6.6 e), relating to an increase in phosphorylated NF-H levels.

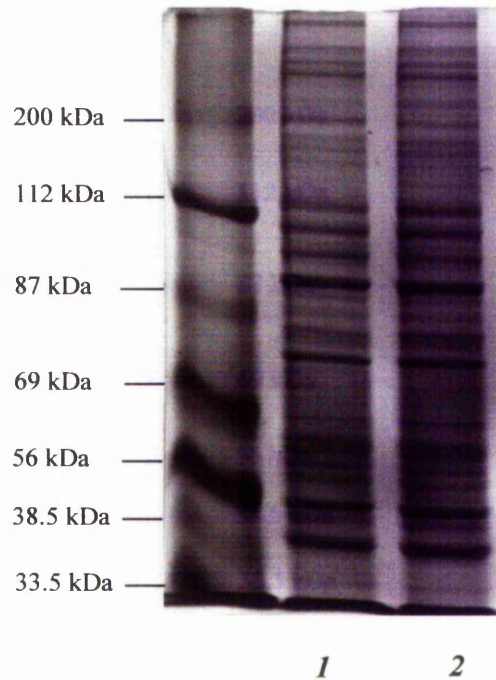
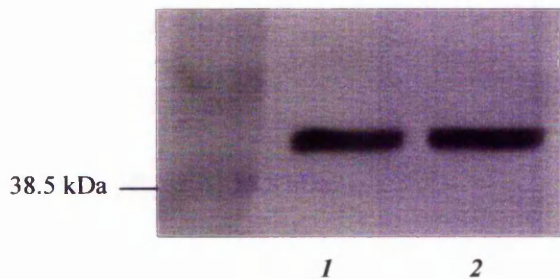


Figure 6.5 Coomassie stained SDS PAGE gel of total cell extracts of pre-differentiated N2a cells exposed to sub-lethal dose of MPTP.

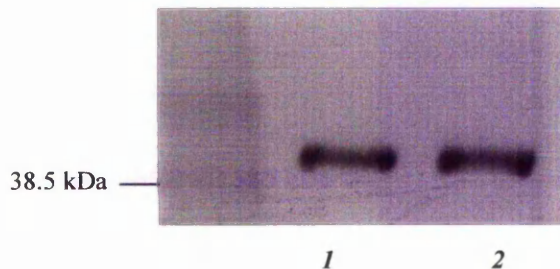
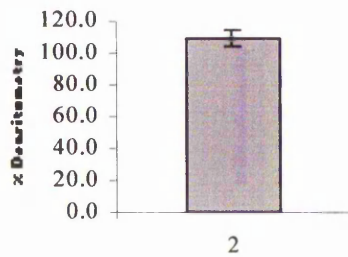
Equal protein aliquots (20 μg) of cell extracts of MPTP exposed differentiating cells were loaded onto a 7.5% SDS-PAGE gel and electrophoresed. Gel was stained with Coomassie blue to reveal protein pattern band formation and confirm the equality of sample loading.

Lanes

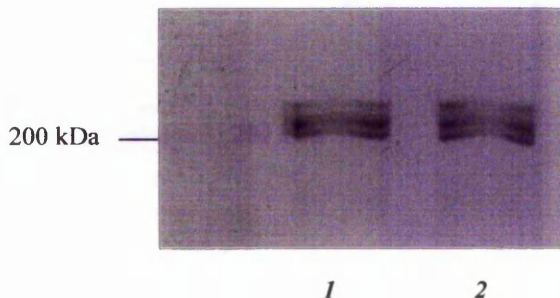
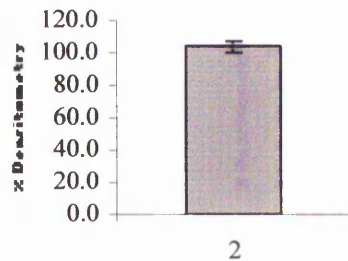
(1) Control (2) 10 μM MPTP



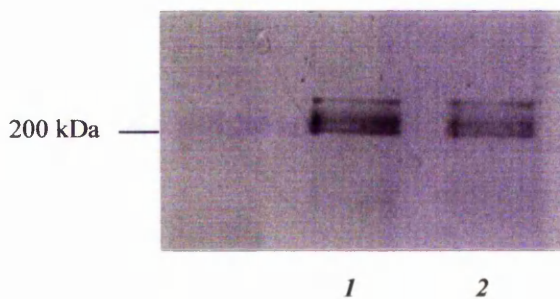
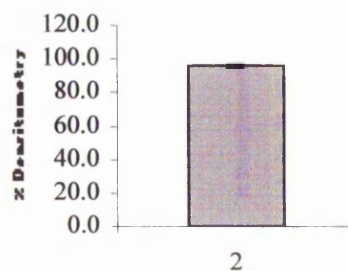
A. *α-tubulin*



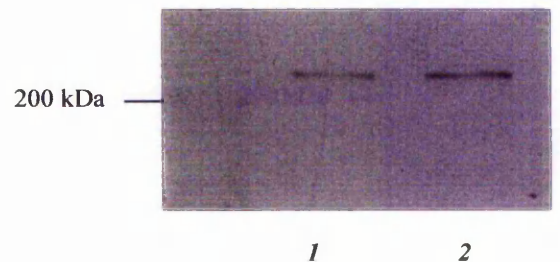
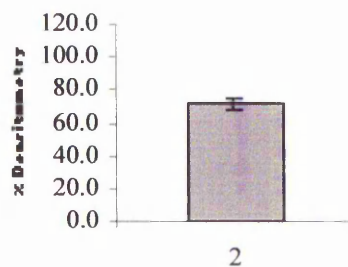
B. *Actin*



C. *N52*



D. *RMd09*



E. *Ta51*

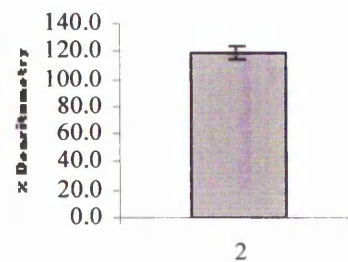


Figure 6.6 *Western blotting analysis of cytoskeletal components from pre-differentiated N2a cells exposed to a sub-cytotoxic concentration of 10 μ M MPTP.*

Left panel: N2a cells were plated out in growth medium at a density 50,000 cells/ml, prior to overnight incubation to allow recovery. Growth medium was carefully aspirated from the wells and replaced with SFM:CM [4:1] containing 0.3 mM dbcAMP to induce differentiation, for a period of 16 hours. Following differentiation medium was again aspirated from the wells and replaced with SFM + 0.3 mM dbcAMP + MPTP. Cells were re-incubated for a further 8 hours prior to extraction of the cell monolayer. Equal protein aliquots (20 μ g) of cell extracts were electrophoresed on a 7.5% SDS-PAGE gel and transferred onto nitrocellulose membrane filters. Blots were then probed with antibodies that recognise anti-actin (a); α -tubulin (b); or neurofilament epitopes (c-e). The signal was developed using either mouse or rabbit alkaline phosphatase secondary conjugates. Shown are control cells (lanes 1) and cells exposed to 10 μ M MPTP (lanes 2) for 8 h post- differentiation.

Right panel: Blots were digitised and changes in antibody reactivity were densitometrically analysed using the Quantiscan Analysis software package. Net area values (arbitrary units) representing the area beneath the peak, automatically corrected for background interference, were obtained. Presented are the mean % Densitometry (y-axes) of three separate experiments \pm SEM, in which the change in densitometry of cells exposed to 10 μ M MPTP (2) is expressed relative to its corresponding control (assigned 100% value).

6.3 Discussion

6.3.1 Characterisation of a post-differentiated neuronal (N2a) cell model.

In order to mimic the physiological state of neuronal cells more closely and substantiate the use of the N2a cell line as a suitable model for analysis of neurodegenerative events that may occur in PD, it was deemed necessary to analyse the effects of MPTP on pre-differentiated N2a cells. Unfortunately, mouse neuroblastoma N2a cells can only be maintained in the differentiated state using serum free medium successfully for up to a maximum of 48 hours whereupon, cell detachment and cell death predominates. Therefore a protocol to maximise N2a cell differentiation was established.

Shea and Beerman (1994) described the morphological differentiation and maintenance of neuroblastoma cells in the presence of serum. However, preliminary experiments in the present study established that serum enhanced cell division thereby reducing the morphological differentiation of the cell population. As glial conditioned medium had previously been shown to markedly enhance N2a cell differentiation (Chapter V), it was used to increase the rate and the proportion of cells exhibiting axon-like processes. Indeed, inducing N2a cells to differentiate in the presence of glial conditioned medium produced a substantial and rapid morphological change in axon outgrowth. Comparison of axon numbers following 'conditioned differentiation' versus 'conventional differentiation' produced a consistently higher percentage of cells with axons. For example, cells induced to differentiate for 16 hours with conditioned C6 medium produced comparable axon counts to cells differentiated by conventional means over 24 hours. In addition, analysis of the NF-H composition confirmed the similarity and relative stability of the axons produced, as both total NF-H levels and NF-H phosphorylation state were comparable in cells induced to differentiate by the two regimes. Indeed, the expression of phosphorylated NF-H (as determined by Ta51 reactivity) within the cell cytoskeleton suggests the a more mature cell phenotype. Although the appearance of various phosphorylated isoforms of NF-H has been associated with axon stability by some workers (Carden *et al.*, 1985), a number of other associated stabilising events have been recognised as contributing to axon maturity and stabilisation (Shea and Beerman, 1994). These include post-

translationally modified tubulin by detyrosination and acetylation and interactions between microtubules and neurofilaments involving MAP1B, tau and extensively phosphorylated NF-H (Hisanaga *et al.*, 1993).

Previous studies utilising conditioned medium, derived from primary astrocytes, indicated that neurite elaboration was unstable and transient in nature, resulting in axon retraction when glial conditioned medium was removed from cells (Shea *et al.*, 1992; Shea and Husain, 1996). However, axon counts of 16 hour pre-differentiated N2a cells (32.16 %, Fig. 6.1) were comparable to axon counts of cells exposed to a further 8 hour incubation in the absence of conditioned medium (29.38 %, Fig. 6.4). Shea and co-workers have induced neuronal differentiation using glial conditioned medium alone in the absence of dbcAMP. In the present study dbcAMP has been supplemented to all stages of the differentiation process, including conditioned differentiation (i.e. 16 hours) and the following neurotoxin exposure period (i.e. 8-24 hours). This lends further support to the 16 hour pre-differentiation protocol suggesting the formation of stable axons. This phenomenon could be related to the idea that glial conditioned medium mediates axon outgrowth via the protein kinase C signal transduction pathway, while dbcAMP mediates outgrowth via the independent protein kinase A pathway (Shea and Husain, 1996). The continual presence of dbcAMP in the pre-differentiation protocol is therefore able to maintain axon stability when conditioned C6 medium is removed. This suggests that the model can be utilised to screen for the initial effects of MPTP neurotoxicity on pre-differentiated cells.

6.3.2 Effect of MPTP on pre-differentiated N2a cells.

N2a cells pre-differentiated for 16 hours with conditioned C6 medium showed a 23 % and 42 % decrease in cell viability when exposed to 1 mM MPTP for 8 hours and 24 hours, respectively. The cell death profile suggests that MPTP-induced cell death is a time-dependent process, with an increase in exposure time to MPTP corresponding to a rise in cell death. In comparison, pre-differentiated N2a cells exhibited an increased sensitivity profile to the cytotoxic effects of MPTP than the differentiating N2a model (see Chapter III, section 3.2.2). Differentiating N2a cells exposed to 1 mM MPTP for 24 hours resulted in a 40 % decrease in cell viability. A

similar extent of cell death was apparent in the pre-differentiated model after only 8 hours exposure to 1 mM MPTP. This increase in MPTP-induced cytotoxicity over time in the pre-differentiated model could be associated with an increase in MAO activity reported in N2a cells following differentiation (Chapter III, section 3.2.4). RT-PCR analysis suggested MAO-A to be the dominant isoform, although MAO-B mRNA was also present; messenger levels for both isoforms increased following differentiation. The associated increase in MAO activity would lead to a concurrent increase in intracellular MPTP metabolism. This in turn would increase MPP⁺ formation resulting in a rise in toxicity.

Establishment of a sub-cytotoxic dose of MPTP enabled a further investigation into its effects on axon maintenance and subsequent cytoskeletal status. The addition of 10 μ M MPTP to pre-differentiated N2a cells produced no measurable increase in cell death after 8 hours incubation, although changes in cell morphology were evident. Indeed, exposure of pre-differentiated cells to MPTP caused a 40 % decrease in axon numbers expressed by the cell population. This phenomenon has also been noted (but not evaluated) by other workers using differentiated PC12 cells (neuronal) exposed to MPTP (Denton and Howard, 1984). In addition an *in vivo* study by Boatell *et al.*, (1992) reported that MPTP could produce a degeneration of striatal axons and dopaminergic terminals within the substantia nigra of MPTP-treated mice, in the absence of significant neuronal loss. These aberrant changes were postulated to be due to retrograde degeneration. The reduction in axon numbers seen in the pre-differentiated N2a model could therefore possibly be associated with either retrograde degeneration or cytoskeletal disruption, leading to axon retraction. However, there is also the possibility that MPTP has caused the inhibition of slow or late developing axon-like processes and may play an additional role in the resultant change in cell morphology.

Further investigation of the characterised morphological changes involved the evaluation of cytoskeletal components within control (untreated) and neurotoxin treated cells. Western blot analysis revealed that total actin and α -tubulin levels were not dramatically affected by exposure to MPTP, as determined by densitometric analysis, suggesting that general cell integrity is maintained during drug exposure. However, it has been reported that 15 μ M MPP⁺ can influence α -tubulin pools in

NGF-differentiated PC12 cells by altering the regulatory balance of α - and β - tubulin subunits (Cappelletti *et al.*, 1995). Indeed, further work has shown that *in situ* soluble α -tubulin levels increase while insoluble α -tubulin levels decrease, resulting in only a small overall increase. These effects have been suggested to be a result of relatively high intracellular MPP⁺ concentrations, since similar concentrations could not interfere with microtubule protein polymerisation *in vitro*; inhibition observed only with 1 mM MPP⁺ (Cappelletti *et al.*, 1999).

Comparison of control and neurotoxin exposed pre-differentiated N2a cells revealed comparable levels of total NF-H. However, a decrease in RMd09 reactivity in MPTP-treated cells (ca. control samples) was countered by an increase in Ta51 reactivity suggesting an alteration in NF-H phosphorylation status. The increase in NF-H phosphorylation state within the pre-differentiated N2a model is not as large as the increase observed within the differentiating model (Chapter IV, Fig. 4.6). It is evident that axons may be undergoing a transition from relatively plastic, rapidly elongating structures in the developing system, to a more mature, stabilised state in the pre-differentiated model. Indeed, a decrease in the rate of outgrowth (as seen in the pre-differentiated N2a model) would reduce the rate of NF-H synthesis and NF-H phosphorylation (Shea, 1995). The presence of a substantial 'soluble pool' of NF-H subunits and their incorporation into the 'insoluble' cytoskeleton both before and during dbcAMP induced differentiation, has been documented in neuroblastoma cells (Shea *et al.*, 1990; Shea, 1995). The ability of MPTP to interfere with this process could influence both axon outgrowth and axon maintenance thereby affecting the extent of NF-H phosphorylation and selective assembly within the cytoskeleton. Therefore the deposition of phosphorylated NF-H subunits from a soluble NF-H pool would be greater in a developing model than in a model expressing pre-formed axons. Although neuronal changes have been observed *in vivo*, immunochemical analysis of mice striata exposed to MPTP, showed no obvious alterations in NF-H subunit levels (Boatell *et al.*, 1992). However, differences in sensitivity and changes at the molecular level do exist between *in vivo* and *in vitro* models and could be related to a number of factors including dosing regimen, duration of neurotoxin treatment, post-treatment period until death of animals, and age of animals (or cellular state i.e. phenotype).

The disclosure of the molecular events involved in MPTP-induced neurotoxicity may provide clues to the mechanisms of cell death and aetiology of PD. The observed aberrant increase in NF-H phosphorylation in MPTP-treated pre-differentiated N2a cells is similar to the observed effects in differentiating N2a cells. This suggests that inducing mouse N2a neuroblastoma cells to express the mature phenotype can provide a simplified, but valuable model for investigating MPTP-induced neurotoxicity. Indeed, the reported changes in the N2a cell model might play an important role in the cascade of events leading to MPTP-induced neuronal cell death and therefore may have implications in PD.

CHAPTER VII

General Discussion & Future Work

7. General Discussion & Future Work

7.1 MPTP-induced neurotoxicity and neurodegeneration

The use of *in vitro* cell models, in this thesis, has allowed the investigation of the direct cytotoxic and neurotoxic effects of MPTP on clonal cell lines of neural origin. The terms cytotoxic and neurotoxic have been used separately to define (a) cytotoxic; toxic insult which has caused apoptotic or necrotic cell death (Chapter III); or (b) neurotoxic; sub-lethal insult which may compromise normal cellular activity/metabolism, prior to measurable cell death (Chapter IV). Cells induced to express the mature phenotype have provided a controlled environment to study MPTP-induced insult on a homogenous cell population. Indeed, this has helped to establish the relative susceptibilities of the two neural cell lines to the neurotoxin and demonstrated subtle intracellular changes at the molecular level following MPTP-induced insult.

In vivo, the classical mechanism of MPTP-induced dopaminergic neurotoxicity is dependent on a number of events. This initially involves the MAO-B mediated 2-electron oxidation of MPTP to MPP⁺ in the central nervous system (Heikkila *et al.*, 1984a) by glial cells. However, *in vitro*, MPTP administered to either C6 or N2a cells leads to cell death in a dose dependent manner. MAO activity profiles demonstrated glioma cells to express greater total activity than neuroblastoma cells, mimicking the *in vivo* situation (see Konradi *et al.*, 1988; Westlund *et al.*, 1988). However, determination of specific MAO mRNA isoforms demonstrated the presence of both isotypes with a predominance of MAO-A in both cell lines. Assuming that these mRNAs are expressed one would thus expect more MAO-A than MAO-B activity in the two cell lines; indeed this was established in C6 cells. To obtain a more detailed (quantifiable) profile of relative MAO isoforms in the two cell lines, the co-amplification of so-called "house-keeping" genes as internal standards, such as β -actin or glyceraldehyde-3-phosphate dehydrogenase, could be undertaken. This would allow an alternative approach to monitor gross changes in MAO expression in the N2a cell line, following neurotoxic insult or neuroprotective treatment.

The cytotoxicity of MPTP to N2a and C6 cells suggests the presence of sufficient MAO activity to produce the toxic metabolite MPP⁺. *In vivo*, the metabolite,

MPP⁺, selectively enters the dopaminergic neurones via active uptake using the dopamine transporter (Javitch *et al.*, 1985), whereupon it accumulates in mitochondria (Tipton *et al.*, 1993). N2a cells demonstrated a less than efficient dopamine uptake system due to their lack of susceptibility to MPP⁺. However, the additional presence of ATP did increase MPP⁺-induced cytotoxicity, suggesting ATP could be a factor in enhancing the catecholamine uptake system as demonstrated by Dunigan and Shamoo (1996).

Once inside the mitochondria MPP⁺ can cause inhibition of complex I of the electron transport chain (Nicklas *et al.*, 1985). Uncoupling of mitochondrial respiration can produce a number of secondary events including loss of neuronal ATP, elevations in intracellular calcium levels, and increased oxidative stress (Chan *et al.*, 1991); a cascade of events particularly toxic to nigral neurones. Indeed, exposure of C6 glioma and N2a neuroblastoma cells to increasing toxic concentrations of MPTP, *in vitro*, showed neuroblastoma cells to be more sensitive than C6 cells (Chapter III). This could be attributed to the relative activity of the glycolytic pathway within the two cell lines or the relative abundance of O₂⁻ scavenging enzymes present. Nevertheless, this difference in sensitivity is akin to the *in vivo* situation, where various factors have been implicated in neurone-specific degeneration including mitochondrial/metabolic differences, excitotoxicity, reduced antioxidant mechanisms, deficient trophic support and the accumulation of toxic metabolite (Lozano *et al.*, 1998). However, C6 cells are killed by high concentrations of MPTP following prolonged exposure (Chapter III), a factor not always commented upon *in vivo*. The rapid removal of the toxic metabolite from the brain and activation of gliosis, *in vivo*, may mask the toxic effects of MPTP towards glial cells (DiMonte *et al.*, 1992).

It is becoming increasingly evident that MPTP may exert its neurodegenerative effect via a combination of independent and linked events producing important molecular changes to neuronal cells prior to metabolic inhibition and cell death. In the past, both animal studies and cell studies have involved the use of acute toxic doses of MPTP, although it is now recognised that a low-dose MPTP animal model with long survival times may be more valuable for studying neuronal damage and repair mechanisms (Bezard *et al.*, 1998) with greater relevance to Parkinson's Disease. To address this, the *in vitro* studies carried out in Chapters IV-VI have focused on the use of sub-cytotoxic doses of neurotoxin to allow investigation of the more subtle changes that occur during neuronal degeneration. This has identified progressive changes that

potentially represent early markers of toxicity. A greater understanding of these progressive changes will ultimately lead to the identification of targets for developing novel therapies.

Treatment of differentiating and differentiated N2a neuroblastoma cells with MPTP leads to an inhibition of axon outgrowth and retraction of axons, respectively. This is associated with a specific increase in neurofilament-H (NF-H) phosphorylation in the absence of changes to the total levels of NF-H, actin or α -tubulin. Furthermore, indirect immunofluorescence analysis revealed an abnormal accumulation of NF-H in the cell perikaryon of neurotoxin treated cells, while actin distribution remained largely unaffected. The observations suggest that aberrant NF-H phosphorylation and altered NF-H distribution is associated with the observed effects on cell morphology. Of particular interest for future work would be to assess the effect of MPTP on post-translational modifications of other cytoskeletal elements, such as tubulin (e.g. acetylation/tyrosination).

The modifications observed occur in the absence of changes in energy status or mitochondrial membrane potential suggesting that these aberrant alterations may represent early markers of neurotoxicity. These modifications in NF protein are particularly important given that NF-H plays a vital role in the organisation and stabilisation of the axonal cytoskeleton and alterations in NF phosphorylation *in vivo* have been associated with NF aggregation in a number of chemically induced neuropathies (e.g. Gold *et al.*, 1988). Indeed, aberrant NF-H phosphorylation has also been identified in the pathology of a number of other neurodegenerative diseases. These include Alzheimer's disease (Cork *et al.*, 1986), amyotrophic lateral sclerosis (Manetto *et al.*, 1988) and particularly Parkinson's Disease (Forno *et al.*, 1983), where hyper-phosphorylated NFs are components of the intraneuronal inclusions - Lewy bodies. However, it is important to note that, *in vivo*, MPTP induced Lewy body formation remains controversial, although recent work has reported abnormal neuronal aggregates in MPTP-treated baboons (Kowall *et al.*, 2000). The absence of definitive changes in ubiquitin and synuclein reactivity in MPTP-treated neuroblastoma cells highlights some of the limitations of the model. The abnormal inclusions seen *in vivo* suggests the need for a cell line that can be maintained in the differentiated state for prolonged periods of time to allow investigation of chronic MPTP exposure.

7.2 The role of MPTP-induced signalling cascades

Studies have shown that NF-H subunits undergo continued phosphorylation and dephosphorylation events during axonal development and transport. In addition, incorporation of NF-H into the cytoskeletal lattice is regulated by phosphorylation (Nixon and Sihag, 1991). Neuroblastoma cells contain low levels of phosphorylated NF-H variants which increase during normal dbcAMP-induced differentiation (Shea, 1995) facilitating NF-H transport, assembly and stabilisation under temporal and spatial regulation. One could therefore hypothesise that the presence of sub-cytotoxic MPTP concentrations during this process causes the activation of a cascade of reactions possibly involving neurofilament associated kinases. This leads to the aberrant and untimely phosphorylation of NF-H resulting in the accumulation and residence of phosphorylated NF-H within the cell perikaryon. These NF-H variants persist within the cell perikaryon as visualised by indirect immunofluorescence analysis (Chapter IV).

The observed increase in NF-H phosphorylation in N2a cells following sub-cytotoxic insult was shown to occur alongside activation of the SAPK/JNK pathway, as determined by the appearance of the activated form of JNK kinase (Chapter IV). This suggests the potential involvement of the SAPK pathway in MPTP-induced neuroblastoma degeneration. Activation of the SAPK pathway has been associated with events leading to oxidative stress (Turner *et al.*, 1998; Bhat and Zhang, 1999) and transient increases in intracellular calcium ion concentration (Tibbles and Woodgett, 1999). Since an increase in both reactive oxygen species and intracellular calcium levels have been documented following MPTP exposure (see section 1.1.9.2), perturbation of intracellular homeostasis by MPTP may relay the observed changes to the cell via this stress-signalling cascade. This is further supported by the fact that activation of the SAPK pathway can lead to hyper-phosphorylation of perikaryal NF-H (Giasson and Mushynski, 1996). Indeed, inhibition of the SAPK pathway has been shown to protect against the loss of dopaminergic cells in a low-dose MPTP mouse model. (Saporito *et al.*, 1999). The ability of this inhibitor to alleviate MPTP-induced neurotoxicity in the N2a system would lend further support to this hypothesis.

Recently, treatment of SH-SY5Y cells with acute doses of MPP⁺ has been shown to cause a biphasic early (15 min) and late (12 h) JNK activation in conjunction

with a biphasic activation of NF- κ B. NF- κ B was shown to mediate the increased expression of the antioxidative enzyme Mn-superoxide dismutase, suggesting NF- κ B activation to be a possible protective response to oxidative stress (Cassarino *et al.*, 2000). Although not studied in this thesis it may be of value to investigate the potential activation of NF- κ B in the N2a cell model as an inherent protective mechanism following oxidative stress or injury.

The potential activation of a cascade of reactions following MPTP-induced insult can not be dismissed and therefore the ERK and p38 pathways may also be involved in MPTP-induced neurotoxicity and NF-H phosphorylation. For example, ERK signalling cascades can play multiple roles in the activity-dependent regulation of neuronal function, which include cell differentiation, proliferation, growth and cell death (Grewal *et al.*, 1999). It is also evident that second messengers such as cyclic adenosine monophosphate, protein kinase A and calcium will also effect the role of ERKs in the regulation of neuronal events. ERK activation may therefore be altered in MPTP treated N2a cells, given the observed changes in cell differentiation, i.e. axon outgrowth. Indeed, the mitogen-activated protein kinases (ERK1 and ERK2) have been shown to phosphorylate NF-H suggesting that may play an important role in axon outgrowth (Veeranna *et al.*, 1998).

Inhibition of p38 MAPK in differentiating N2a cells resulted in cells expressing an increasingly mature phenotype, characterised by an increase in axon outgrowth (Chapter V). In addition, inhibition of p38 MAPK repressed the MPTP-induced effects on cell morphology and NF-H phosphorylation state, suggesting a potential protective role by inhibiting the p38 pathway. Indeed, p38 activation is reported to precede PC12 cell death following growth factor withdrawal (Horstmann *et al.*, 1998). In addition, specific inhibitors of the p38 MAPK pathway i.e. SB203580 and SB202190, have been shown to promote chick embryonic neurone survival *in vitro* (Horstmann *et al.*, 1998). In contrast, these p38 inhibitors had no effect on the survival of HeLa cells following H₂O₂ insult (Wang *et al.*, 1998), suggesting that a more complex scenario exists depending on cell type or the nature of the insult. Work carried out using dorsal root ganglia neurones has suggested that p38 kinases are not directly involved in the phosphorylation of perikaryal NF-H (Giasson and Mushynski, 1997). This could imply that SB202190-induced protection is possibly functioning upstream of MPTP activated targets or is via an alternative mechanism that can indirectly affect MPTP-induced NF-

H phosphorylation. Although p38 MAPKs have been implicated both as positive and negative regulators of cell survival it is becoming clear that the nature of the stimulus is all important and might trigger the activation of other signalling pathways, which act in either a synergistic or antagonistic manner with the p38 pathway.

The abundant KSP repeats found in NF-H represent the major phosphorylation sites of the protein. Investigations of the relevant kinases that function in this role has identified a number of kinases within the serine/threonine and proline directed protein kinase superfamilies. These include the glycogen synthase kinase-3, extracellular signal-regulated kinases (ERKs), cyclin dependent kinase-5 and c-jun N-terminal kinase (Giasson and Mushynski, 1996). Interestingly, the serine/threonine kinase, cyclin-dependent kinase 5 (cdk5) and p35 (the regulatory subunit that associates with cdk5 to cause kinase activation) are known to regulate the phosphorylation of NF-H at KSPXK motifs (Sun *et al.*, 1996) and therefore have implications in neurodegeneration. Over expression of p25 (a truncated form of p35; which also associates with cdk5 to cause increased kinase activation) can cause cytoskeletal disruption characterised by tau phosphorylation, but also NF-H hyperphosphorylation and accumulation in primary cortical neurones (Patrick *et al.*, 1999). Indeed, p25 has been found to accumulate in the brains of patients with Alzheimer's disease and correlates with an increase in cdk5 kinase activity (Patrick *et al.*, 1999).

In contrast to the activation of potential kinases, the changes in NF-H phosphorylation may potentially be mediated by inhibition of particular protein phosphatases. For example, the dual specificity phosphatases, such as MAP kinase phosphatases (MKP-1 and MKP-2), and individual serine:threonine (i.e. type 2a, PP2A) or tyrosine (type 1, PP1) protein phosphatases regulate the phosphorylation of a large number of key elements in the cytoskeleton and in various signalling processes (Toviola and Ericksson, 1999). Indeed, immunocytochemical analysis of spinal cord has revealed the association of a number of protein phosphatase subunits with neurofilaments. In particular, it has been suggested that neurofilament-associated PPI and PP2A play an important role in the regulation of neurofilament phosphorylation (Strack *et al.*, 1997). It has also been reported that MKPs can inactivate the stress-activated protein kinases. Therefore it is possible that inhibition of particular phosphatases can lead to alterations in cytoskeletal integrity and function, involving hyper-phosphorylation of intermediate filament proteins. Although beyond the scope of this thesis, a study of the effects of inhibitors of specific protein phosphatases could

help establish their potential role in altered NF-H phosphorylation state, following MPTP-induced insult.

7.3 Neuroprotection

It was demonstrated in Chapter V that treatment of differentiating N2a cells with potential neuroprotective agents such as deprenyl, conditioned C6 medium and to a lesser extent estradiol, was able to attenuate the neurotoxic and cytotoxic effects of MPTP. The mechanism of action of these neuroprotective agents is likely to function through a number of linked pathways perhaps working in synergy. For example, deprenyl will primarily inhibit MAO activity thereby preventing MPP⁺ formation. However, deprenyl is also proposed to exhibit other neuroprotective properties independent of its MAO inhibitory effects (see section 5.3.1). C6 conditioned medium enhanced morphological cell differentiation and subsequently alleviated the inhibition in axon outgrowth produced by MPTP-insult. In addition, C6 conditioned medium could reverse the imbalance in NF-H phosphorylation state, produced by sub-cytotoxic concentrations of MPTP.

Although beyond the scope of this thesis, fractionation of conditioned medium and purification of the neurotrophic factors present would help to establish the components present and allow investigations into the mechanisms of action. However, it has been demonstrated in Chapter V that C6 cells secrete GDNF into culture medium. The potential of GDNF as a neuroprotective agent has been proposed by Tomac *et al.*, (1995) who showed it could exert cytoprotective and regenerative effects, *in vivo*, on dopaminergic neurones in the MPTP mouse model. Indeed, like GDNF, C6 conditioned medium was also able to protect N2a cells from MPTP-induced cell death following exposure to cytotoxic concentrations over a 48 hour period. One could therefore speculate that the protective effects seen could be due, at least in part, to the presence of GDNF in conditioned C6 medium. The molecular basis of protection would involve a glycosylphosphatidylinositol linked GDNF receptor (GDF α 1) interacting with a transmembrane Ret receptor tyrosine kinase (Jing *et al.*, 1996). The intracellular events following GDNF-dependent Ret activation are complex, but it is likely that the cascade of signalling events counteract the MPTP-

induced stress response leading to enhanced neurite outgrowth, differentiation and ultimately cell survival.

7.4 Summary

In summary, the results from this thesis show that exposure of differentiating and differentiated N2a cells to MPTP disrupts normal NF-H phosphorylation, thereby affecting NF assembly and inhibiting axon outgrowth. Since aberrant NF phosphorylation state *in vivo* is associated with a number of neurodegenerative conditions, the identification of similar aberrant changes in N2a cells following neurotoxic insult suggests it may represent a useful cellular model. Indeed, these alterations can be monitored more easily using cell model systems that express a mature phenotype and has also been used to assess organophosphate-induced delayed neurotoxicity (Flaskos *et al.*, 1998). The aberrant morphological and biochemical changes following MPTP insult therefore represent useful *in vitro* makers of neurotoxicity. Indeed, inhibition of aberrant NF-H phosphorylation provides a mechanism by which neuroblastoma cells can potentially moderate MPTP-induced neurotoxicity. This is suggested by the ability of various neuroprotective agents to attenuate MPTP-induced hyper-phosphorylation and also alleviate cell death.

The close association demonstrated by MPTP with the pathology seen in Parkinson's disease suggests that deciphering the molecular events that cause cellular damage following MPTP-induced neurotoxic insult may well provide useful information in understanding neurodegeneration. To examine these events a combination of animal models (wild-type/transgenic), examination of tissue from the human Parkinsonian brain and *in vitro* cell-culture paradigms will be needed. In this respect, cell culture models will allow detailed and systematic analysis of the signalling events involved during neurotoxic insult. This could be initially achieved through the use of a combination of specific kinase and phosphatase inhibitors and commercially available phospho-specific antibodies.

One of the primary objectives for future Parkinson's disease therapy is the development of neuroprotective agents that will slow or prevent neuronal cell death. This form of therapy will be achieved following a better understanding of the basic mechanism of neurodegeneration. In this instance, the use of a simplified neuronal cell

model, which expresses subtle changes following neurotoxic insult, could provide a valuable tool in investigating potential neuroprotective agents.

REFERENCES

References

- Adams J.D. Jr., Odunze I.N. (1991) Biochemical mechanisms of 1-methyl-4-phenyl-1,2,3,6-tetrahydropyridine toxicity. *Biochem. Pharmacol.* **41**, 1099-1105.
- Airaksinen M.S., Titievsky A., Saarma M. (1999) The biology of glial-derived neurotrophic factor. *Mol. Cell. Neurosci.* **13**, 313-325.
- Akaneya Y., Takahashi M., Hatanaka H. (1995) Involvement of free radicals in MPP⁺ neurotoxicity against rat dopaminergic neurones in culture. *Neurosci. Letts.* **193**, 53-56.
- AlvesRodrigues A., Gregori L., FigueiredoPereira M.E. (1998) Ubiquitin, cellular inclusions and their role in neurodegeneration. *Trend. Neurosci.* **21**, 516-520.
- Andersen J.K., Frim D.M., Isacson O., Beal M.F., Breakefield X.O. (1994) Elevation of MAO-B in a transgenic mouse model has no effect on MPTP sensitivity. *Brain Res.* **656**, 108-114.
- Anderson M. E. (1985) Determination of glutathione and glutathione disulphide in biological samples. *Meth. Enzymol.* **70**, 548-554.
- Armstrong R. A., Cairns N. J., Lantos P. L. (1998) The spatial patterns of Lewy bodies, senile plaques, and neurofibrillary tangles in dementia with Lewy bodies. *Exp. Neurol.* **150**, 122-127.
- Baas P.W. (1997) Microtubules and axonal growth. *Curr. Opin. Cell Biol.* **9**, 29-36.
- Baas P.W., Deitch J.S., Black M.M., Banker G.A. (1988) Polarity orientation of microtubule in hippocampal neurons, uniformity in the axon and non-uniformity in the dendrite. *Proc. Natl. Acad. Sci. USA.* **85**, 8335-8339.
- Bach A.W.J., Lan N.C., Johnson D.L., Abell C.W., Bembenek M.E., Kwan S-W., Seeburg P.H., Shih J.C. (1988) cDNA cloning of human liver monoamine oxidase A and B, molecular basis of differences in enzymatic properties. *Proc. Natl. Acad. Sci. USA.* **85**, 4934-4938.
- Basma A.N., Heikkila R.E., Saporito M.S., Philbert M., Geller H.M., Nicklas W.J. (1992) 1-methyl-4-(2'-ethylphenyl)-1,2,3,6-tetrahydropyridine-induced toxicity in PC12 cells is enhanced by preventing glycolysis. *J. Neurochem.* **58**, 1052-1059.
- Behl C., Holsboer F. (1999) The female sex hormone oestrogen as a neuroprotectant. *TIPS.* **20**, 441-444.
- Benda *et al.* (1968) Cell culture of a rat glioma cell line. *Science* **161**, 370
- Berridge M.V., Tan A.S., McCoy K.D., Wang R. (1996) The biochemical and cellular basis of cell proliferation assays that use tetrazolium salts. *Biochemica.* **4**, 15-20.
- Berry M.D., Juorio A.V., Paterson I.A. (1994) The functional role of monoamine oxidases A and B in the mammalian central nervous system. *Prog. Neurobiol.* **42**, 375-391.
- Bezard E., Imbert C., Gross C.E. (1998) Experimental models of Parkinson's disease, from static to the dynamic. *Rev. Neurosci.* **9**, 71-90.
- Bhat N.R., Zhang P.S. (1999) Hydrogen peroxide activation of multiple MAPK in an oligodendrocyte cell line, Role of extracellular signal-regulated kinase in hydrogen peroxide-induced cell death. *J. Neurochem.* **72**, 112-119.
- Birkmayer W., Knoll J., Riederer P. (1985) Improvement of life expectancy due to l-deprenyl addition to madopar treatment in Parkinson's disease. *J. Neural Transm.* **12**, 113-127.
- Blaschko H., Richter D., Schlossmann H. (1937) The oxidation of adrenaline and other amines. *Biochem J.* **31**, 2187-2196.

- Boatell M. Ll., Mahy N., Cardozo A., Ambrosio S., Tolosa E., Cruz-Sanchez F. F. (1992) Neuronal changes in the nigrostriatal pathway of MPTP-treated mice. *Meth. Find. Exp. Clin. Pharmacol.* **14**, 781-787.
- Bohets H.H., Nouwen E.J., Debroe M.E., Dierickx P.J. (1994) Effects of fetal calf serum on cell viability, cytotoxicity and detoxification in the kidney-derived cell lines LLC-PK1 and MDCK. *Toxicol. In Vitro* **8**, 559-561.
- Borg J., Spitz B., Hamel G., Mark J. (1985) Selective culture of neurones from rat cerebral cortex, morphological characterisation, glutamate uptake and related enzymes during maturation in various culture medium. *Dev. Brain Res.* **18**, 37-49.
- Boyce S., Kelly E., Reavill C., Jenner P., Marsden C.D. (1984) Repeated administration of N-methyl-4-phenyl-1,2,3,6-tetrahydropyridine to rats is not toxic to striatal dopamine neurones. *Biochem. Pharmacol.* **33**, 1740-1752.
- Bradford H.F. (1986) Function of Glial cells. In *Chemical Neurobiology, An introduction to neurochemistry*. W.H. Freeman and Company. 152-174.
- Brooks W.J., Jarvis M.F., Wagner G.C. (1989) Astrocytes as a primary locus for the conversion of MPTP into MPP⁺. *J. Neural Transm.* **76**, 1-12.
- Burns R.S., Chiueh C.C., Markey S.P., Ebert M.H., Jacobowitz D.M., Kopin I.J. (1983). A primate model of parkinsonism, selective destruction of dopaminergic neurones in the pars compacta of the substantia nigra by 1-methyl-4-phenyl-1,2,3,6-tetrahydropyridine. *Proc. Natl. Acad. Sci.* **80**, 4546-4550.
- Buckman T.D. (1991) Toxicity of MPTP and structural analogues in clonal cell lines of neuronal origin expressing B type monoamine oxidase activity. *Mol. Chem. Neuropathol.* **15**, 87-102.
- Camins A., Sureda F.X., Gabriel C., Pallas M., Escubedo E., Camarasa J. (1997) Effect of 1-methyl-4-phenylpyridinium (MPP⁺) on mitochondrial membrane potential in cerebellar neurons, interaction with the NMDA receptor. *J. Neural Transm.* **104**, 569-577.
- Cappelletti G., Camatini M., Brambilla E., Maci R. (1991) N-methyl-4-phenyl-1,2,3,6-tetrahydropyridine (MPTP) induces cytoskeletal alterations on Swiss-3T3 mouse fibroblasts. *Neurosci Lett.* **129**, 149-152.
- Cappelletti G., Incani C., Maci R. (1995) Involvement of tubulin in MPP⁺ neurotoxicity on NGF-differentiated PC12 cells. *Cell Biol. Int.* **19**, 687-693.
- Cappelletti G., Maggioni M.G., Maci R. (1999) Influence of MPP⁺ on the state of tubulin polymerisation in NGF-differentiated PC12 cells. *J. Neurosci. Res.* **56**, 28-35.
- Carden M.J., Schlaepfer W.W., Lee V.M. (1985) The structure, biochemical properties, and immunogenicity of neurofilament peripheral regions are determined by phosphorylation state. *J. Biol. Chem.* **260**, 9805-9817.
- Carden M.J., Trojanowski J.Q., Schlaepfer W.W., Lee V.M. (1987) Two-stage expression of neurofilament polypeptides during rat neurogenesis with early establishment of adult phosphorylation patterns. *J. Neurosci.* **7**, 3489-3504.
- Carlo P., Del Rio M., Violani E., Sciaba L., Picotti G. (1996) Influence of culture conditions on monoamine oxidase A and B activity in rat astrocytes. *Cell. Biochem. and Func.* **14**, 19-25.
- Cassarino D.S., Halvorsen E.M., Swerdlow R.H., Abramova N. N., Davis Parker W., Sturgill T. W., Bennett J. P. (2000) Interaction among mitochondria, mitogen-activated protein kinases, and nuclear factor κ B in cellular models of Parkinson's disease. *J. Neurochem.* **74**, 1384-1392.

- Castagnoli N. Jr., Chiba K., Trevor A. (1985) Potential bioactivation pathways for the neurotoxin 1-methyl-4-phenyl-1,2,3,6-tetrahydropyridine (MPTP). *Life Sci.* **36**, 225-230.
- Cawthorn R.M., Breakefield X.O. (1979) Differences in A and B forms of monoamine oxidase revealed by limited proteolysis and peptide mapping. *Nature* **281**, 692-694.
- Chan P., Delaney L.E., Irwin I., Langston J.W., DiMonte D. (1991) Rapid ATP loss caused by 1-methyl-4-phenyl-1,2,3,6-tetrahydropyridine in mouse-brain. *J. Neurochem.* **57**, 348-351.
- Chiba K., Trevor A., Castagnoli N. Jr. (1984) Metabolism of the neurotoxic tertiary amine, MPTP, by brain monoamine oxidase. *Biochem. Biophys. Res. Commun.* **120**, 574-578.
- Chomczynski P., Sacchi N. (1987) Single-step method of RNA isolation by acid guanidinium thiocyanate-phenol-chloroform extraction. *Anal. Biochem.* **162**, 156-159.
- Cleeter M.W.J., Cooper J.M., Schapira A.H.V. (1992) Irreversible inhibition of mitochondrial complex I by 1-methyl-4-phenyl pyridinium (MPP⁺), evidence for free radical involvement. *J. Neurochem.* **58**, 786-789.
- Cohen G., Pasik P., Cohen B., Leist A., Mytilineou C., Yahr M. (1984) Pargyline and deprenyl prevent the neurotoxicity of 1-methyl-4-phenyl-1,2,3,6-tetrahydropyridine (MPTP) in monkeys. *Europ. J. Pharmacol.* **106**, 209-210.
- Cork L.C., Sternberger N.H., Sternberger L.A., Casanova M.F., Struble R.G., Price D.L. (1986) Phosphorylated neurofilament antigens in neurofibrillary tangles in Alzheimer's disease. *J. Neuropathol. Exp. Neurol.* **45**, 56-64.
- Corongiu F.P., Dessi M.A., Banni S., Bernardi F., Piccardi M.P., Del Zompo M., Corsini G.U. (1987) MPTP fails to induce lipid peroxidation *in vivo*. *Biochem. Pharmacol.* **36**, 2251-2253.
- Cookson M.R., Mead C., Austwick S.M., Pentreath V.W. (1995) Use of the MTT assay for estimating toxicity in primary astrocytes and C6 glioma cell cultures. *Toxicol. in Vitro.* **9**, 39-48.
- D'Amato R.J., Benham D.F., Snyder S.H. (1987) Characterisation of the binding of N-methyl-4-phenylpyridine, the toxic metabolite of N-methyl-4-phenyl-1,2,3,6-tetrahydropyridine, to neuromelanin. *J. Neurochem.* **48**, 653-658.
- Damier P., Kastner A., Agid Y., Hirsch E.C. (1996) Does monoamine oxidase type B play a role in dopaminergic nerve cell death in Parkinson's disease. *Neurology* **46**, 1262-1269.
- Davey G., Tipton K.F., Murphy M.P. (1992) Uptake and accumulation of MPP⁺ by rat liver mitochondria measured using an ion-selective electrode. *Biochem J.* **288**, 439-443.
- Davis G.C., Williams A.C., Markey S.P., Ebert M.H., Caine E.D., Reichert C.M., Kopin I.J. (1979). Chronic Parkinsonism secondary to intravenous injection of meperidine analogues. *Psych. Res.* **1**, 249-254.
- Denny R.M., Fritz R.R., Patel N.T., Abell C.W. (1982) Human liver MAO-A and MAO-B separated by immunoaffinity chromatography with MAO-B specific monoclonal antibody. *Science* **215**, 1400-1403.
- Denton T., and Howard B.D. (1984). Inhibition of dopamine uptake by MPTP, a cause of Parkinsonism. *Biochem. Biophys. Res. Commun.* **119**, 1186-1190.
- Denton T., Howard B.D. (1987) A dopaminergic cell line variant resistant to the neurotoxic 1-methyl-4-phenyl-1,2,3,6-tetrahydropyridine. *J. Neurochem.* **49**, 622-630.
- Dexter D.T., Carter C.J., Wells F.R., Lees A.J., Agid F., Agid Y., Jenner P., Marsden C.D. (1989) Basal lipid peroxidation in substantia nigra is increased in Parkinson's disease. *J. Neurochem.* **52**, 381-389.

- Di Monte D., Jewell S.A., Ekstrom G., Sandy M.S., Smith M.T. (1986) 1-Methyl-4-phenyl-1,2,3,6-tetrahydropyridine (MPTP) and 1-methyl-4-phenylpyridinium (MPP⁺) cause rapid ATP depletion in isolated hepatocytes. *Biochem. Biophys. Res. Commun.* **137**, 310-315.
- Di Monte D., Wu E.Y., Irwin I., DeLanney L.E., Langston J.W. (1992) Production and disposition of 1-methyl-4-phenylpyridinium in primary cultures of mouse astrocytes. *Glia* **5**, 48-55.
- Doering L.C. (1993) Probing modifications of the neuronal cytoskeleton. *Mol. Neurobiol.* **7**, 265-291.
- Dunigan C.D., Shamo A.E. (1996) Identification of the major transport pathway for the parkinsonism-inducing neurotoxin 1-methyl-4-phenylpyridinium. *Neurosci.* **75**, 37-41.
- ElAgnaf O.M.A., Jakes R., Curran M.D., Middleton D., Ingenito R., Bianchi E., Pessi A., Neill D., Wallace A. (1998) Aggregates from mutant and wild-type α -synuclein and NAC peptide induce apoptotic cell death in human neuroblastoma cells by formation of β -sheet and amyloid like filaments. *FEBS Letts.* **440**, 71-75.
- Eshleman A., Dunigan C.D., Shamo A.E., Eldefrawi M. (1995) ATP enhances catecholamine uptake into PC12 cells. *Life Sci.* **56**, 1613-1621.
- Flann S., Hawkes R.B., Riederer B.M., Rider C.C., Beesley P.W. (1997) Changes in ubiquitin immunoreactivity in developing rat brain, A putative role for ubiquitin and ubiquitin conjugates in dendrite outgrowth and differentiation. *Neurosci.* **81**, 173-187.
- Flaskos J., McLean W.G., Fowler M.J., Hargreaves A.J. (1998) Tricresyl phosphate inhibits the formation of axon-like processes and disrupts neurofilaments in cultured mouse N2a and rat PC12 cells. *Neurosci. Lett.* **242**, 101-104.
- Forno L.S., Langston J.W., DeLanney L.E., Irwin I., Ricaurte G.A. (1986) Locus coeruleus lesions and eosinophilic inclusions in MPTP-treated monkeys. *Ann. Neurol.* **20**, 449-455.
- Forno L.S., Strefling A.M., Sternberger L.A., Sternberger N.H., Eng L.F. (1983) Immunocytochemical staining of neurofibrillary tangles and the periphery of Lewy bodies with a monoclonal antibody to neurofilaments. *J. Neuropath. Exp. Neurol.* **42**, 342-345.
- Fowler C.J., Mantle T.J., Tipton K.F. (1982) The nature of the inhibition of rat liver MAO-A and B by the acetylenic inhibitors clorgyline, L-deprenyl, and pargyline. *Biochem. Pharmacol.* **31**, 3555.
- Fowler C.J., Wiberg A., Orelund L., Winblad B. (1980) Titration of human brain type B monoamine oxidase. *Neurochemical Research.* **5**, (7) 697-708.
- Freyaldenhoven T.E., Ali S.F. (1996) Heat shock proteins protect cultured fibroblasts from the cytotoxic effects of MPP⁺. *Brain Res.* **735**, 42-49.
- Geisler N., Kaufmann E., Fischer S., Plessmann U., Weber K. (1983) Neurofilament architecture combines structural principles of intermediate filaments with carboxy-terminal extensions of increasing size between triplet proteins. *EMBO J.* **2**, 1295-1302.
- Geisler N., Kaufmann E., Weber K. (1985) Antiparallel orientation of the double stranded coiled-coils in the tetrameric protofilament unit of intermediate filaments. *J. Mol. Biol.* **182**, 173-177.
- Giasson B.I., Mushynski W.E. (1996) Aberrant stress-induced phosphorylation of perikaryal neurofilaments. *J. Biol. Chem.* **271**, 30404-30409.
- Giasson B.I., Mushynski W.E. (1997) Study of proline-directed protein kinases involved in phosphorylation of the heavy neurofilament subunit. *J. Neurosci.* **17**, 9466-9472.
- Gibb J.W.G., Lees A.J. (1988) The relevance of Lewy Body to the pathogenesis of idiopathic Parkinson's disease. *J. Neurol. Neurosurg. Psychiatry.* **51**, 745-752.

- Giros B., El Mestikawy S., Godinot N., Zheng K., Han H., Yang-Fen T., Caron M.G. (1992) Cloning, pharmacological characterisation, and chromosome assignment of the human dopamine transporter. *Mol. Pharmacol.* **42**, 383-390.
- Gold, B.G., Price D.L., Griffin J.W., Rosenfeld J., Hoffman P.N., Sternberger N.H., Sternberger L.A. (1988) Neurofilament antigens in acrylamide neuropathy. *J. Neuropathol. Exp. Neurol.* **47**, 145-157.
- Goldman J.E., Yen S-H., Chiu F-C., Peress N.S. (1983) Lewy bodies of Parkinson's disease contain neurofilament antigens. *Science* **221**, 1082-1084.
- Greenamyre J.T. (1998) Glutamate and Parkinson's disease. *Biochem. Soc. Trans.* **26**, vii.
- Grewal S.S., York R. D., Stork P.J.S. (1999) Extracellular-signal-regulated kinase signalling in neurones. *Curr. Opin. Neurobiol.* **9**, 544-553.
- Grimsby J., Chen K., Wang L.J., Lan N.C., Shih J.C. (1991) Human monoamine oxidase A and oxidase B genes exhibit identical exon intron organisation. *Proc. Natl. Acad. Sci. USA.* **88**, 3637-3641.
- Gupta M., Gupta B.K., Thomas R., Bruemmer V., Sladek J.R.J., Felten D.L. (1986) Aged mice are more sensitive to 1-methyl-4-phenyl-1,2,3,6-tetrahydropyridine treatment than young adults. *Neurosci. Lett.* **70**, 326-331.
- Haffke S.C., Seeds N.W. (1975) Neuroblastoma, the E.coli of neurobiology. *Life. Sci.* **16**, 1649-1658.
- Han J., Cheng F-C., Yang Z., Dryhurst G. (1999) Inhibitors of mitochondrial respiration, Iron (II), and hydroxyl radical evoke release and extracellular hydrolysis of glutathione in rat striatum and substantia nigra, Potential implications to Parkinson's disease. *J. Neurochem.* **73**, 1683-1695.
- Hantraye P., Brouillet E., Ferrante R., Palfi S., Dolan R., Matthews R.T., Beal M.F. (1996) Inhibition of neuronal nitric oxide synthase prevents MPTP-induced parkinsonism in baboons. *Nature. Med.* **2**, 1017-1021.
- Hantraye P., Varastet M., PescHanski M., Riche D., Cesaro P., Willer J.C., Maziere M. (1993). Stable parkinsonian syndrome and uneven loss of striatal dopamine fibres following chronic MPTP administration in baboons. *Neurosci.* **53**, 169-178.
- Hare M.L.C. (1928) Tyramine oxidase. A new enzyme system in liver. *Biochem J.* **22**, 968-979.
- Hargreaves A.J. (1997) The cytoskeleton as a target in cell toxicity. *Adv. Mol. and Cell Biol.* **20**, 119-144.
- Hargreaves A.J., Yusta B., Avila J., Hesketh J.E., Aranda A., Pascual A. (1989) Sodium butyrate induces major morphological changes in C6 glioma cells that are correlated with increased synthesis of a spectrin-like protein. *Develop. Brain. Res.* **45**, 291-295.
- Hartley C.L., Anderson V.E.R., Anderson B.H., Robertson J. (1997) Acrylamide and 2,5-hexanedione induce collapse of neurofilaments in SH-SY5Y human neuroblastoma cells to form perikaryal inclusion bodies. *Neuropath. Appl. Neurobiol.* **23**, 364-372.
- Hasegawa E, Takeshiga K, Oishi T, Murai Y, Minikami S. (1990) 1-methyl-4-phenyl pyridinium (MPP⁺) induces NADH-dependent superoxide formation and enhances NADH-dependent lipid peroxidation in bovine heart submitochondrial particles. *Biochem. Biophys. Res. Commun.* **170**, 1049-1055.
- Heikkila R.E., Hess A., Duvoisin R.C. (1984a) Dopaminergic neurotoxicity of 1-methyl-4-phenyl-1,2,3,6-tetrahydropyridine in mice. *Science.* **224**, 1251-1253.
- Heikkila R.E., Manzino L., Cabbat F.S., Duvoisin R.C. (1984b) Protection against the dopaminergic neurotoxicity of 1-methyl-4-phenyl-1,2,3,6-tetrahydropyridine by monoamine oxidase inhibitors. *Nature.* **311**, 467-469.

Henschler D., Schmuck G., van Aerssen M., Schiffmann A. (1992) The inhibitory effect of neuropathic organophosphate esters on neurite outgrowth in cell cultures, a basis for screening for delayed neurotoxicity. *Toxic. In Vitro* **6**, 327-335.

Hershko A., Ciechanover A. (1982) Mechanisms of intracellular protein breakdown. *Ann. Rev. Biochem.* **51**, 335-364.

Hess A., Desiderio C., McAuliffe W.G. (1990) Acute neuropathological changes in the caudate nucleus caused by MPTP and methamphetamine, immunohistochemical studies. *J. Neurocytol.* **19**, 338-342.

Hisanaga S-I., Yasugawa S., Yamakawa T., Miyamoto E., Ikebe M., Uchiyama M., Kishimoto T. (1993) Dephosphorylation of microtubule binding sites at the neurofilament-H tail domains by alkaline and protein phosphatases. *J. Biochem.* **113**, 705-709.

Hoffman P.N., Lasek R.J. (1975) The slow component of axonal transport, Identification of major structural polypeptides of the axon and their generality among mammalian neurones. *J. Cell Biol.* **66**, 351-366.

Hoffman P.N., Cleveland D.W., Griffin J.W., Landes P.W., Cowan N.J. (1987) Neurofilament gene-expression - a major determinant of axonal caliber. *Proc. Natl. Acad. Sci. USA.* **84**, 3472-3476.

Hornykiewicz O. (1988). Neurochemical Pathology and the Etiology of Parkinson's disease, Basic facts and Hypothetical possibilities. *Mount Sinai J of Med.* **55**, 11-20.

Horstmann S., Kahle P.J., Borasio G.D. (1998) Inhibitors of p38 mitogen-activated protein kinase promote neuronal survival in vitro. *J. Neurosci. Res.* **52**, 483-490.

Hou J.G.G., Lin L.F.H., Mytilineou C. (1996) Glial cell line derived neurotrophic factor exerts neurotrophic effects on dopaminergic neurones in vitro and promotes their survival and re-growth after damage by 1-methyl-4-phenylpyridinium. *J. Neurochem.* **66**, 74-82.

Hunot S., Bernard V., Faucheux B., Boissiere F., Leguern E., Brana C., Gautris P.P., Guerin J., Bloch B., Agid Y., Hirsch EC. (1996) Glial cell-line derived neurotrophic factor (GDNF) gene expression in the human brain - a post-mortem in situ hybridisation study with special reference to Parkinson's disease. *J. Neural Transm.* **103**, 1043-1052.

Inestrosa N.C., Marzolo M.P., Bonnefont A.B. (1998) Cellular and molecular basis of estrogen's neuroprotection - Potential relevance for Alzheimer's disease. *Mol. Neurobiol.* **17**, 73-86.

Irwin I., Langston J.W. (1985) Selective accumulation of MPP⁺ in the substantia nigra, a key to neurotoxicity. *Life Sci.* **36**, 207-212.

Itano Y., Kitamura Y., Nomura Y. (1994) MPP⁺-induced cell death in PC12 cells, inhibitory effects of several drugs. *Neurochem. Int.* **25**, 419-424.

Ito A., Kuwahara T., Inadome S., Sagara Y. (1988) Molecular cloning of cDNA for rat liver monoamine oxidase B. *Biochem. Biophys. Res. Comm.* **157**, 970-976.

Jackson-Lewis V., Neystat M., Lynch T., Vukosavic S., Burke RE., Przedborski S. (1998) Increased expression of α -synuclein in the MPTP mouse model of Parkinson's disease. *Neurology.* **50**, A97.

Jakes R., Spillantini M.G., Goedert M. (1994) Identification of two distinct synucleins from human brain. *FEBS Letts.* **345**, 27-32.

Javitch J.A., D'Amato R.J., Strittmatter S.M., Snyder S.H. (1985) Parkinsonism-inducing neurotoxin, N-methyl-4-phenyl-1,2,3,6-tetrahydropyridine, uptake of the metabolite N-methyl-4-phenylpyridine by dopamine neurones explains toxicity. *Proc. Nat. Acad. Sci.* **82**, 2173-2177.

- Javitch J.A, Snyder S.H. (1984) Uptake of MPP⁺ by dopamine neurons explains selectivity of parkinsonism-inducing neurotoxin, MPTP. *Eur. J. Pharmacol.* **106**, 455-456.
- Javitch J.A, Uhl G.R., Snyder S.H. (1984) Parkinsonism-inducing neurotoxin *N*-methyl-4-phenyl-1,2,3,6-tetrahydropyridine, Characterisation and localisation of receptor binding sites in rat and human brain. *Proc. Natl. Acad. Sci. USA*, **81**, 4591-4595.
- Jing S., Wen D., Yu Y., Holst P. L., Luo Y., Fang M., Tamir R., Antonio L., Hu Z., Cupples R. (1996) GDNF-induced activation of the ret protein tyrosine kinase is mediated by GDNFR- α , a novel receptor for GDNF. *Cell* **85**, 1113-1124.
- Johannessen J.N., Chiueh C.C., Burns R.S., Markey S.P. (1985) Differences in metabolism of MPTP in the rodent and primate parallel differences in the sensitivity to its neurotoxic effects. *Life Sci.* **36**, 219-214.
- Johnson G.V.W., and Jope R.S. (1988) Phosphorylation of rat-brain cytoskeletal proteins is increased after orally-administered aluminum. *Brain Res.* **456**, 95-103.
- Johnston J.P. (1968) Some observations of a new inhibitor of monoamine oxidase in brain tissue. *Biochem. Pharmacol.* **17**, 1285-1297.
- Johnston H.B., Thomas S.M, Atterwill C.K. (1993) Aluminium and iron induced metabolic changes in neuroblastoma cell lines and rat primary neural cultures. *Toxicol. In Vitro* **7**, 229-233.
- Julien J.P., Mushynski W.E. (1983) The distribution of phosphorylation sites among identified proteolytic fragments of mammalian neurofilaments. *J. Biol. Chem.* **258**, 4019-4025.
- Kass G.N., Wright J.M., Nicotera P., Orrenius S. (1988) The mechanism of 1-methyl-4-phenyl-1,2,3,6-tetrahydropyridine toxicity, role of intracellular calcium. *Arch. Biochem. Biophys.* **269**, 789-797.
- Kearney E.B., Salach J.I., Walker W.H., Seng R.L., Kenny W., Zeszotek E., Singer TP. (1971) The covalently bound flavin of hepatic monoamine oxidase. 1. Isolation and sequence of a flavin peptide and evidence for binding at the 8 α position. *Eur. J. Biochem.* **24**, 321-327.
- Keilbaugh S.A., Prusoff W.H., Simpson M.V. (1991) The PC12 cell as a model for studies of the mechanism of induction of peripheral neuropathy by anti-HIV-I dideoxynucleoside analogs. *Biochem. Pharmacol.* **42**, R5-R8.
- Kitamura Y., Kosaka T., Kakimura J. I., Matsuoka Y., Kohno Y., Momura Y., Taniguchi T. (1998) Protective effects of antiparkinsonian drugs talipexole and pramipexole against MPP⁺-induced apoptotic death in human neuroblastoma SH-SY5Y cells. *Mol. Pharmacol.* **54**, 1046-1054.
- Klebe R.J., Ruddle F.H. (1967) Neuroblastoma, Cell culture analysis of a differentiating stem cell system. *Abst. 9th Ann. Meet. Amer. Soc. Cell Biol.* **165**, p69a.
- Knoll J., Ecsery Z., Kelemen K., Nievel J., Knoll B. (1965) Phenylisopropylmethylpropinylamine (E-250), a new spectrum psychic energiser. *Arch.Int. Pharmacodyn.* **155**, 154.
- Knoll J., Magyar K. (1972) Some puzzling pharmacological effects of monoamine oxidase inhibitors. In, *Monoamine oxidases-New Vistas*, pp393-408. Eds. E. Costa and M. Sandler. Raven Press. New York.
- Kochersperger L.M., Parker E.L., Siciliano M., Darlington G.J., Denny R.M. (1986) Assignment of genes for human monoamine oxidases A and B to the X chromosome. *J. Neurosci. Res.* **16**, 601-616.
- Konradi C., Kornhuber J., Froelich L., Fritze J., Heinsen H., Beckmann H., Schultz E Riederer P. (1989) Demonstration of monoamine oxidase-A and -B in the human brainstem by a histochemical technique. *Neuroscience.* **33**, 383-400.

- Konradi C., Svoma E., Jellinger K., Riederer P., Denny R., Thibault J. (1988) Topographic immunocytochemical mapping of monoamine oxidase A, monoamine oxidase B and tyrosine hydroxylase in human post mortem brain stem. *Neuroscience*. **26**, 791-802.
- Kowall N.W., Hantraye P., Brouillet E., Beal M.F., McKee A.C., Ferrante R.J. (2000) MPTP induces alpha-synuclein aggregation in the substantia nigra of baboons. *NeuroReport* **11**, 211-213
- Kromidas L., Trombetta L.D., Jamall I.S. (1990) The protective effect of glutathione against methylmercury cytotoxicity. *Toxicol. Letters*. **51**, 67-80.
- Kruh J. (1982) Effects of sodium butyrate, a new pharmacological agent, on cells in culture. *Mol. & Cell. Biochem.* **42**, 65-82.
- Kumar S., Weingarten D.P., Callahan J.W., Sachar K., de Vellis J. (1984) Regulation of mRNAs for three enzymes in the glial cell model C6 cell line. *J. Neurochem.* **43**, 1455-1463.
- Kwan S-W., Abell C.W. (1992) cDNA cloning and sequencing of rat MAO-A, comparison with the human and bovine enzymes. *Comm. Biochem. Physiol.* **102B**, 143-147.
- Laemmli U.K. (1970) Cleavage of structural proteins during the assembly of the head of bacteriophage T₄. *Nature*. **227**, 680-685.
- Lai M., Griffiths H., Pall H., Williams A., Lunec J. (1993) An investigation into the role of reactive oxygen species in the mechanism of MPTP toxicity using neuronal cell lines. *Biochem. Pharmac.* **45**, 927-933.
- Lan N.C., Heinzmann C., Gal A., Klisak I., Orth U., Lai E., Grimsby J. (1989) Human MAO-A and B genes map to Xp11.23 and are deleted in a patient with Norrie disease. *Genomics* **4**, 552-559.
- Langston J.W., Ballard P., Tetrud J.W., Irwin I. (1983) Chronic parkinsonism in humans due to a product of meperidine-analogue synthesis. *Science*. **219**, 979-980.
- Langston J.W., Forno L.S., Robert C.S., Irwin I. (1984a). Selective nigral toxicity after systemic administration of 1-methyl-4-phenyl-1,2,3,6-tetrahydropyridine (MPTP) in the squirrel monkey. *Brain Res.* **292**, 390-394.
- Langston J.W., Irwin I., Langston E.B., Forno L.S. (1984b) 1-methyl-4-phenylpyridinium ion (MPP⁺), Identification of a metabolite of MPTP, a toxin selective to the substantia nigra. *Neurosci. Lett.* **48**, 87-92.
- Langston J.W. (1985) MPTP neurotoxicity, An overview and characterisation of phases of toxicity. *Life Sci.* **36**, 201-206.
- Lapchak P.A., Miller P.J., Jiao S., Araujo D.M., Hilt D., Collins F. (1996) Biology of GDNF, Implications for the use of GDNF to treat Parkinson's disease. *Neurodegen.* **5**, 197-205.
- LaRosa F.G., Kumar S., Prasad K.N. (1996) Increased expression of ubiquitin during adenosine 3',5'-cyclic monophosphate-induced differentiation of neuroblastoma cells in culture. *J. Neurochem.* **66**, 1845-1850.
- Lee J., Ziering A., Berger L., Heineman S.D. (1946). *Jubile Vol. Emil Barell* 264-305. (*Chem Abstr.* **41**, 6251g).
- Lee V.M-Y., Carden M.J., Schlaepfer W.W., Trojanowski J.Q. (1987) Monoclonal antibodies distinguish several differentially phosphorylated states of the two largest rat neurofilament subunits (NF-H and NF-M) and demonstrate their existence in the normal nervous system of adult rats. *J. Neurosci.* **7**, 3474-3488.

- Lee H.-W., Eghbali-Webb M. (1998) Estrogen enhances proliferative capacity of cardiac fibroblasts by estrogen receptor- and mitogen activated protein kinase-dependent pathways. *J. Mol. Cell. Cardiol.* **30**, 1359-1368.
- Lees J.F., Shneidman P.S., Skuntz S.F., Carden M.J., Lazzarini R.A. (1988) The structure and organisation of the heavy neurofilament subunit (NF-H) and the gene encoding it. *EMBO J.* **7**, 1947-1955.
- Levitt P., Pintar J.E., Breakefield X.O. (1982) Immunocytochemical demonstration of MAO-B in brain astrocytes and serotonergic neurones. *Proc. Natl. Acad. Sci. USA.* **79**, 6385-6389.
- Lin L.-F.H., Doherty D.H., Lile J.D., Bektesh S., Collins F. (1993) GDNF, a glial cell-line derived neurotrophic factor for midbrain dopaminergic neurones. *Science* **260**, 1130-1132.
- Lotharius J., Dugan L.L., O'Malley K.L. (1999) Distinct mechanisms underlie neurotoxin mediated cell death in cultured dopaminergic neurones. *J. Neurosci.* **19**, 1284-1293.
- Lowe J., Blanchard A., Morrell K., Lennox G., Reynolds L., Billett M., Landon M., Mayer R.J. (1988) Ubiquitin is a common factor in intermediate filament inclusion bodies of diverse type in man, including those of Parkinson's disease, Pick's disease and Alzheimer's disease, as well as Rosenthal fibres in cerebellar astrocytomas, cytoplasmic bodies in muscle, and Mallory bodies in alcoholic liver disease. *J. Pathol.* **155**, 9-15.
- Lowry O.H., Rosebrough N.J., Farr A.L., Randall R.J. (1951) Protein measurement with the Folin phenol reagent. *J. Biol. Chem.* **193**, 265-275.
- Lozano A.M., Lang A.E., Hutchison W.D., Dostrovsky J.O. (1998) New developments in understanding the etiology of Parkinson's disease and its treatment. *Curr. Opin. Neurobiol.* **8**, 783-790.
- Makar T. K., Nedergaard M., Preuss A., Gelbard A. S., Perumal A. S., Cooper A. J. L. (1994) Vitamin E, ascorbate, glutathione, glutathione disulphide, and enzymes of glutathione metabolism in cultures of chick astrocytes and neurones, evidence that astrocytes play an important role in antioxidative processes in the brain. *J. Neurochem.* **62**, 45-53.
- Manetto V., Sternberger N.H., Perry G., Sternberger L.A., Gambetti P. (1988) Phosphorylation of neurofilaments is altered in amyotrophic lateral sclerosis. *J. Neuropathol. Exp. Neurol.* **47**, 642-653.
- Mann D.M.A., Yates P.O., Barton C.M. (1977) Neuromelanin and RNA in cells of the substantia nigra. *J. Neuropath. Exp. Neurol.* **36**, 379-384.
- Marchisio P.C., Osborn M., Weber K. (1978) Changes in intracellular organisation of tubulin and actin in N-18 neuroblastoma cells during the process of axon extension induced by serum deprivation. *Brain Res.* **155**, 229-237.
- Marder K., Tang M.X., Alfaro B., Mejia H., Cote L., Jacobs D., Stern Y., Sano M., Mayeux R. (1998) Post-menopausal estrogen use and Parkinson's disease with and without dementia. *Neurol.* **50**, 1141-1143.
- Mari Z., Bodis-Wollner I. (1997) MPTP-induced parkinsonian syndrome in humans and animals, How good is the model? In Beal M.F., Howell N., Bodis-Wollner I. (eds). *Mitochondria & Free Radicals in Neurodegenerative diseases*. New York. Wiley-Liss, pp189-229.
- Markey S.P., Johannessen J.N., Chiueh C.C., Burns R.S., Herkenham M.A. (1984) Intraneuronal generation of a pyridinium metabolite may cause drug induced parkinsonism. *Nature.* **311**, 464-467.
- Maroteaux L., Campanelli J.T., Scheller R.H. (1988) Synucelin, a neuron specific protein localised to the nucleus and presynaptic nerve terminal. *J. Neurosci.* **8**, 2804-2815.
- Meister A. (1984) New aspects of glutathione biochemistry and transport, selective alterations of glutathione metabolism. *Fed. Proc.* **43**, 3031-3042.

- Minamiura N., Yasunobu K.T. (1978) Bovine liver monoamine oxidase, a modified purification procedure and preliminary evidence for two subunits and one FAD. *Archs. Biochem. Biophys.* **189**, 481-489.
- Moldeus P., Hogberg J., Orrenius S., (1978) Isolation and use of liver cells. *Methods Enzymol.* **52**, 60-71.
- Moll G., Moll R., Riederer P., Heisen H., Denny R.M. (1988) Distribution pattern of MAO-A and MAO-B in human substantia nigra shown by immunofluorescence cytochemistry on thin frozen sections. *Pharmac. Res. Commun.* **20**, 89-90.
- Monard D., Solomon F., Rebsch M., Gysin R. (1973) Glial induced morphological differentiation in neuroblastoma cells. *Proc. Natl. Acad. Sci. USA.* **78**, 1894-1897.
- Mytilineou C., Cohen G., Heikkila R.E. (1985) 1-methyl-4-phenylpyridine (MPP⁺) is toxic to mesencephalic dopamine neurones in culture. *Neurosci. Lett.* **57**, 19-24.
- Mytilineou C., Cohen G. (1984) 1-methyl-4-phenyl-1,2,3,6-tetrahydropyridine destroys dopamine neurones in explants of rat embryo mesencephalon. *Science.* **225**, 529-531.
- Nagatsu T., Nakano T., Kato H., Higashida H. (1981) Expression of A and B types of monoamine oxidase in neuroblastoma hybrid cells. *Neurochem. Int.* **3**, (2) 137-142.
- Narotzky R., Bondareff W. (1974) Biogenic amines in cultured neuroblastoma cells. *J. Cell. Biol.* **69**, 64-70.
- Nicklas W.J., Vyas I., Heikkila R.E. (1985) Inhibition of NADH-linked oxidation in brain mitochondria by 1-methyl-4-phenyl-1,2,3,6-tetrahydropyridine. *Life Sci.* **36**, 2503-2508.
- Nixon R.A. (1993) The regulation of neurofilament protein dynamics by phosphorylation - clues to neurofibrillary pathobiology. *Brain Pathol.* **3**, 29-38.
- Nixon R.A. (1998) The slow axonal transport of cytoskeletal proteins. *Curr. Opin. Cell Biol.* **10**, 87-92.
- Nixon R. A., Sihag R. K. (1991) Neurofilament phosphorylation, a new look at regulation and function. *Trend. Neurosci.* **14**, 501-506.
- Notter M.F.D, Irwin I., Langston J.W., Gash D.M. (1988) Neurotoxicity of MPTP and MPP⁺ in vitro, characterisation using specific cell lines. *Brain Res.* **456**, 254-262.
- OhtaniKaneko R., Asahara M., Takada K., Kanda T., Iigo M., Hara M., Yokosawa H., Ohkawa K., Hirata K. (1996) Nerve growth factor (NGF) induces increase in multi-ubiquitin chains and concomitant decrease in free ubiquitin in nuclei of PC12h. *Neurosci. Res.* **26**, 349-355.
- Oreland L., Shaskan E.G. (1983) Monoamine oxidase activity as a biological marker. *TIPS* **6**, 339-341.
- Packer M.A., Miesel R., Murphy M.P. (1996) Exposure to the Parkinsonian Neurotoxin 1-methyl-4-phenylpyridinium (MPP⁺) and nitric oxide simultaneously causes cyclosporin-A sensitive mitochondrial calcium efflux and depolarisation. *Biochem. Pharmacol.* **51**, 267-273.
- Parsons B., Rainbow T.C. (1984) High-affinity binding sites for [³H]MPTP may correspond to monoamine oxidase. *Euro. J. Pharmacol.* **102**, 375-377.
- Patrick G. N. Zukerberg L., Nikolic M., de la Monte S., Dikkes P., Tsai L-H. (1999) Conversion of p35 to p25 deregulates cdk5 activity and promotes neurodegeneration. *Nature.* **402**, 615-622.
- Pekiner C., and McLean W.G. (1991) Neurofilament phosphorylation in spinal cord of experimentally diabetic rats. *J. Neurochem.* **56**, 1362-1367.

- Perry T.L., Young V.W., Clavier R.M., Jones K., Wright J.M., Foulkes J.G., Wall R.A. (1985) Partial protection from the dopaminergic neurotoxin MPTP by four different antioxidants in the mouse. *Neurosci. Lett.* **60**, 109-114.
- Pifl C., Giros B., Caron M.G. (1993) Dopamine transporter expression confers cytotoxicity to low doses of the parkinsonism-inducing neurotoxin 1-methyl-4-phenylpyridinium. *J. Neurosci.* **13**, 4246-4253.
- Polotrak M., Freed W. J. (1988) Immunoreactive phosphorylated epitopes on neurofilaments in neuronal perikarya may be obscured by tissue preprocessing. *Brain Res.* **480**, 349-354.
- Polymeropoulos M.H., Higgins J.J., Golbe L.I., Johnson W.G., Ide S.G., Di Iorio G., Sanges G., Stenroos E.S., Pho L.T., Schaffer A.A., Lazzarini A.M., Nussbaum R.L., Duboisin .RC. (1996) Mapping of a gene for Parkinson's disease to chromosome 4q21-q23. *Science.* **274**, 1197-1199.
- Powell J.F., Hsu Y-P.P., Weyler W., Chen S., Salach J., Andrikopoulos K., Mallet J., Breakefield X.O. (1989) The primary structure of bovine MAO-A, comparison with peptide sequences of bovine MAO-B and other flavoenzymes. *Biochem J.* **259**, 407-413.
- Prasad K. N., Sinha P.K. (1976) Biochemical differentiation of neuroblastoma cells. *In Vitro* **12**, 125-132.
- Przedborski S., Kostic V., Jackson-Lewis V. (1992) Transgenic mice with increased C/Zn-superoxide dismutase activity are resistant to MPTP-induced neurotoxicity. *J. Neurosci.* **12**, 1658-1667.
- Rainbow T.C., Parsons B., Wieczorek C., Manaker S. (1985) Localisation in rat brain of binding sites for parkinsonian toxin MPTP, similarities with [³H]pargyline binding to monoamine oxidase. *Brain Res.* **330**, 337-342.
- Ramsey R.R., Salach J.I., Dadgar J., Singer T.P. (1986) Inhibition of mitochondrial NADH dehydrogenase by pyridine derivatives and its possible relation to experimental and idiopathic Parkinsonism. *Biochem. Biophys. Res. Commun.* **135**, 269-275.
- Ramsey R.R., Kowal A.T., Johnson M.K., Salach J.I., Singer T.P. (1987) The inhibition site of MPP⁺, the neurotoxic product of MPTP is near the Q-binding site of NADH dehydrogenase. *Arch. Biochem. Biophys.* **259**, 645-649.
- Ramsey R.R., Krueger M.J., Youngster S.K., Gluck M.R., Casida J.E., Singer T.P. (1991) Interaction of MPP⁺ ion and its analogues with the rotenone/piericidin binding site of NADH dehydrogenase. *J. Neurochem.* **56**, 1184-1190.
- Ransom B.R., Kunis D.M., Irwin I., Langston J.W. (1987) Astrocytes convert the parkinsonism inducing neurotoxin, MPTP, to its active metabolite, MPP⁺. *Neurosci. Lett.* **75**, 323-328.
- Reagan K.E., Wilmarth K.R., Friedman M., Aboudonia M.B. (1994) Acrylamide increases *in-vitro* calcium and calmodulin-dependent kinase mediated phosphorylation of rat brain and spinal cord neurofilament proteins. *Neurochem. Int.* **25**, 133-143.
- Reinhard J.F., Daniels A.J., Painter G.R. (1990) Carrier independent entry of MPP⁺ into adrenal chromaffin cells as a consequence of charge delocalisation. *Biochem. Biophys. Res. Commun.* **168**, 1143-1148.
- Ricaurte G.A., Irwin I., Forno L.S., DeLanney L.E., Langston E., Langston J.W. (1987) Ageing and 1-methyl-4-phenyl-1,2,3,6-tetrahydropyridine-induced degeneration of dopaminergic neurones in the substantia nigra. *Brain Res.* **403**, 43-51.
- Riederer P., Sofic E., Rausch W.D. (1989) Transition metals, ferritin, glutathione and ascorbic acid in parkinsonian brains. *J. Neurochem.* **52**, 515-520.
- Rossetti Z.L., Sotgiu A., Sharp D.E., Hadjiconstantinou M., Neff N.H. (1988) 1-methyl-4-phenyl-1,2,3,6-tetrahydropyridine (MPTP) and free radicals *in vitro*. *Biochem. Pharmacol.* **37**, 4573-4574.

Russell S.M., Mayer R.J. (1983) Degradation of transplanted rat liver mitochondrial outer membrane proteins in hepatoma cells. *Biochem. J.* **216**, 163-175.

Salach J.I., Singer T.P., Castagnoli N. Jr., Trevor A. (1984) Oxidation of the neurotoxic amine 1-methyl-4-phenyl-1,2,3,6-tetrahydropyridine (MPTP) by monoamine oxidases A and B and suicide inactivation of the enzymes by MPTP. *Biochem. Biophys. Res. Commun.* **125**, 831-835.

Saporito M.S., Brown E.M., Miller M.S., Carswell S. (1999) CEP-1347/KT-7515, an inhibitor of c-jun N-terminal kinase activation, attenuates the 1-methyl-4-phenyl tetrahydropyridine-mediated loss of nigrostriatal dopaminergic neurons *in vivo*. *J. Pharmacol. Exp. Therap.* **288**, 421-427.

Schubert D., Humphreys S., Baroni C., Cohn M. (1969) In vitro differentiation of a mouse neuroblastoma. *Proc. Natl. Acad. Sci. USA.* **64**, 316-323.

Scotcher K.P., Irwin I., DeLanney L.E., Langston J.W., DiMonte D. (1991) Mechanism of accumulation of 1-methyl-4-phenylpyridinium species into mouse brain synaptosomes. *J. Neurochem.* **56**, 1602-1607.

Shaw G. (1991) Neurofilament proteins. In *The Neuronal Cytoskeleton*. Wiley-Liss, pp185-214.

Shea T.B., Beermann M.L., Nixon R.A. (1989) Appearance and localisation of phosphorylated variants of the high molecular weight neurofilament protein in NB2a/d1 cytoskeleton during differentiation. *Dev. Brain. Res.* **50**, 142-146.

Shea T.B., Sihag R.K., Nixon R.A. (1990) Dynamics of phosphorylation and assembly of the high molecular weight neurofilament subunit in NB2a/d1 neuroblastoma. *J. Neurochem.* **55**, 1784-1792.

Shea T.B., Beermann M.L., Leli U., Nixon R.A. (1992) Opposing influences of protein-kinase activities on neurite outgrowth in human neuroblastoma-cells -initiation by kinase-A and restriction by kinase-C. *J. Neurosci. Res.* **33**, 398-407.

Shea T.B. (1994) Toxic and trophic effects of glial-derived factors on neuronal cultures. *Neurorep.* **5**, 797-800.

Shea T.B., Beermann M.L. (1994) Respective roles of neurofilaments, microtubules, MAP1B, and tau in neurite outgrowth and stabilisation. *Mol. Biol. Cell* **5**, 863-875.

Shea T.B., Beermann M.L., Nixon R.A. (1995) Aluminium treatment of intact neuroblastoma cells alters neurofilament subunit phosphorylation, solubility, and proteolysis. *Mol. & Chem. Neuropathol.* **26**, 1-14.

Shea T.B. (1995) Differential synthesis and cytoskeletal deposition of neurofilament subunits before and during axonal outgrowth in NB2a/d1 cells, evidence that segregation of phosphorylated subunits within the axonal cytoskeleton involves selective deposition. *J. Neurosci. Res.* **40**, 225-232.

Shea T.B., Husain T. (1996) Induction of neurite outgrowth in neuroblastoma cells by astroglial-secreted factors is mediated by protein kinase C. *Neurosci. Res. Commun.* **18**, 57-61.

Shea T.B., Wheeler E., Jung C. (1997) Aluminium inhibits neurofilament assembly, cytoskeletal incorporation and axonal transport. *Mol. & Chem. Neuropathol.* **32**, 17-39.

Shih J.C., Zhu Q.S., Grimsby J., Chen K. (1994) Identification of human monoamine oxidase A and B gene promoters. *J. Neural. Transm. Suppl.* **41**, 27-33.

Singer T.P., Salach J.I., Crabtree D. (1985) Reversible inhibition and mechanism-based irreversible inactivation of monoamine oxidases by MPTP. *Biochem. Biophys. Res. Commun.* **127**, 707-712.

Singer T.P., Salach J.I., Castagnoli N. Jr., Trevor A. (1986) Interactions of the neurotoxic amine MPTP with monoamine oxidases. *Biochem. J.* **235**, 785-789.

Singer T.P., Castagnoli N. Jr., Ramsey R.R., Trevor A.J. (1987) Biochemical events in the development of parkinsonism induced by 1-methyl-4-phenyl-1,2,3,6-tetrahydropyridine. *J. Neurochem.* **49**, 1-8.

Skaper S.D., Adelson G. L., Seegmiller J.E. (1976) Metabolism of biogenic amines in neuroblastoma and glioma cells in culture. *J. Neurochem.* **27**, 1065-1070.

Smith T.S., Swerdlow R.H., Parker W.D.J., Bennett J.P.J. (1994) Reduction of MPP⁺ induced hydroxyl radical formation and nigrostriatal MPTP toxicity by inhibiting nitric oxide synthetase. *Neuroreport* **5**, 2598-2600.

Song X., Perkins S., Jortner B.S., Ehrich M. (1997) Cytotoxic effects of MPTP on SH-SY5Y human neuroblastoma cells. *Neurotoxicol.* **18**, 341-353.

Spillantini M.G., Schmidt M.L., Lee V.M.-Y., Trojanowski J.Q., Jakes R., Goedert M. (1997) α -Synuclein in Lewy bodies. *Nature.* **388**, 839-840.

Sriram K., Pai K.S., Boyd M.R., Ravindranath V. (1997) Evidence for generation of oxidative stress in brain by MPTP, *In vitro* and *in vivo* studies in mice. *Brain Res.* **749**, 44-52.

Sternberger L.A., Sternberger N.H. (1983) Monoclonal antibodies distinguish phosphorylated and non-phosphorylated forms of neurofilaments in situ. *Proc. Natl. Acad. Sci. USA.* **80**, 6126-6130.

Strack S., Westphal R.S., Colbran R.J., Ebner F.F., Wadzinski B.E. (1997) Protein serine/threonine phosphatase 1 and 2A associate with and dephosphorylate neurofilaments. *Mol. Brain Res.* **49**, 15-28.

Sun D., Leung C. L., Liem R. K. H. (1996) Phosphorylation of the high molecular weight neurofilament protein (NF-H) by cdk5 and p35. *J. Biol. Chem.* **271**, 14245-14251.

Sunstrom E., Mo L.L. (1995) Effects of MPP⁺ on radioligand binding to the NMDA receptor complex. *Res. Commun. Mol. Pathol. Pharmacol.* **88**, 131-136.

Suter-Crazzolaro C., Unsicker K. (1996) GDNF mRNA levels are induced by FGF-2 in rat C6 glioblastoma cells. *Mol. Brain Res.* **41**, 175-182.

Tatton W.G., Ju W.Y.L., Holland D.P., Tai C., Kwan M. (1994) (-)-Deprenyl reduces PC12 cell apoptosis by inducing new-protein synthesis. *J. Neurochem.* **63**, 1572-1575.

Tatton W.G., Chalmers-Redman R.M.E. (1996) Modulation of gene expression rather than monoamine oxidase inhibition, (-)-deprenyl-related compounds in controlling neurodegeneration. *Neurol.* **47**, S171-S183.

Tetrad J.W., Langston J.W. (1992) Tremor in MPTP-induced parkinsonism. *Neurology.* **42**, 407-410.

Tibbles L.A., Woodgett J.R. (1999) The stress-activated protein kinase pathways. *Cell. Mol. Life Sci.* **55**, 1230-1254.

Tipton K.F., Singer T.P. (1993) Advances in our understanding of the mechanisms of neurotoxicity of MPTP and related compounds. *J. Neurochem.* **61**, 1191-1206.

Tomac A., Lindqvist E., Lin L-F.H., Ogren S.O., Young D., Hoffer B.J., Olson L. (1995) Protection and repair of the nigrostriatal dopaminergic system by GDNF *in vivo*. *Nature* **373**, 335-339.

Toran-Allerand C. D., Singh M., Setalo G. Jr. (1999) Novel mechanisms of estrogen action in the brain, new players in an old story. *Front. Neuroendocrinol.* **20**, 97-121.

Toviola D.M., Eriksson J.E. (1999) Toxins affecting cell signalling and alteration of cytoskeletal structure. *Toxicol. In Vitro.* **13**, 521-530.

Towbin H., Staehelin T., Gordon J. (1979) Electrophoretic transfer of proteins from polyacrylamide gels to nitrocellulose sheets, procedure and some applications. *Proc. Natl. Acad. Sci. USA.* **76**, 4350-4354.

Treanor J.J., Goodman L., de Sauvage F., Stone D.M., Poulsen K.T., Bck C.D., Gray C., Armanini M.P., Pollack R.A., Hefti F., Phillips H.S., Goddard A., Moore M.W., Buj-Bello A., Davies A.M., Asai N., Takahashi M., Vandlen R., Hebderson CE., Rosenthal A. (1996) Characterisation of a multicomponent receptor for GDNF. *Nature* **382**, 80-83.

Turner N.A. Xia F., Azhar G., Zhang X.M., Liu L.X. Wei J.Y. (1998) Oxidative stress induces DNA fragmentation and caspase activation via the c-jun N terminal kinase pathway in H9c2 cardiac muscle cells. *J. Mol. Cell. Cardiol.* **30**, 1789-1801.

Turski L., Bressler K., Rettig K.J., Loschmann P.A., Wachtel H. (1991) Protection of substantia-nigra from MPP⁺ neurotoxicity by N-methyl-D-aspartate antagonists. *Nature*. **349**, 414-418.

Umemura T., Naoi M., Takahashi T., Fukui Y., Yasue T., Ohashi M. Nagatsu T. (1990) Cytotoxic effect of MPP⁺ ion on human-melanoma cell lines, HMV-II and SK-MEL-44, is dependent on the melanin contents and caused by inhibition of mitochondrial electron transport. *Biochem. Medicin. Metabol. Biol.* **44**, 51-58.

Urani C., Brambilla E., Santagostino A., Camatini M. (1994) 1-methyl-4-phenyl-1,2,3,6-tetrahydropyridine (MPTP) affects the actin cytoskeleton and calcium level of Swiss 3T3 mouse fibroblasts. *Toxicol.* **91**, 117-126.

Varshesky A. (1997) The ubiquitin system. *TIBS* **22**, 383-387.

Veeranna, Amin N.D., Ahn N.G., Jaffe H., Winters C.A., Grant P., Pant H.C. (1998) Mitogen-activated protein kinases (Erk1,2) phosphorylate Lys-Ser-Pro (KSP) repeats in neurofilament proteins NF-H and NF-M. *J. Neurosci.* **18**, 4008-4021.

Vila M., Vukosavic S., Jackson-Lewis V., Neystat M., Jakowec M., Przedborski S. (2000) α -synuclein up-regulation in substantia nigra dopaminergic neurons following administration of the Parkinsonian toxin MPTP. *J. Neurochem.* **74**, 721-729.

Vyas I., Heikkila R.E., Nicklas W.J. (1986) Studies on the neurotoxicity of MPTP, Inhibition of NAD-linked substrate oxidation by its metabolite MPP⁺. *J. Neurochem.* **46**, 1501-1507.

Wang X.T., Martindale J.L., Liu Y.S., Holbrook N.J. (1998) The cellular response to oxidative stress, influences of mitogen-activated protein kinase signalling pathways on cell survival. *Biochem J.* **333**, 291-300.

Watson D.F., Fittro K.P., Hoffman P.N., Griffin J.W. (1991) Phosphorylation-related immunoreactivity and the rate of transport of neurofilaments in chronic 2,5-hexanedione intoxication. *Brain Res.* **539**, 103-109.

Waymire J.C., Weiner N., Prasad K.N. (1972) Regulation of tyrosine hydroxylase activity in cultured mouse neuroblastoma cells, elevation induced by analogues of adenosine 3',5'-cyclic monophosphate. *Proc. Nat. Acad. Sci. USA.* **69**, 2241-2245.

Wei Q., Yeung M., Jurma O.P., Andersen J.K. (1996) Genetic elevation of monoamine oxidase levels in dopaminergic PC12 cells results in increased free radical damage and sensitivity to MPTP. *J. Neurosci. Res.* **46**, 666-673.

Weiss H., Friedrich T., Hofhaus G., Preis D. (1991) The respiratory-chain NADH dehydrogenase (complex I) of mitochondria. *Eur. J. Biochem* **197**, 563-576.

Westlund K.N., Denny R.M., Rose R.M., Abell C.W. (1988) Localisation of distinct monoamine oxidase B cell populations in human brainstem. *Neuroscience.* **25**, 439-456.

Weyler W. (1989) Monoamine oxidase A from human placenta and monoamine oxidase B from bovine liver both have one FAD per subunit. *Biochem. J.* **260**, 725-729.

Wullner U., Loschmann P.A., Schulz J.B., Schmid A., Dringen R., Ebeln F., Turski L., Klockgether T. (1996) Glutathione depletion potentiates MPTP and MPP⁺ toxicity in nigral dopaminergic neurones. *NeuroReport* 7, 921-923.

Yasuhara H., Parvez S.H., Oguchi K., Sandler M., Nagatsu T. (1993) Monoamine oxidase, basic and clinical aspects. New York. VSP, 15-48.

Youdim M.H., Finberg J.P.M. (1991) New directions in monoamine oxidase A and B, selective inhibitors and substrates. *Biochem. Pharmacol.* 41, 155-162.

Yu P.H. (1981) Studies on the pargyline binding site of different types of MAO. *Can. J. Biochem.* 59, 30-37.